1.0

4.5
5.0
5.6
6.3

2.8   2.5

3.2   2.2

3.6

4.0   2.0

1.1

1.8

1.25   1.4   1.6

MICROCOPY RESOLUTION TEST CHART
NATIONAL BUREAU OF STANDARDS-1963-A

SSC-268

ENVIRONMENTAL WAVE DATA FOR DETERMINING HULL STRUCTURAL LOADINGS

DDC
RECEIVED
DEC 2 1977
B

SHIP STRUCTURE COMMITTEE
1977

The Ship Structure Committee recognizes that information concerning the
environmental conditions under which ships and marine structures are
operated is of utmost importance for structural design, and particularly
so for estimating their survival limitations. Recent progress in proba-
bilistic approaches to design permits design loads to be estimated with
reasonable accuracy where ocean wave spectra in the operating areas of
the ship (or marine structure) are sufficiently known.

Although there is a great deal of data on visually observed wave heights
and periods in the North Atlantic and in the North Pacific Oceans, these
data are not in a form which the designer can use; they are not in a con-
sistent form which can be easily processed; they cover only a small por-
tion of the geographical and sea state range necessary for design purposes;
and even some of these are of somewhat questionable validity. Therefore,
it became necessary to undertake a study directed toward developing a body
of complete and reliable ocean wave loading data.

This report describes the study and presents a research plan directed
toward the development of wave loading data in a form which can be used
in rational hull structure design.

W. M. BENKERT
Rear Admiral, U.S. Coast Guard
Chairman, Ship Structure Committee

SSC-268

FINAL TECHNICAL REPORT.

on

Project SR-223

"Wave Loading Data Plan"

ENVIRONMENTAL WAVE DATA FOR

DETERMINING HULL STRUCTURAL LOADINGS.

62754N

1977   236 p.

by

D. Hoffman and D. A. Walden   F43422

with contributions by

V. J. Cardone, and   SF43422703
W. J. Pierson, Jr.

WEBB INSTITUTE OF NAVAL ARCHITECTURE

under

Department of the Navy
Naval Sea Systems Command
Contract No. N00024-75-C-4209

D D C
RECEIVED
DEC 2 1977
B

*This document has been approved for public release
and sale: its distribution is unlimited.*

U.S. Coast Guard Headquarters
Washington, D.C.
1977

372 720

ABSTRACT

A summary is given of the trade routes of U.S. ships, followed by suggestions
for new projects and extension and improvement of current projects to meet the
need for additional data on sea conditions encountered by U.S. ships. It is
concluded that the greatest benefit can be obtained by making a direct effort
to obtain wave spectra for the ocean areas on important sea routes that are known
to experience severe sea conditions, probably by the use of moored buoys, and
by further verification and improvement of wave hindcast techniques for eventual
application to obtaining wave spectra for design. At the same time, steps should
be initiated that may lead to the availability of wave data in the future, such as
seeking oil company data.

It is felt that attention should also be given to the further analysis of
available data, and of new data produced by buoy deployment and hindcast procedures,
including the measurement of directional spectra and their application to design.
Hindcast techniques should be extended to the southern hemisphere, and new
techniques for wave data collection -- disposable buoys and satellite systems --
should continue to be developed.

A survey evaluation is given of observed and measured wave data covering
major U.S. routes, with appendices, tabulations and maps. The introduction
of theoretical formulations leads to the discussion and evaluation of wave spectral
hindcasting techniques. The methods used to predict ship motions and loads are
explained followed by a section discussing the wave data format required for
predicting short and long-term loads and motions as well as numerical examples
showing the effect on and sensitivity of predictions to variation in wave data
format.

Based on the preceding discussion, presently available data suggested for
use in determining ship loads are given. The use of a combination of statistics
based on observations on the frequency of occurrence of various wave heights
and a spectral family of measured spectra grouped by wave height is recommended.
Finally, a survey of current and planned data collection projects is given.

11

CONTENTS

LIST OF TABLES

LIST OF FIGURES

LIST OF FIGURES (cont'd)

LIST OF FIGURES (cont'd)

SHIP STRUCTURE COMMITTEE

The SHIP STRUCTURE COMMITTEE is constituted to prosecute a research program to improve the hull structures of ships by an extension of knowledge pertaining to design, materials and methods of fabrication.

RADM W. M. Benkert, USCG (Chairman)
Chief, Office of Merchant Marine Safety
U.S. Coast Guard Headquarters

Mr. P. M. Palermo
Asst. for Structures
Naval Ship Engineering Center
Naval Ship Systems Command

Mr. M. Pitkin
Asst. Administrator for
Commercial Development
Maritime Administration

Mr. John L. Foley
Vice President
American Bureau of Shipping

Mr. C. J. Whitestone
Engineer Officer
Military Sealift Command

SHIP STRUCTURE SUBCOMMITTEE

The SHIP STRUCTURE SUBCOMMITTEE acts for the Ship Structure Committee on technical matters by providing technical coordination for the determination of goals and objectives of the program, and by evaluating and interpreting the results in terms of ship structural design, construction and operation.

NAVAL SEA SYSTEMS COMMAND

Mr. R. Johnson - Member
Mr. J. B. O'Brien - Contract Administrator
Mr. C. Pohler - Member
Mr. G. Sorkin - Member

U.S. COAST GUARD

LCDR E. A. Chazal - Secretary
LCDR S. H. Davis - Member
CAPT C. B. Glass - Member
LCDR J. N. Naegle - Member

MARITIME ADMINISTRATION

Mr. F. Dashnaw - Member
Mr. N. Hammer - Member
Mr. R. K. Kiss - Member
Mr. F. Seibold - Member

MILITARY SEALIFT COMMAND

Mr. T. W. Chapman - Member
CDR J. L. Simmons - Member
Mr. A. B. Stavovy - Member
Mr. D. Stein - Member

AMERICAN BUREAU OF SHIPPING

Mr. S. G. Stiansen - Chairman
Dr. H. Y. Jan - Member
Mr. I. L. Stern - Member

NATIONAL ACADEMY OF SCIENCES
SHIP RESEARCH COMMITTEE

Prof. J. E. Goldberg - Liaison
Mr. R. W. Rumke - Liaison

SOCIETY OF NAVAL ARCHITECTS &
MARINE ENGINEERS

Mr. A. B. Stavovy - Liaison

WELDING RESEARCH COUNCIL

Mr. K. H. Koopman - Liaison

INTERNATIONAL SHIP STRUCTURES
CONGRESS

Prof. J. H. Evans - Liaison

U.S. COAST GUARD ACADEMY

CAPT W. C. Nolan - Liaison

STATE UNIV. OF N.Y. MARITIME COLLEGE

Dr. W. R. Porter - Liaison

AMERICAN IRON & STEEL INSTITUTE

Mr. R. H. Sterne - Liaison

U.S. NAVAL ACADEMY

Dr. R. Bhattacharyya - Liaison

I. INTRODUCTION

Background

The dynamics of ships or other types of marine structures is determined
to a large extent by their responses to the environment in which they operate.
Wind, waves, current and ice are the four environmental factors which individually
and interactively contribute to the forces imposed on the system and hence to
the resulting responses. The definition of the excitation function is therefore
of critical importance and a prerequisite for a prediction of the behavior
of a ship in a realistic environment. Each of the above four categories is
of a complex nature and involves several physical phenomena. The waves,
however, are the major influence on the behavior of marine vehicles.

Ever since the probabilistic approach was developed by St. Denis
and Pierson (1953),[*] the complex problem of ship behavior in waves has been
conveniently separated into two components, i.e., the waves and the transfer
function. While the latter has received rather extensive treatment over the
past 20 years, the wave description has been left to the oceanographers studying
basic prinicples such as generation of waves, the energy balance in the waves,
growth of waves with wind, etc. Understanding the mechanism of wave generation
has led oceanographers to formulate the shape of idealized wave spectra, par-
ticularly the spectra of fully-developed storm seas, although the shapes of
developing and decaying spectra have also been studied. They have also reported
spectra obtained from actual measurements at various ocean locations, but have
not given much attention to the variations in shape that these spectra show.
Thus cross seas, as created by local wind sea superimposed on swell or several
swells, are not adequately represented by the ideal formulations; yet these
conditions are very common.

Actual wave records and, particularly, wave spectra are available only
for limited ocean areas, and the present design practice in most cases is to
apply the above ideal mathematical formulations as defined by the observed
significant wave height and period. This procedure requires cautious evaluation,
as discussed in this report.

The state of the art of wave load prediction has thus reached a stage
in which the continuous refinement and exact mathematical solution of transfer
functions cannot be satisfactorily applied to ship design without at least an
equivalent refinement in the wave description. The time has come when designer
should actively seek the wave data needed, rather than to wait for the ocean-
ographer to supply them. Hence, a major objective of this report is to make
recommendations regarding further research to obtain the needed wave information.

Wave Data Requirements

The definition of the type of wave data desired by the ship designer is

---

[*]See references listed at the end of this report.

unfortunately often determined by the designer's knowledge of available data. It is therefore important to define present needs as well as idealized requirements assuming unlimited wave data availability. Only such an approach can lead to effective pursuance of future wave data collection and the correct application of such data in the statistical prediction of ship loadings in the environment.

The method formulated by St. Denis and Pierson (1953) to obtain the response of a ship or other system to waves utilizes the wave spectrum, which can be expressed mathematically by analysis of a measured wave record of 20 - 30 minutes length or by estimate from the average characteristics of the seaway. From the spectrum of the waves and the characteristic ship response to different frequencies (transfer function or response amplitude operator) the response spectrum can be obtained, and hence the statistical properties of the ship response can be determined. For design purposes the response of the system to all possible sea conditions is of prime importance, and hence extensive wave data in spectral form are felt to be essential.

Ideally, these wave spectra should be directional, i.e., should define the wave components by direction as well as by frequency. They should describe both growing and decaying storm seas, as well as fully-developed seas. They should describe combinations of storm seas and swells that are typical of winter weather conditions in northern and southern latitudes, as well as slow-moving circular storms of the tropics.

However, in view of the extreme cost and time associated with an extensive data gathering plan, a more exact assessment is required today with regard to the influence of variations in wave spectra on response. As mentioned previously, different wave data can affect the prediction of the design loads and hence the structural design. Such influence can only be determined in terms of the final product, i.e., the loads predicted on the ship. It has already been shown (Hoffman, 1973, 1974, 1975) that such effects will vary from one size to another and most likely will be a function of the type of response in question, such as bending moment or acceleration. Hence, further study is needed of the degree of detail needed in wave spectral data.

In contrast to the ultimate need of the designer for optimum wave data formatting, an important interim stage considers the best application of presently available data. Acquisition of reliable wave data is a lengthy process and an interim solution is needed for the immediate years.

Thus, a survey and assessment of available ocean wave data and of its suitability for design use is first required. Then a plan must be developed for obtaining needed additional data in suitable format.

Trade Routes of U.S. Ships

An important question that arises in surveying available and needed ocean wave data is what ocean areas are of greatest interest. A study has been made to establish the most important world trade routes, with particular attention

to those served by U.S. ships. The routes of greatest volume of cargo and number of ships are those from the U.S. East (and Gulf) coasts to Europe. There are three branches, one north of the British Isles to Scandinavia, one to northern Europe via the English Channel and the third to the Mediterranean, but all are vitally affected by weather and sea conditions in the North Atlantic Ocean.

Another important group of trade routes is between U.S. East and Gulf coasts and the Caribbean and South America. These lend importance to sea conditions in the vicinity of Cape Hatteras and to the conditions prevailing during hurricanes in the Gulf of Mexico and North Atlantic.

Also of importance are routes in the Pacific Ocean, which however are widely scattered -- covering U.S. ports on West, East and Gulf coasts (Panama Canal) and connecting with Japan, the Asian continent, Indonesia, Australia, New Zealand, etc. From the viewpoint of the effect of sea conditions on ship operation, however, the ocean area of greatest potential interest is the North Pacific. Increased trade between West coast ports and Alaska has resulted in growing interest in sea conditions in the Gulf of Alaska.

Although relatively few U.S. flag ships transit the Indian Ocean, the eastern part of the area is of interest during the monsoon season. The South Atlantic and South Pacific oceans, as a whole, are also of secondary interest.

Finally, consideration should be given to bulk petroleum movements to U.S. ports, which are carried on ships of which few are U.S. flag but many of U.S. ownership. The predominant route is from the Persian Gulf and Cape of Good Hope to Caribbean and U.S. Gulf ports. Sea conditions in the vicinity of the Cape are of particular concern, as discussed in detail later in this report. The opening of the Suez Canal can be expected to divert some of this traffic through the Mediterranean, but there can be no doubt that sea conditions around the Cape of Good Hope will continue to be of great importance.

Scope of Project

The scope of work for the project reported here was stated as follows in the contract schedule: "Conduct a survey and assessment of the type and scope of wave loading data presently available, and that which is needed, and establish a research plan to acquire a sufficient quantity of the needed wave data in a form which can be used in hull structural design."

This report describes the work done and presents the results of the study carried out in accordance with the above. For convenience the proposed plan for further research on ocean wave data, developed in the course of the project, is presented in the following Chapter II. A survey is then presented of various types of ocean wave data, and their reliability (Chapters III, IV, V, VI). Next the use of such wave data for the determination of hull loads is discussed, and the effect of variations in the wave data format is considered (Chapters VII and VIII). Finally, recommendations are made regarding the best available data and current data collection projects are surveyed. (Chapter IX).

II. A RESEARCH PLAN

General

One of the principal objectives of this project was to develop a research plan for the acquisition of required additional ocean wave data, and their translation into a form useable by hull structural designers. On the basis of the survey given in the following chapters, recommendations for short and long-range research are given here. In addition to the proposed research projects themselves, however, consideration should be given to setting up a central management or coordinating project to oversee the acquisition of data for use by naval architects. One object would be to keep all interested parties informed as to what projects are being undertaken and who is sponsoring them.

Some of the projects listed below could produce immediately useful data if undertaken promptly, while others would not be productive for some time. A discussion of recommended priorities is given at the end of the chapter.

Hindcast Techniques

1. Evaluation and refinement of existing wave hindcast programs. The only suitable procedure in active operation is that of the Navy Fleet Numerical Weather Central (FNWC) in Monterey. A continuing, routine checking and verification process should be carried out, comparing hindcast spectra with those calculated from wave measurements at data buoys or weather ships. As improvements in the hindcast procedures are made, they should be evaluated by this continuous routine checking. It is understood that such checking is now being done by FNWC to some degree.

From the long-range viewpoint, attention should be directed to private forecasting and hindcasting procedures (such as that of Ocean Routes, Inc., Palo Alto, California) which are being developed to serve oil well drilling activities but could perhaps be extended to serve shipping lines.

2. Development of a comprehensive hindcast data base. After the validity of the FNWC hindcast system has been established, the data base can be developed by statistical analysis of daily spectra for at least a year at selected locations over the entire North Atlantic and North Pacific Oceans, and in the Mediterranean Sea. Such a data base has been referred to as a "wave spectra climatology." See NAVSEA (1975).

It should be noted that funds have already been allocated to FNWC for hindcasting directional spectra back to 1955, using the latest refinements in the hindcast model. Since this is a project of considerable magnitude, considerable effort should be devoted to improving and refining the prediction model (item 1) in parallel with this large-scale hindcasting effort.

3. Extension of the hindcast system to cover the South Atlantic Ocean and the Western Indian Ocean, including the ocean area in the vicinity of the Cape of Good Hope. After such a system becomes operational, it should be verified, analyzed and applied as in 1) and 2) above.

This project may require direct support from shipping and ship design interests, since the Navy has not given it high priority. Since a long time is required for this work, no short-term results can be expected.

Development and Use of Wave Buoys

4. Deployment of buoys. A number of buoys should be set out, with telemetered wave records regularly transmitted to shore and spectrally analyzed. See Steele (1974) for a description of the National Oceanic and Atmospheric Administration (NOAA) Data Buoy Office (NDBO) system. The buoys would be located on important steamship routes, particularly at locations where inadequate wave data are available. Resulting spectra would be used directly to increase the bank of data for designers' use. See Appendix E.

Consideration should be given to incorporating slope, as well as vertical acceleration measurements. Such slope measurements, while not sufficient to define the directional spectra completely, can give some directional information. Cartwright (1961) discusses the limits of such slope measurements.

Tentative buoy locations:

    (a) North Atlantic (Grand Banks, Faraday Sea Mount)
    (b) Near entrance to English Channel
    (c) North Pacific (South of Aleutians)
    (d) Off South Africa.

Consideration should also be given to the possible future use of smaller moored buoys intermediate in size between the NOAA and the WAVERIDER (Dutch) buoys. However, the problem of collecting and processing the data -- which has been solved by NOAA on an almost worldwide basis -- must be dealt with before making practical use of such buoys. Hence, no immediately useful results can be expected.

5. Analysis of buoy data. Statistical analysis of wave spectra should be carried out in a manner similar to that described in the survey portion of this report, i.e., stratified by wave height and analyzed to obtain mean values and standard deviations of spectral ordinates. Spectra should be used directly as a basis for checking and evaluating the regular hindcast procedures discussed under items 1 and 3.

It is recognized that although this approach may be the most practical and useful for immediate problems in ship hull design, different types of analysis in order to improve the underlying theory of wave generation, propagation and decay should also be carried out for long-range usefulness.

Data from Fixed Platforms

6. Oil company data. Companies engaged in off-shore drilling operations in various parts of the world have been vigorously collecting proprietary wave data in various formats. Efforts should be made to devise a procedure for making data for areas of interest to ship operation available generally. This should be more readily accomplished when a government is involved in the data collection (as in the case of the British Government in the areas around the British Isles).

Measurement of Directional Spectra

7. Development of techniques. Further development of methods of obtaining accurate directional spectra -- such as stereo photographic techniques -- should be pursued, since other methods (including wave buoys, item 4) are not completely satisfactory. Such accurate directional spectra would provide the ultimate basis for verifying hindcast directional spectra.

A more long-range approach is the use of airborne synthetic aperture radars (SAR), which still requires further theoretical development. This approach can potentially provide directional spectra with a very large number of degrees of freedom per frequency band.

8. Application of directional spectra. As more data in the form of directional spectra become available, both from measurement and hindcasting, research is needed on how to describe them in a generalized format for design use. After grouping the spectra by wave height, as has been done with point spectra, it is necessary to describe the variability of wave energy with direction as well as with frequency.

Improvement in Shipboard Data

9. Analysis of weather ship data. All wave data currently being collected by the various weather ships should be regularly analyzed on a continuing basis, in a manner similar to the data from Stations I, K and P, in parallel with wave buoy and FNWC hindcasting data collection and analysis.

10. Analysis of observational wave height information. Data accumulated from ships should be analyzed for several major routes across the Atlantic and the Pacific based on the 6-hourly reports obtained by NOAA, as a means of up-dating and improving available studies. At least 2 - 3 years of past data should be included and the work should continue on a routine basis (as is now being done for coastal wave data).

Up-dating and extension of wave atlas publication should be encouraged, as for example the extension of Hogben and Lumb (1967) to the North Pacific.

11. Development of disposable buoy. Effort should be continued toward the development of a small buoy which can be "shot" off the side of a ship, capable of transmitting a signal for $\frac{1}{2}$ hour when the ship is moving at 20 - 30 knots. Its accuracy need not be greater than that of existing small buoys. Although such a device might have its primary application to improving the quality of operational wave data, it would also provide data of value in ship design.

Satellite Systems

12. Continued development of satellite wave measurement. The enormous potential of satellite wave measuring systems dictates the continuation of efforts to develop a workable system for measuring wave spectra from spacecraft, since current efforts are only partially successful. See Pierson (1976).

Priorities

The above plan covers a large number of areas for further work, with varying time frames and cost factors. The following paragraphs attempt to assign priorities to the various areas of effort on the basis of obtaining the most useful information at the least cost in the least time.

It is believed that the _first_ priority should be given to a direct effort to obtain wave spectra for the ocean areas on important sea routes that are known to experience severe sea conditions. The most immediately available method is the use of moored buoys, as outlined in item 4.

Of almost equal importance is believed to the further verification and improvement of wave hindcast techniques, item 1, in order to prepare the way for eventual application of this approach to obtaining wave spectra for design.

At the same time, steps should be initiated that may lead to the availability of wave data in the future, as seeking oil company data, item 6.

Second priority should be given to further analysis of available data, items 9 and 10, and of new data produced by buoy deployment and hindcast procedures, items 2 and 5.

Attention should also be given to the measurement of directional spectra and their application to design, items 7 and 8.

Third priority should be given to the extension of hindcast techniques to the southern hemisphere, item 3, and to the development of new techniques for wave data collection, disposable buoys and satellite systems, items 11 and 12.

Included in this category should also be certain long-term aspects of the various research items, such as:

- New hindcast procedures (item 1)
- Development and use of small wave buoys (item 4)
- Development of airborne synthetic aperture radar (item 7).

III. OBSERVED WAVE DATA

Shipboard Operations

Continuous information has been gathered on observed wave heights and directions for approximately the last 100 years, and on wave periods for the last 25. This information comes from weather ships, voluntary observing ships and on a more limited basis from research ships, light vessels, fishery protection vessels, etc. Since the largest number of the observations comes from voluntary observing ships such as merchant ships, there is extensive coverage of shipping routes.

Wave observation statistics are a collection of subjective judgments made by many different observers. The accuracy of the observations of course varies greatly from observer to observer. The reporting code used from 1949 to 1968 had discontinuities at 5 meters and 10 meters, e.g., 8 = 4m., 9 = 4.5m., 10 = 5.0m., and a similar change at 10 m. This led to bias in favor of 4.5 m. and 9.5m. There is also a preference for whole meter wave heights in the higher ranges. The newer code reduces these biases.

Three other factors also tend to bias observational data:

1. Fair weather bias occurs because ships in passage tend to avoid bad weather, resulting in lower average winds.

2. Observers frequently fail to code wave observations if wave conditions are calm; this reduces the percentage of <u>reported</u> fair weather conditions.

3. Observers tend to underestimate following seas and overestimate head seas because of the difference in ship behavior.

Since it is impossible to quantify these factors, there is no way to correct systematically for the biases they induce.

Verploegh (1961) estimates the standard error based on comparison between ships as follows:

Wave direction	10°-13°
Wave period	1.8 seconds
Wave height	0.3 m. at 1.5 m. (1 ft. at 5 ft.)
	1.0 m. at 6 m. (3 ft. at 20 ft.)

In most cases, observations have been found to yield an adequate approximation in the range of practical interest, 5 to 30 feet (2 to 10 meters), which represents over 95% of the expected frequency of occurrence. For values above 30 feet (10 meters) or below 5 feet (2 meters) the observers' ability to estimate adequately is doubtful, in the former case due to the conditions on board ship and in the latter case due to cross seas, swell, etc.

In view of the large amount of observed data available and the uncertainty of its reliability, it is not surprising that a number of comparisons have been made between visual and measured wave estimates. Fig. 1 from Hoffman (1974) shows significant wave height versus observed wave height. It should be noted that all the observations included in Hoffman's data were made by trained observers on ocean weather ships. Hoffman's data also include more cases of severe weather since weather ships must remain on station and are not free to avoid storms. It may be seen that below 30 ft. observers tend to underestimate the wave heights. A reasonably good linear fit over the entire range is shown to be,

$$H_{1/3} = 7.0 + 0.775 \ H_v.$$

Table 1 from Hogben (1970) summarizes the results of several investigations of correlations between observed and measured wave heights (maxima in individual records). The measurements were made with Tucker wave recorders, with appropriate frequency dependent corrections included. The observations were made by officers aboard merchant ships, rather than by professional weather ship observers. The table gives the coefficients A and B which gave the best linear fit to the data points, when plotted in a manner similar to Fig. 1, and the coefficient C which gave the best fit for a line passing through the origin.

Also shown in Table 1 are the standard deviation, σ, of the data points about the lines and the correlation coefficient, ρ. The latter is defined as follows:

$$\rho = \frac{\overline{H_m \cdot H_v} - \overline{H_m} \cdot \overline{H_v}}{\sigma_{H_m} \cdot \sigma_{H_v}}$$

where the lines over letters indicate averages.

It may be seen that the first three sets of data show very similar straight line fits. Where correlation coefficients are available, they show good agreement between observations and measurement.

The material factors used to relate observations to measurements can only be expected to yield good results when applied to data of the same nature as that from which they were derived. This presents a difficulty in that whenever comparisons are made between observed and measured values the observer on board a weather ship is a trained observer, whereas the largest number of observers are not. It is likely, however, that various types of observers will agree most closely in the range of 5 to 30 feet (2 to 10 meters), as previously noted.

The ability to estimate the significant wave height by means of observed wave height is extremely important because of the large amount of available observational data. It is apparent that the several different realtionships in Table 1 show very slight differences.

In the case of wave direction it is difficult to compare observation with measurement, since wave direction is not routinely measured. (The measurement of directional spectra, being a special problem, is discussed later). Direction is, however,
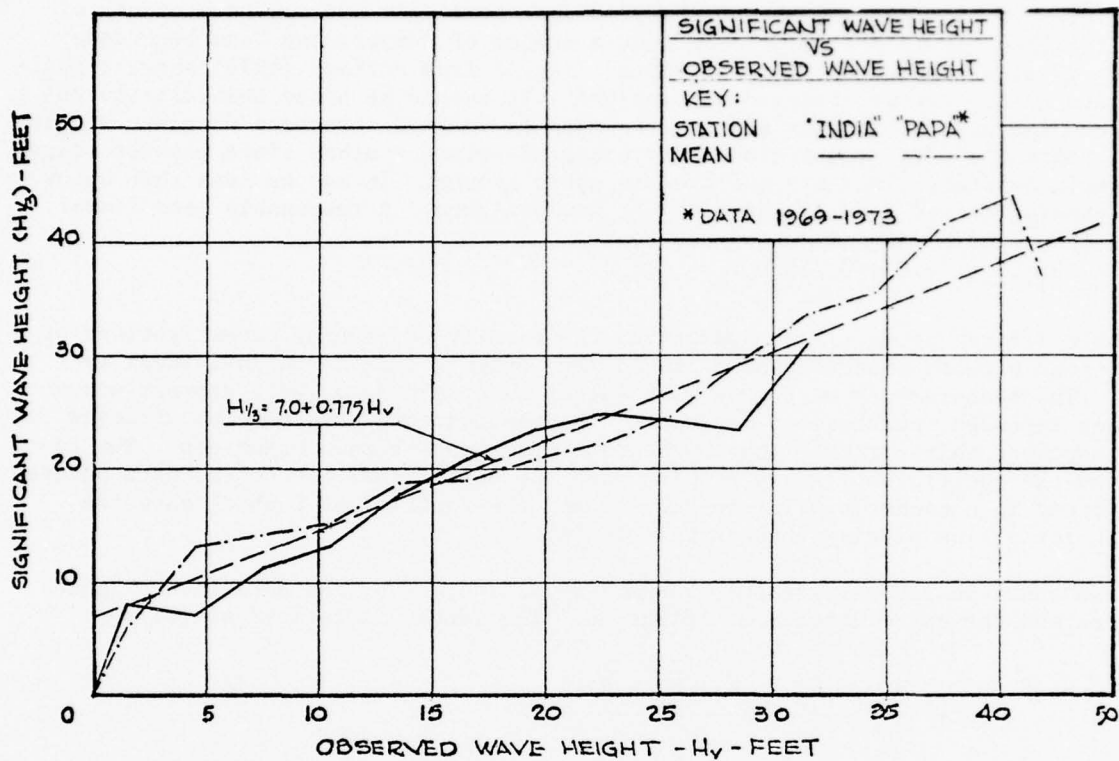
Figure 1. Significant and Observed Wave Height Relationships.

Table I
Correlation of Measured Maximum and Observed Wave Heights
for Individual Weather Ship Records

Reference	A	B(ft.)	σ(ft.)	C	σ(ft.)	N	ρ
Hogben & Lumb (1964)	1.41	6.72	4.59	1.89	5.41	905	
Hogben & Lumb (1967)	1.41	6.46	4.17	1.70	4.43	317	0.86
Hogben (1970)	0.83	6.26	3.25	1.42	5.03	527	0.73

A, B, and C are coefficients found using linear regression.

$$H_m = A H_v + B \qquad \text{(best straight line)}$$

$$H_m = C H_v \qquad \text{(best straight line through the origin)}$$

where H_m is measured maximum, except in Hogben (1970) where it is derived from $H_m = 1.6 H_{1/3}$.

H_v is observed wave height.

σ standard deviation.

N number of comparisons.

ρ correlation coefficient.

the easiest observation to make visually. It is usually apparent when one is sighting along a crest line 90° to the direction of the waves. This shows up in the smaller percentage error in direction found in comparisons between ships. However, when the sea is reported as a combination of sea and swell the direction definition becomes a problem.

In a similar way Table 2 shows the results of several comparisons between measured and observed wave periods. As can be seen by looking at the correlation factors and standard deviations, the correlation between observed and measured periods is much less satisfactory than the correlation between observed and measured wave heights.

The poor correlation of period estimates may be at least partly due to the fact that period must be estimated by timing wave crests whereas heights can be directly observed. The combination of sea and swell, the periodic motion of the ship, and the random nature of the waves contribute to the difficulty in observing period. Hence, all tabulations of period statistics must be viewed with extreme caution.

The National Climatic Center[*] can prepare Summaries of Synoptic Meteorological Observations (SSMO) based on a world-wide collection of observations from 1964 to present. SSMOs can be prepared for individual $1° \times 1°$ squares or for any desired marine area so long as the boundaries are specified. The approximate number of recorded observations within an area of interest can be furnished when desired. It can then be decided if the area contains an adequate number of observations. Cost/time estimates can be obtained from NCC.

The Naval Weather Service Command in 1969 began funding a continuing program at the National Climatic Center to publish complete SSMOs for selected ocean areas. Copies of these publications are available. Each volume contains a complete set of tables for two or more ocean areas. Information concerning the geographical boundaries of areas for which summaries have been prepared and/or published is given in Appendix B. They are at present limited to coastal areas and the Great Lakes.

Tables 18 and 19 in the SSMOs are the only ones including information on waves. (See example in Appendix C.) Other tables contain information on wind conditions, etc. SSMOs include both monthly tabulations and annual summaries.

Collections of Observed Data

The World Meteorological Organization (WMO) has designated specific areas to various national organizations who have collected the observed data on wave height, period and direction and coded them onto punched cards. Fig. 2 shows the areas of responsibility. Appendix A describes the extent and availability of these coded data. This coded information, along with monthly climatological summaries which include wind and wave information, is also available through the WMO. This type of information has been available for many years and considerable use of it has been made.

Of greater immediate usefulness are published compilations of wave data. The following four figures show the results of several compilations of wave statistics.

---

[*] NCC, Federal Building, Asheville, North Carolina, 28801 (704) 254-0961.

Table II

Correlation of Measured and Observed Wave Period

Reference	Symbol for Meas. Per.	A	B(sec)	σ(sec)	C	σ(sec)	N	ρ
Hogben & Lumb (1964)	T_c	0.37	5.19	1.12	0.86	1.41	834	0.48
Hogben & Lumb (1967)	T_s	0.32	4.70	0.88	0.73	1.20	294	0.50
	T_o	0.76	4.10	2.15	1.12	2.23	294	0.50
Hogben (1970)	T_z	---	----	----	1.37	2.71	467	0.04

In addition to the notation used in Table 1:

T_c = crest-to-crest period from record.

$T_s = \sqrt{\dfrac{m_o}{m_2}}$ where m_o and m_2 are the zeroth and second moments of the spectra.

T_o = modal period, period corresponding to the peak of the spectrum.

T_z = zero crossing period.
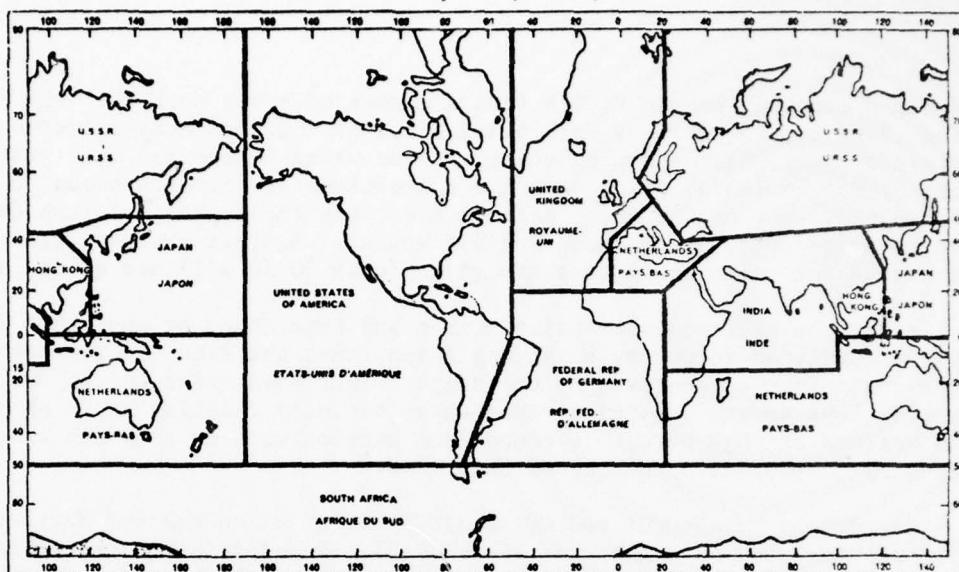
The addresses of the nine responsible WMO Members:

1. Germany, Federal Republic of
   Director
   Deutscher Wetterdienst
   Seewetteramt
   Bernhard Nocht Strasse 76
   2 Hamburg 4

2. Hong Kong
   Director
   Royal Observatory
   Nathan Road, Kowloon

3. India
   Director General
   Observatories
   Lodi Road, New Delhi 3

4. Japan
   Director General
   Japan Meteorological Agency
   Ote-machi
   Chiyoda-ku, Tokyo

5. Netherlands
   Director-in-Chief
   Koninklijk Nederlands
   Meteorologisch Instituut
   Utrechtseweg 297, De Bilt

6. South Africa
   Director
   Weather Bureau
   Private Bag 97, Pretoria

7. USA
   Director
   National Climatic Center
   Federal Building
   Asheville, North Carolina   28801

8. UK
   Director-General
   Meteorological Office
   Met 0 12, London Road
   Bracknell, Berkshire   RG 12 2SZ

9. USSR
   Institute of Aeroclimatology
   Molodezhnaya 3
   Moscow, B-296

Figure 2. Areas of Coverage of Responsible WMO Members.

Appendix C contains sample tables from a number of these sources. The first source listed (Fig. 3), the work by Hogben and Lumb, is the most comprehensive. It includes coverage of most major shipping routes. When using Hogben and Lumb statistics, the report by Hogben (1974) which contains corrections to the directional classes, should be consulted. One of the great deficiencies with the Hogben and Lumb data is that there is no coverage of Northern Pacific routes. Another shortcoming is that the area blocks for which statistics are given (only 50 in all) are quite large.

It must be realized when using Hogben and Lumb data, or any other statistics based primarily on voluntary observing ships, that the data are representative only of the conditions encountered by the ships. This means that on the average the data represent less severe conditions than those actually existing since ships try to avoid regions of high waves. A comparison between weather ship and transient ship records by Quayle (1974) describes this bias.

The work by Yamanouchi and Ogawa (1970) (Fig. 4) covers the Northern Pacific region not included in Hogben and Lumb (1967), In addition to the tables in this work which give the same information as in Hogben and Lumb, there are roses and histograms which make it easy to see the relations among conditions in different areas and at different times. It should be noted that the tables in this publication include all waves higher than 7.7m (25.6 ft.) in one group. This lack of definition in the probability of occurrence of the large waves makes these data inadequate for accurately predicting long-term ship loads.

Fig. 5 indicates that the U.S. Naval Oceanographic publication (1963) which covers the North Atlantic does not give as much information as Hogben and Lumb in that numbers of observations are not tabulated and thus percentage occurrences of large wave heights cannot be obtained to an accuracy of greater than 1%. But it does give information for much smaller areas (5° squares). This type of subdivision may be needed for some purposes.

Fig. 6 shows that information on observations in the norther North Atlantic, a region not covered in Hogben and Lumb, is available in Ewing and Hogben (1966). Appendix C contains sample tables from all these various collections of wave observations.

The 1964 ISSC Committee 1 report (ISSC 1964) includes statistical data for ship route areas. The wave height bands used were so broad, however, that the data are of limited usefulness.

Unusual Conditions

Bad weather areas and seasons are indicated by reference letters in the world map, Fig. 7. Table 3 lists special hazards which are also indicated on the map. The table also indicates the cause or tentative explanation of the hazard. In the cases where currents are listed they may be important not only in themselves but for their effect on waves. Fig. 8 indicates the effect a current can have on waves.

This current effect is thought to be a factor off the Southeast Coast of South
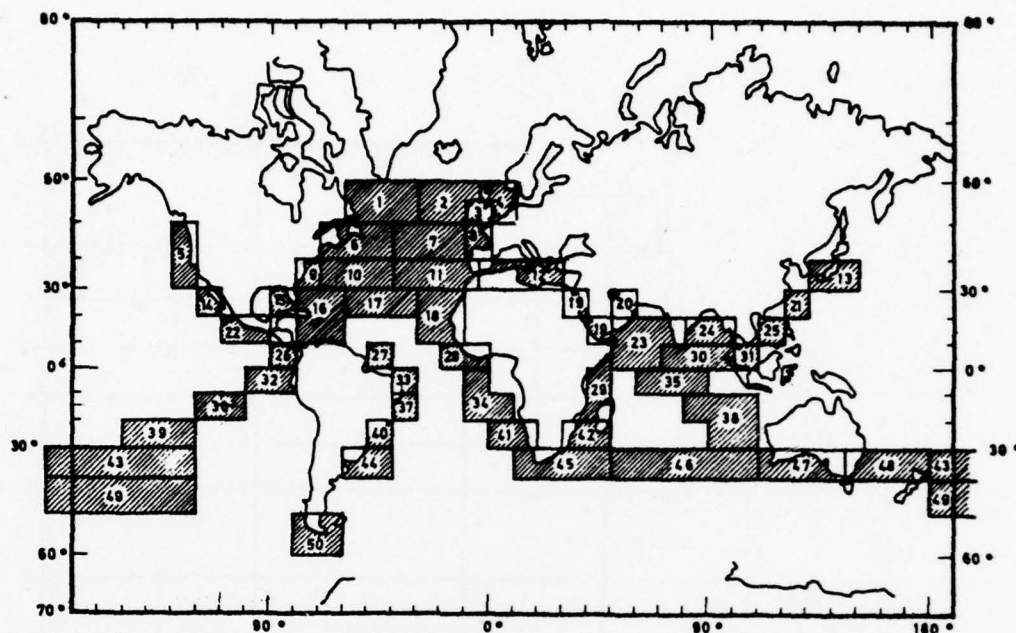
Notes

For each of 50 areas and each of four seasons (plus the whole year), the following information is presented:

Tables for each of 12 direction classes (plus all directions combined) showing numbers of observations in cells corresponding to every combination of wave height and period code number (i.e., height intervals in 1/2 meters and period intervals of 2 seconds) for which observations have been reported.

About a million observations reported in the years 1953 to 1961 are covered.

Figure 3   Worldwide Wave Data (except North Pacific)
          Source: Hogben and Lumb (1967)
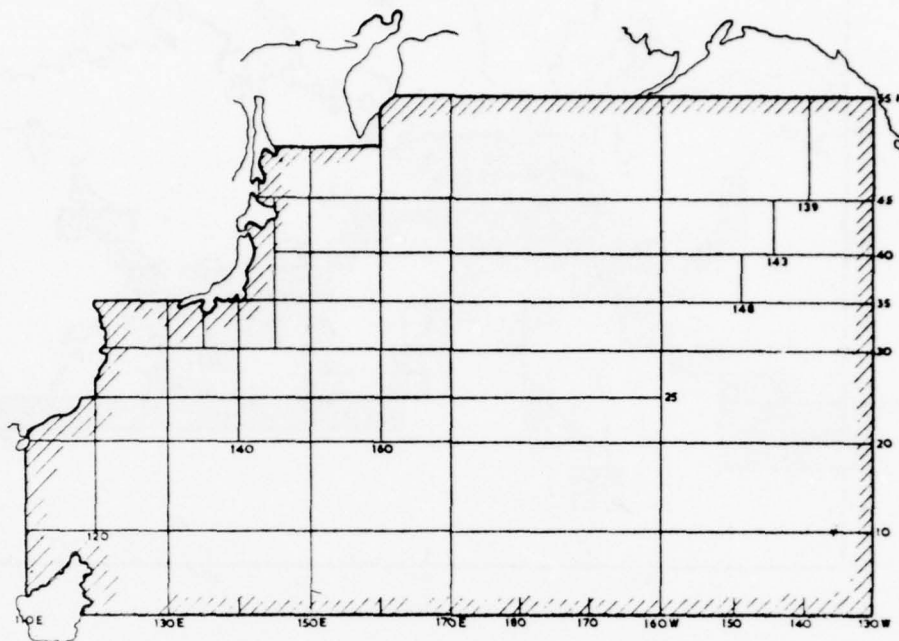
Notes

For each of 54 zones (as defined by the grid lines shown in the map above) and each of 12 months (plus the whole year), the following information is presented:

(i)   Wind velocity rose with 12 direction classes
        Wave height rose with 12 direction classes
        Wave period rose with 12 direction classes

(ii)   Mean of wind speed, percentage of gale force (34 knots and above)
        Mean of wave height
        Mean of wave period

(iii)   Histogram of wave height
        Histogram of wave period
        Histogram of wave speed

(iv)   Tables of percentage frequency of ocurrence for wave height vs. wave
            period

About 1,500,000 observations reported in the years 1954-1963 are covered.

Figure 4   North Pacific Wave Data
            Source: Yamanouchi (1970)
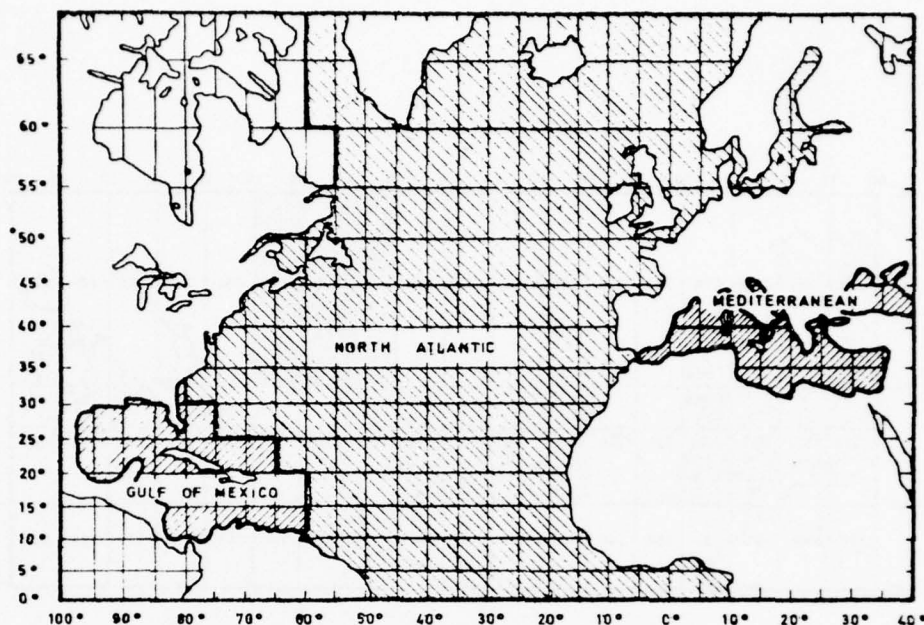
Notes

For each of 3 main areas, No. Atlantic, Mediterranean and Gulf of Mexico (sub-divided into alternate 5° squares), and each month, the following information is presented:

(i) Wind roses with 8 direction classes

(ii) State of Sea:
Roses with 8 direction classes
Isolines of frequency of exceeding various wave heights
Predominant sea direction

(iii) Swell:
Same as for state of sea

(iv) Persistence diagrams of wave height
At weather stations by seasons not months

(v) Cumulative cross frequencies of wave height, period, and direction
By seasons not months

The information is presented graphically in the form of graphs and roses rather than in tables of numbers of observations. The graphs and plots cannot be read to an accuracy greater than 1%

The alternate 5% squares summarize about 600,000 observations.

Figure 5   North Atlantic Wave Data
Source: Naval Oceanographic Office (1963)
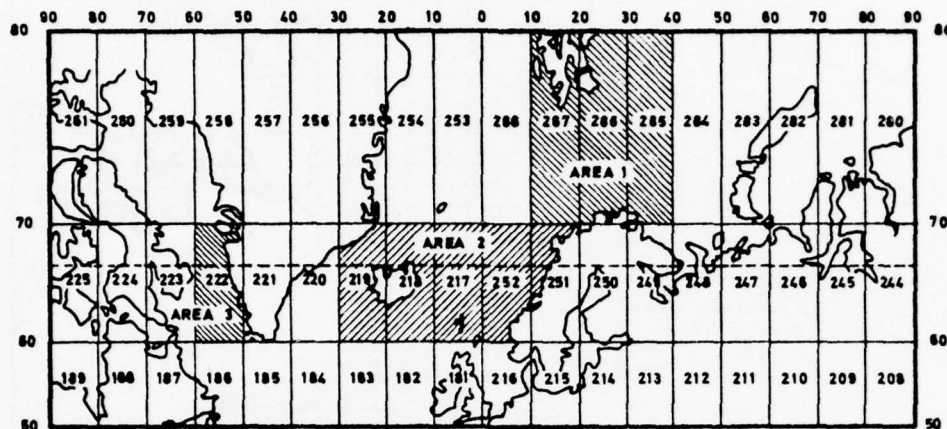
Notes

For each of 3 areas and 2 seasons, the following information is presented:

(i)   Cumulative frequency curves of wave height and period and rosettes of
        Beaufort wind force with 8 direction classes.

(ii)   Tables giving numbers of observations for
         Wave height vs. wave period
         Wind direction vs. wind force
         Wave height vs. wind force
         Wave length vs. wave period

About 4,000 observations reported in the years 1953-1965 are covered.

Figure 6   Extreme North Atlantic Wave Data
             Source: Ewing and Hogben (1966)
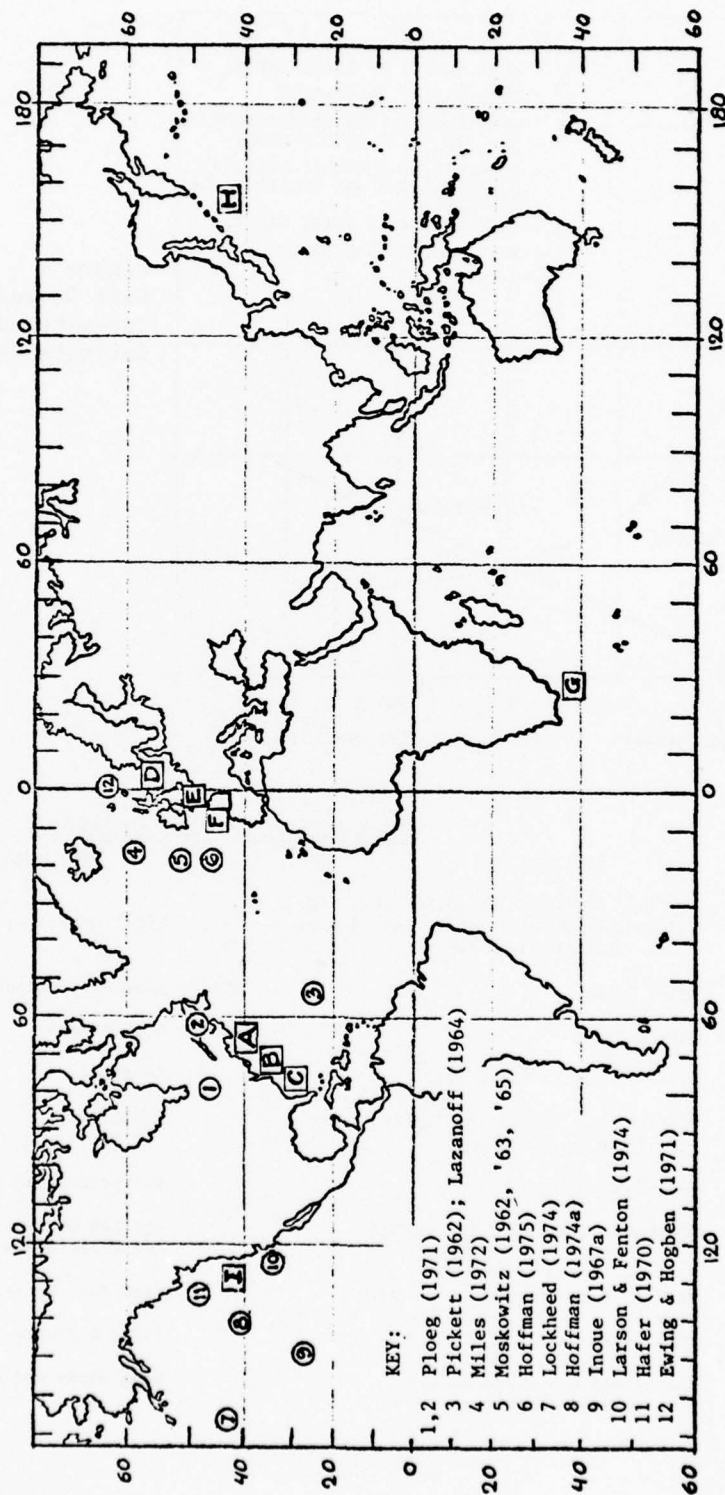
Fig. 7 - Areas with Special Hazards (Indicated by Letters -- see Table III) and Locations of Measured Spectra (Indicated by Numbers -- Sey Key)

KEY:

1,2 Ploeg (1971)
3 Pickett (1962); Lazanoff (1964)
4 Miles (1972)
5 Moskowitz (1962, '63, '65)
6 Hoffman (1975)
7 Lockheed (1974)
8 Hoffman (1974a)
9 Inoue (1967a)
10 Larson & Fenton (1974)
11 Hafer (1970)
12 Ewing & Hogben (1971)

H_O — WAVE HEIGHT IN STILL WATER
H_C — WAVE HEIGHT IN CURRENT
C_O — WAVE VELOCITY IN STILL WATER $C_O = 3T$ (T = WAVE PERIOD)
U — VELOCITY OF CURRENT, POSITIVE FOR FOLLOWING AND NEGATIVE FOR OPPOSING
L_O — WAVE LENGTH IN STILL WATER
L_C — WAVE LENGTH IN CURRENT

Figure 8 – Change in Wave Dimensions for Opposing and Following Currents (Wiegel, 1964)

TABLE III – SPECIAL HAZARDS

Location	Nature of Hazard
A[*] Entrance Nantucket Sound (Pollack Rip), Nantucket Shoals (Rips), tip of Cape Cod (Race Point), Bay of Fundy	Tidal currents, shoaling
B Grand Banks	Labrador Current, shoaling
C Cape Hatteras	Gulf Stream
D Eastern side of North Sea	Shoaling
E Western part of English Channel (continental shelf)	Shoaling
F Bay of Biscay	Reflection and refraction
G Southeast Coast of South Africa	Agulhas Current and swell from Antarctic Ocean
H Pacific Ocean Northeast of Japan	Kuro Shio Current
I Seymour Narrows, BC	Tidal currents
Hurricanes and Typhoons in various locations	High winds and waves

---

[*] letters refer to locations shown in Figure 7.

-20-

Africa. Large waves can occur there when an area of low pressure moving to the
east-northeastward produces a strong southwesterly wind blowing against the flow of
the Agulhas Current. This combination of conditions has produced waves of 7 to 8 m
(23 to 26 ft.) with a period of about 10 seconds and length 60-90 m (200 to 700 ft.)
moving to the northeast. There may also be wave trains emanating from severe Ant-
arctic storm centers further south having periods greater than 14-15 sec. These
long swells, or "Cape rollers" may in themselves be a hazard for large super tankers.
But when these swells move in the same direction as the storm seas (Quayle, 1974 a)
and the crests of the two wave trains coincide, a "freak wave" of 20 m (66 ft.) in
height may result. The lifetime of such a wave is short, and it will only extend
over a limited distance.

IV. MEASURED WAVE DATA

Sources of Wave Measurements

The measured data are limited in quantity and location compared with the vast systematic accumulations of visual observations. The need for measured data has, however, been fully established and collection programs are expanding.

The number of wave measuring instruments that have been used in limited quantity is quite large. Although most have served a useful scientific purpose, few have been widely used for long periods. The Tucker recorder (SBWR) is the most successful shipborne instrument, and has been used on weather ships for generating large quantities of measured data for the North Atlantic, and lesser amounts for the North Pacific and elsewhere. It is somewhat restricted by the requirement that the ship be hove to. (A number of measurements have been made using the Tucker recorder on ships at speed, but the validity of these measurements is in doubt, as discussed later). The reliability of the Tucker recorder is critically dependent on the application of a frequency dependent calibration correction which depends on the size and characteristics of the vessel on which the recorder is mounted.

The British National Institution of Oceanography (NIO) has used ocean weather ships (OWS) equipped with Tucker wave recorders to record long series wave records. The equipment is built into the ships. Other ships have also been equipped with NIO Tucker recorders, including several American flag merchant ships. However, the latter results obtained are inadequate because of the forward speed of the ship, Webb (1974), Wheaton (1975). Appendix F describes the extent of the data accumulated using these instruments.

In locations where fixed towers are available, such as in the Gulf of Mexico, a resistance wire wave meter -- such as the Baylor gage -- is useful as a simple yet accurate measuring instrument. The Vibratron, a low-noise transducer used to measure pressure variations, has been used to measure wave heights from the bottom, and from the top of the Cobb Sea Mount off the West coast of Canada. It has also been used in combination with an accelerometer on floating drilling platforms.

Recently, the NOAA Data Buoy Office (NDBO) has used accelerometers mounted in 40-feet diameter buoys to make measurements. The results thus far have been good and their program is expanding. The Waverider buoy, a 1-meter sphere with accelerometer, designed and manufactured in the Netherlands, has been used to measure lake and coastal wave elevations. It has been used in open ocean locations in conjunction with specific ship test and measuring projects, but has not been used routinely to obtain open ocean spectra. Buoys in the intermediate size range are being developed by oil companies for use in obtaining wave data for use in drilling platform design and operation; most of this information is proprietary.

Data from other wave measuring systems, such as wave towers and pressure transducers in shallow water, the pitch/roll buoy, the clover leaf buoy, aerial photography, imaging radars, airborne laser altimeters, over-the-horizon high-frequency radio waves, and a nanosecond airborne radar, have yet to be used extensively for naval architectural purposes.

-22-

The four instruments for measuring waves and providing data of importance to naval architecture in deep water or on the continental shelf are the Tucker Shipborne Wave Recorder, the NOAA Data Buoy Office Discus Buoy, the Baylor Gauge and the Waverider Buoy. See Appendix D for a full description of these instruments.

Reliability of Wave Measuring Techniques

Of the four important instruments mentioned in the preceding section, all but the Baylor Gauge, the instrument used on oil platforms, measure an acceleration and convert the data during processing to an elevation spectrum by means of either a double integration in the time domain or its equivalent in frequency space. Those that measure acceleration attempt to correct for ship or buoy response to the high frequencies in one way or another.

Each of the systems using an accelerometer measures something slightly different. The ship with the SBWR does not follow the orbital motion of the shorter waves. The Discus buoy of NDBO probably follows the orbital motions of the larger waves. The Waverider buoy being small is almost equivalent to a freely floating particle of water on the free surface.

In addition, each of the systems has the equivalent of some kind of a band-pass filter acting on what would have been a "pure" record of acceleration. This filter is a function of the dimensions and response of the platform and of the range of the accelerations sensed by the recorder. The low-pass filter, defined as a function of frequency, say, $F(\omega)$, operates on the true elevation spectrum $S(\omega)$ to produce,

$$S^*(\omega) = F(\omega) \, S(\omega)$$

The low-frequency range of the band-pass filter, say $\omega = 0$ through $\omega = 2\pi/25$, presents particular problems, at least with the SBWR and perhaps with the other two. Fortunately, the long waves with frequencies this low (lengths greater than 3000 ft.) seldom need to be considered for practical purposes. However, certain aspects of non-linear wave theory suggest they may prove to have theoretical importance.

For most wave frequencies of importance to naval architecture, the filter $F(\omega)$ can be found and the output spectrum $S^*(\omega)$ can be used to calculate $S(\omega)$ as in

$$S(\omega) = S^*(\omega) \ / \ F(\omega)$$

However, as $F(\omega)$ approaches the high-frequency cut-off, there will be a range of ω where a substantial amplification of $S^*(\omega)$ is required, and when $F(\omega)$ becomes nearly zero, the procedure yields poor results.

For these reasons, the SBWR yields useful spectra only over the frequency range,

$$2\pi/25 \ < \ \omega \ < \ 2\pi/5 \ \text{or} \ 2\pi/4$$

or the wave length range,

$$100 \text{ ft.} \ < \ L \ < \ 3000 \text{ ft.}$$

-23-

An additional problem with the SBWR is that the final output is the sum of two measurements -- pressure and acceleration -- each of which ideally should have a different calibration factor.

The NDBO Discus Buoy must also have important filter effects for $\omega > 2\pi/4$. The Waverider buoy seems to be a good standard for calibration and appears to have the widest frequency range.

The Baylor wave gauge was used to measure hurricane waves in the Gulf of Mexico. It has an unknown roll-off starting at $\omega \cong 2\pi/3$, but still responds to high-frequency waves in a useful way. Additional study of the electronics in these gauges could provide further information on $F(\omega)$.

Waves shorter than 100 ft. ($\omega < 2\pi/4$) are seldom of importance to larger ships, but they are important to small craft, surface effect-ships and hydrofoils. They also contribute to problems in deck wetness and slamming. There is increasing evidence that strange things happen in the frequency range, $2\pi/4 < \omega < 2\pi$ ($5 < L < 80$ ft.) and that this range is wind-speed dependent. Growth of the spectrum with wind speed in this range adds several feet to the significant wave height. New systems and new techniques are required to measure these spectral components and new basic research programs to develop these spectral systems need to be funded.

Analysis of Records

Once a record of wave height has been obtained, it can be analyzed in several ways. The simplest is the Draper method of analysis in which the number of peaks and troughs, number of zero crossings, and highest positive and negative maxima are determined from visual examination of the record. These values are then used to determine various parameters of the record. The other method is to compute the energy spectrum by taking the Fourier transform of the auto-correlation function or by means of a Fast Fourier analysis. The parameters are then determined by the relations between the various moments of the spectrum. A detailed comparison of the results using each of these methods with the same data is given in Appendix H.

This comparison is important because analysis of all the records from the British NIO Tucker Recorders is being done solely by the Draper method. It can be concluded that the $H_{1/3}$ values derived by this method are quite good and these data should be made available.

The original problem with the energy spectrum method of analysis was the large amount of computation required to produce the spectrum from the record. This problem has been solved with the advent of the large high-speed digital computer. The remaining difficulty is that much of the data, as for example that from the Tucker wave recorder, is in the form of strip charts, which require a great deal of manual effort to read and to put into digital form. This problem is being eliminated in that most recording is now being done in a form that is directly compatible with computers.

The number of spectra available is limited but increasing. The map, Fig. 7 shows the locations where spectra have been measured, as indicated by reference num-

bers. A table giving details is given in Appendix E, with typical results from the various sources given in Appendix I.

If specific information is required about the availability of measured data for a particular coastal location, Appendix G can be consulted. It is a table compiled by PIANC (Permanent International Association of Navigation Congresses) of organizations which can provide detailed information concerning wave recording sites in their countries.

As can be seen from the study of large samples of spectra from a single location there is considerable variation in spectral shape. It is difficult to draw conclusions about "typical" or mean spectra for a location without having a large sample.

Such large samples of spectra are currently available for the following locations: weather stations I, J and K in the eastern North Atlantic; station P in the eastern North Pacific; Cobb Seamount; and the Great Lakes. NOAA Data Buoys in the Gulf of Alaska, the Gulf of Mexico and off the eastern U.S. Coast have been providing an increasing amount of data.

The number of directional spectra available is limited to a mere handful. Such spectra, which specify the energy as a function of both direction and frequency, require sophisticated measurements. The methods available to obtain directional information include arrays of wave height measuring devices, slope measuring instruments, and stereo photography. Table 4 describes the directional spectra available.

Table IV

Available Directional Spectra

	Cote, L.J., et al (1960)	Canham, H.J.S., et al (1962)	Longuet-Higgins, M.S., et al (1961)
Record Length	1300' x 2700'	12 min.	same instrument and procedure as Canham, H.J.S., et al (1962)
Sample Rate	x = 30'	.5 sec.	
Analysis Method	Correlation 20 x 40 lags	Correlation 60 lags	
Smoothing	2-dimensional Hamming	factors $\frac{1}{4}, \frac{1}{2}, \frac{1}{4}$	
Corrections	tilt of zero level	noise correction	
Units (ordinate)	ft^4	$ft^2 \cdot sec.$	
Units (abscissa)	ft^{-1} (wave number)	sec^{-1}	
Instrument	Stereo cameras	NIO pitch-roll buoy	
Time	1954	1959	1953-1956
Location	$40°N-65°W$	North Atlantic	North Atlantic
Number of Spectra	1	3	5

V. THEORETICAL SPECTRAL FORMULATIONS

Basic Formulations

The short-term description of the sea is the basic input required in order to determine the response of a vehicle in such a sea. The definition of short-term is a period of time short enough to make it possible to describe the sea as a stationary random process. The stationary property does not imply that the surface of the sea remains unchanged. On the contrary, at any given instant of time the surface pattern is unique. However, the statistical properties of the short-term sea, defined by its spectrum, may be regarded as constant over such a period of time. The significant wave height and average period alone cannot characterize the short-term sea; hence, the actual wave spectrum, describing how the components of the surface pattern are distributed over frequency, is required. When the random process is stationary the spectrum remains essentially unchanged.

Two records taken at different times having the same height and period would, of course, not in general have the same spectrum. For the spectrum to remain the same, all moments must also remain the same. The height and the period are functions of the zero and second moments of the spectrum. Characteristic periods and other parameters are functions of higher order moments, all of which will change with variations in spectral shape.

On the other hand, the first three or four moments do not exactly define the shape. It can be seen from Figures 25, 34 and 48 that wave spectra are highly irregular. While some of this irregularity in measured spectra is due to sampling variability, this does not account for it completely. This characteristic irregularity should be kept in mind whenever theoretical formulations are considered.

General Form of Theoretical Spectra

The lack of availability of measured spectra in a form suitable for application to response calculations has led to the use of mathematically formulated spectra. Although this approach has been extensively used, Pierson has cautioned that great care must be taken in choosing values of the parameters based on samples of spectra. (See Appendix J). The mathematical formulation commonly used is of the general form shown below:

$$S_\zeta (\omega) = A\omega^{-p} \exp(-B\omega^{-q}) \tag{1}$$

where $S_\zeta (\omega)$ is the variance spectrum ordinate $(ft.^2 \cdot sec)$ or $(m^2 \cdot sec)$
ω is the circular frequency $= 2\pi/T$ (sec^{-1})
A, B, p, q are the parameters of the spectrum

The various moments of the spectrum are defined as:

$$m_c = \int_0^\infty S_\zeta (\omega) \cdot \omega^c \, d\omega$$

-27-

Introducing the Gamma function, for convenience,

$$\Gamma(x) = \int_0^\infty y^{x-1} e^{-y} dy$$

and letting

$$y = B \omega^{-q} \quad \text{and}$$

$$x = \frac{p-c-1}{q}$$

the equation for the moment of order c becomes,

$$m_c = \frac{A}{q B^{\frac{p-c-1}{q}}} \Gamma\left(\frac{p-c-1}{q}\right) \qquad [2]$$

Thus,

$$m_{-1} = \frac{A}{q B^{p/q}} \Gamma\left(\frac{p}{q}\right) \qquad [3]$$

$$m_o = \frac{A}{q B^{\frac{p-1}{q}}} \Gamma\left(\frac{p-1}{q}\right) \qquad [4]$$

$$m_1 = \frac{A}{q B^{\frac{p-2}{q}}} \Gamma\left(\frac{p-2}{q}\right) \qquad [5]$$

$$m_2 = \frac{A}{q B^{\frac{p-3}{q}}} \Gamma\left(\frac{p-3}{q}\right), \text{ etc.} \qquad [6]$$

Expressions using various combinations of the moments are often used in describing spectra. For example,

significant wave height $\qquad H_{1/3} = 4\sqrt{m_o} \qquad [7]$

average mean period $\qquad T_1 = 2\pi \, m_o/m_1 \qquad [8]$

energy average period $\qquad T_{-1} = 2\pi \, m_{-1}/m_o \qquad [9]$

average zero crossing period	T_2	$=$	$2\pi \ (m_o/m_2)^{\frac{1}{2}}$	[10]
average crest-to-crest period	T_4	$=$	$2\pi \ (m_2/m_4)^{\frac{1}{2}}$	[11]
skewness	γ	$=$	$m_3/m_2^{3/2}$	[12]
broadness	ε	$=$	$\left(1 - \dfrac{m_2}{m_o m_4}\right)^{\frac{1}{2}}$	[13]
flatness	β	$=$	m_4/m_2^2	[14]

Specific Theoretical Formulations

By substituting the definition of the moments in terms of the spectral parameters, (14) and (15), into the above definitions for $H_{1/3}$ and T_1, we find:

$$T_1 = 2 \ B^{-1/q} \ \frac{\Gamma \ (\frac{p-1}{q})}{\Gamma \ (\frac{p-2}{q})}$$

and

$$H_{1/3} = 4 \ \left[\frac{A}{q \ B^{\frac{p-1}{q}}} \ \Gamma \ (\tfrac{p-1}{q}) \right]^{\frac{1}{2}}$$

Solving for A and B,

$$A = \frac{q}{16} \ \left(\frac{2\pi}{T_1}\right)^{p-1} \ \frac{[\ \Gamma \ (\frac{p-1}{q}) \ ]^{p-2}}{[\ \Gamma \ (\frac{p-2}{q}) \ ]^{p-1}} \ H_{1/3}^2$$

$$B = \left(\frac{2\pi}{T_1}\right)^q \ \left[\frac{\Gamma \ (\frac{p-1}{q})}{\Gamma \ (\frac{p-2}{q})} \right]^q$$

The form for the spectrum is now,

$$S_\zeta(\omega) = \frac{q}{16} \ \left(\frac{2\pi}{T_1}\right)^{p-1} \ \frac{[\Gamma(\frac{p-1}{q})]^{p-2}}{[\Gamma(\frac{p-2}{q})]^{p-1}} \ H_{1/3}^2 \ \omega^{-p} \ \exp\left\{ [-\left(\frac{2\pi}{T_1}\right)^q] \ \left[\frac{\Gamma(\frac{p-1}{q})}{\Gamma(\frac{p-2}{q})} \right]^q \ \omega^{-q} \right\} \qquad [15]$$

-29-

To find the frequency at which the peak of the spectrum occurs, we set the derivative with respect to ω equal to zero:

$$\frac{d}{d\omega} \, S_\zeta(\omega) \; = \; 0$$

Carrying out this differentiation, setting the result equal to zero, and calling the frequency at which the peak occurs, ω_o, we have:

$$\omega_o \; = \; (\frac{q}{p} \, B)^{1/q}$$

or

$$T_o \; = \; 2\pi \, (\frac{q}{p} \, B)^{1/q}$$

Letting p = 5 and q = 4 in [15] yields a formulation which is generally referred to as the modified Pierson-Moskowitz spectrum,

$$S_\zeta(\omega) \; = \; 0.11 \, (\frac{2\pi}{T_1})^4 \; H_{1/3}^2 \quad \omega^{-5} \quad \exp \quad [-0.44 \, \left(\frac{\omega T_1}{2\pi}\right)^{-4}]$$

This is the ISSC recommended spectral formulation, ISSC (1970). For this case,

$$T_{-1}/T_1 \; = \; 1.1114$$

$$T_2/T_1 \; = \; 0.9208$$

$$\epsilon \; = \; \text{indeterminate}$$

$$\gamma \, H_{1/3} \; = \; 6.1438$$

$$\beta \, H_{1/3} \; = \; \text{indeterminate}$$

$$\omega_o \, T_1 \; = \; 4.8492$$

-30-

It is possible to calculate ε by truncating the spectral density function at high frequencies. It has been shown in Loukakis (1970) that the spectral broadness factor for the above spectrum is given approximately by $\varepsilon = 0.59$.

If $p = 6$ and $q = 2$ in [15], the Neumann spectrum is obtained:

$$S_\zeta(\omega) = 0.39 \left(\frac{2\pi}{T_1}\right)^5 H_{1/3}^2 \, \omega^{-6} \, \exp\left[-1.767 \left(\frac{\omega T_1}{2\pi}\right)^{-2}\right]$$

For this case,

$$T_2/T_1 = 0.9217$$

$$\varepsilon = 0.816$$

$$\gamma \, H_{1/3} = 5.5279$$

$$\beta \, H_{1/3} = 14.8043$$

$$\omega_o \, T_1 = 4.8223$$

Two additional spectral formulations based on the above general formulation were presented in Mirakhin and Kholodilin (1975) and are based on measurements:

Voznesenski-Netsvetayev spectrum,

$$\frac{S(\omega)\,\bar{\omega}}{D_\zeta} = 1.97 \left(\frac{\omega}{\bar{\omega}}\right)^{-6} \exp\left[-0.53 \left(\frac{\omega}{\bar{\omega}}\right)^{-4}\right]$$

where

$$\bar{\omega} = \frac{2\pi}{T_1} = \text{mean wave frequency}$$

$$D_\zeta = m_o = \frac{H_{1/3}^2}{16} = \text{zero moment}$$

They define the spectrum peak as,

$$\left[\frac{S(\omega)\,\bar{\omega}}{D_\zeta}\right]_{max} = 2.10; \quad \frac{\omega_o}{\bar{\omega}} = 0.77$$

Krylov spectrum,

$$\frac{S(\omega)\,\bar{\omega}}{D_\zeta} = 3.12 \left(\frac{\omega}{\bar{\omega}}\right)^{-7} \exp\left[-0.79 \left(\frac{\omega}{\bar{\omega}}\right)^{-4}\right]$$

$$\left[\frac{S(\omega)\ \bar{\omega}}{D_\zeta}\right]_{max} = 2.21; \quad \frac{\omega_o}{\omega} = 0.82$$

Spectral Shape Definition

It is evident from the preceding presentation that, as long as the basic formulation given by [1] is used for the spectral representation, the only way one can control the shape of the spectrum is by assigning different values to the parameters, p and q.

In a recent study at Webb Institute, Walden and Hoffman (1975),an attempt was made to determine revised values for p and q. This was done by determining the flatness and skewness in terms of p and q from the theory and then choosing the combination of p and q which provided the best fit to measured values. The measured values were determined from the spectra available from Stations I, K and P.

It was found that p and q are quite sensitive to the skewness and flatness. This means that if skewness and flatness could be determined accurately, p and q could also be determined. Unfortunately, it also means that if there is a small uncertainty in skewness and flatness there is a large uncertainty in p and q. It was found that the differences in measured skewness and flatness values which resulted from different averaging procedures resulted in p's from 6.2 - 5.7 and q's from 5.9 - 3.9. Fig. 9 shows the skewness data from Station "Papa." The intercepts from this plot and from a similar plot of the flatness data provided the basis for the choice of p and q.

It was also found that adjusting the values of p and q in the theoretical formulation to provide better agreement between the measurement and theoretical values of the broadness and flatness factors led to greater disagreement between the values of other measured and theoretical parameters. In particular, the agreement was worse for the frequently referred to relation between ω_o and T_1.

It follows from the form of Eq. [1] that any combination of p and q predicts a relation of the form,

$$\omega_o T_1 = c$$

when c is a function of p and q. The c resulting from the revised p and q resulted in a worse fit to the measured data.

It can be seen from Fig. 10 that the actual relation is of the form

$$\omega_o^x T_1 = c$$

Figure 10 – Theoretical and Measured Relationship Between Frequency of Maximum Spectral Ordinates and Average Period (Walden and Hoffman, 1975)

KEY:
+ MEASURED VALUES
⊕ CALCULATED VALUES

$\omega_o, RAD/SEC$

$T_1, SEC.$

$\omega_o T_1 = CONST = 4.83$
$p = 5, q = 4$

$T_1 \omega_o^{0.51} = 6.0$

Figure 9 – Spectral Skewness Parameter, Y, vs. Significant Wave Height, $H_{1/3}$ (Walden and Hoffman, 1975)

ln Y

ln $H_{1/3}$

LINE OF SLOPE = -1, PASSING THROUGH DATA POINT AT MID RANGE
INTERCEPT = 1.64

LEAST SQUARES FIT TO DATA
SLOPE = -0.968
INTERCEPT = 1.56

-33-

where x is some power less than 1. This relation can never be accurately described by a spectral formulation of the form in [1].

Ferdinande, et. al. (1975) have also conducted an investigation into determining p and q. Their work was of a more limited scope and their measured values were based on a much smaller sample. They found for their limited sample that p = 4.9 and q = 3.5 provides a better fit, based on measured and theoretical T_{-1}/T_O and T_1/T_O ratios. Fig. 11 shows the data on which they based their choice of p and q.

Some recent work with spectral formulations other than [1] has also been attempted, Ewing (1974). The Joint North Sea Wave Project (JONSWAP) was initiated primarily to study the form of the source function of the energy-balance equation for the wave spectrum during conditions of wave growth. The formulation is for spectra corresponding to fetch-limited off-shore wind conditions and is a variance spectrum expressed as a function of frequency, $f = 1/T$

$$E(f) = \frac{\alpha g^2}{(2\pi)} \quad \exp\left[-\frac{5}{4}\left(\frac{f}{f_m}\right)^{-4}\right] \cdot \gamma \exp\left[-\frac{(f - f_m)^2}{2\sigma^2 f_m^2}\right] \quad [16]$$

where

$$\sigma = \begin{cases} \sigma_a & \text{for } f \le f_m \\ \sigma_b & \text{for } f > f_m \end{cases}$$

and there are five parameters, f_m, α, γ, σ_a and σ_b. As shown in Fig. 12, f_m is the frequency of the spectral peak, γ is the ratio of the maximum spectral energy to the maximum of the corresponding Pierson-Moskowitz spectrum and σ_a and σ_b are measures of the left and right-sided widths of the spectrum.

It can be seen that if the last factor in [16],

$$\gamma \exp\left[-\frac{(f - f_m)^2}{2\sigma^2 f_m^2}\right] = 1$$

the latter reduces to the same form as the basic fully-developed spectral formulations [15], with p = 5 and q = 4. The additional factor or scaling function yields a wider variety of spectral shapes than the basic formulation and consequently it makes it possible to obtain a better fit with measured spectra.

The JONSWAP spectrum has recently been presented in terms of the parameters $H_{1/3}$ and T_1, Ewing (1975); in its original form, it was based on wind speed and fetch. It is now possible to compare JONSWAP with corresponding Pierson-Moskowitz spectra as currently recommended by ISSC. Fig. 13 shows the ISSC and JONSWAP spectra for $H_{1/3}$ = 47.7 ft. and T_1 = 11.5 seconds. It can be seen that the JONSWAP spectrum is much more sharply peaked than the ISSC; there is thus less energy in the high and low-frequency regions above and below the peak. Figs. 14 - 19 show some typical comparisons between measured, ISSC and JONSWAP spectra.

-34-
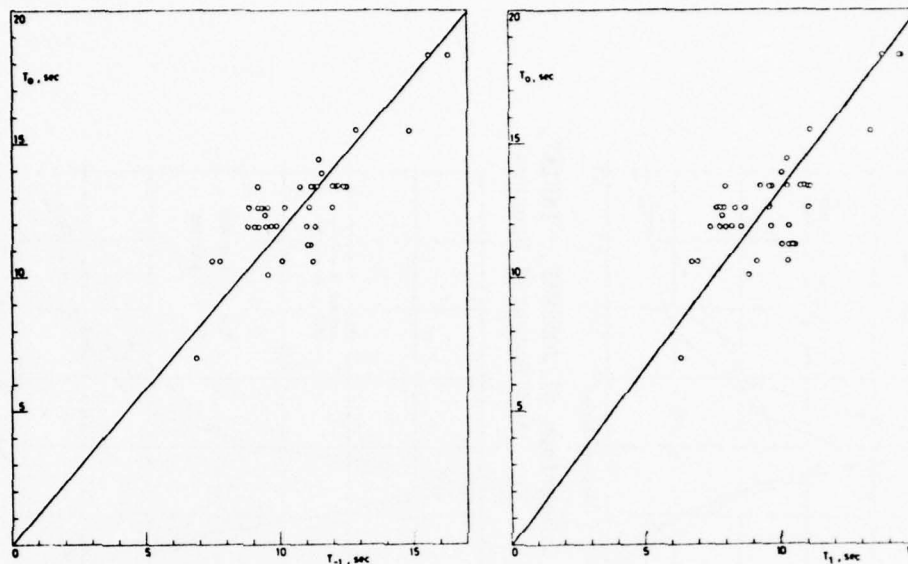
Figure 11. Relationship Between Different Period Definitions.
(Ferdinande, et. al., 1975)
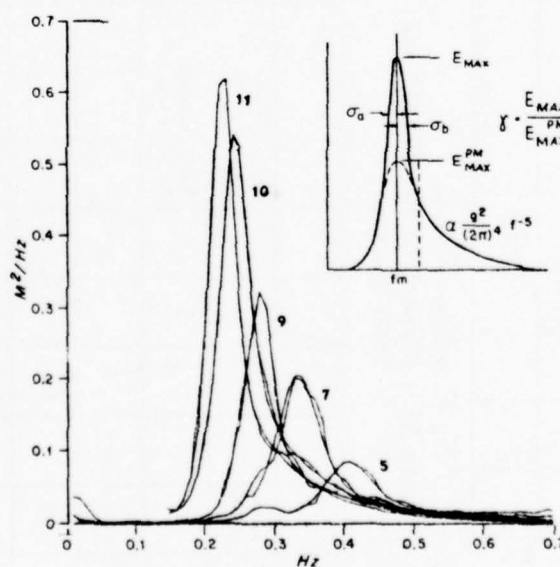
Figure 12. Typical Fit Using JONSWAP Spectral Formulation
(Ewing, 1974)

Figure 15 – Comparison of JONSWAP, "INDIA", and Measured Spectra

Figure 16 – Comparison of JONSWAP, "INDIA", and Measured Spectra
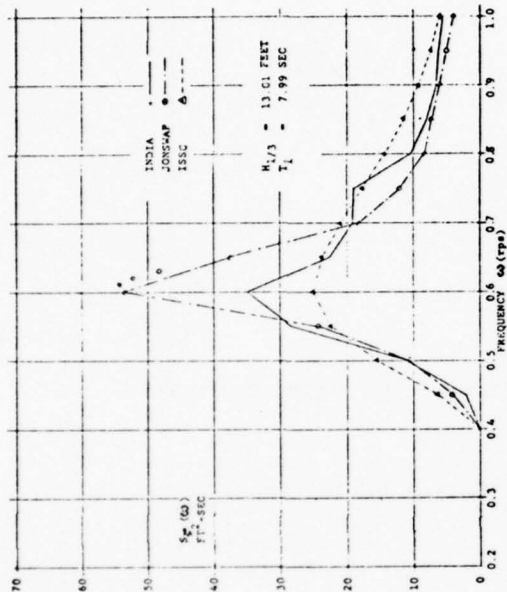
Figure 13 – Comparison of JONSWAP and ISSC Spectra
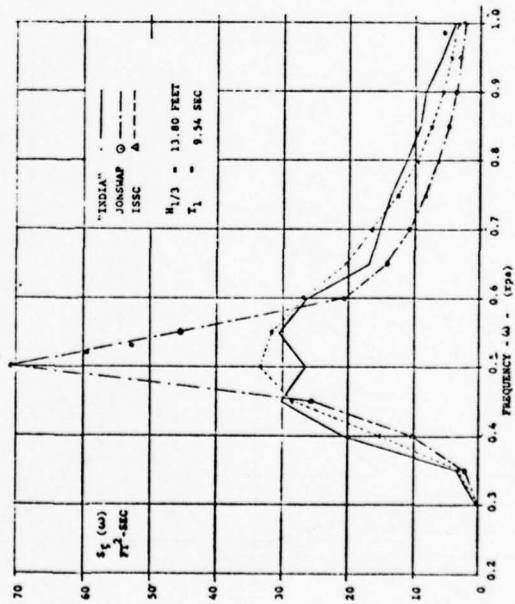
Figure 14 – Comparison of JONSWAP, "INDIA", and Measured Spectra

-36-

Figure 19 - Comparison of JONSWAP, "INDIA", and Measured Spectra

Figure 17 - Comparison of JONSWAP, "INDIA", and Measured Spectra
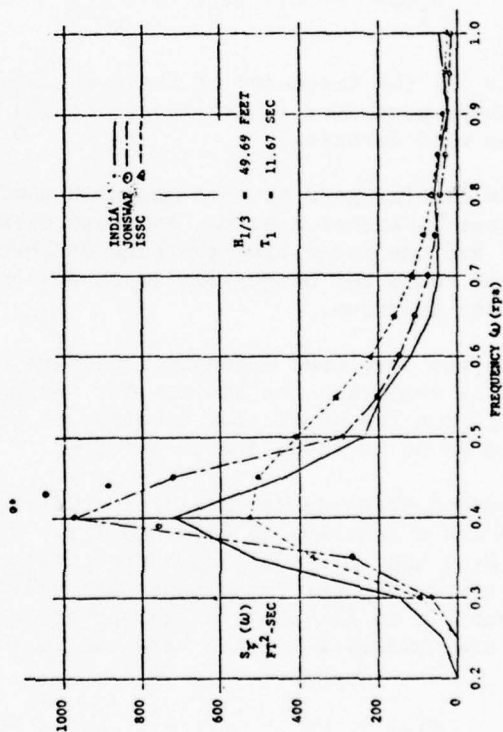
Figure 18 - Comparison of JONSWAP, "INDIA", and Measured Spectra

It is apparent that cases can be found where the JONSWAP matches best, Figs. 16 and 19, where the ISSC matches best, Figs. 14 and 17 and where neither is particularly close, Figs. 15 and 18. The lines labeled JONSWAP in the figures indicate the effective spectrum actually used in the program. The points represent the actual JONSWAP spectrum.

The JONSWAP form is of doubtful use for the open ocean because of the fetch-limited and relatively shallow water nature of the measurements on which it is based. W.J. Pierson (1975) raises serious questions about the procedures used in determining the parameters in the JONSWAP spectrum, particularly the discarding of double-peaked spectra.

Ochi (1975) has developed a three-parameter formulation of the following form,

$$S_\zeta(\omega) = c_1 \ (\omega_o, \lambda) \ \frac{H_{1/3}}{\omega^{\lambda+1}} \ e^{-c_2 \ (\omega_o, \lambda) \ \frac{1}{\omega^4}} \qquad [17]$$

where ω_o is the frequency of the peak, $H_{1/3}$ is the significant wave height and λ is a shape parameter (which he eventually hopes to relate to an observed quantity such as wind duration).

He obtains good fits to measured spectra, as shown in Fig. 20, by combining two three-parameter spectra, one describing the low-frequency region with ω_m', $H_{1/3}'$, and λ' and one describing the high-frequency region with ω_m'', $H_{1/3}''$ and λ''. He found he could not adequately represent the measured spectra with a single three-parameter spectrum.

He has developed a computer program which chooses ω_m', $H_{1/3}'$, λ', ω_m'', $H_{1/3}''$, and λ'' by computing the spectra for various combinations of these parameters and then picking the particular combination which provides the best fit in the least squares sense to the measured spectra.

Gospodnetic and Miles (1974) studies the shape of 307 spectra from Station "India" as a function of $H_{1/3}$ and T_{-1}. They non-dimensionalized $S_\zeta(\omega)$ and ω using $H_{1/3}$ and T_{-1}. They then grouped the 307 available spectra by $H_{1/3}$ and T_{-1}, using a second-order two-dimensional polynomial regression in the parameters $H_{1/3}$ and T_{-1} to fit the average spectra obtained by the grouping process. Thus, their six-parameter spectra have the form:

$$S(\omega, T, H) = A_{00} + A_{10} (H - H_0) + A_{01} (T - T_0) + A_{20} (H - H_0)^2$$
$$+ A_{11} (H - H_0) (T - T_0) + A_{02} (T - T_0)^2$$

where T and H are substituted for T_{-1} and $H_{1/3}$, respectively, and T_0 and H_0 are average values for the entire sample of spectra. The six A-parameters were plotted as functions of ω.

The difficulty is that their analysis is based on only 295 measured spectra. Thus, some of their $H_{1/3}$, T_{-1} groups have as few as five spectra. This method accurately represents the average of the $H_{1/3}$, T_{-1} groups but for 80 frequencies requires 480 coefficients, which vary in no systematic way. So theirs is essentially a 480-parameter spectrum. Fig. 21 illustrates their results.

-38-
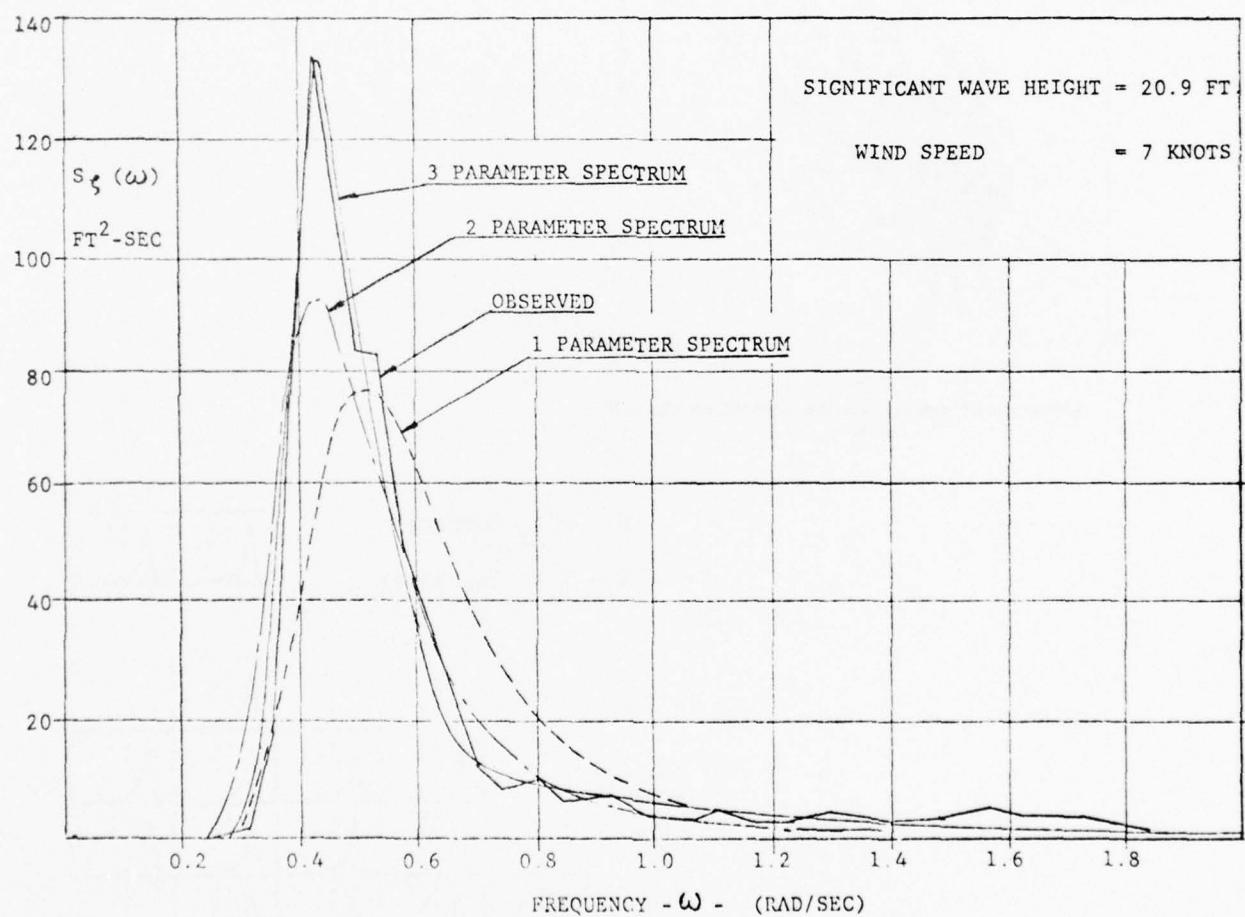
Figure 20 — Typical Fit Using Ochi's Three-Parameter, Two-Stage Spectra
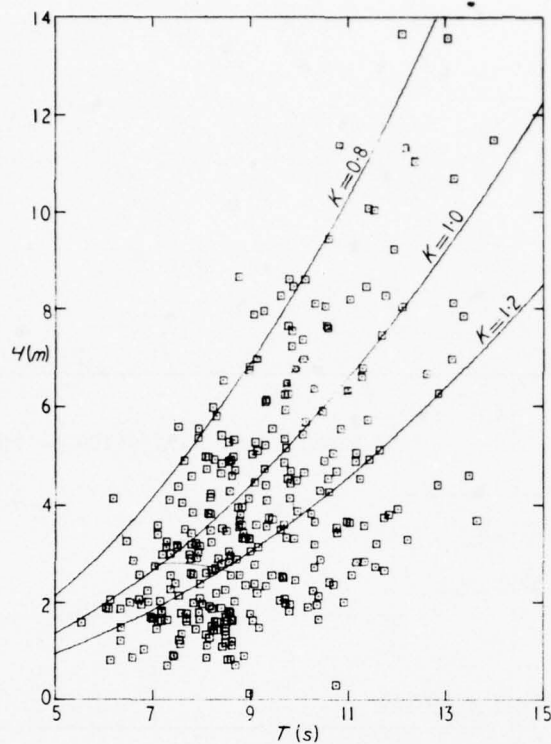
Locations of measured wave spectra on the T, H plane.

$H - H_{1/3}$ (meters)

$T - T_1$ (seconds)
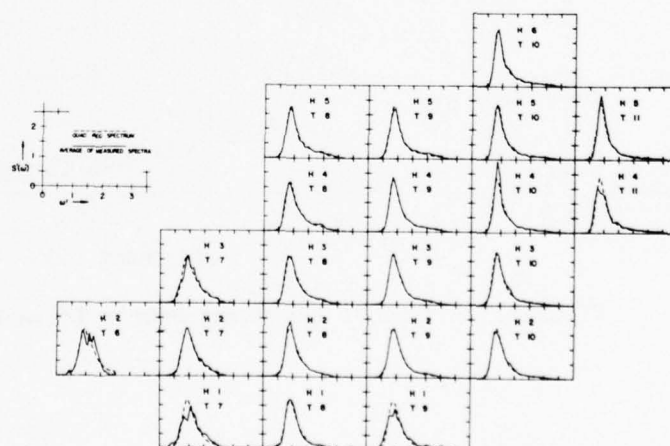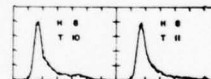
Figure 21. Comparison of Quadratic Regression Spectrum and Averages of Measured Spectra. (Gospodnetic and Miles, 1974)

In all the above examples, Ewing (1974), Ochi (1975) and Gospodnetic and Miles (1974), the spectral formulation was obtained through curve-fitting of many wave spectral estimates obtained from wave records, and the additional parameters controlling the shape were not related to physical conditions. Hence, the ability to generalize is rather limited in all the above three cases. Another possible way of generalizing such data is through the classification of spectra, as discussed in the following section.

In Appendix J, Pierson discusses the entire process of parameterization of spectra. He concludes that often too little thought is given to what the parameterized spectra are supposed to represent. He suggests that the sample be stratified to the greatest extent possible. These considerations will become increasingly important as more measured or accurately hindcast spectra become available.

VI.   WAVE DATA FROM HINDCAST MODELS

Introduction

As noted elsewhere in this report, the quantity of measured wave data remains very limited compared to visual estimates, despite the continued development of new techniques to measure waves and the rather intense activities being undertaken to test and implement the new techniques in the field. Measurement programs are expanding rapidly, most notably the NOAA data buoy program and the various special measurement programs sponsored by the oil industry in the Gulf of Mexico, the Gulf of Alaska and the North Sea. Nevertheless, these measurements are limited to the continental shelf zone. Spacecraft measurement systems may be able to provide wave measurements on a global scale within the next decade. The concept is being tested currently on GEOS-C and will again be used on SEASAT A in 1978. Until global-scale measurements become available, wave spectra calculated by means of hindcast procedures using wave generation and propagation models may be the only recourse for general climatological wave studies. This section therefore reviews the available sources of hindcast data, outlines the models used to generate the data and describes the sources of hindcast data that may become available soon on the basis of current and planned wave hindcast programs.

Hindcast wave data have been generated within the context of three basic activities:

1. Case studies associated with wave prediction model development. These data are usually limited in area coverage and in time to match an available wave measurement data set and are available usually only in the specific form analyzed and published for the purpose of model validation.

2. Climatological studies. In this activity a wave prediction model is used to compute a long history of wave data from which a wave climatology may be developed.

3. Operational models. When a wave prediction model is used in an operational hindcast/forecast cycle, two types of spectra are regularly produced:
   - Forecast spectra based on forecast wind fields, and
   - Hindcast spectra based on observed wind fields (which constitute the initial conditions for the next forecast).

Prior to the introduction of digital computers to wave hindcast studies, the quantity of wave hindcast data was very limited and consisted mainly of significant wave height hindcast data calculated by means of wave models. These early models will be reviewed here briefly, but the emphasis will be on spectral wave hindcast data, as they are potentially the most useful data, and current and planned wave hindcast programs will employ the spectral approach to wave prediction almost exclusively.

-42-

Significant Wave Hindcast Models

Most significant wave prediction methods are derived from the original work of Sverdrup-Munk (1947). The empirical relationships between the wind, its fetch and duration and the significant wave characteristics have been revised several times (e.g., Bretschneider, 1952 and 1958, U.S. Army CERC, 1966). Prior to the mid 1960's the methods were applied manually to subjectively analyzed wind fields to produce operational wave forecasts for marine forecast services. Hindcast data prior to this period were limited to specific locations and storms. Walden (1957), for example, evaluated several methods by comparing their hindcasts of swell observed off the coast of Angola in January 1955. As another example, Bretschneider (1963) applied the method to the hindcast of significant wave conditions at Station J for the December 1959 storm. The hindcast data generated in this type of case study are not very reliable because of the very subjective nature of the application of the method, are not very extensive and are intrinsically not very useful since they closely overlap measured wave data.

Hindcast Data Produced by the FNWC Significant Wave Forecast Model. The implementation of the significant wave method in an objective computerized wave forecast program was first accomplished at the U.S. Navy Fleet Numerical Weather Central (FNWC), as reported by Hubert (1964). The method is an adaptation of the Sverdrup-Munk-Bretschneider system and was the operational wave forecast model of FNWC until December 1974 when it was replaced by a spectral model, as described below. That FNWC model routinely produced a daily wave analysis that was achieved and today provides the largest existing hindcast data base of the significant wave variety. Specifically, the hindcast wave data are available on the North Atlantic and North Pacific portions of the JNWP grid system (Fig. 22) in the form of combined sea-swell heights (the square root of the sum of the squares of the sea and swell heights) and the average period and direction of the sea and swell. The data are available twice daily (00GMT and 12GMT) between 1964 and 1970 and 4 times daily from 1970 - 1974. To produce an enhanced wave hindcast data set, FNWC has extended the hindcasts back to 1946 on a once-a-day basis. The data are stored on computer-compatible magnetic tape.

The FNWC significant wave hindcast data set is not homogeneous in that the procedures for the specification of the meteorological input to the wave analysis forecast program was continually updated and refined. The most recent hindcast data are probably the most reliable, as the input fields benefitted from a larger data base of weather observations and were updated more frequently. The evolution of the method is described more recently by Hubert and Mendenhall (1970) and Schwartz and Hubert (1973). Bunting (1970) has evaluated the hindcasts and forecasts of the FNWC model and compared the results to a spectral model and to wave measurements made at Argus Island and at several North Atlantic Ocean Stations between March 1966 and March 1967.

Hindcast Data Produced by NOAA Significant Wave Forecast Models. On October 1, 1968, NOAA introduced its first operational automated wave forecast model. The method is a straightforward adaptation of the FNWC model described above. It con-
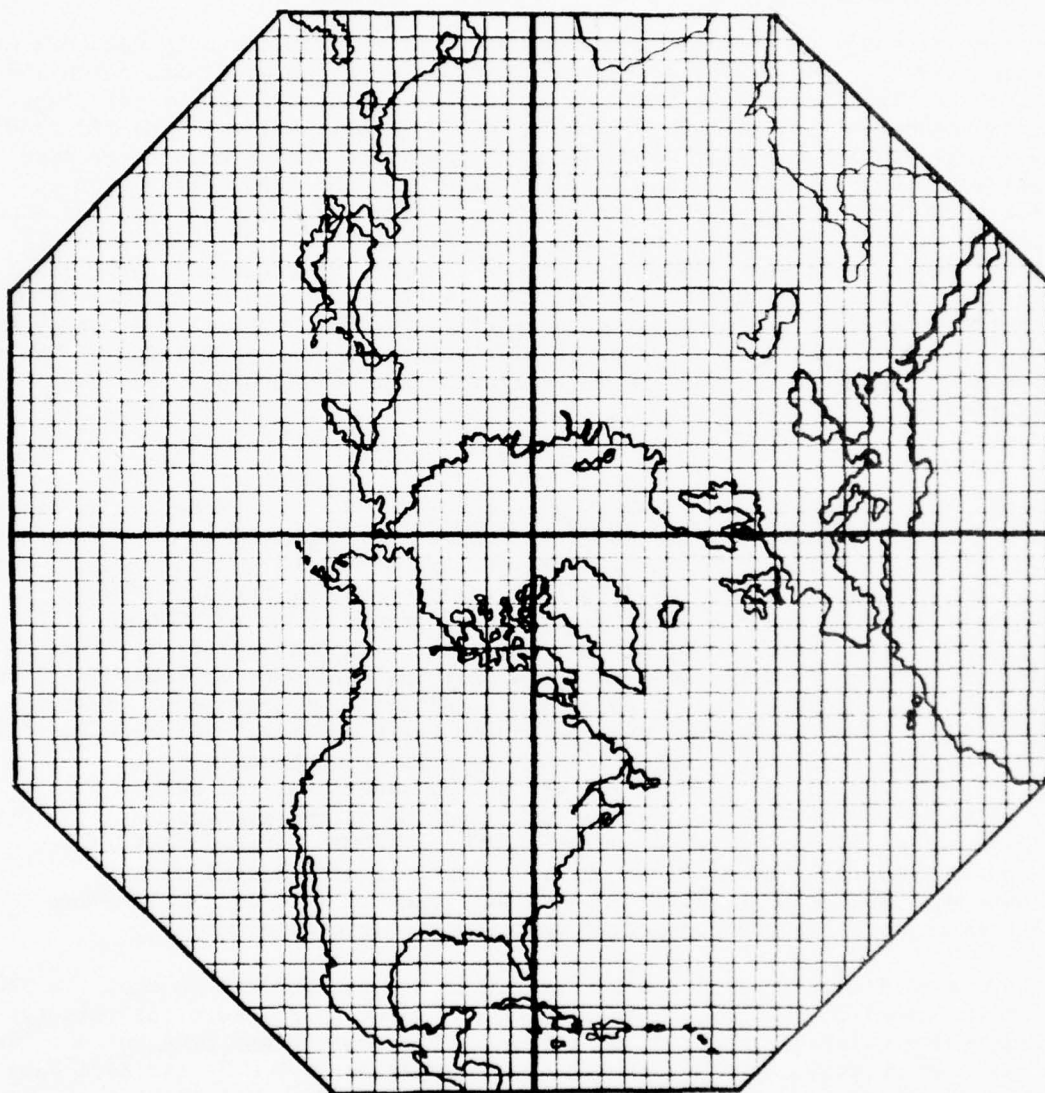
Figure 22   JNWP Grid System of Northern Hemisphere.

tinues as the operational NOAA global wave forecast model. Forecasts are run twice daily at the National Meteorological Center (NMC) and provide analysis and forecasts on the portions of the NMC grid (JNWP) covering the North Atlantic and North Pacific Oceans. The technique is described in detail by Pore (1970).

The NOAA model produces wind wave forecasts in terms of significant wave height, period and direction to 48 hours in 12-hour steps, as well as a wave specification at initialization time (either 0000 or 1200 GMT). Swell information is not available as an analyzed (hindcast) quantity but as forecast out to 24, 36 and 48 hours. Since 1968, changes have been made in the way the surface wind fields that drive the model are derived from the operational NMC hemisphere analysis and forecast models are described by Pore and Richardson (1969).

The NOAA wave forecast model has recently been extended to the Great Lakes, whereby significant wave information is specified every 12 hours from analysis time (again either 1200 or 0000 GMT) to +48 hours on a special grid of points extending over all of the Great Lakes. A statistical procedure is used to provide the winds on the relatively fine grid of points from the large-scale NMC analysis and forecasts. The wind and wave specification procedures for the Great Lakes are described in detail by Barrientos (1970).

As far as the author has been able to determine, there is no systematic effort within NOAA to archive the NOAA hindcast wave data generated within the context of the analysis (hindcast)/forecast cycle just described. However, inasmuch as most analysis/forecast products generated at NMC are intercepted and stored at the National Climatic Center at Asheville, North Carolina, it may be possible to retrieve some or all of the wave hindcast data generated by NOAA since the inception of the models.

It is difficult to assess the accuracy of the NOAA wave hindcast data just described, since verification programs have heretofore been limited to the use of visual wave estimates (e.g., Pore and Richardson, 1969).

Significant Wave Hindcast Data Produced in Climatological Studies. Significant wave hindcast models have been applied in climatological studies for both extratropical and tropical wind systems. Neu (1971), for example, used wind data for one year on the Canadian Atlantic Coast to calculate a wave climatology for the region. This approach is feasible for regions not affected significantly by swell, such as the upper east coast, but may be quite unrepresentative for say the Gulf of Alaska.

The significant wave method has been applied to hurricanes on the basis of its adaptation to moving fetches (Wilson, 1961). Patterson (1971) calibrated such a hindcast model with wave measurements obtained near and in intense hurricanes in the Gulf of Mexico. The calibrated model has been used to develop a significant wave climatology of hurricane-generated waves for the deep water portions of the Gulf of Mexico coast from Mississippi to Texas (Bea, 1974).

More general wave climatologies can be calculated from the time series of significant wave hindcasts produced by the FNWC and NOAA significant wave hindcast pro-

gram. However, this has not been done, at least not in the public domain. It is probably not worthwhile at this point to proceed with such an endeavor, as global scale wave hindcast series are currently being calculated from more advanced and apparently more accurate spectral models, as will be described below.

Spectral Wave Hindcast Models

As early as 1953, the concepts of stochastic processes and spectra had already been incorporated into a practical wave forecasting method. This technique, referred to as the PNJ method (Pierson, Neumann and James, 1953 and 1955) was based on the spectrum proposed by Neumann (1953) which in turn was derived with the use of data on wave heights and periods obtained by visual observing methods. This imaginative derivation was in a sense verified when Pierson (1954) interpreted the observable properties of waves in terms of the wave spectrum.

Among the innovative aspects of the PNJ method was the recognition of directional properties of waves -- fetch width as well as length were considered. The concept of moving fetch was introduced, and the "period increase" of swell was correctly explained in terms of spectral component group velocity dispersion effects.

One important weakness of all wave prediction schemes in existence in the early 1950's was the subjectivity of their application. Wave hindcasting and forecasting was still an art -- only practitioners with considerable experience could produce consistent results. With the development of numerical weather prediction, however, it became evident that large digital computers could be applied to the wave prediction problem. Gelci and Chavy (1961) and Baer (1962) were among the first to use a computer to make predictions of wave spectra.

Baer's work represented an early attempt to build a comprehensive and completely computerized wave prediction scheme. His model represented the North Atlantic ocean with a grid of 519 points spaced 120 nautical miles apart. At each grid point the spectrum was described by 120 numbers that represented ten frequencies and 12 directions. Wind speed and direction were supplied to the grid and updated each 6 hours, while the 120 numbers were systematically modified each two hours, to account for wave generation and propagation.

The PNJ spectral component wave growth was coupled to the angular dispersion relationship given by Project SWOP (Cote et al, 1960) and expressed in the form of a large table. At each time step, growth was allowed only for components travelling within 90° of the wind direction, with the Neumann fully developed spectrum used to limit growth. No other form of implicit or explicit attentuation was assumed.

Wave propagation was approximated by the so-called jump technique -- that is, spectral components were simply translated to adjacent grid points after a sufficient number of time steps had elasped to account for the grid spacing. This technique allowed the wave energy to retain the quasi-discontinuous characteristics imparted by moving fetches, as occurs for example near meteorological fronts. Baer tested his model by hindcasting the severe wave conditions observed in the North Atlantic in December 1959.

The suitability of this model to further development was soon realized. By 1964, a revised version had been used to hindcast the two-dimensional wave spectrum on the 519-point grid for the year 1959. This project, sponsored by the U.S. Naval Oceanographic Office and carried out at New York University, has been summarized in detail by Bunting (1966). Briefly, the revisions included the introduction of objective wind field analysis techniques (Thomasell and Welsh, 1963), the adoption of the Pierson-Moskowitz fully-developed spectrum as a limiting state and the addition of a dissipation mechanism based on gross Austausch turbulence to simulate the attenuation of swell travelling against wind-generated seas.

The end product of the project consisted of 30 reels of magnetic tape containing 6-hourly wave spectra and wind data over a 15-month period at 519 grid points of the North Atlantic Ocean. The data were for the months of December 1955, November 1956, December 1968, and January through December 1959.

For each of the grid points throughout the period there are available 222 pieces of six-hourly information consisting of the following:

1) 180 numbers describing the directional wave spectrum for 15 frequency ranges and 12 directions.

2) 15 numbers summing the wave spectra for each of the frequency bands.

3) 12 numbers summing the wave spectra for each of the 12 direction ranges.

4) 12 numbers giving the percentages of total energy in each direction range.

5) 2 numbers giving the wind speed and direction.

6) 1 number giving the significant wave height equivalent to the spectral energy.

The results have been used by Wachnik and Zarnick (1965) in the study of aircraft carrier motions. The continued availability of this source depends upon the condition of the magnetic tape copies that are in the possession of the Naval Oceanographic Office.

The climatology described above will soon be replaced by a more extensive and accurate file of spectra as a result of the operational status of a contemporary spectral wave prediction at FNWC. The hindcast data presently available from this effort will be described after the nature of contemporary models in general is outlined.

Modern Spectral Model. The framework of contemporary spectral wave prediction can be traced through the work of Gelci et al. (1956), Hasselmann (1960), Pierson et al. (1966) and Barnett (1968). These models are based on the numerical integration of the energy balance equation:

$$\frac{\partial}{\partial t} E(f,\theta,x,t) = -C_g (f,\theta) \cdot \nabla E(f,\theta,t,x) - S$$

where E is the directional wave spectrum defined as a function of frequency, f, direction, θ, position, x, and time t. C_g is the deep water group velocity and S, the source function, represents all physical processes that transfer energy to or from the spectrum. In principle, if S could be specified in terms of E and the wind field, the above equation could be numerically integrated, subject to appropriate initial and boundary conditions, to yield wave predictions with an accuracy limited only by errors in the wind field and in the numerical methods.

Propagation. The physical nature of wave propagation in deep water is well understood as a result of the work of Barber and Ursell (1948), Groves and Melcer (1961) and Snodgrass, et al. (1966). Each component in the two-dimensional spectrum travels along a great circle in its direction at the deep water group velocity appropriate to its frequency.

Baer (1962) demonstrated that propagation by a simple first order finite difference analog was inadequate if the quasi-discontinuous nature of the spatial distribution of wave energy is to be preserved. Such a scheme has been used by Gelci, er al. (1966) and Barnett (1968).

The jump technique, as developed by Baer (1962) partially overcame this difficulty but was at best only an approximation to propagation for most spectral components and it could lead to serious errors for large propagation distances. Pierson, Tick and Baer (1966) proposed a technique that combines the finite difference and jump techniques. Their propagation algorithm attempts to keep track of discontinuities in the energy field and employs jump techniques in such regions, while the finite differences scheme is applied where the fields vary smoothly. Uzi and Isozaki (1972) have developed a more complicated version of the jump technique whereby lateral spreading and longitudinal dispersion associated with discrete directional spectral components are simulated. Ewing (1971) has proposed a model in which a fourth-order differencing scheme is used to simulate propagation.

Most numerical models have used grid systems on conformal map projections because of their minimal distortion, small-scale variation and conservation of angle. Grid paths on such projections are not, in general, great circles, though for distances less than one quarter of the earth's circumference, errors are not too large. For global scale predictions, Baer and Adamo (1966) proposed a grid system based upon the gnomonic projection -- on which all straight lines are great circles. A multi-projection system was devised in which the earth was mapped onto 20 faces of an icosahedron circumscribed about the earth. This "Icosahedral-Gnomonic Projection" is shown in Fig. 23. Within each triangular subprojection, a hexagonal coordinate system defines a 1225 point grid of average spacing 95 nautical miles. A modified jump technique has been used on the Northern Hemisphere portion of this grid system and appears to give reasonable results.
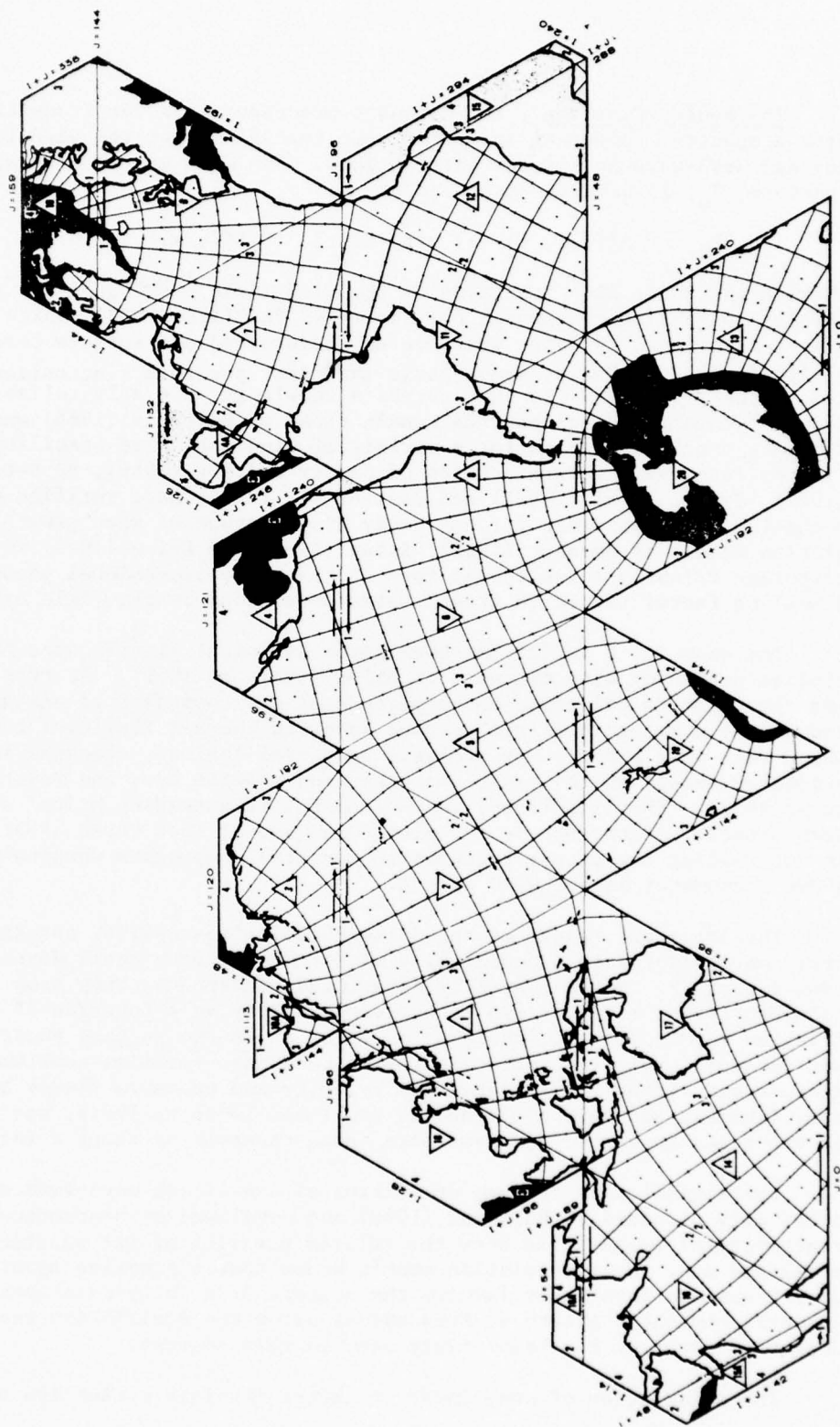
Figure 23. The Icosahedral-Gnomonic Projection of the Earth Designed for Global Numerical Wave Prediction. (Baer and Adams, 1966.)

The Source Function. The dominant processes that can transfer energy to or from a spectral component include direct transfers from the wind field, wave breaking and wave-wave non-linear interactions. The wind generation part of the source function, S_w, is usually expressed as

$$S_w = A(f, x, t) + B(f, x, t) \cdot E(f, x, t)$$

where A and B are also functions of the wind field. The quantity A has been given physical significance through the theory of Phillips (1957), which explains the initial generation of gravity waves on an undisturbed sea surface through a resonant excitation by incoherent atmospheric turbulent pressure fluctuations being convected by the mean wind. To this author's knowledge, the only reliable field measurements of this pressure spectrum remain those of Priestly (1965) who obtained measurements over mowed grass for a variety of wind speed and stability conditions. The limited fetch wave growth studies of Snyder and Cox (1966), Barnett and Wilkerson (1967), Schule et al. (1971) and Ross et al. (1971) have verified that the resonance mechanism is responsible for the early linear stage of wave growth. The wave prediction models of Barnett (1968), Inoue (1967) and Ewing (1971) and others all incorporate Priestly's functional form of the three-dimensional pressure spectrum with a scaling factor fitted to growth rates determined in the field experiments.

The quantity B in (2) has been given dynamical significance through a series of studies beginning with the work of Miles (1957 and 1959). In those studies Miles was the first to calculate the amplitude of the component of atmospheric pressure, induced by a prescribed free surface wave, in the air flow over the wave and in phase with wave slope. His analysis was quasi-laminar, atmospheric turbulence being neglected except in the sense that the wind profile over the waves was specified as logarithmic. Phillips (1966) was successful in extending Miles' model to include some aspects of atmospheric turbulence and showed that these effects were important in determining the energy transfer to spectral components possessing phase speeds above anemometer height wind speeds.

The important result of the Miles-Phillips instability theories is that spectral energy increases exponentially with time or fetch until dissipative effects become important. For a neutrally stratified atmosphere, they show that the dimensionless growth rate B/f can be expressed solely as a function of dimensionless friction velocity, u_*/c, where $u_* = \sqrt{\tau/\rho}$ (τ is the surface shear stress and ρ is air density). The instability theories have been verified qualitively by direct measurement of the wave-induced air velocity and pressure fields both in the laboratory (Shemdin and Hsu, 1967) and in the field (Dobson, 1971), but the theoretical growth rates appear to underestimate those observed by about a factor of 4.

The significance to wave prediction of non-linear wave-wave energy transfers as originally proposed by Phillips (1960) and developed by Hasselmann (1963) remains a controversial subject, as does the related question of the existence of a fully-developed sea. Wave prediction models whose source function ignores non-linear energy transfers invariably involve the concept of a fully-developed spectrum to limit spectral component growth at frequencies below the equilibrium range. The Pierson-Moskowitz spectrum has been widely used in this context.

The calculation of non-linear transfers involves evaluation of quadruple inte-

grals over the directional spectrum. Even with the fastest computers available, such calculations are impractical in a wave prediction model. The wave-wave transfer rates have therefore been computed only for typical spectral shapes and applied to a given spectrum parameterized in terms of total energy, mean frequency and mean direction. The wave prediction models of Barnett (1968) and Ewing (1971) have included a wave-wave interaction component in their source function through such parameterization.

Hindcast Data Generated Through Model Development. A very limited amount of wave data has been generated in the process of model development for the various spectral models described above. Ewing's (1971) model, for example, was run only to simulate two three-day periods in November 1966 and June 1967, for which wave measurements were available at Stations I and J in the North Atlantic Ocean.

The limited applicability of most spectral models has made model intercomparisons difficult except for ideal imposed wind conditions. Several hindcasts of the severe storm in the North Atlantic in December 1959 have been compared by Hayes (1973). The comparison is significant because each hindcast was made by a numerical spectral model applied on the same exact grid system (Baer, 1962) and driven with the same wind fields. The differences between the hindcasts therefore reflect mainly differences in the source function and propagation method. The time history of hindcast and observed significant wave height for this storm at ocean station J is shown in Fig. 24, with the hindcast and observed one-dimensional spectra at peak storm conditions shown in Fig. 25. It is clear that the "second generation" spectral wave prediction models (Inoue, 1967; Barnett, 1968; Isozaki and Uji, 1973) significantly improved upon the original Baer (1962) results. The source function of Barnett's model included a non-linear interaction parameterization but its hindcasts are not significantly better than those models that do not include non-linear transfers explicitly. Those models that include a dissipation mechanism for turbulent attenuation of spectral components propagating against locally wind generated seas (Inoue, 1967, and Isozaki and Uji, 1973) appear to simulate better the decay of seas after peak storm conditions.

The observed spectrum at peak conditions (Fig. 25) appears to be narrower than all hindcast spectra, and this discrepency cannot be completely explained by sampling variability or the limited frequency resolution of the hindcast spectra. Further refinement of these hindcasts would appear to require two-dimensional measurements and a further reduction of the remaining differences between the grid wind fields and the true wind distribution.

More recently, Feldhausen, et al. (1973) have also compared hindcasts for the same storm. Both spectral and significant wave methods were intercompared. For the best models, the correlation coefficient between hindcast and measured significant wave height at station J averaged 0.85, but there was a systematic tendency for all methods to overspecify sea states between storm periods.

Operational Spectral Wave Prediction Models. The potential for the rapid accumulation of a global scale wave hindcast data bank through the implementation of
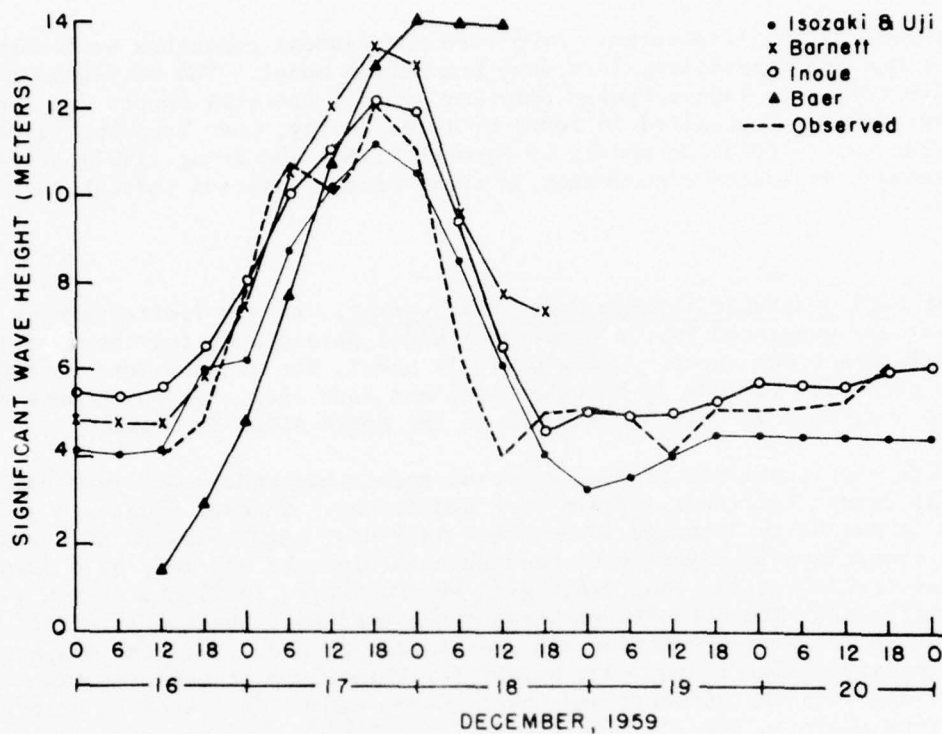
Fig. 24 — A comparison of various spectral hindcast model predictions of the time history of significant wave height at the position of the Ocean Station Vessel 'J' (52° 40' N, 20°W) in the eastern North Atlantic, during the severe storm of December, 1959. (Hayes, 1973).
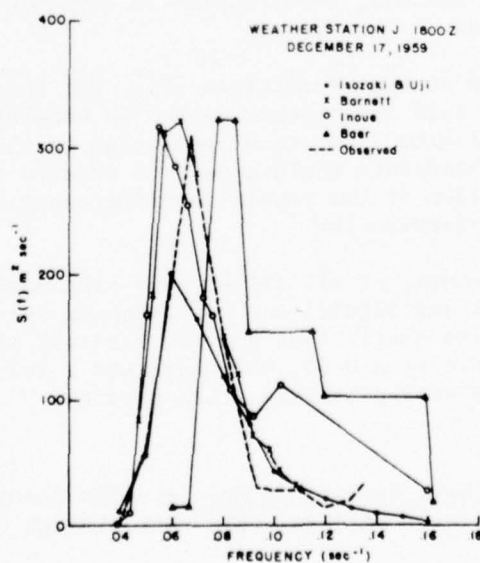
Fig. 25 — Observed and hindcast spectra at station 'J'. (Hayes, 1973).

spectral models in operational wave forecast programs was realized in December 1974 when the model described by Pierson, Tick and Baer (1966) became the operational model of the FNWC. Two years earlier, a Mediterranean wave spectral model was placed into operational use at FNWC (Lazanoff, Stevenson, and Cardone, 1973). As a result, hindcast wave spectra are now produced routinely for the entire Northern Hemisphere and are archived at FNWC in the format to be described below.

Mediterranean Sea Wave Hindcast Data. Twice a day, the wave spectrum resolved into 15 frequencies and 12 directions is updated and forecast to 48 hours on a grid of points with average grid spacing of 40 nautical miles (Fig. 26) that represents the Mediterranean. The forecasts have been verified against measured wave staff and laser profilometer data with good results. Shallow water effects are not yet in the model. FNWC is presently saving and archiving all grid point hindcast spectra, available 4 times per day, on magnetic tape along with the significant height field. This complete archiving system began in October 1975. Between April 1972 and October 1975, the significant wave height field is available on microfilm and for most of the period complete spectra are available for about 30 grid points distributed across the grid, also on microfilm.

Northern Hemisphere Icosahedral Grid Hindcast Data. The Icosahedral hemispheric spectral wave prediction model has been operational at FNWC since December 1974. Forty-eight-hour forecasts and 12-hour hindcast updates of the spectral field are made twice daily for the North Atlantic Ocean, the North Pacific Ocean and adjacent basins, the Gulf of Mexico and northern half of the Indian Ocean. With regard to Fig. 23, the model uses seven subprojections for the North Pacific, six for the North Atlantic and Gulf and one for the Indian Ocean. There are 325 grid points on each subprojection with a spacing of 350 km at the point of tangency and 194 km at the vertices. As in the Mediterranean model, at each grid point the spectrum is resolved into 180 discrete variance elements representing 15 frequencies and 12 directions of propagation.

Since October 1975, the wave hindcast spectra have been saved at all grid point points and are available four times a day at six hour intervals (03GMT, 09GMT, 15GMT, 21 GMT). Prior to October 1975, a small subset of grid points was available covering portions of the Gulf of Alaska, the West Coast of the U.S., the Gulf of Mexico and portions of the North Atlantic.

Lazanoff and Stevenson (1975) have described the model itself as implemented at FNWC and have presented a preliminary evaluation of the hindcasts and forecasts as verified against measured wave data. They conclude that the method "produces far superior results than the previous FNWC operational singular wave model" for significant heights.

More recently, comparisons of the hindcast data with wave spectra measured at locations of NOAA data buoys (e.g., Appendix K) suggest that systematic errors may be present in the FNWC model. These effects are probably caused by errors of a systematic nature in the wind input to the FNWC model. Beginning in late 1975, specification of the winds was changed (Kaitala, personal communication) to conform more

SACLANT WAVE BUOY
10-15 APRIL 1972

SACLANT WAVE BUOY
25-29 MAY 1972

NAVOCEANO AIRPLANE TRACK
1106Z-1230Z, 29 MAY 1972
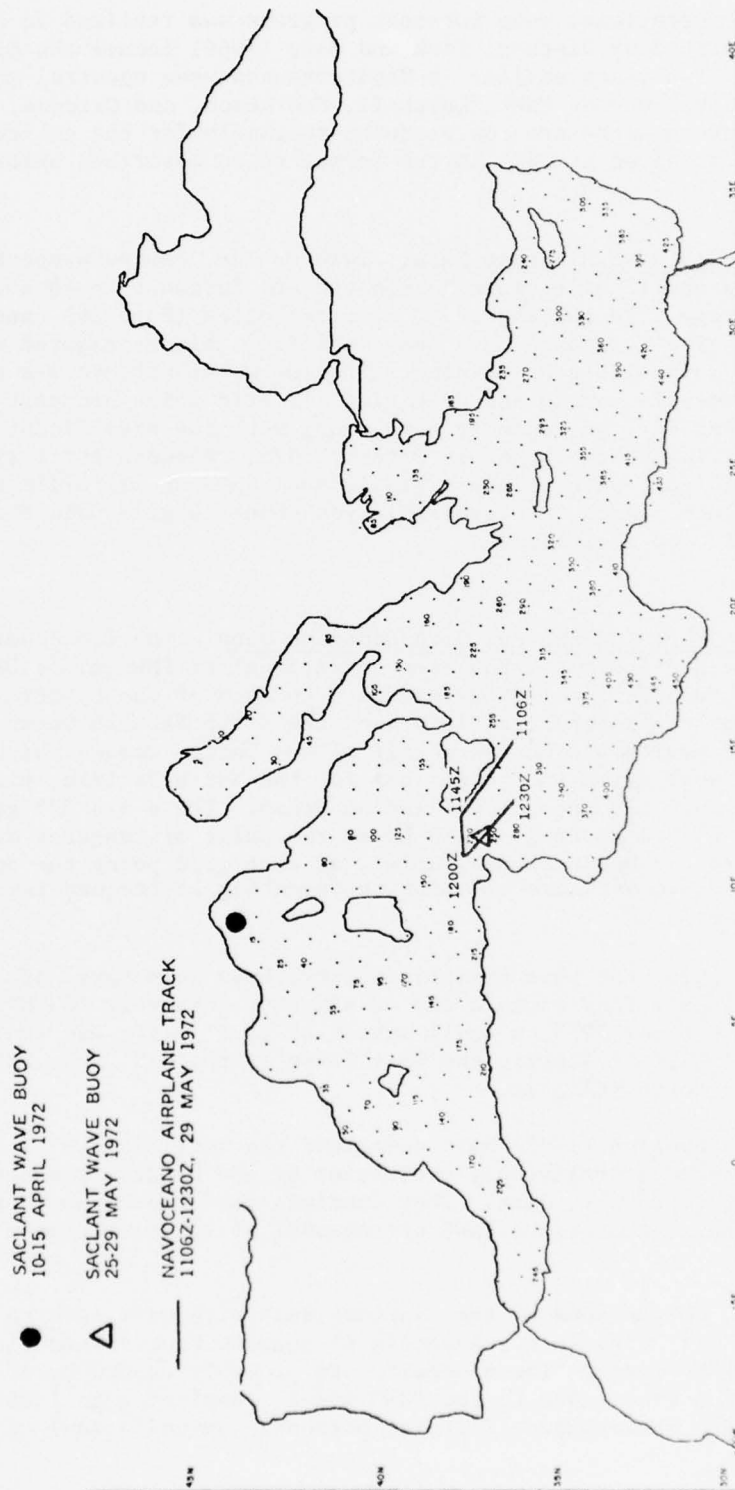
Figure 26.   The Grid System of the FNWC Operational Mediterranean Sea Wave Spectral Model Grid.
(Lazanoff, Stevenson and Cardone, 1973)

-54-

closely with the procedure described by Cardone (1969). Hindcasts made with the new wind input have yet to be evaluated. Currently, a hindcast series is being generated on the Univac 1108 machine at the U.S. Naval Oceanographic Office. The hindcasts will initially extend for a month period (mid December 1973 - mid January 1974) and only for the North Atlantic portions of the grid system. The winds for that hindcast were calculated precisely according to the procedure described by Cardone. The hindcasts will be compare to special Tucker meter wave measurements made at the ocean stations in the eastern North Atlantic during the SKYLAB experiment. This study should be completed within a few months and could provide insights as to the role fo the wind input in the discrepencies observed in the FNWC operational output.

Current and Planned Wave Hindcast Activities

The operation FNWC spectral model will provide an ever-expanding data base of hindcast wave spectral data, since the total hindcast output continues to be archived. This source will therefore rapidly increase and should supersede all existing sources in quantity and probably in accuracy as well. To extend this data base, FNWC plans to hindcast a twenty-year period with the hemispheric spectral model. The effort will begin this year with a complete hindcast of the year 1975, and then will be extended back in time year by year. The rapidity with which this effort will proceed is not yet determinable as it depends on the exact nature of computer resources that will become available this year at FNWC.

Development of Operational Spectral Wave Forecast Models Elsewhere

Several countries are engaged in the development of spectral models for eventual operational application. The model described by Ewing (1971) could now produce operational spectral wave forecast and hindcasts for the eastern North Atlantic but has not been implemented.

In Japan, the model developed by Isozaki and Uji (1974) has been programmed for a portion of the North Pacific Ocean. Recently, Isozaki and Uji (1974) performed a test hindcast with the model for a seven-day period in January 1972, using the marine boundary layer model of Cardone (1969) to provide the winds. The hindcasts were compared to visual wave estimates provided by ships. The comparisons were favorable. However, there is no indication that the model will be implemented operationally in the near future.

Australia is also engaged in the development of a spectral model for application to the southern oceans. The form this model will likely take was indicated in the study of Dexter (1974) in which four spectral models were tested against simple idealized wind fields. The study suggest the form an operational model will likely take, but does not indicate when such a model will be implemented.

-55-

Development of Shallow Water Spectral Wave Hindcast Models

The emphasis in the development of new wave hindcast models appears to be on the applicability to shallow seas. Cardone et al. (1975) have developed a model that can be applied to small time and space-scale meteorological phenomena such as hurricanes, with particular application to the continental shelf zone of the Gulf of Mexico. Hindcasts of shallow water spectra associated with several hurricanes compared quite favorably with spectra measured from specially instrumented oil rigs. The oil industry will probably use that model to calculate a climatology of hurricane-generated wave conditions in the Gulf of Mexico within the next year. In a study supported by Shell Development Co. and NOAA, the model is being adapted to the east coast of the U.S. (deep water), and may be applied to forecast hurricane generated sea states quasi-operationally this summer, using NOAA's computer in Miami.

Collins (1972) and Barnett (1969) have also developed spectral wave prediction models for shallow seas but the models have not been used extensively enough to provide hindcast wave data.

A major research effort is currently underway in Great Britain to develop a wave prediction model for application to the shallow and deep portions of the North Sea. The model will employ a parametric approach (Hasselmann et al. 1976) for the wind sea, while swell will be tracked separately. Bottom friction but not refraction will be modelled.

The model will be used to hindcast a sample of 50 of the most severe storms that occurred between 1965-1975. Wave records from oil rigs and weather ships available recently for the North Sea will be used to calibrate the model. The effort is scheduled to be completed by the end of 1976.

VII. PREDICTION OF LOADS

Ship Response Prediction

So far general wave characteristics and wave spectra -- theoretical, measured and hindcast -- have been discussed. Consideration must be given next to the use to which the wave data are to be put -- namely, the determination of the responses of ships and other floating structures to the waves. This leads to the question of the characteristics and variability of the response spectra. In general, the main interest is in the <u>area</u> of the response spectrum representing the root-mean-square of the process, which defines the principal statistical properties of the response. By contrast the <u>shapes</u> of the wave spectra are of great importance, since they affect the response spectrum area, yielding some scatter about the mean area. This statement will be clarified in the following paragraphs.

In general, on the basis of the superposition principle whose applicability to ship motions was first demonstrated by St. Denis and Pierson (1953), the response spectrum, S_R, is obtained by multiplying a sea spectrum, S_ζ, by the response amplitude operator (RAO), Y, obtained from model tests in regular waves or by theoretical calculation. Hence, for the point spectrum,

$$S_R(\omega) = S_\zeta(\omega) \ Y(\omega)$$

It is apparent that the magnitude of the response spectrum ordinate at any frequency is directly proportional to the sea spectral ordinate at that frequency. For highly tuned responses such as roll, with sharply peaked RAO's, seemingly minor changes in the shape of the sea spectrum can have large effects on the response spectrum.

These changes in the sea spectral shape can be due to several causes. There is first the obvious variability of sea conditions. Changes in ship speed or heading can also affect the shape of the encounter spectrum, i.e., the waves which the ship actually sees and responds to, as discussed later.

It is often assumed that the ship response is a narrow-band process and therefore that the short-term peak-to-mean responses are Rayleigh distributed, i.e.,

$$p(r_0) = \frac{r_0}{rms^2} \ e^{-\frac{r_0^2}{2rms^2}}$$

when r_0 is peak-to-mean response and $\quad rms^2 = \int_0^\infty S_R(\omega) \ d\omega \quad$ and

$$p(r > r_0) = e^{-\frac{r_0^2}{2rms^2}}$$

Thus the probability of exceeding a certain response over a limited period of time, during which sea conditions are stationary, depends only on the rms response, i.e., on the response spectrum area and not on its shape.

When the variability of ocean wave spectra is considered, the problem of determining the response is more complicated than when only one wave spectrum is consid-

ered, but a prediction for longer periods of time, such as several hours or the lifetime of the ship, is possible. It will be assumed that a representative random sample of wave spectra is available, all falling within a relatively small band of significant wave heights (hence spectral areas). For a particular ship speed, heading and wave component direction;

$$\int S_R(\omega) \, d\omega = \int S_\zeta(\omega) \, Y(\omega) \, d\omega$$

$$\simeq \sum_{n=1}^{N} S_R(\omega_n) \, \Delta\omega = \sum_{n=1}^{N} S_\zeta(\omega_n) \, Y(\omega_n) \, \Delta\omega$$

In this summation, $Y(\omega_n)$ has specific values depending on ω_n and relative wave direction. However, each $S_\zeta(\omega_n)$ is a random function, assumed to be normally distributed, as illustrated in Fig. 27, for which the mean and standard deviation are known for each value of ω_n. Hence, the mean and standard deviation of each product in the sum is also known.

Assuming that the functions $S_\zeta(\omega_n)$ for different values of ω_n are independent or uncorrelated, then the mean and standard deviation of the rms values, $[S_R(\omega_n) \, \Delta\omega]^{\frac{1}{2}}$, can be determined by standard statistical techniques, as shown below.

Theory for Approximating the Distribution of a Function of Random Variables

We wish to approximate the distribution of a function of random variables of the form

$$g(X_1, X_2, \ldots X_N)$$

where the X_N are N random variables with means μ_n, and standard deviations, σ_n.

If g is represented by its first-order Taylor series expansion,

$$g(X_1, X_2, \ldots, X_N) = g(\mu_1, \mu_2, \ldots, \mu_N) + \sum_{n=1}^{N} \{\frac{\partial}{\partial X_n} g(\mu_1, \mu_2, \ldots, \mu_N)\} \{X_n - \mu_n\}$$

So g is now approximated by a linear combination of functions, for which the following relations are easily derived. First,

$$\mu_g = g(\mu_1, \mu_2, \ldots, \mu_N)$$

And if the X_n's are independent

$$\sigma_g^2 = \sum_{n=1}^{N} \{\frac{\partial}{\partial X_n} g(\mu_1, \ldots, \mu_N)\}^2 \, \sigma_n^2$$

-58-
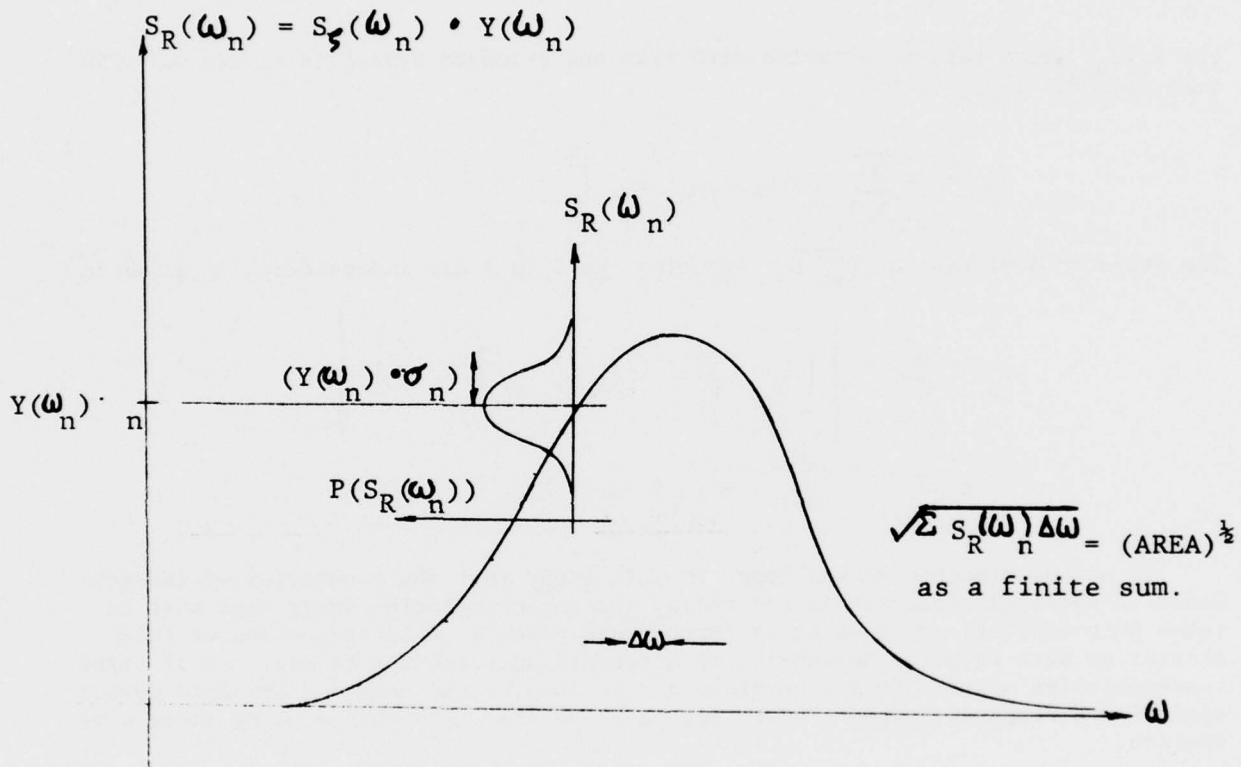
Figure 27   Calculation of rms Response

Application of the Theory

Now consider the function

$$\sqrt{\sum S_R \; \Delta\omega} \;=\; \left| \sum_{n=1}^{N} \; S_\zeta(\omega_n) \; Y(\omega_n) \; \Delta\omega \right|^{\frac{1}{2}} \qquad \text{which defines the rms response, where}$$

the $S_\zeta(\omega_n)$ are N random variables with mean and standard deviation μ_n and σ_n. The mean of $\sqrt{\Sigma S_R}$ is given by:

$$\mu_R \;=\; \left| \sum_{k=1} \; Y(\omega_n) \; \omega_n \; \Delta\omega \right|^{\frac{1}{2}}$$

The standard deviation of $\sqrt{\sum S_R}$ assuming the $S_\zeta(\omega_n)$ are independent, is given by:

$$\sigma^2_R \;=\; \sum_{n=1}^{N} \left\{ \left[\frac{1}{2} \; \frac{1}{\mu_R} \; Y(\omega_n) \; \Delta\omega \right]^2 \; \sigma_n^2 \right\}$$

$$=\; \frac{1}{4 \; \mu_R^2} \; \sum_{n=1}^{N} \; Y^2(\omega_n) \; \Delta\omega^2 \; \sigma_n^2$$

In actual practice it was found in this study that the assumption of independence of spectral ordinates is not valid, and the correlation among them must be taken into account. This point is further discussed in a later section of this chapter on data format. Meanwhile, an alternate approach was to make use of eight representative spectra from each group and to compute the mean and standard deviation of rms response based on eight rms response spectra obtained using these wave spectra.

Either method can be extended to short-crested seas by considering the directional components of the sea and the corresponding response amplitude operators. The final response spectrum can be obtained by integrating over wave direction.

$$S_R(\omega) \;=\; \int_0^{2\pi} S_\zeta(\omega,\psi) \; Y(\omega,\psi) \; d\psi$$

The integral that determines the statistical properties of the response can then be obtained,

$$\int_0^\infty S_R(\omega) d\omega \;=\; \int_0^\infty \int_0^\infty S_\zeta(\omega,\psi) \; Y(\omega,\psi) \; d\psi \; d\omega$$

In practice this result is usually obtained by numerical summation rather than by integration. It applies to a specific ship speed and relative heading angle,

$$\int_0^\infty S_R(\omega)d\omega = \sum_{n=1}^N \sum_{m=1}^M S_\zeta(\omega_n, \psi_m) \ Y(\omega_n, \psi_m) \ \Delta\psi \ \Delta\omega$$

If it is assumed that for each ship heading the rms response, which is a result of contributions from all wave directions, as well as all frequencies, is normally distributed, then the mean and standard deviation can be calculated in the manner just outlined. (Of course, this assumption might not be true in the case of spectra from two storms superimposed, or a sea spectrum made up of sea and swell coming from different directions.)

Certain responses, acceleration at the forward perpendicular, for example, are strongly dependent on frequency of encounter and thus ship heading relative to the waves. Wave bending moment, which depends on effective wave length, is also dependent on heading angle. This means that for accurate predictions, reliable estimates are required of the percentage of time spent at various headings of the ship relative to the waves. This information can be obtained by combining information on the ship's course over its route with information on occurrence of various wave directions from a statistical source. It has been found by experience that the increment in relative heading must not be larger than 15°.

Hence, finally, the whole procedure described above must be carried out for each ship heading relative to the dominant wave direction. The final distribution of rms response is a weighted sum (the contribution for each heading being weighted by the expected percentage of time to be spent at that heading) of all the normal distributions resulting from the calculation for each ship heading; it may not necessarily be a normal distribution. The final result applies to one ship speed and one band of significant wave heights.

It is recognized that any calculated wave spectra is an estimate whose confidence bounds depend on the length of the record and the spacing of data points. In principle, therefore, it would be expected that the standard deviations of spectral ordinates in a sample of wave spectra would include the effect of this sampling variability.

If the above calculation is made for a number of different wave height groups, the result can be presented in the form of a plot of mean rms and standard deviation of rms response vs. wave height. (See Chapter VIII).

One procedure, Band (1966), Hoffman and Lewis (1969), Hoffman et al. (1972), for making long-term predictions of wave bending moment (or other ship responses) is to integrate the Rayleigh distributions using the above assumption with regard to the distribution of rms values (Rayleigh parameters) for each wave height group. Finally, these long-term distributions can be combined into a single distribution on the basis of the expected probability of each heading and wave height group.

It should be noted, however, that since the results of each individual wave height group are combined to yield the long-term trend, a consistent approach must be adopted for each of these groups, i.e., number of spectra in the group used to obtain the rms response, the method of calculation or statistical combination of the data, etc.

Details of Ship Response Prediction

Details will be given in this section of the procedure for the long-term prediction of wave loads, assuming that families of wave spectra of different severity are available.

It is assumed that a family of wave spectra has been defined; for each of ten significant wave height groups, eight spectra have been chosen as representative, $S_{g,n}$ where $g = 1....10$, $n = 1....8$. This family is used in making long-term predictions. The procedure is given as follows:

1) Assume a spreading function, most often the cosine-squared function;

$$S_\zeta(\omega,\psi) = S_\zeta(\omega) \cdot f(\psi)$$

where

$$f(\psi) = \frac{2}{\pi} \cos^2 \psi \quad \text{for} -\frac{\pi}{2} \leq \psi \leq \frac{\pi}{2} \quad \text{and} \quad f(\psi) = 0 \quad \text{elsewhere}$$

$$\int_0^{2\pi} f(\psi) \, d\psi = 1$$

where ψ is the angle between a particular wave component and the dominant wave direction.

2) Assume probabilities, P, of various ship headings relative to the dominant waves, χ_i, where $\sum_{i=1}^{12} P(\chi_i) = 1$, based on details of ship's route and operation. Usually seven headings are used in the computation which, because of the symmetry, give results for 12 headings.

3) Obtain probability of occurrence of the 10 significant wave height ranges, $P(g)$, where $\sum_{i=1}^{10} P(g) = 1$. This distribution depends on ship route and operating seasons. This information is currently obtained from summaries of large numbers of visual observation such as Hogben and Lumb or NOAA Summaries of Synoptic Meteorological Observations. (See Chapter IX).

4) Obtain RAOs for response of interest from model tests or theoretical calculations, $Y(\omega,\chi_i-\psi)$.

5) Compute rms response for each of 80 spectra for each of 7 headings, χ_i,

$$RESP(\chi_i, S_{g,n}) = \left| \int_\omega \int_\psi Y(\omega,\chi_i-\psi) \, S_{g,n}(\omega) \, f(\psi) \, d\psi \, d\omega \right|^{\frac{1}{2}}$$

resulting in 7 x 80 = 560 responses.

6) For each of the ten wave height groups, g, find mean and standard deviation at each of seven headings, χ_i.

$$\mu_g(\chi_i) = \frac{1}{8} \sum_{n=1}^{8} RESP \ (\chi_i, \ S_{g,n})$$

$$\sigma_g^2(\chi_i) = \frac{1}{8} \sum_{n=1}^{8} [\ RESP^2(\chi_i, \ S_{g,n}) - \mu_g^2(\chi_i) \ ]$$

7) Assume at each heading in each wave height group, the rms response, RESP, is normally distributed.

$$P(rms) = \frac{1}{\sqrt{2\pi} \ \sigma_g(\chi_i)^2} \ e^{- \frac{[rms - \mu_g(\chi_i) \ ]^2}{2 \ \sigma_g(\chi_i)^2}}$$

Thus the probability of exceeding a particular value, rms_o, is given by,

$$P(rms > rms_o) = \int_{rms_o}^{\infty} P(rms) \ d \ rms$$

8) For each rms, the peak-to-mean responses, r, are Rayleigh distributed.

$$P(r \mid rms) = \frac{2r}{rms^2} \ e^{- \frac{r}{2rms^2}}$$

where $P(a \mid b)$ is read, "the probability of a for a given b."
The probability of r exceeding a particular value, r_o, is given by

$$P(r > r_o \mid rms) = e^{- \frac{r_o^2}{2rms^2}}$$

Thus the total probability of exceeding r_o for a given heading in a given group,

$$P(r > r_o \mid i,g)$$

is given by the product the probability of each rms value for that heading and group times the probability of exceeding r_o for that rms, summed over rms values. That is,

$$P(r > r_o \mid i,g) = \int_{0}^{\infty} P(r > r_o \mid rms) \ P(rms \mid i,g) \ d \ rms$$

which is the integral of a Rayleigh distribution times a normal distribution.

-63-

9) The total probability of r exceeding r_o is given by,

$$P(r > r_o) = \sum_{g=1}^{10} \sum_{i=1}^{7} P(g) \ P(\chi_i) \ P(r > r_o \mid i,g)$$

where $P(g)$ is the probability of occurrence of each wave height group and $P(\chi_i)$ is probability of occurrence of each heading.

Wave Data Format

As has been explained in the previous sections, both the methods being used to predict ship loads and motion are based on the probability of occurrence of a number of wave height groups, and the mean and standard deviation, due to variation in spectral shape, ship heading, etc. of rms ship response for each wave height group. The required wave data format differs for the two methods.

The first approach, discussed in a previous section, was based on the use of a mean value and standard deviation of the wave spectral ordinate at each frequency for each wave height group. These values are obtained from measured spectra by the following procedure. First the spectra are sorted into wave height groups. Then for each group the values of the spectral ordinate are assumed to be normally distributed at each frequency. The mean and unbiased estimation of standard deviation of spectral ordinates are then computed. It can be seen that by using this method any number of spectra can be included in each group, each contributing to the mean and standard deviation of spectral ordinates at each frequency. The mean and standard deviation of response spectral ordinates can then be computed.

It was previously explained that the assumption of independence of the spectral ordinates was not valid. This means that the effect of the dependence must be included. Thus the correlation coefficients must be computed and their effect included in the method for predicting rms response variation. This is feasible, but it is complicated, and this approach has not yet been developed and applied.

The other method, multiplying a number of spectra from each group by the response operators, and then using the rms response values thus obtained to determine the mean and standard deviation of rms response, was adopted here, as described in the preceding section. The number of spectra in the highest groups was limited to eight by the number available. In the lower wave height groups, the number of spectra was limited to eight in order to maintain consistency of the short-term trends and to limit computer time needed to make the response predictions. In groups where more than eight spectra were available, the eight were chosen using a Monte Carlo technique designed to match as closely as possible four parameters, the $H_{1/3}$, T_1 and ε (the broadness factor, see Chapter V), of the average spectrum of the whole available sample with the $H_{1/3}$, T_1 and ε of the average of eight selected spectra. Furthermore, the standard deviation of $H_{1/3}$ of the whole available sample was matched with the standard deviation of $H_{1/3}$ of the group of eight.

A typical example showing the characteristics of the total number of available spectra and the selected eight is shown in Tables 5 and 6. The tables show excellent agreement for Station "India." Hence, the Monte Carlo selection procedure seems reasonable, and it was adopted instead of a purely random choice.

Such families of wave spectra have been developed at Webb Institute of Naval Architecture from available wave records obtained at Stations "India", Hoffman (1972), and "Kilo", Hoffman (1975), in the North Atlantic and Station "Papa" in the North Pacific, Hoffman (1974). The differences are not great among these families, but the one that is believed to have the best statistical basis because of the method of selection and to be generally the most useful for ship design purposes is the Station "India" family. Figs. 28 to 37 show the eight spectra in each of the ten wave height groups in this family. Also shown in Figs. 38 to 47 are the means and standard deviations of spectral ordinates for each of the ten wave height groups.

Table V

Average Characteristics of Wave Spectra
from both "Papa" and "India"
Whole Sample

			PAPA					INDIA			
Group	Wave Ht. Band Width	No. of Recs.	$H_{1/3}$ ft.	T_1 sec.	ε	ω_o	No. of Recs.	$H_{1/3}$ ft.	T_1 sec.	ε	ω_o
1	< 3	14	2.44	6.42	.614	.52	12	2.36	7.06	.568	.75
2	3 – 6	31	4.70	6.95	.629	.52	39	4.91	7.41	.590	.70
3	6 – 9	42	7.60	7.24	.629	.73	43	7.36	8.15	.626	.65
4	9–12	55	10.64	7.69	.662	.63	43	10.63	8.25	.638	.60
5	12–16	87	14.18	8.24	.685	.58	40	13.97	8.86	.677	.55
6	16–21	103	18.43	8.70	.701	.52	28	17.97	8.73	.673	.55
7	21–27	65	23.35	9.11	.715	.52	25	24.08	9.45	.708	.50
8	27–34	40	30.82	10.11	.753	.47	5	30.20	9.87	.737	.45
9	34–42	12	37.93	10.53	.769	.42	8	37.22	11.21	.764	.40
10	> 42	5	43.59	10.88	.775	.42	8	47.69	11.49	.784	.40
		454					251				

Table VI

Average Characteristics
of Wave Spectra
from "India"
Samples of Eight Spectra

Group	Wave Ht. Band Width	No. of Recs.	$H_{1/3}$ ft.	T_1 sec.	ε	ω_o
1	< 3	8	2.40	7.06	.571	.75
2	3 – 6	8	4.90	7.48	.591	.75
3	6 – 9	8	7.34	8.35	.628	.65
4	9–12	8	10.51	8.34	.640	.55
5	12–16	8	13.90	8.93	.674	.55
6	16–21	8	17.82	8.78	.675	.55
7	21–27	8	23.34	8.85	.704	.50
8	27–34	8	28.89	9.98	.722	.45
9	34–42	8	37.05	11.34	.760	.40
10	>42	8	47.47	11.64	.782	.40

Figure 29 – Scatter of Spectral Height Family – Group 2, 3-6 ft. Station 'India'
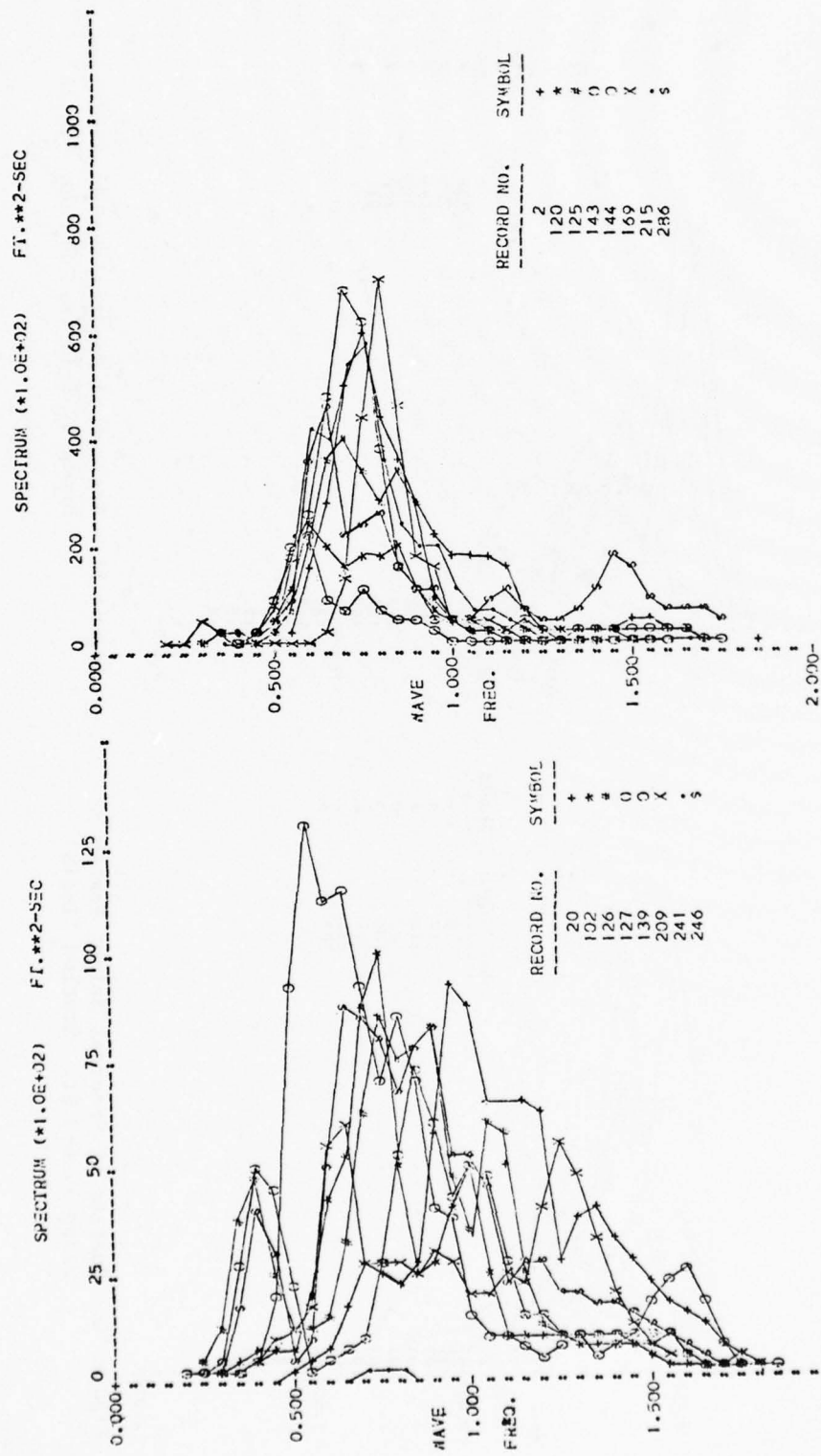
Figure 28 – Scatter of Spectral Height Family – Group 1, 0-3 ft. Station 'India'

Figure 31 – Scatter of Spectral Height Family – Group 4, 9-12 ft. Station 'India'
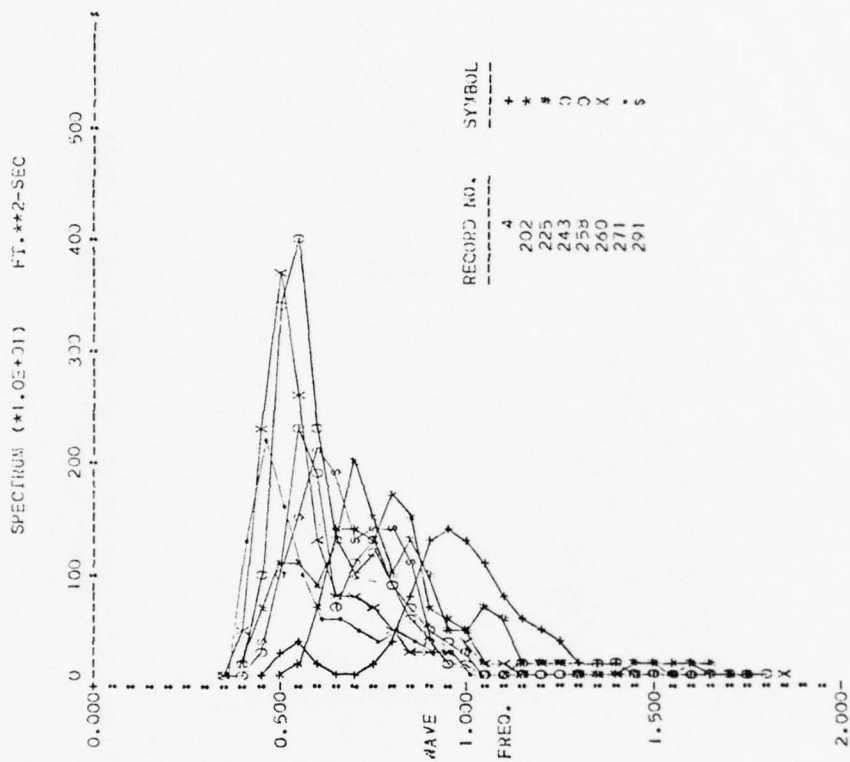
Figure 30 – Scatter of Spectral Height Family – Group 3, 6-9 ft. Station 'India'
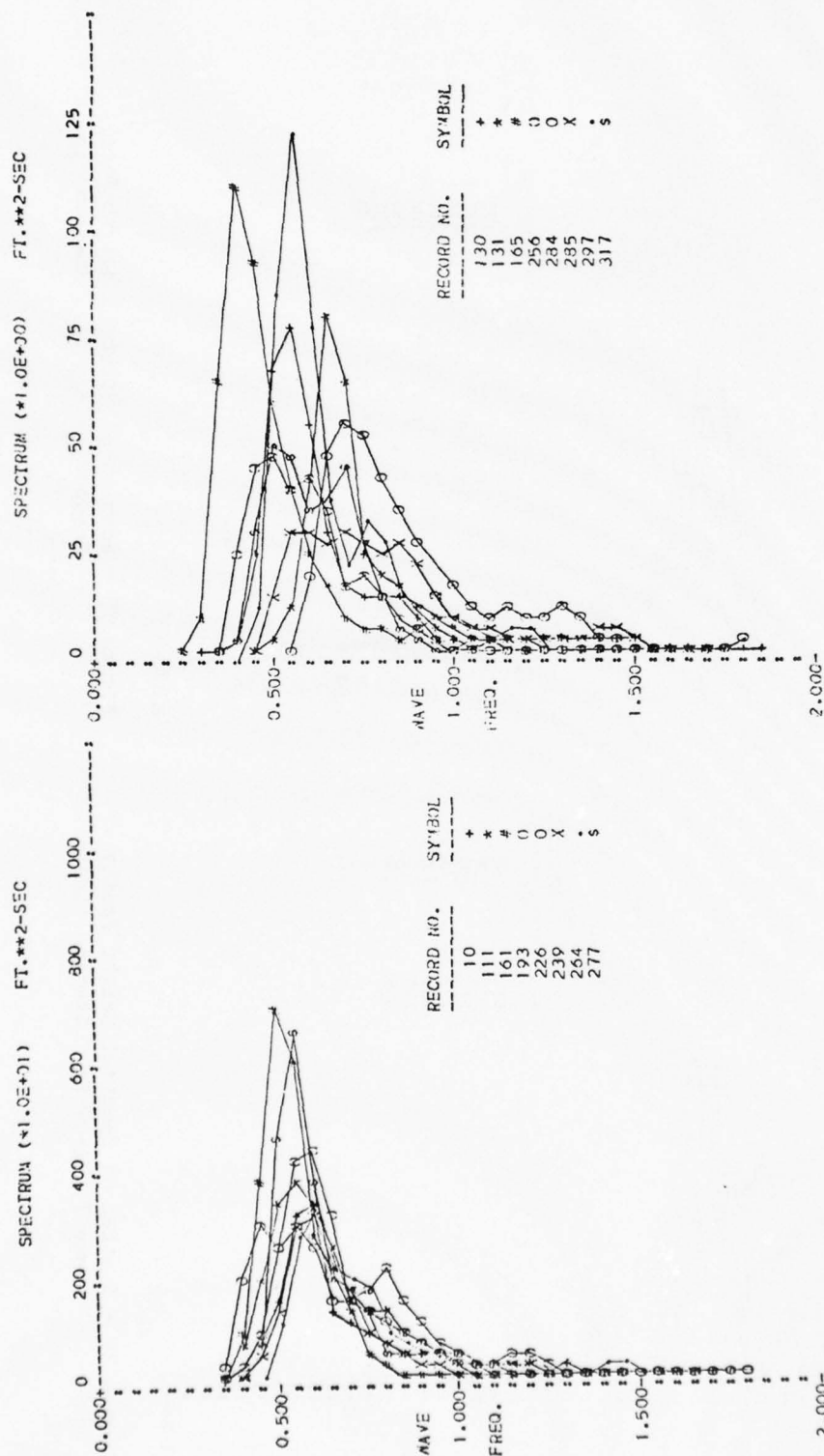
Figure 32 - Scatter of Spectral Height Family - Group 5, 12-16 ft. Station 'India'

Figure 33 - Scatter of Spectral Height Family - Group 6, 16-21 ft. Station 'India'

Figure 35 – Scatter of Spectral Height Family – Group 8, 27-34 ft. Station 'India'
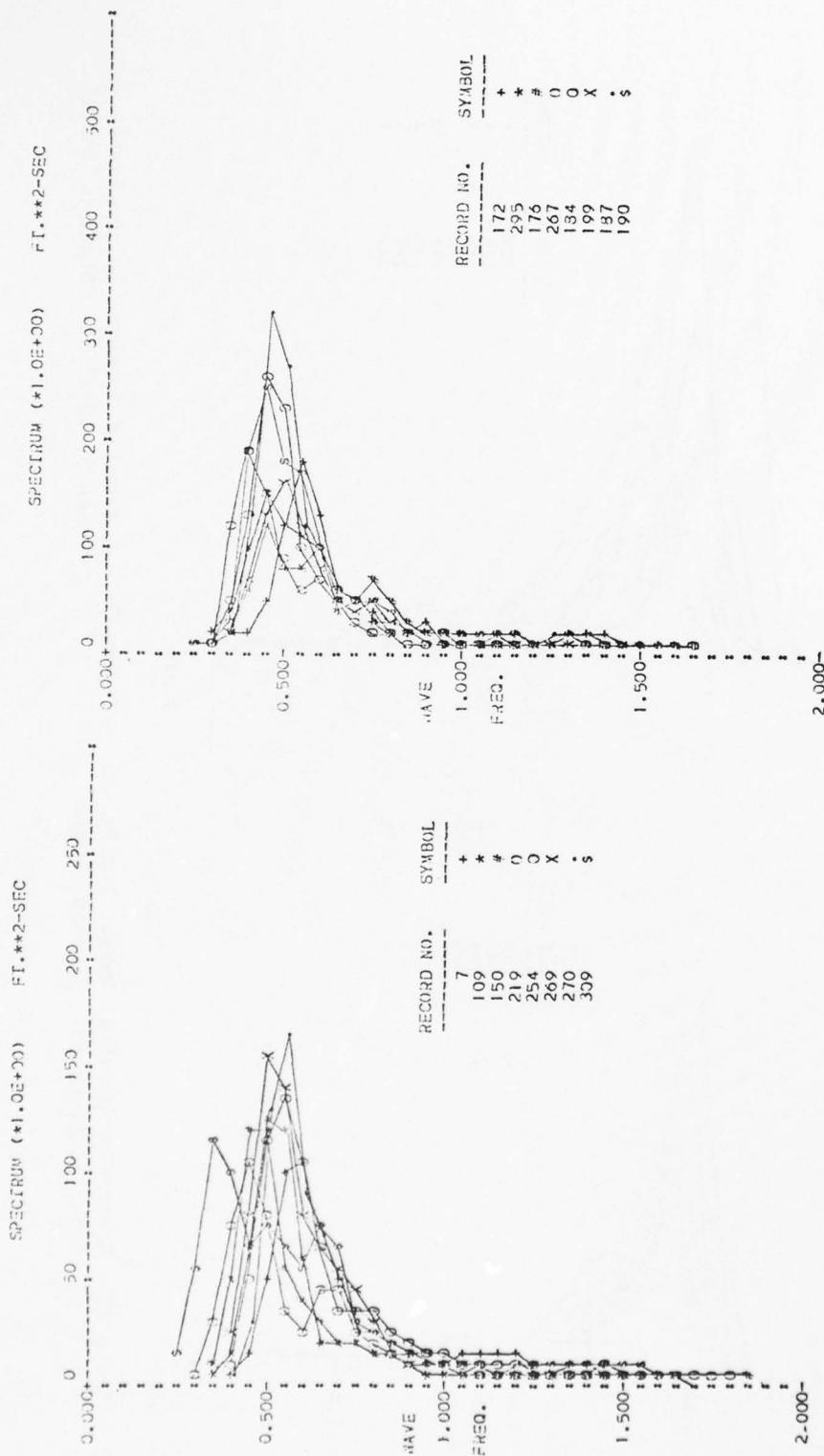
Figure 34 – Scatter of Spectral Height Family – Group 7, 21-27 ft. Station 'India'
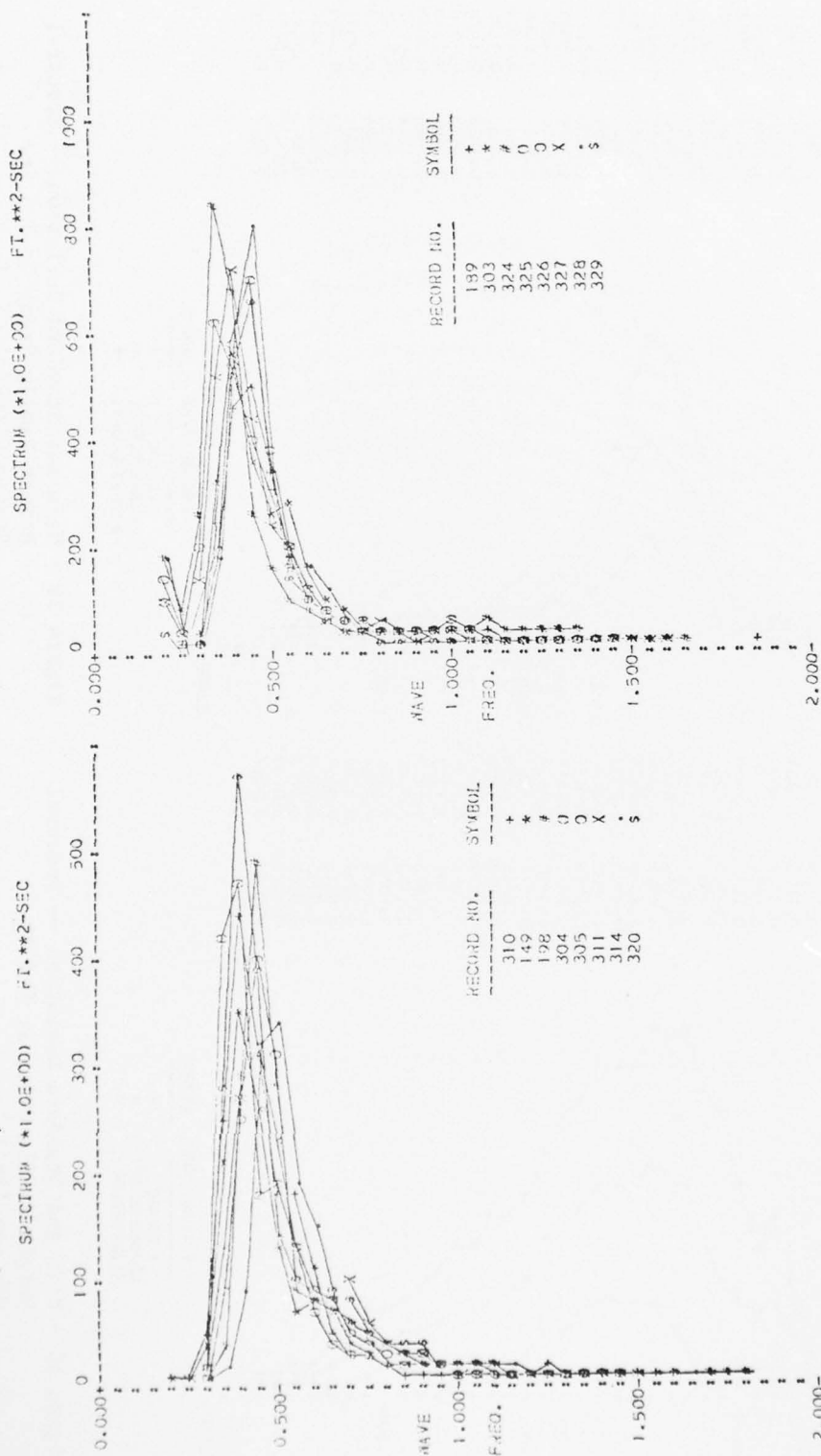
Figure 36 – Scatter of Spectral Height Family – Group 9, 34-42 ft. Station 'India'
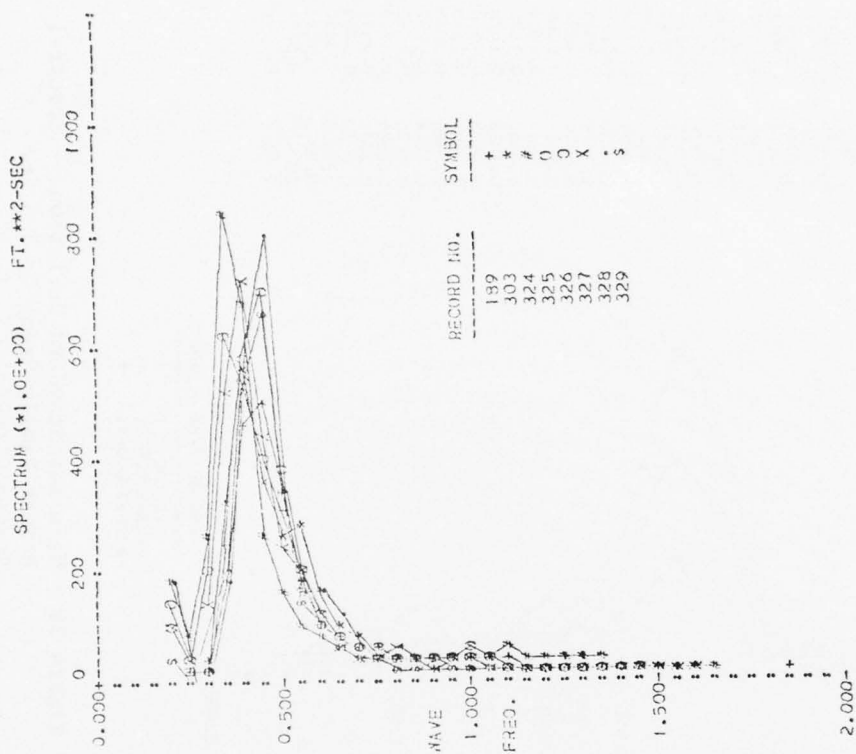
Figure 37 – Scatter of Spectral Height Family – Group 10, >42 ft. Station 'India'

SPECTRUM (*1.0E+02)   FT.**2-SEC

0.0139	0.0367
0.0502	0.0908
0.1060	0.1697
0.1794	0.1607
0.2126	0.1593
0.2994	0.0949
0.5543	0.2663
1.2198	0.7256
2.3553	1.1563
2.9263	1.5306
3.4500	2.0417
3.8542	1.8821
3.3368	1.7143
2.4477	1.2380
1.6689	0.7370
1.2358	0.6084
0.7929	0.4548
0.6409	0.4359
0.6861	0.5064
0.6051	0.4824
0.4346	0.2535
0.3232	0.1029
0.3123	0.1668
0.3101	0.1835
0.3586	0.3482
0.4214	0.4959
0.4159	0.4682
0.3326	0.3213
0.2711	0.2575
0.2333	0.2494
0.1858	0.2239
0.1214	0.1543
0.0420	0.0261
0.0182	0.0402

WAVE FREQ.

Figure 39 – Mean and Standard Deviation -- Spectral Height Family Group 2, 3-6 ft. Station 'India'

SPECTRUM (*1.0E+02)   FT.**2-SEC

0.0020	0.0053
0.0132	0.0147
0.0365	0.0369
0.1185	0.1303
0.2021	0.2009
0.1834	0.1375
0.1948	0.2860
0.2488	0.4001
0.3601	0.3514
0.4647	0.3730
0.4965	0.3405
0.5229	0.3328
0.4791	0.2681
0.4702	0.2827
0.4782	0.2671
0.4253	0.2437
0.3370	0.2510
0.3408	0.2183
0.2581	0.1897
0.2165	0.1853
0.2099	0.1909
0.1777	0.1538
0.1729	0.1531
0.1524	0.1293
0.1276	0.0961
0.1153	0.0744
0.1086	0.0666
0.0962	0.0685
0.0792	0.0772
0.0546	0.0567
0.0353	0.0258
0.0268	0.0169
0.0117	0.0133
0.0043	0.0092

WAVE FREQ.

Figure 38 – Mean and Standard Deviation -- Spectral Height Family Group 1, 0-3 ft. Station 'India'

SPECTRUM (*1.0E+01)   FT.**2-SEC

0.0000	0.0000	0.0000
0.0191	0.0171	0.0300
0.0889	0.0915	0.1020
0.2555	0.4353	0.4581
1.2853	2.9869	4.1217
3.5990	8.7719	8.4679
5.6983	15.2130	12.6011
6.3015	16.1682	11.7836
7.1357	12.4201	7.1257
8.9254	9.9642	5.2736
6.8554	10.2268	5.3224
4.1008	9.9761	4.7179
4.0273	9.0978	4.5382
3.0595	8.2108	3.7424
1.7968	6.1510	3.4437
1.9871	5.1621	3.6231
1.6547	4.3695	3.4038
0.9652	3.3386	3.3430
1.2289	2.5665	2.5450
0.6338	1.8311	1.6056
0.6506	1.7474	1.2090
0.7321	1.5707	0.9805
0.7470	1.1414	0.5885
0.7797	1.0912	0.5321
0.4704	1.0768	0.4620
0.3459	1.0576	0.3902
0.3249	1.0220	0.4450
0.2765	0.9834	0.5675
0.1631	0.8942	0.5830
0.1528	0.7533	0.4594
0.2385	0.5931	0.4530
0.2704	0.4080	0.3480
0.1479	0.2367	0.1699
0.1182	0.0889	0.1754
0.0487		

Figure 41 – Mean and Standard Deviation -- Spectral
Height Family Group 4, 9-12 ft.
Station 'India'

RECORD TYPE   SYMBOL
-----------   ------
AVERAGE   +
MEAN-STD.DEV.   *
MEAN+STD.DEV.   #

SPECTRUM (*1.0E+01)   FT.**2-SEC

0.0000
0.0505
0.1057
0.2142
1.3618
4.3747
5.9829
4.1038
2.0029
5.3567
3.9071
2.4752
2.7494
1.7968
1.9871
1.0547
0.9289
0.6338
0.6506
0.7321
0.7470
0.7797
0.4704
0.3459
0.3249
0.2765
0.1631
0.1528
0.2385
0.2704
0.1479
0.1182
0.0487

Figure 40 – Mean and Standard Deviation -- Spectral
Height Family Group 3, 6-9 ft.
Station 'India'

RECORD TYPE   SYMBOL
-----------   ------
AVERAGE   +
MEAN-STD.DEV.   *
MEAN+STD.DEV.   #

-73-

SPECTRUM (*1.0E+00)   FT.**2-SEC
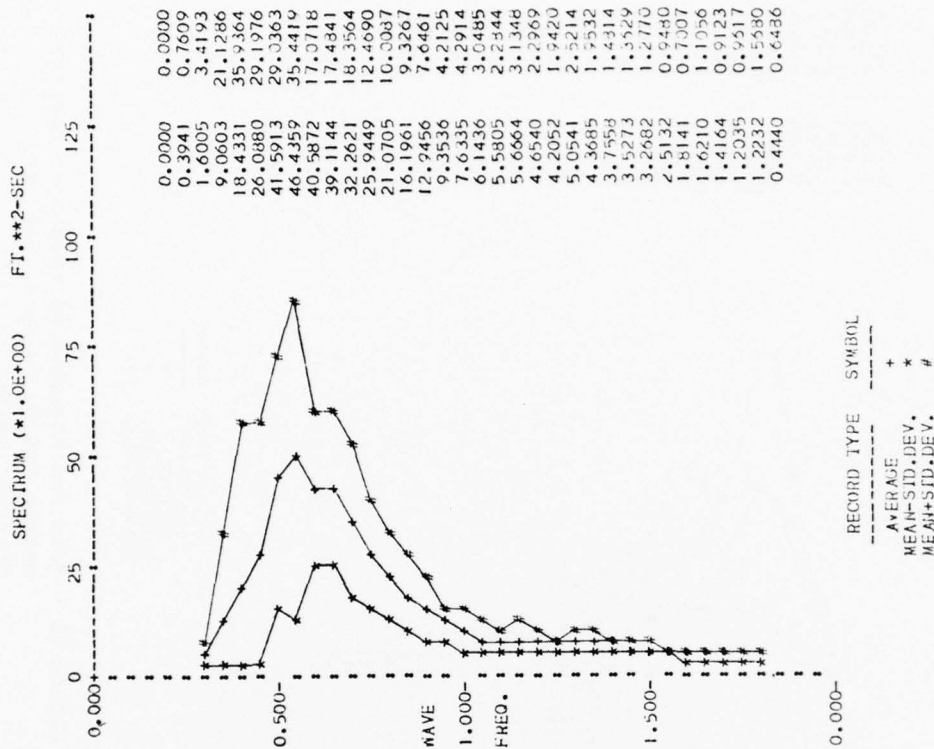
Figure 43 – Mean and Standard Deviation -- Spectral Height Family Group 6, 16-21 ft. Station 'India'

SPECTRUM (*1.0E+01)   FT.**2-SEC

Figure 42 – Mean and Standard Deviation -- Spectral Height Family Group 5, 12-16 ft. Station 'India'

SPECTRUM (*1.0E+00)   FT.**2-SEC

0.2499	0.6611
3.3618	1.7628
7.6591	5.6021
37.8569	31.9896
111.1989	57.7978
179.2877	83.2645
157.1213	61.1390
116.8767	39.0965
92.7993	19.7671
54.1333	5.9901
45.5175	7.7476
39.4263	15.8720
27.4957	11.2758
20.5170	4.1752
16.7729	5.0726
13.6727	3.2539
11.8770	4.5513
10.4970	3.9753
12.0326	5.4490
11.9805	6.1021
8.6382	4.2407
8.1771	4.6246
10.0329	7.6488
9.5912	6.1005
8.7651	4.8341
7.3916	4.0588
5.8654	3.4638
4.3387	2.4584
3.6051	1.5938
3.6227	1.8293
2.4359	1.0715
0.7906	0.6180
0.5335	0.9202
0.0390	0.1032

RECORD TYPE   SYMBOL

AVERAGE	-
MEAN-STD.DEV.	+
MEAN+STD.DEV.	*
	#

Figure 45 - Mean and Standard Deviation -- Spectral Height Family Group 8, 27-34 ft. Station 'India'

SPECTRUM (*1.0E+00)   FT.**2-SEC

0.1438	0.3937
2.6560	5.5199
8.3075	17.6983
21.2975	37.4098
34.6921	32.5947
66.1179	33.8770
106.1445	32.9378
101.3971	43.1075
70.2815	27.9345
56.1685	19.4755
42.4107	14.4955
29.4702	8.2006
25.1109	6.6461
18.2739	4.7446
15.7954	2.4426
12.0440	2.8884
10.8422	2.3712
9.3437	3.1000
7.4056	3.8012
6.4804	3.5079
7.2290	3.8799
7.4116	3.4764
6.0847	2.6247
5.9477	2.6306
6.2302	2.7984
5.7978	2.1703
4.7223	1.9815
3.9953	2.1805
3.0641	1.7946
1.8823	1.3681
1.2750	1.2700
1.2210	0.8695
1.1867	1.0530
0.9452	0.9028

RECORD TYPE   SYMBOL

AVERAGE	-
MEAN-STD.DEV.	+
MEAN+STD.DEV.	*
	#

Figure 44 - Mean and Standard Deviation -- Spectral Height Family Group 7, 21-27 ft. Station 'India'

Figure 46 - Mean and Standard Deviation -- Spectral Height Family Group 9, 34-42 ft. Station 'India'
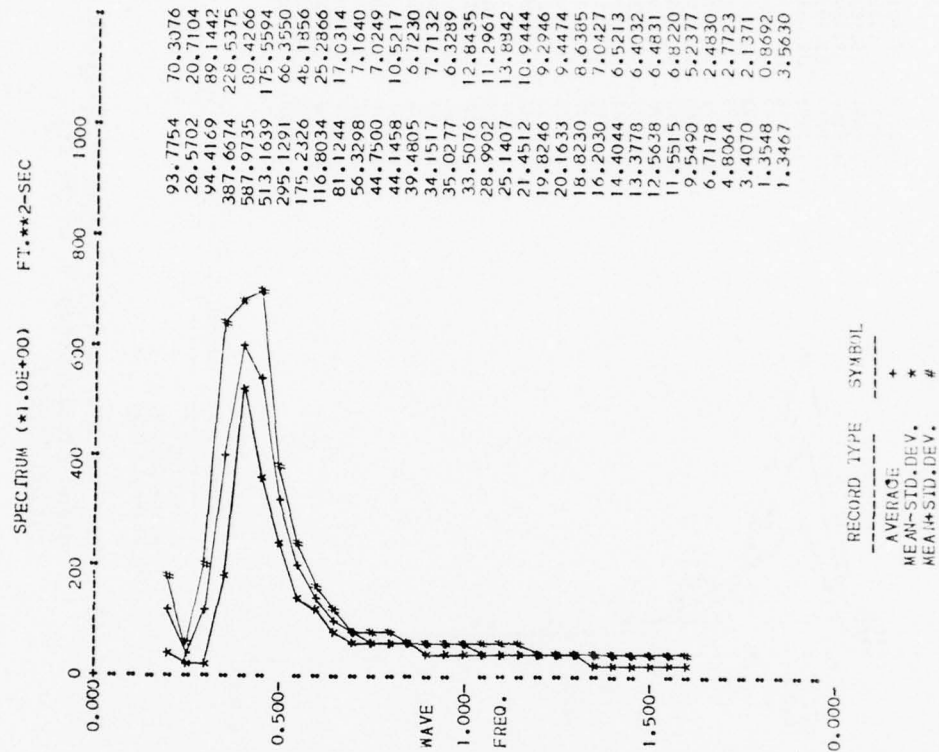
Figure 47 - Mean and Standard Deviation -- Spectral Height Family Group 10, >42 ft. Station 'India'

VIII.   EFFECT OF VARIATION IN WAVE DATA FORMAT ON LOAD PREDICTIONS

Comparative Calculations

From the point of view of the naval architect, the only variations in wave data which are of concern are those which affect his predictions of ship motions and loads. It follows that those variations in wave data which have the greatest effect on the accuracy of his predictions are of greatest concern. The following discussion will indicate the effect of a number of variations in wave data format on load predictions, using as examples vertical bending moment for the 496-foot general cargo carrier Wolverine State, the 880-foot SL-7 high-speed container ship, the 1082-foot tanker Universe Ireland, and the design for a 1300-foot 600,000-ton VLCC (based on theortically derived RAOs).

As previously noted, the determination of the adequacy of specific wave data for ship response calculations is a function not only of the wave parameters but also of the wave spectral shape characteristics. Hence, the availability of wave data, such as the height and period values and their frequency of occurrence for certain locations as a function of the season or direction of propagation, is not adequate for performing the prediction of ship responses and loads in irregular seas. A definition of the sea surface in the form of spectra must be available, along with the basic transfer function given as the response to unit wave height as a function of wave frequency. Ideally, as previously discussed, measured spectra for the specific area of interest are preferred. However, the limited availability of such wave data has led to the substitution of mathematical formulations for the actual spectra. The usual input parameters required to generate a theoretical spectrum include wave height and period, though other additional parameters such as fetch, or the spectral peak frequency, have been shown to define a more realistic spectral shape. (See Chapter V).

Fig. 48 illustrates seven spectra, all having roughly the same period and height parameters, plotted in a non-dimensional form. Also shown are the mean line and the equivalent two-parameter ideal spectrum corresponding to the mean height and period of the seven records. When plotted non-dimensionally in this way, the theoretical spectrum is represented by a single line for all choices of $H_{1/3}$ and T_1, thus eliminating variations in the spectra resulting from small differences in $H_{1/3}$ and T_1. Hence, the difference between each of the seven spectral shapes and the single mean theoretical spectrum represents actual variations in shape.

The large scatter of measured spectra about the mean over the entire frequency range is of great significance and would naturally lead to scatter in the response spectra as well as in the rms values. Even though the mean spectrum is not appreciably different from the mean theoretical line, this fact bears no significance as to the suitability of the theoretical spectrum to represent sea conditions of this severity.

One approach commonly used to obtain short and long-term response predictions when measured spectra are not available is to obtain some indication
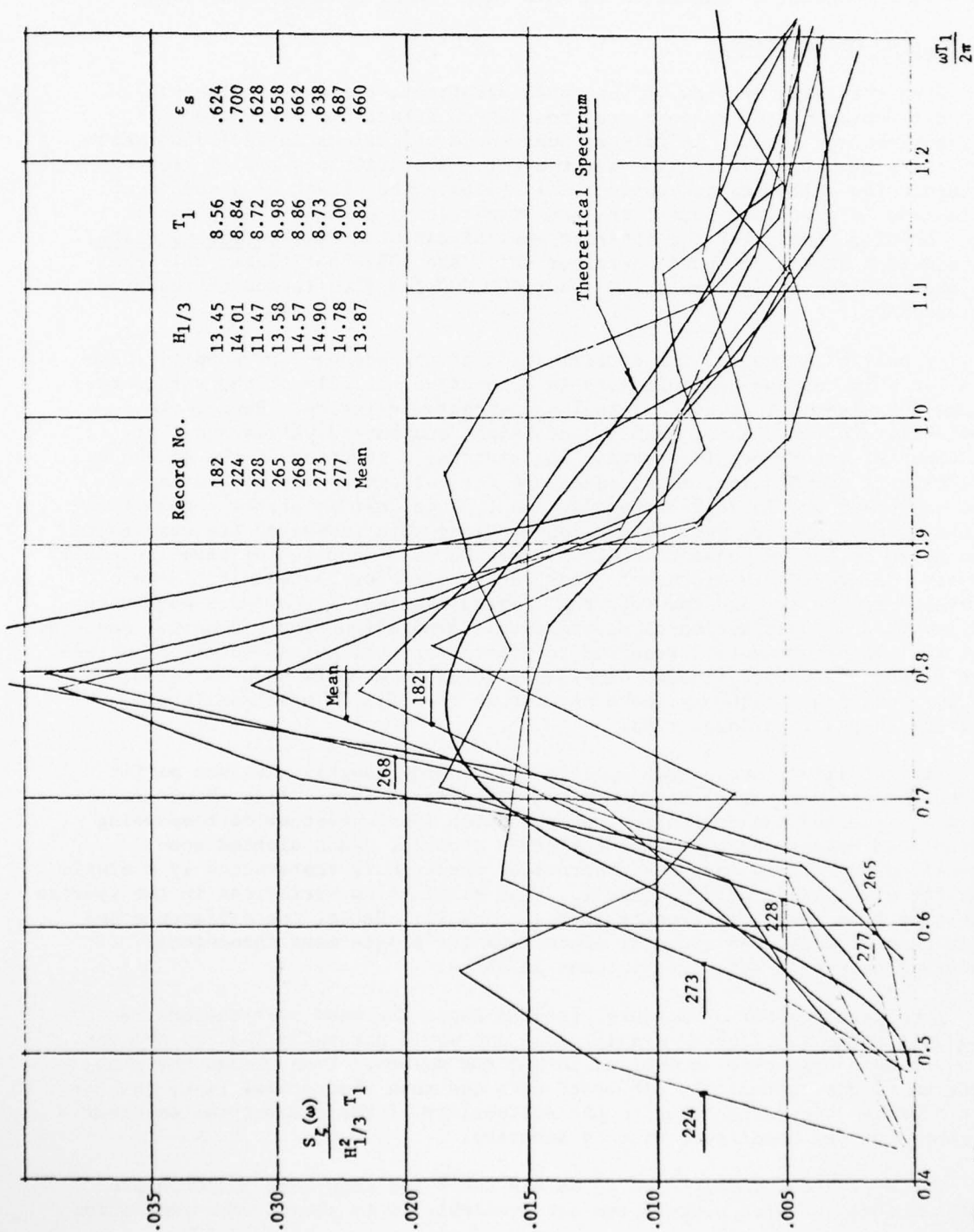
Fig. 48 – Comparison of Spectral Shape Variation.

Record No.	$H_{1/3}$	T_1	ϵ_s
182	13.45	8.56	.624
224	14.01	8.84	.700
228	11.47	8.72	.628
265	13.58	8.98	.658
268	14.57	8.86	.662
273	14.90	8.73	.638
277	14.78	9.00	.687
Mean	13.87	8.82	.660

$$\frac{S_\zeta(\omega)}{H_{1/3}^2\, T_1}$$

$$\frac{\omega T_1}{2\pi}$$

of scatter by means of the distribution of the various period groups within the bounds of each wave height group, using a mathematical formulation to describe the various spectra, each defined by its own characteristic period. While this method yields some measure of scatter, it fails to take into account the variation in spectral shapes discussed above. This would naturally result in a lower predicted long-term extreme value, due to the smaller standard deviation in RMS response. Further doubt is cast on this method by the extreme uncertainty in the observed period information. Of the three commonly observed parameters, height, period and direction, period is by far the most uncertain.

Finally, we may consider the approach described in the preceding chapter-- the use of a random sample of wave spectra classified by area or significant height. In this chapter the use of various formulations will be compared to the results obtained by this method. To summarize, the following formats are compared:

Formulations

ITTC   one-parameter spectrum, in which wave height is the only parameter,

ISSC   two-parameter spectrum, in which both significant height and average period are included.

Families

"H-Family"   original Webb random sample, Lewis (1967)

Station "India"   new Webb samples from the
Station "Kilo"   North Atlantic, Hoffman (1972, 1975)

Station "Papa"   New Webb sample from N. Pacific, Hoffmann (1974)

The effect on short-term bending moment predictions of using a number of data sources is shown in Figs. 49 through 51. See also Hoffman (1975a) and Hoffman (1975b). These figures show the mean and standard deviation of rms bending moment as a function of significant wave height. The various spectral families were created by classifying measured spectra from the various sources by significant wave height ($H_{1/3}$) and then choosing a number (usually eight) to represent each wave height range, as outlined in the previous chapter. It may be seen from the figures there are significant differences in the case of the small Wolverine State, less differences in the SL-7, and relatively small differences in the case of the large tanker, Universe Ireland.

In order to evaluate the effect of these different sources of wave data on long-term predictions Figs. 52 through 54 compare the long-term predictions based on the means and standards deviations discussed above. The wave height distributions used in these calculations are given in Table 7. It can be seen

-79-
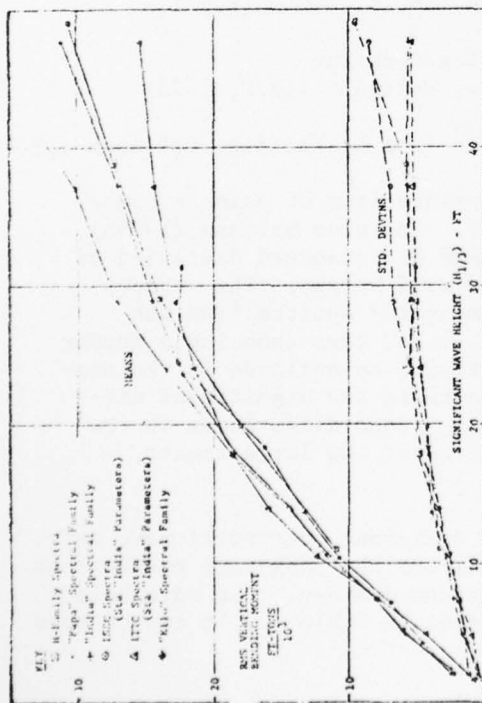
Fig. 49 – Short-Term Bending Moment Responses for Light Load *WOLVERINE STATE* — Mean RMS and Standard Deviation.
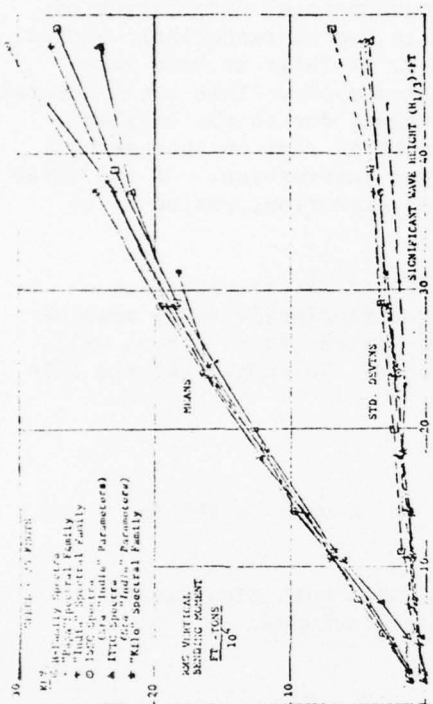
Fig. 50 – Short-Term Bending Moment Responses for Full Load SL-7 Containership — Mean RMS and Standard Deviation.
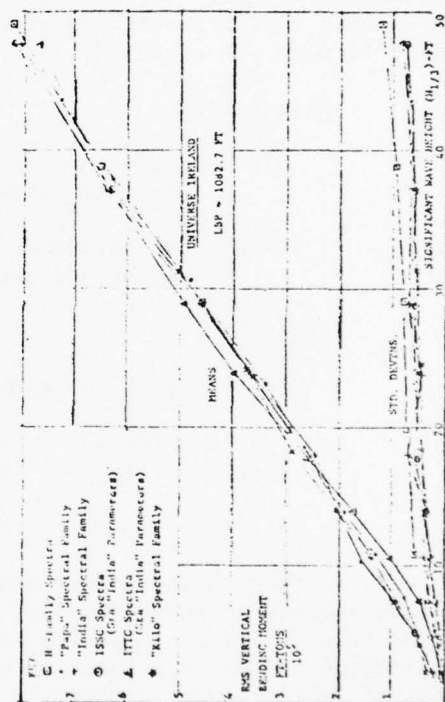
Fig. 51 – Short-Term Bending Moment Responses for *UNIVERSE IRELAND*, Mean RMS and Standard Deviations.
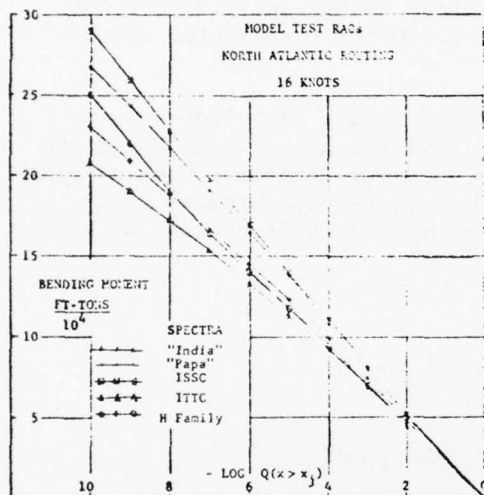
Fig. 52 - Long-Term Vertical Bending
Moment for Light Load
WOLVERINE STATE for Five
Spectral Families.
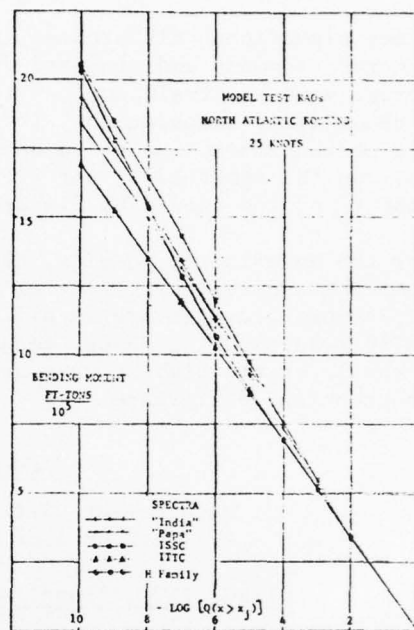
Fig. 53 - Long-Term Vertical Bend-
ing Moment for Full-Load
SL-7 Containership for
Five Spectral Families.
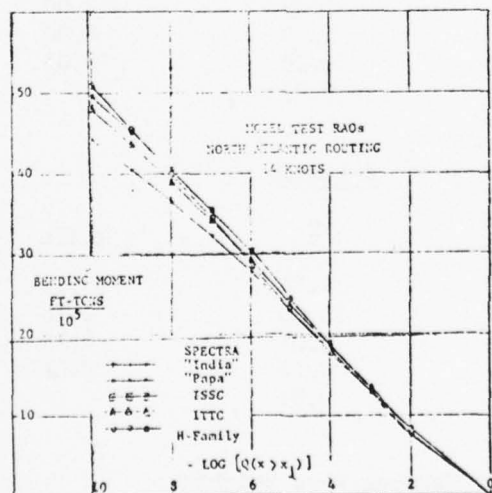
Fig. 54 - Long-term Vertical Bending
Moment for Full-Load
UNIVERSE IRELAND for Five
Spectral Families.

that there are significant differences in the results, because of the variations in both mean rms response and standard deviation. Since the calculation based on actual wave spectral families is believed to be more accurate than use of the theoretical formulations, it is concluded that in most cases the ISSC formula overestimates the trend and therefore is not satisfactory for general use. On the other hand, the ITTC one-parameter formulation under-estimates the trend and should be discarded.

As for the wave family results, the "India" family is believed to be the most complete and reliable,especially for a wide range of ship types and sizes. Furthermore, results are in all cases in close agreement with simpler early H-family results. The "Papa" results differ, perhaps because of an inadequate sample of the highest wave height groups, as well because of pos-sible oceanographical difference.

Table VII

Wave Height Distributions Used in
Section 1 of Chapter VIII

ISSC, ITTC, 'Papa' and 'India' Families

Range (ft)	%	Cum.
0- 3	8.75	91.25
3- 6	23.75	67.50
6- 9	30.70	36.80
9-12	20.35	16.45
12-16	6.90	9.55
16-21	4.95	4.60
21-27	2.69	2.00
27-34	1.70	0.30
34-42	0.25	0.05
>42	0.05	

H-Family

Range (ft)	%	Cum.
5-15	84.54	15.46
15-25	13.30	2.16
25-35	2.01	0.15
35-45	0.14	0.01
>45	0.01	

Probability of Occurrence of Various Wave Heights

The previous predictions of long-term responses utilized an assumed probability of occurrence of wave height, usually expressed in groups covering

various ranges, as well as the rms response distribution for each of these wave height groups. Thus, in evaluating the reliability of long-term predictions the accuracy of the wave height distribution, as well as the accuracy of the rms response and its scatter in each wave height group, must be considered.

In the previous section, where the effect of spectral shape was explored, the distribution of wave heights was taken to be -- as nearly as possible -- the same. However, as might be expected, the long-term prediction, i.e., the value to be exceeded once in say 10^8 cycles, is quite sensitive to the probability of occurrence of the highest few wave groups. This is due to the fact that, in spite of their small probability of occurrence, the magnitude of response when these wave height ranges do occur, is expected to be quite high.

Table 8 shows several different wave height distributions for the North Atlantic. The column labeled "Hogben & Lumb" was obtained by combining the results in Hogben (1967) of areas 2, 6, 7 (the areas covering the North Atlantic) weighing 2 twice and 6 and 7 once each. The column labeled "H. Walden" was derived using data on the probability of occurrence of various wave heights at weather ships in the North Atlantic given in Walden (1964). In the distribution labeled "H. Walden modified" the percentage occurrence of the highest group was arbitarily increased to simulate possible extremely severe conditions.

The following Table 9 shows the effect of the different wave height distributions on calculated long-term vertical bending moments for three ships. It may be seen that the small differences above 21 feet between the two H. Walden distributions has a significant effect on response. The results from Hogben and Lumb data are somewhat lower, possibly because the ships on board which observations were obtained tended to avoid heavy seas whenever possible.

Table VIII

North Atlantic Wave Height Distributions

$H_{1/3}$ Range (ft)	H. Walden (modified) %	Cumm.	H. Walden %	Cumm.	Hogben & Lumb %	Cumm.
0- 3	8.75	91.25	8.75	91.25	11.210	88.79
3- 6	23.75	67.50	23.75	67.50	36.524	52.27
6- 9	30.70	36.80	30.70	36.80	25.916	26.35
9-12	20.35	16.45	20.35	16.45	13.690	12.66
12-16	6.90	9.55	6.90	9.55	7.544	5.12
16-21	4.95	4.60	4.95	4.60	2.232	2.88
21-27	2.69	2.00	3.350	1.25	2.126	0.076
27-34	1.70	0.30	1.060	0.190	0.743	0.015
34-42	0.25	0.05	0.168	0.022	0.0121	0.0029
>42	0.05*		0.022		0.0029	

* Percentages for highest groups were changed, as discussed in text.

MICROCOPY RESOLUTION TEST CHART

NATIONAL BUREAU OF STANDARDS-1963
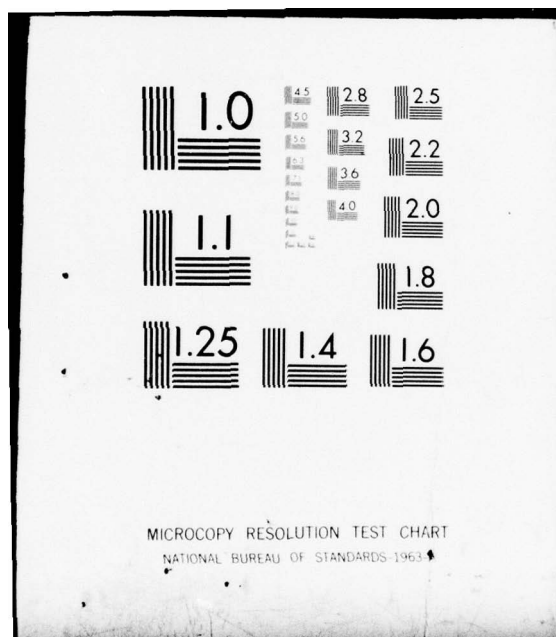
Table IX

Long-Term Vertical Bending Moment Predictions for Various North Atlantic Wave
Height Distributions
Values expected to be exceeded once in 10^8 cycles, ft -tons

	H. Walden (modified)	H. Walden	Hogben and Lumb
Wolverine State 496 ft., 16-knot, light load	1.882×10^5	1.846×10^5	1.770×10^5
SL-7 880.5 ft., 15-knot, full load	1.542×10^5	1.475×10^5	1.3034×10^6
Universe Ireland 1082.7 ft., 14-knot, full load	4.043×10^6	3.872×10^6	3.4210×10^6

Another set of wave height distributions, developed by Hoffman from
Hogben and Lumb (1967) data for eight different world shipping routes, is
summarized in Table 10 in cumulative form. It may be seen that No. 1 "Most
Severe North Atlantic," is the same as "H. Walden modified" in Table 8.
Calculated long-term bending moments for a 600,000-dwt VLCC design are
given in Table 11 for all of the above routes. It may be seen that a wide
variation in wave height distributions produces considerable variation in
long-term response.

Thus it can be seen that for accurate long-term predictions reliable
values for probability of occurrence of the various wave height groups
are necessary. If the 10^8 value is required, the highest three wave groups
seem to be of greatest importance.

Table X

Wave Height Distributions – World Routes
Frequency of Exceedance of
Average Significant Wave Height $H_{1/3}$

Route No.	1	2	3	4	5	6	7	8
Mean $H_{1/3}$(ft)								
2	100.00	100.00	100.00	100.00	100.00	100.00	100.00	100.00
4	91.25	86.37	88.79	77.62	82.26	82.72	74.56	79.64
8	67.50	68.17	71.14	35.12	56.62	57.60	29.16	54.38
10	36.80	35.41	36.01	13.07	19.03	19.96	9.32	20.50
15	16.45	17.51	17.18	2.83	6.46	6.82	3.03	8.81
20	9.55	4.88	4.55	1.41	1.07	1.13	0.51	2.14
25	4.60	2.70	2.56	0.80	0.42	0.48	0.18	1.10
30	2.00	1.07	0.97	0.43	0.12	0.15	0.09	0.40
35	0.30	0.35	0.31	0.17	0.03	0.04	0.04	0.13
50	0.05	0.02	0.01	0.02	0.01	0.01	0.01	0.01

1. Most severe North Atlantic
2. North Atlantic (Northern Europe)
3. North Atlantic (Southern Europe)
4. Europe -- Persian Gulf via South Africa
5. North Pacific
6. Europe -- Persian Gulf via Suez Canal
7. Persian Gulf -- USA
8. Europe -- USA West Coast

Table XI

Long-term Vertical Bending Moment Predictions for
Different World-Wide Wave Height Distributions
600,000 dwt VLCC, Full Load
Value expected to be exceeded once in 10^8 cycles, ft.-tons

Speed 30.06 ft/sec., 17.8 knots

	Route							
	1	2	3	4	5	6	7	8
Vertical Bending Moment $\times 10^{-6}$	7.3806	7.0596	6.7469	6.7012	7.0074	6.7473	6.7460	6.7580

-85-

Directional Information

A third factor in addition to spectral shape and probability of occurrence of wave heights which affects ship motions and load predictions is the probability distribution of relative angles between ship heading and wave directions. As refinement in the incorporation of variation in spectral shape takes place and more accurate information on the probability of occurrence of wave height groups becomes available, more attention must be given to directional information. Certain responses such as acceleration at the F.P. are very sensitive to heading angle. Others, such as vertical bending moment, are not quite as sensitive.

The following figures illustrate the magnitude of the contributions from various heading angles and wave height groups to the total probability of exceeding particular acceleration and vertical bending moment values for the Wolverine State, assuming equal probabilities of all headings. A cosine-squared spreading function has been used. In Fig. 55, the total volume of the solid is the probability that the amplitude of the acceleration at the forward perpendicular will exceed 58.2 ft/sec^2. If the average period is approximately 11 seconds, the acceleration of 58.2 ft/sec^2 will be expected to occur once in 20 years, the approximate lifetime of a ship. It can be seen that the largest contribution comes from head seas in the largest wave height group. This occurs because, even though the probability of occurrence of the lower wave height groups is larger, the probability of exceeding 58.2 ft/sec^2 is extremely remote for those groups.

Fig. 56 shows a similar plot, in this case for the probability of acceleration at the F.P. exceeding 29.4 ft/sec^2. Here the largest contribution comes from the eighth wave height group. This happens because the large probability of exceeding the stated value in the large wave height group is outweighed by the larger probability of occurrence of the eighth wave height group.

Fig. 57 shows the probability of the amplitude of the vertical bending moment exceeding 9.6 x 10^4 ft.-tons. Again it can be noted that the largest contribution does not come from the highest wave height group.

These figures show the trends in importance of various heading and wave height groups relative to predicted ship responses. These plots also show the importance of the role played by the largest wave height groups. The lower wave height groups make no contribution to the maximum value expected in the lifetime of the ship. The large variation in the contributions of different heading angles indicates the need for reliable ship heading and wave direction information.

It should be noted that the method used in the treatment of heading angle here and outlined in Chapter VII is different from that used in Lewis (1967) and as derived in the appendix by Karst to Hoffman (1972a). Previously, it was assumed that the rms response was normally distributed in each wave height group, involving all headings. Now the more accurate assumption is made that the rms response is only normally distributed at each heading, with the result that the actual distribution of all rms values obtained by combining all headings is not normal.
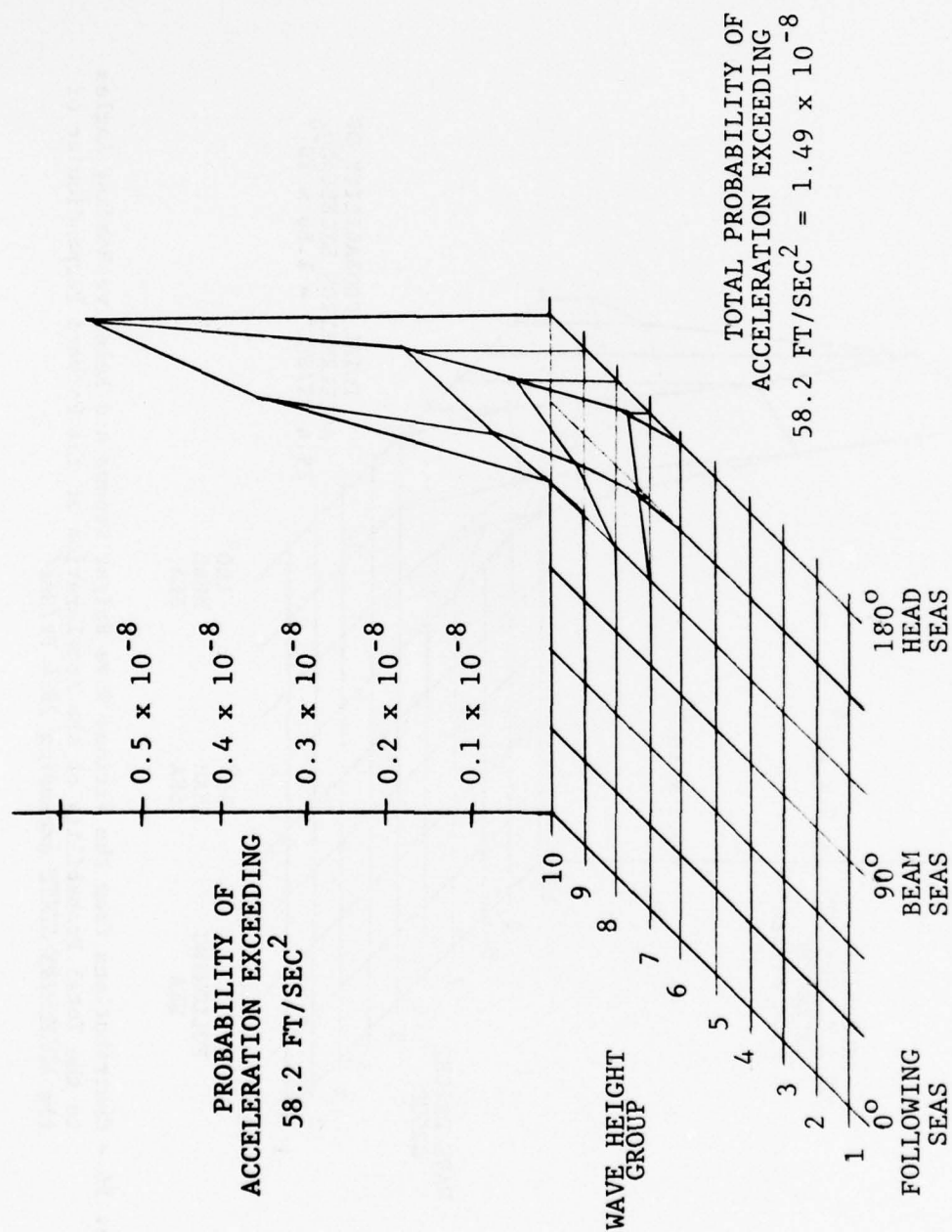
Figure 55 Contributions from the Various Wave Height Groups and Relative Heading Angles to the Total Probability of the Acceleration at the Forward Perpendicular of the Wolverine State exceeding 58.2 ft./sec^2.
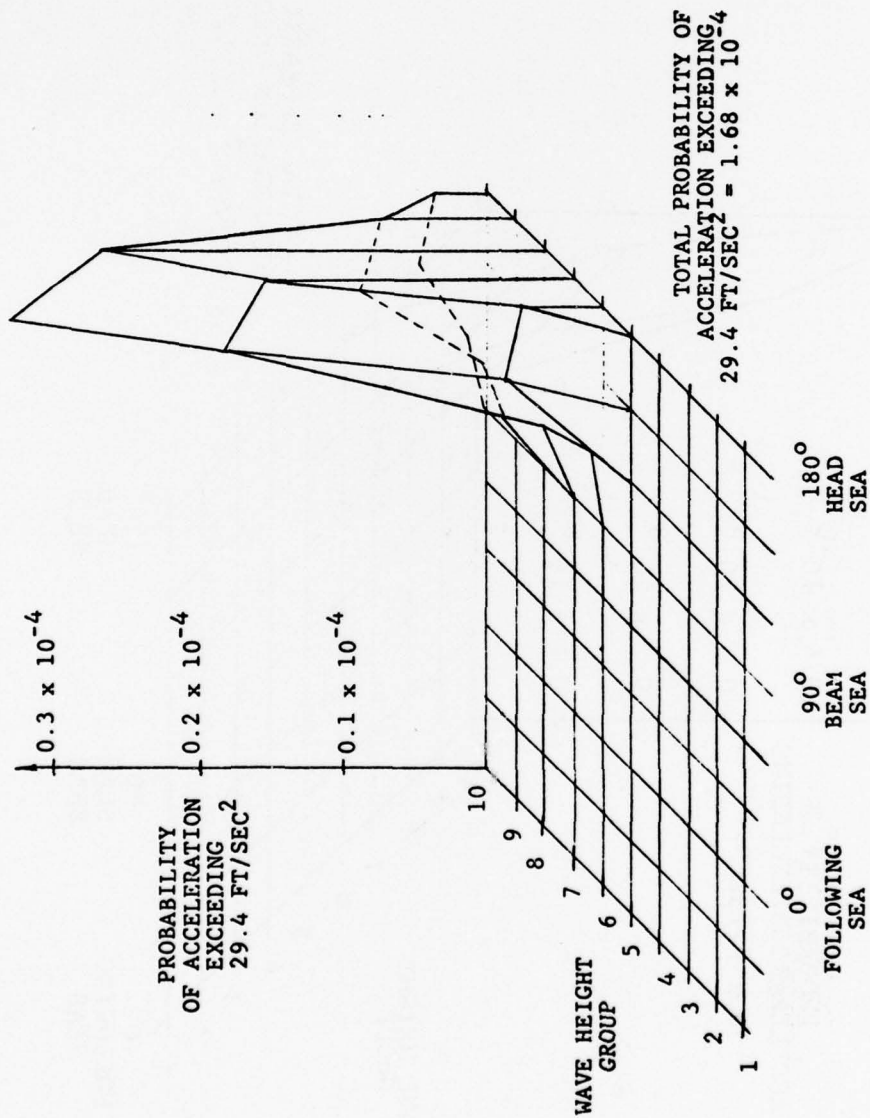
Fig. 56 – Contributions from the Various Wave Height Groups and Relative Heading Angles to the Total Probability of the Acceleration at the Forward Perpendicular of the *WOLVERINE STATE* exceeding 29.4 Ft/Sec^2.
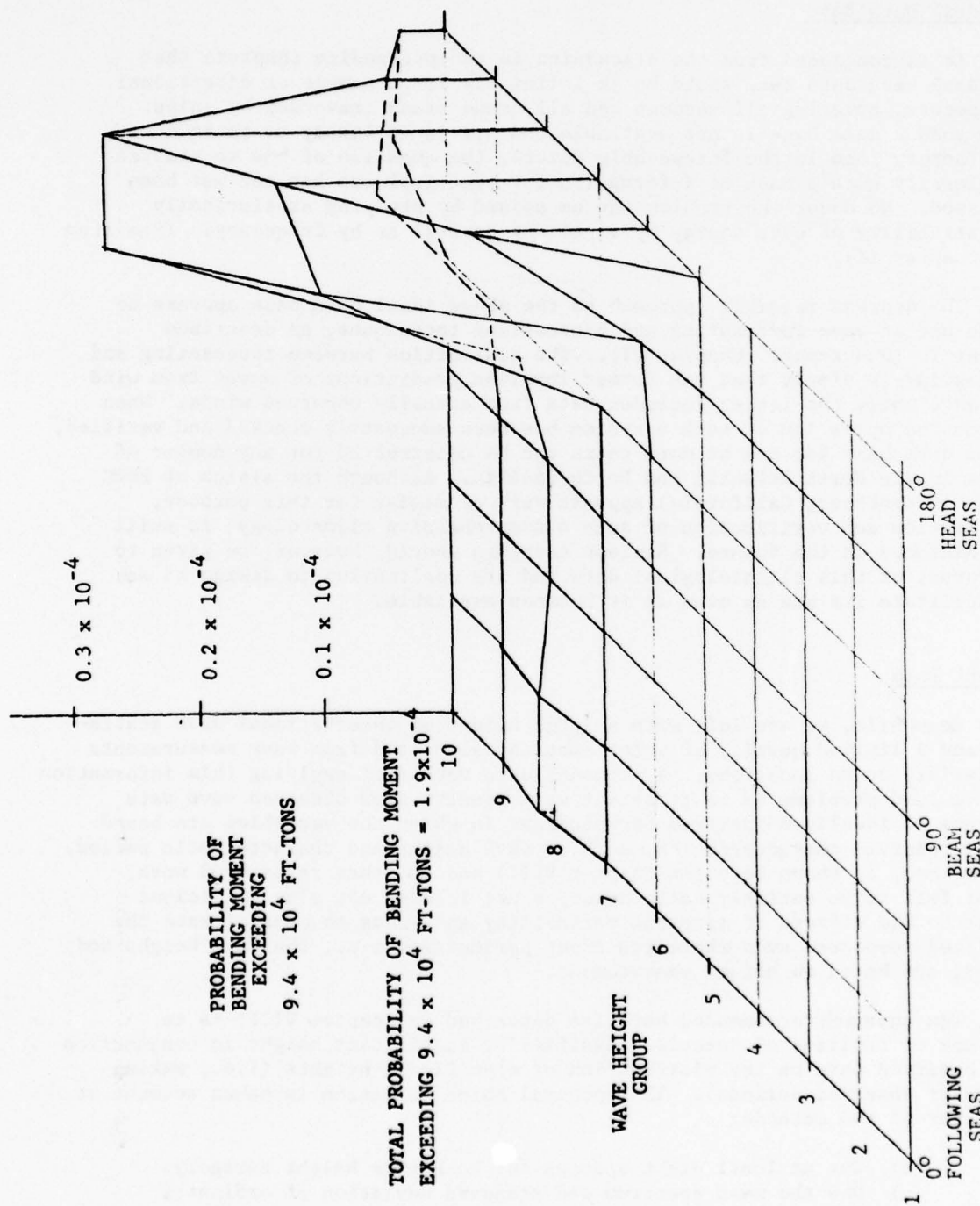
Fig. 57 – Contributions from the Various Wave Height Groups and Relative Heading Angles to the Total Probability of the Vertical Bending Moment of the *WOLVERINE STATE* Exceeding 9.6 x 10⁴ Ft-Tons.

IX.   WAVE DATA FOR USE IN DESIGN

The Ideal Data Base

It is concluded from the discussion in the preceeding chapters that
the ideal wave data base would be an infinitely large sample of directional
sea spectra, covering all seasons and all ocean areas traversed by ships.
Since such a data base is not available now nor is it likely to be in a
satisfactory form in the foreseeable future, the question of how to analyze
and classify such a mass of information for practical use has not yet been
addressed. No doubt the problem can be solved by studying statistically
the variability of wave energy by direction as well as by frequency. (See item
8 in Chapter II).

The nearest feasible approach to the above ideal data base appears to
be the use of wave forecasting and hindcasting techniques, as described
earlier in this report (Chapter VI). The distinction between forecasting and
hindcasting is simply that the former involves predictions of waves from wind
forecasts while the latter includes data from actually observed winds. When
the routine operation of such a system has been adequately checked and verified,
then a data base for one or more years can be constructed for any number of
points in the North Atlantic and North Pacific. Although the system of FNWC
(based in Monterey, California) appears very promising for this purpose,
the creation and verification of such a comprehensive climatology is still
some distance in the future. Serious thoughts should, however, be given to
the format of this climatological data and its application to design so as
to facilitate its use as soon as it becomes available.

Present Data

Meanwhile, we are left with a large amount of observational wave statis-
tics and a limited quatity of point spectra calculated from wave measurements
at specific ocean locations. A commonly used method of applying this information
to wave load problems is to construct wave spectra from observed wave data
by means of idealized spectrum formulations in which the variables are based
on the observed characteristics, such as wave height and characteristic period.
This method, as shown here (in Chapter VIII) and in other referenced work,
is not felt to be entirely satisfactory since it does not give sufficient
weight to the effects of spectrum variability and seems to overestimate the
predicted responses even where the input parameters, i.e., the wave height and
period, are based on actual measurement.

The approach recommended here (as described in Chapter VIII) is to
make use of families of spectra classified by significant height in conjunction
with observed data on the distribution of significant heights (i.e., making
no use of observed periods). The spectral shape variation is taken account of
by either of two methods:

      a)   Use at least eight spectra for each wave height category.
      b)   Use the mean spectrum and standard deviation of ordinates
         for each wave height category.

A standard cosine-squared spreading function would be applied to take
account approximately of short-crestedness, and unless information to the
contrary is available equal probability of all headings would be assumed.

Speed can be accounted for by selecting RAOs for the maximum reasonable
speed to suit each wave height category. No specific allowance need be made
for the possible effect of more than one storm -- or sea and swell -- com-
bined, other than the inclusion of such conditions in the statistical sample
of wave spectra used.

The effect of variation in ship cargo loadings on wave bending moment
can in many cases be ignored. But where large variations in draft are
possible -- as between full load and ballast conditions of mammoth tankers --
completely separate calculations should be made for these two conditions of
loading. See Lewis, et. al. (1973).

As indicated in Chapter III, the recommended sources of observational
data for determining the wave height distribution are as follows:
>   Hogben and Lumb (1967) for the North and Central Atlantic,
>   Indian Ocean, and South Pacific.
>   Yamanouchi and Ogawa (1970) for the North Pacific.
>   U.S. Navy, Summaries of Synoptic Meteorological Observations
>   for regions which they cover (see Appendix B).

The recommended wave spectral families are those derived by Hoffman (1975)
from Station 'India' records, as given in Chapter VIII in the two forms:
>   a) Eight representative spectra for each group.
>   b) A mean spectrum and standard deviations for each group.

The Future

The previous chapters have indicated the continuing need for more
data in order, for example, to stratify spectra further, to improve statistics
of wave height occurrence and to evaluate hindcasts and forecasts. A number
of projects that will help fulfill these needs, some still in the planning
stage and some already operational on an experimental basis, are discussed below.

Satellites. The GEOS-3 satellite now in operation has on board a radar
altimeter. This instrument is being used, experimentally at present, to
measure significant wave heights. Reliable measurements have been made of sig-
nificant wave heights of from 2 to 10 meters by analyzing the changing shape
of the radar return pulse. The accuracy of the method in measuring storm seas
generated by high winds, where the waves are long, is still being investigated.

When the GEOS-3 system becomes fully operational and starts collecting
data routinely, the potential volume of information is almost overwhelming.
Data will be available from all portions of the oceans, even those far from
land and traveled only infrequently by ships. The information will be avail-
able both night and day. By the very nature of this acquisition and transmis-
sion these data will be in directly computer-compatible form and their management
should be straightforward.

SEASAT-A is scheduled for launch in 1978. This satellite will include
a radar altimeter similar to that on GEOS-3 that will be able to provide
data on significant wave height. It had been hoped that the synthetic
aperture radar to be included on this satellite would provide a system for
imaging waves, thus allowing the estimation of wave spectra. There is
some question now as to whether it will be possible to obtain wave images,
and hence spectral estimates, from spacecraft. The task does not appear to
be hopeless and investigations in this area are continuing.

A system to provide accurate wind speed measurements is to be included
on SEASAT-A. These wind speed measurements, which will cover all oceans,
will be used as inputs for the FNWC weather forecasting and hindcasting model.
Since the current limiting factor in the FNWC wave predictions is the accuracy
of the wind fields, the more accurate wind data -- combined with the more ac-
curate adjustment of the empirical factors in the model based on the significant
wave height measurements -- should greatly improve the accuracy of the FNWC
predictions.

Data from Platforms
The oil companies, in connection with their interest in exploring the
possibilities of oil production off the U.S. East and West Coasts and British
Isles, will be collecting large amounts of environmental data including infor-
mation on waves. Unfortunately, as has been the case with large amounts of
data collected by the oil companies in the North Sea, Gulf of Mexico and near
Alaska, most of this information will be considered proprietary and will not
be immediately available. If this information were made available to FNWC,
whose predictions the oil companies use routinely, and to interested scientists,
the accuracy of their predictions would undoubtedly increase. Furthermore,
some of the areas covered are near shipping lanes and would be of considerable
value, especially because of the effect of shoaling water and wave steepness.

Data Buoys
As noted in Chapter IV the NOAA Data Buoy Office (NDBO) has deployed
a number of 40-foot discus buoys for the collection of environmental data.
The information collected includes wind speed and the vertical component
of buoy acceleration from which spectra are computed. Figs. 58 and 59 show
the current and planned location of these buoys.

NDBO has over the years deployed several different measurement systems
for recording the waves. These included accelerometer data subjected to
double integration, an auto-covariance analysis and a wave spectrum analysis.
Plans for the future include a wave directional analysis (summer/fall 1976).
While not providing the wide scale coverage of the satellite systems, they
do provide year round information for specific areas. Their spectra can
be used for checking and verifying the output of the FNWC hindcast model
and other large-scale data collection systems. Furthermore, if additional
funding were made available buoys could be deployed in locations where ad-
ditional data are particularly needed -- as off the coast of South Africa.
(See Appendix L).

-92-
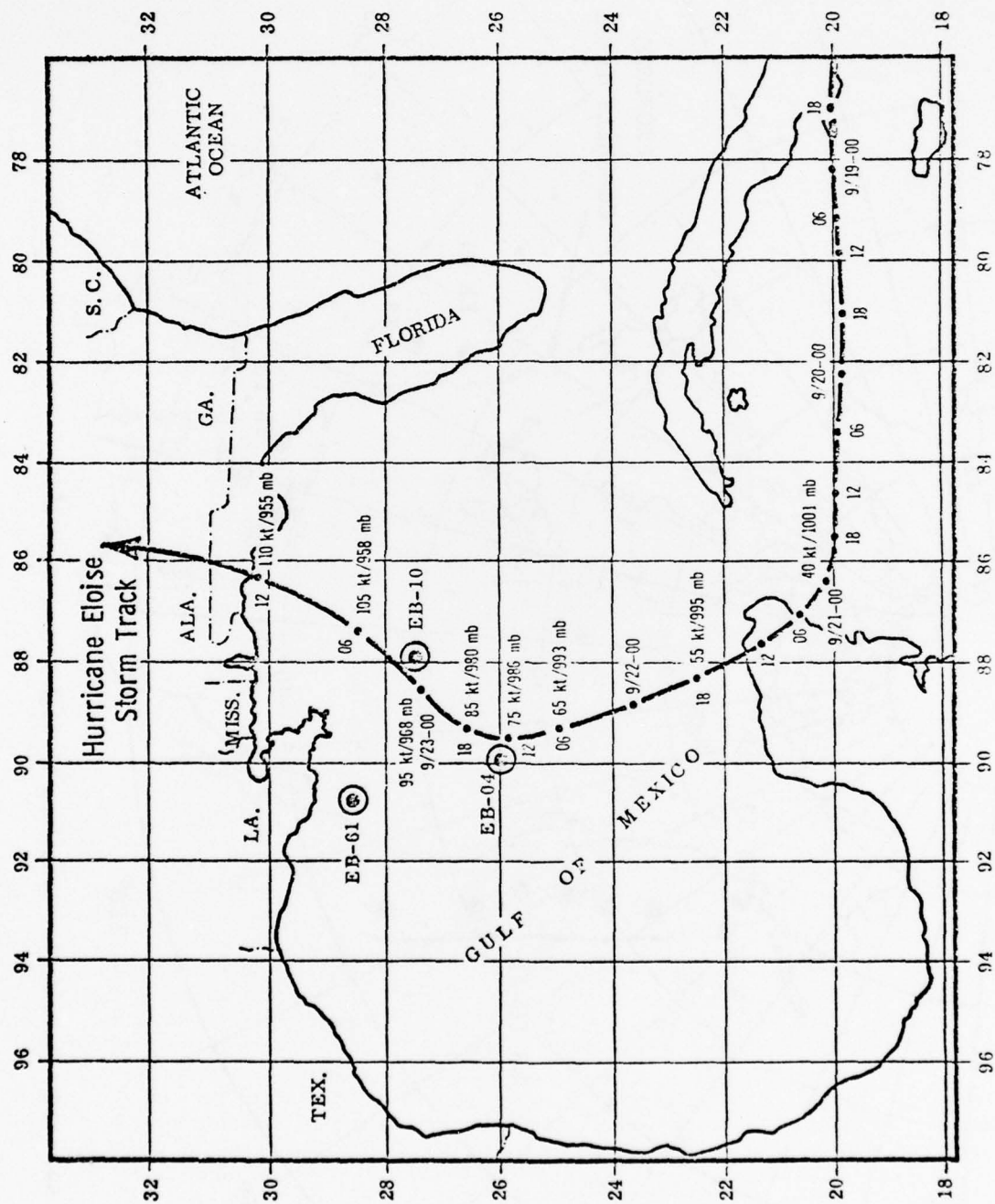
Fig. 58 - Location of NDBO Buoys in the Gulf of Mexico from "Data Report: Buoy observations during Hurricane ELOISE [Sept. 19 to Oct. 11, 1975]", Environmental Sciences Div. NDBO Nov. 1975.
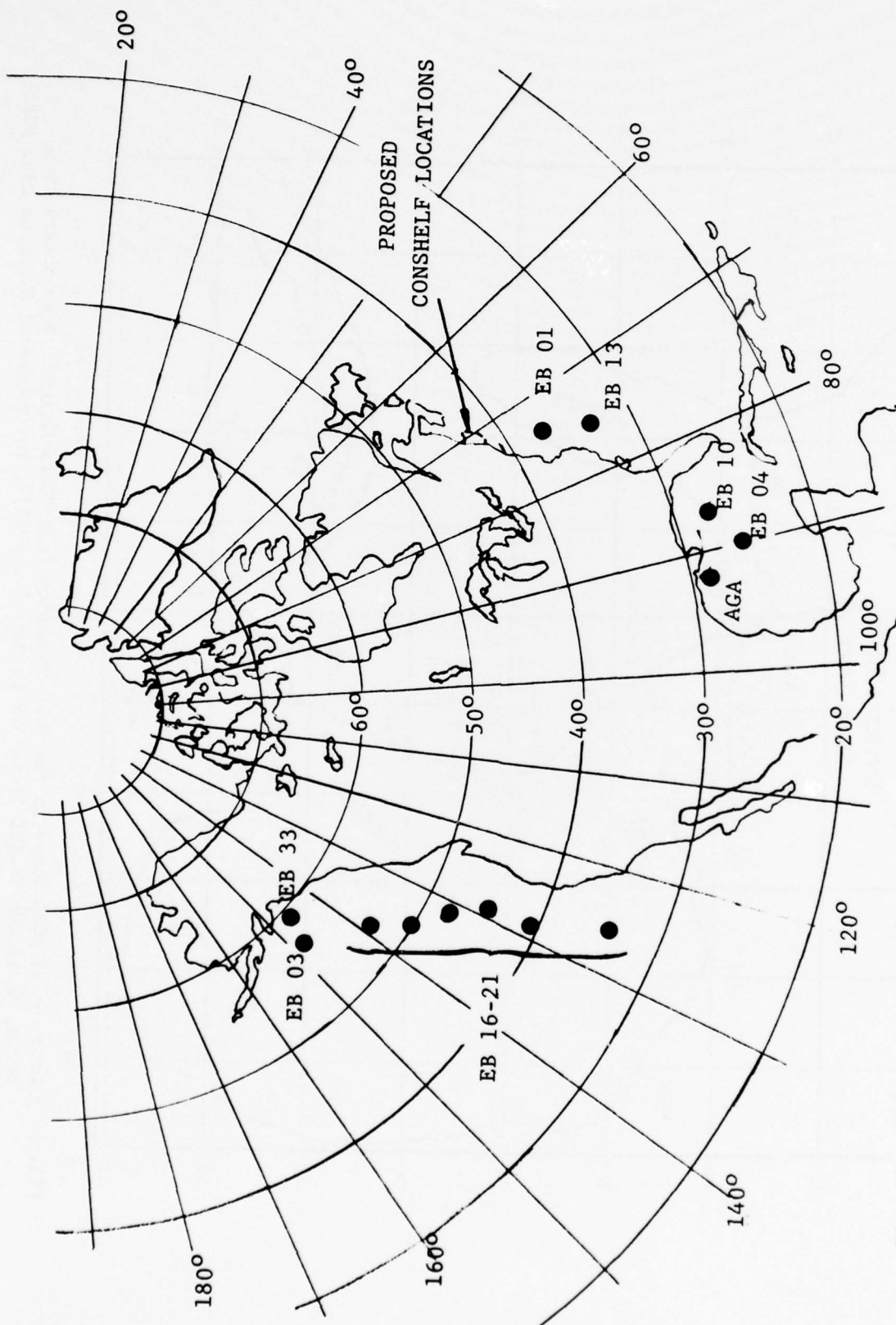
Fig. 59 – NDBO Planned Buoy Locations Through Fiscal Year 1976.

ACKNOWLEDGMENTS

REFERENCES

Baer, L., 1962: "An Experiment in Numerical Forecasting of Deep Water Ocean Waves," Report No. LMSC-801296, Lockheed California Co.

Baer L. and L.C. Adams, 1966: "The Icosahedral Gnomonic Projection and Grid of the World Ocean for Wave Studies," Report No. LR 20157, Lockheed California Co.

Band, E. G. U., 1966: "Analysis of Ship Data to Predict Long-Term Trends of Hull Bending Moments," Webb Report to A. B. S., November 1966.

Barber, N.F., and Ursell, 1948: "The Generation and Propagation of Ocean Waves and Swell," Philos. Trans. R. Soc. A, Vol. 240, p. 527.

Barnett, T.P., 1968: "On the Generation, Dissipation and Prediction of Ocean Wind Waves," Jo. Geophys. Res., Vol. 73, pp. 513-529.

Barnett, T.P., 1969: "Wind Waves in Shallow Water," Westinghouse Ocean Research Laboratory, San Diego, California.

Barnett, T.P. and J.C. Wilkerson, 1967: "On the Generation of Wind Waves as Inferred from Airborne Measurements of Fetch-Limited Spectra," Journal of Marine Research, Vol. 25, pp. 292-328.

Barricutos, C.S., 1970: "An Objective Method for Forecasting Winds Over Lake Erie and Lake Ontario," ESSA Technical Memorandum WBTM TDL 34, U.S. Department of Commerce, Washington, D.C., p. 20.

Bea, R.G., 1974: "Gulf of Mexico Hurricane Wave Heights," OTC Paper No. 2110, Offshore Technology Conference, Houston, Texas.

Bennet, C.M., 1968: "A Directional Analysis of Sea Waves from Bottom Pressure Measurements," Transactions Marine Tech. Society.

Bretschneider, C.L., 1952: "Revised Wave Forecasting Relationships," Proceedings of 2nd Conference on Coastal Engineering, pp. 1-5.

Bretschneider, C.L., 1952: "Revision in Wave Forecasting, Deep and Shallow Water," Proceeding of 6th Conference on Coastal Engineering, pp. 30-67.

Bretschneider, C.L., 1963: "Significant Wave Hindcasts for Station J North Atlantic Storm," Technical Report, National Engineering Science Co., No. SN-77-1.

Briscoe, M.G., and Goudriaan, E., 1972: "Research Use of the Waverides Buoy in Deep Water," Underwater Journal, Aug., 1972, pp. 142-148.

Brown, D.W., Scringer, J.A., and Kelly, C.E., 1966: "Ocean Wave Measurements Using a Wave Pole," Report 66-1, Pacific Naval Lab. Defence Research Board, Canada, August, 1966.

Bunting, D.C., 1966: "Wave Hindcast Project North Atlantic Ocean," TR-183, U.S. Naval Oceanographic Office, Washington, DC.

Bunting, D.C., 1970: "Evaluating Forecasts of Ocean-Wave Spectra," Jo. Geophys. Res., Vol. 75, pp. 4131-4143.

Canham, H.J.S., Cartwright, D.E., Goodrich, G.J., and Hogben, N., 1962: "Seakeeping Trials in OWS Weather Reporter," Royal Institute of Naval Architects.

Cardone, V.J., 1969: "Specification of the Wind Distribution in the Marine Boundary Layer for Wave Forecasting," TR-69-1, Geophysical Science Laboratory, New York University.

Cardone, V.J., W.J. Pierson and E.G. Wand, 1975: "Hindcasting the Directional Spectrum of Hurricane Generated Waves," Paper No. OTC 2332, Offshore Technology Conference, Houston, Texas.

Cartwright, D.E., 1961: "The Use of Directional Spectra in Studying the Output of a Wave Recorder on a Moving Ship," Conference on Ocean Wave Spectra, Easton, MD., National Academy of Sciences, Washington, DC.

Cartwright, D.E. and Longuet-Higgins, M.S., 1956: "The Statistical Distribution of the Maximum of a Random Function," Proc. Royal Soc. of London Series A, Vol. 237.

Caul, R.D. and Brown, N.L., 1967: "A Comparison of Wave Measurements form a Free-Floating Wave Meter and the Monster Buoy," Transactions 2nd International Buoy Technical Symposium/Expo.

Chang, M.S., 1968: "Mass Transport in Seep Water Long Crested Random Gravity Waves," Jo. Geophys. Res., Vol. 24, pp.1515-1536.

Collins, J.I., 1972: "Prediction of Shallow Water Spectra," Jo. Geophys. Res., Vol. 77, pp.2693-2707.

Cote, L.J., J.O. Davis, R.J. McGough, E. Mehr, W.J. Pierson, F.J. Ropek, G. Stephenson and R.C. Vetter, 1960: "The Directional Spectrum of a Wind Generated Sea as Determined From Data Obtained by the Stereo Wave Observation Project," Meteor. Pap. Vol. 2, p. 88, New York University Press (New York).

Crutcher, H.L., 1975: "A Note on the Possible Misuse of the Kolmogorov-Smirnov Test," Journal of Applied Meteorology, Vol. 14, No. 8, pp. 1600-1603, December 1975.

Dexter, P.E., 1974: "Tests of Some Programmed Numerical Wave Forecast Models," Jo. of Phy. Oceanog., Vol. 4, No. 4.

Dobson, F.W., 1971: "Measurements of Atmospheric Pressure on Wind Generated Sea Waves," Jo. Fluid Mech., Vol. 48, pp. 91-127.

Draper, L., 1966: "The Analysis and Presentation of Wave Data--A Plea for Uniformity," Proceedings of 10th Conference of Coastal Engineering, Tokyo, Sept., 1966.

Draper, L., 1971: "Waves at North Carr Light Vessel, off Fife Ness," NJO Int. Report A.50, Aug., 1971.

Draper, L., and Humphrey, J.D., 1973: "An Investigation into Large-Wave-Height Response of two Wave Recorders," National Institute of Oceanography, Wormley, Godalming, Surrey, NIO Internal Report A-63.

Draper, L., and Fortnum, B.C.H., 1974: "Wave Recording Instruments for Civil Engineering Use," Institute of Oceanographic Science, Wormley, July, 1974.

Draper, L., and Squire, E.M., 1967: "Waves at OWS India (59° N, 19° W)", Trans. Roy. Inst. Nav. Arch., Vol. 109, pp. 85-93.

Draper, L. and Whitaker, M.A.B., 1965: "Waves at Ocean Weather Ship Station 'Juliet'," Drutschen Hyd. Zeitschrift Band 8.

Ewing, J.A., 1969: "Some Measurements of the Directional Wave Spectrum," Journal of Marine Research, Vol. 27, No. 2, May 1969.

Ewing, J.A., 1971: "A Numerical Wave Prediction for the North Atlantic Ocean," Deutsche Hydrogr. Zeit., Vol. 24, pp. 241-261.

Ewing, J.A., 1974: "Some Results from the JONSWAP of Interest to Engineers," International Symposium on the Dynamics of Marine Vehicles and Structures in Waves, London, April 1974.

Ewing, J.A., 1975: "The Use of the JONSWAP Spectrum Given Values of Significant Wave Height and Period," Contribution to the 1976 ISSC Committee I Report.

Ewing, J.A., and Hogben, N., 1966: "Some Wave and Wind Data From Trawlers," Marine Observer, No. 36, pp. 71-80.

Ewing, J.A., and Hogben, N., 1971: "Wave Spectra From Two British Research Trawlers," National Physical Laboratory, Ship Division, Ship Report 150, National Institute of Oceanography, Wormley, Godalming, Surrey, England.

Feldhausen, P.H., Chakrabarti, S.K., and Wilson, B.W., 1974: "Comparison of Wave Hindcasts of Weather Station 'J' for the North Atlantic Storm of December, 1959," Deutsche Hydrog. Zeit., Vol. 26, No. 10.

Ferdinande, V., De Lembre, R., and Aertessen, G., 1975: "Spectres de Vagues de l'Atlantique Nord (Sea Spectra from the North Atlantic)", Association Technique Maritime et Aeronautique, Session 1975,

Gelci, R., Cazale, H., and Vassal, J., 1956: "Utilization des Diagrammes de Propagation a la Provision Energetique de la Houle," Bull. Inform. Comite Central d'Etude, Cotes, Vol. 9, pp. 416-425.

Gelci, R.H. and Chavy, P., 1961: "Technical Aspects of Numerical Forecasting of Swell," Conference on Ocean Wave Spectra, Easton, Maryland.

Gospodnetic, D., and Miles, M., 1974: "Some Aspects of the Average Shape of Wave Spectra at Station 'India' (50° N, 19°W)", International Symposium on the Dynamics of Marine Vehicles and Structures in Waves, London, April, 1974.

Groves, G.W., and J. Melcer, 1961: "On the Propagation of Ocean Waves on a Sphere," Geofis. Int. Mexico, Vol. 1, p. 77.

Hafer, R.A., 1970: "Wave Measurements from the Drilling Rig SEDCO 135 F off the Coast of British Columbia," Report 70-3, Defense Research Board, Canada, July, 1970.

Hasselmann, K., 1960: "Grundgleichungen der Seegangesvoraussage," Schiffstechnik, Vol. 7, pp. 191-195.

Hasselmann, K., 1963: "On the Non-linear Energy Transfer in a Gravity Wave Spectrum P3: Evaluation of the Energy Flux and Swell-Sea Interaction for a Neumann Spectrum," Jo. Fluid Mech., Vol. 15, p. 385

Hasselmann, K., D.B. Ross, P. Mullen and W. Sell, 1976: "A Parametrical Wave Prediction Model," To appear in Jo. of Physical Oceanog.

Hayes, J., 1973: "A Review of Ocean Wave Forecasting Techniques," Master's Thesis, New York University.

Hoffman, D., 1972: "Further Analysis of Ocean Wave Spectra at Station 'India'," Webb report submitted to SNAME, March 1972.

Hoffman, D., 1974: "Analysis of Measured and Calculated Data," Proceedings of International Symposium on the Dynamics of Marine Vehicles and Structures in Waves, University College, London.

Hoffman, D., 1974a: "Analysis of Wave Spectra at Station 'Papa'," Webb report submitted to Sea Use Foundation, December 1974.

Hoffman, D., 1975: "Analysis of Wave Spectra at Station 'Kilo'," Webb report submitted to NSRDC under GHR program, October 1975.

Hoffman, D., 1975a: "Wave Data Application for Ship Response Predictions," Final Webb Report under GHR Program.

Hoffman, D., and Lewis, E.V., 1969: "Analysis and Interpretation of Full-Scale Data on Midship Bending Stresses of Dry Cargo Ships," Report SSC-196.

Hoffman, D., and Marks, W., 1973: "Application of Wave Inputs to Seakeeping," Seakeeping 1953-1973 T & R Symposium S-3, SNAME.

Hoffman, D., Hsiung,C., and Zielinski, T., 1975: "Wave Load Distributions on Large Ships," Paper presented at SNAME STAR Symposium, Washington, DC, August 1975.

Hoffman, D. Williamson, J., and Lewis, E.V., 1972: "Correlation of Model and Full-Scale Results in Predicting Wave Bending Moment Trends," Report SSC-233.

Hoffman, D., and Zielinski, T., 1974: "Load Analysis of Atomic-Powered Vessels," Hoffman Maritime Consultants report prepared for G.G. Sharp under contract to Babcock & Wilcox, September 1974.

Hoffman, D., and Zielinski, T., 1975: "Effects of Spectral Shape on Ship Response Predictions," Webb report for ABS, September 1975.

Hogben N., 1970: "Measured and Visual Wave Data From Trawlers," Marine Observer, April 1970.

Hogben, N., 1974: "Ocean Wave Statistics -- 'Five Minutes Slow' After Six Years," National Physical Lab., Report Ship-180, England.

Hogben, N., and Lumb, F.L., 1964: "The Presentation of Wave Data from Voluntary Observing Ships," National Physical Lab, England, Ship Division Report No. 49, 1964. (Appendix by Cartwright).

Hogben, N., and Lumb, F.L., 1967: "Ocean Wave Statistics," Her Majesty's Stationary Office, London.

Hubert, W.E., 1964: "Operational Forecasts of Sea and Swell," First U.S. Navy Symposium on Military Oceanography, 17-19 June, 1964, pp. 113-124.

Hubert, W.E. and B.R. Meudenhall, 1970: "The FNWC Singular Sea/Swell Model," FNWC Technical Note 59.

Inoue, T., 1967: "On the Growth of the Spectrum of a Wind Generated Sea According to a Modified Miles-Phillips Mechanism and its Application to Wave Forecasting," TR-67-5, Geophysical Sciences Laboratory Report, New York University, New York.

Inoue, T., 1967a: "Ocean Wave Spectra Estimated from Three Hour Pressure Records Obtained by FLIP," New York University, Geophysical Science Lab., Rpt. No. 67-1, Feb. 1967.

Isozaki, I., and T. Uji, 1973: "Numerical Prediction of Ocean Wind Waves," Meteorological Research Institute, Tokyo.

Isozaki, I., and T. Uji, 1974: "Numerical Model of Marine Surface Winds and its Application to the Prediction of Ocean Wind Waves," Papers in Meteorology and Geophysics, Vol. 25, pp. 197-231.

ISSC, 1970: 4th ISSC, Committee 1 (Enviromental Conditions) Report, Tokyo.

Larson, L.H. and Fenton, D., 1974: "Open Ocean Wave Studies," University of Washington Data Report 1-73, February 1974.

Lazanoff, M., 1964: "Wave Power Spectra from Argus Island, September 1962," Unpublished manuscript, IMB No. 0-46-64, Marine Science Department, U.S. Naval Oceanographic Office, Dec. 1964.

Lazanoff, S.M., N. Stevenson and V.J. Cardone, 1973: "A Mediterranean Sea Wave Spectral Model," Technical Note 73-1, Fleet Numerical Weather Central, Monterey, California.

Lazanoff, S., and N. Stevenson, 1975: "An Evaluation of a Hemispheric Operational Wave Spectral Model," Technical Note 75-3, Fleet Numerical Weather Central, Monterey, California.

Lewis, E.V., 1967: "Predicting Long-Term Distribution of Wave-Induced Bending Moments on Ship Hulls," SNAME Spring Meeting Proceedings.

Lewis, E.V., van Hooff, R., Hoffman, D., Zubaly, R.B., and Maclean, W.M., 1973: "Load Criteria for Ship Structural Design," Report SSC-240.

Lockheed 1971: "Wave Spectra Estimated from 355 North Pacific Wave Records Collected at Station 'Papa' During 1969-71," Lockheed Shipbuilding and Co-struction Co. Report.

Lockheed 1973: "Wave Spectra Estimated from 305 North Pacific Wave Records Collected at Station 'Papa' During 1972-73," Lockheed Shipbuilding and Construction Co. Report.

Lockheed Shipbuilding and Construction Company, 1974: "Instrumentation and Analysis of Data Collected on the S.S. Japan Mail and S.S. Phillipine Mail from December 1971 to July 1973," Report to Sea Use Foundation, Seattle, 1974.

Longuet-Higgins, M.S. 1952: "On the Statistical Distribution of the Heights of Sea Waves," Journal of Marine Research, Vol. XI, No. 3.

Longuet-Higgins, M.S., Cartwright, D.E. and Smith, N.S., 1961: "Observations of the Directional Spectrum of Sea Waves Using the Motions of a Floating Buoy," Conference on Ocean Wave Spectra, Easton, Maryland, National Academy of Sciences, Washington, DC, 1961.

Loukakis, T.A., 1970: "Experimental and Theoretical Determination of Wave Form and Ship Response Extremes," MIT Report 69-7, May, 1970.

Mallory, J.K., 1975: "Abnormal Waves off the South African Coast -- a Danger to Shipping," The Naval Architect, July 1975.

Miles, J.W., 1957: "On the Generation of Surface Waves by Shear Flows," Journal of Fluid Mech., Vol. 3, pp.185-204.

Miles, J.W., 1959: "On the Generation of Surface Waves by Shear Flows, Part II," Journal of Fluid Mech. Vol.,6, pp. 568-582.

Miles, M., 1972: "Wave Spectra Estimated from a Stratified Sample of 323 North Atlantic Wave Records," Report LTR-SH-118A, Division of Mechanical Engineering, National Research Council, Canada, May, 1972.

Mirakhin and Kholodilin, 1975: "Probability Characteristics of Ship Inclination Due to Erupting Wave Impulse," 14th ITTC, Ottawa, 1975.

Moskios, A., and Deleonibus, P., 1965: "Performance of a Shipboard Wave Height Sensor," Informal Manuscript Report No. 0-4-65, Marine Science Department, U.S. Naval Oceanographic Office, March, 1965.

Moskowitz, L., 1964: "Estimates of the Power Spectrums for Fully Developed Seas for Wind Speed of 20 to 40 Knots," Journal of Geophysical Research, Vol. 69, No. 24, pp. 5161-5179.

Moskowitz, L., Pierson, W.J. and Mehr, E., 1962, 1963, 1965: "Wave Spectra Estimates from Wave Records Obtained by the OWS Weather Explorer and the OWS Weather Reporter (I, II and II), New York University, Department of Meterology and Oceanography, Geophysical Sciences Laboratory.

NAVSEA, 1975: "Seakeeping in the Ship Design Process," Report of the Seakeeping Workshop at U.S. Naval Academy, June 1975, NAVSEA, NAVSEC and DTNSRDC Report, July, 1975.

Neumann, G., 1953: "On Ocean Wave Spectra and a New Method of Forecasting Wind Generated Sea," U.S. Beach Erosion Board, Technical Memo. 43.

Neu, H.A., 1971: "Wave Climate of the Canadian Atlantic Coast and Continental Shelf -- 1970," Atlantic Oceanographic Laboratory Report, 1971-10.

Ochi, M., 1975: Personal communication, July, 1975.

Patterson, M.M., 1971: "Hindcasting Hurricane Waves in the Gulf of Mexico," Paper No. 1345, Proceedings 1971 Offshore Technology Conference, Houston, Texas.

Phillips, O.M., 1957: "On the Generation of Waves by Turbulent Wind," Journal of Fluid Mech., Vol 2, pp. 417-445.

Phillips, O.M., 1960: "On the Dynamics of Unsteady Gravity Waves of Finite Amplitude, Part I," Journal of Fluid Mech., Vol. 9, pp. 193-217.

Phillips, O.M., 1966: The Dynamics of the Upper Ocean, Cambridge University Press, England.

Pickett, R.L. 1962: "A Series of Wave Power Spectra," Unpublished manuscript, IMB No. 0-63-62, Marine Science Department, U.S. Naval Oceanographic Office, 1962.

Pierson, W.J., 1954: "The Interpretation of the Observable Properties of Sea Waves in Terms of the Energy Spectrum of the Gaussian Record," Transactions, American Geophysical Union, Vol. 35, pp. 747-757.

Pierson, W.J., 1975: Comments on "A Parametric Wave Prediction Model," Personal communication, Oct. 1975, revised, May, 1976.

Pierson, W.J., 1976: "The Theory and Applications of Ocean Wave Measuring Systems At and Below the Sea Surface, on the Land, from Aircraft, and from Spacecraft," NASA Contractor Report CR-2646, New York University.

Pierson, W.J., Jr. and Marks W., 1952: "The Power Spectrum Analysis of Ocean Wave Records," Transactions, Amer. Geophys. Union, Vol. 33, No. 6, December 1952.

Pierson, W.J. and Moskowitz, L., 1964: "A Proposed Spectral Form for Fully Developed Wind Seas Based on the Similarity Theory of S.A. Kitaigorodskii," Journal of Geophysical Research, Vol. 69, (24), pp. 5181-5190.

Pierson, W.J., Neumann, G. and James, R.W., 1955: "Practical Methods for Observing and Forecasting Ocean Waves by Means of Wave Spectra and Statistics," H.O. Pub. No. 603, U.S. Navy Hydrographic Office, Washington, D.C.

Pierson, W.J., Tick, L.J. and Baer, L., 1966: "Computer Based Procedures for Preparing Global Wave Forecasts and Wind Field Analyses Capable of Using Wave Data Obtained by a Spacecraft," Proceedings of the Sixth Naval Hydrodynamics Symposium.

Ploeg, J., 1971: "Wave Climate Study -- Great Lakes and Gulf of St. Lawrence," SNAME T & R Bulletin No. 2-17.

Pore, N.A., 1970: "Summary of Selected Reference Material on the Oceanographic Phenomena of Tides, Storm Surges, Waves and Breakers," ESSA Technical Memo. WBTM TDL 30, U.S. Dept. of Commerce, Washington, D.C.

Pore, N.A. and Richardson, W.S., 1969: "Second Interim Report on Sea and Swell Forecasting," ESSA Technical Memo. WBTM TDL 17.

Priestly, J.T., 1965: "Correlation Studies of Pressure Fluctuations on the Ground Beneath a Turbulent Boundary Layer," National Bureau of Standards, NBS Report 8942.

Quayle, 1974: "A Climatic Comparison of Ocean Weather Stations and Transient Ship Records," Mariner's Weather Log, Sept. 1974.

Quayle, 1974a: "Cape Rollers -- Unusually High Swells off the South African Coast," Mariner's Weather Log, May 1974.

Ross, D.B., Cardone, V.J. and Conaway,, J.W., Jr., 1971: "Laser and Microwave Observations of Sea Surface Conditions for Fetch Limited to 17 to 25 m/s Winds," IEEE Transactions on Geoscience Electronics, GE-8, 326-336.

Rudnick, P., 1969: "Wave Directions from a Large Spar Buoy," Journal of Marine Research, Vol. 27, No. 1.

St. Denis, M. and Pierson, W.J., 1953: "On the Motions of Ships in Confused Seas," Transactions, SNAME.

Saetre, H.J., 1974: "On High Wave Conditions in the Northern North Sea," Institute of Oceanographic Sciences, Surrey, England, Report No. 3.

Schule, J.J., Simpson, L.S. and DeLeonibus, P.S., 1971: "A Study of Fetch-Limited Wave Spectra with an Airborne Laser," Journal of Geophysical Research, Vol. 76, pp. 4160-4171.

Schwartz, E. and Hubert, W.E., 1973: "The FNWC Singular Advective Wind Wave/ Swell Analysis and Forecast Model." Fleet Numerical Weather Central, Technical Note No. 73-2, Monterey, California.

Shemdin, O.H., and Hsu, E.Y., 1967: "Direct Measurement of Aerodynamic Pressure Above a Simple Progressive Gravity Wave," Journal of Fluid Mech., Vol. 30, pp. 403-417.

Snodgrass, F.E., Groves, G.E., Hasselmann, et. al., 1966: "Propagation of Ocean Swell Across the Pacific," Philos. Trans. R. Soc., A. Vol. 259, p. 431.

Snyder, R. and Cox, C.S., 1966: A Field Study of the Wind Generation of Ocean Waves," Jo. Mar. Res., Vol. 24, pp. 141-177.

Steele, K., 1975: "Buoys Now Provide Real Time Wave Spectra Data," N.D.B.O. Data Buoy Technical Bulletin, Vol. 1, No. 6.

Steele, Michelena and Hall, 1974: "NDBO Wave Data -- Current and Planned," Proceedings of the International Symposium on Ocean Wave Measurement and Analysis, Sept. 1974.

Thomasell, A. and Welsh, J.G., 1963: "Studies of the Specification of Surface Winds over the Ocean," Traveler's Research Center, Inc.

Tukey, J.W., 1949: "The Sampling Theory of Power Spectral Estimates," Symposium at Woods Hole Oceanographic Institute, NAVEXOS-0-735, ONR.

U.S. Army Coastal Engineering Research Center (CERC), 1966: "Shore Protection Planning and Design," Technical Report No. 4, Third Edition.

U.S. Department of Commerce, 1972: NOAA Technical Procedures Bulletin No. 72, Silver Springs, Maryland.

U.S. Naval Oceanographic Office, 1963: "Oceanographic Atlas of the North Atlantic Ocean, Section IV, Sea and Swell," U.S. Naval Oceanographic Office, Publication No. 700.

Verploegh, 1961: "On the Accuracy and the Interpretation of Wave Observations from Selected Ships," WMO working papers.

Wachnick, Z.G. and Zarnick, E.E., 1965: "Ship Motions Prediction in Realistic Short Crested Seas," Trans. SNAME, Vol. 73, pp. 100-134.

Walden, D.A. and Hoffman, D., 1975: "An Investigation into the Effects of Varying the Shape Parameters in the Standard Spectral Formulation," Webb Report.

Walden, H. 1957: "Methods of Swell Forecasting Demonstrated with an Extraordinary High Swell Off the Coast of Angola," Proceedings of the Symposium on the Behavior of Ships in a Seaway, Netherlands Ship Model Basin, Wageningen.

Walden, H., 1964: "Die Eigenschaften der Meereswellenim Nordatlantischen Ozean," Deutscher Wetterdienst Seewetteramt, Publication No. 41.

Webb, 1974: "Analysis of Data Obtained on Board Two American Mail Line Vessels," Webb report prepared for Sea Use Foundation.

Wheaton and Boentgen, 1975: "Ship Response Instrumentation Aboard the Containership S.S. Sea-Land McLean -- Results from the Second Operational Season in the No. Atlantic Service," Teledyne Report to Ship Structure Committee, Project SR-211.

Wiegel, R.L., 1964: Oceanographic Engineering, Prentice-Hall, Englewood Cliffs, N.J. p. 171.

Wilson, B.W., 1961: "Deep Water Wave Generation by Moving Wind Systems," Jo. of Waterways and Harbors, Div. ASCE, WW2, pp. 113-141.

Yamanouchi, Y., 1969: "On the Encounter Wave Recorder for Free Running Model and for Actual Ship," Proceedings of 12th International Towing Tank Conference, Rome, Italy.

Yamanouchi and Ogawa, 1970: "Statistical Diagrams on the Winds and Waves on the North Pacific Ocean," Paper of the Ship Research Institute, Tokyo, Japan, March 1970.

APPENDIX A

INDEX OF PUNCHED CARDS
CARRYING WIND AND WAVE DATA
AVAILABLE FROM VARIOUS SOURCES

TABLE I - Index of Punched Card Decks Carrying Wave and Wind Data.

Country and Holding Agent	Deck Nos. or Series No.	Approximate No. of Cards	Areas Covered	Years Covered	Waves Elements	Waves Intervals or Code	No. of Groups	Wind Elements	Wind Intervals or Code	Temp. Air/Sea	Remarks
GERMANY											
Deutscher Wetterdienst		10,890,000	All	1890 to 1939	State of Sea Direction	Nautical Scale 32 Points		Speed Direction	Beaufort	Yes	
		790,000	All	1949 to 1957	State of Sea Direction	Nautical Scale 10°	2	Speed Direction	Beaufort	Yes	
Seewetteramt		430,000	All	1959 to 1965	Height Period Direction	½ Metre 1 Second 10°	1	Speed Direction	Beaufort	Yes	
Hamburg			All	Since 1966	Height Period Direction	½ Metre 2 Second 10°	2	Speed Direction	Beaufort	Yes	
JAPAN		1,260,000	All	1933 to 1953	State of Sea Direction	Nautical Scale 32 Points	2	Speed Direction		Yes	
		2,000,000	Mainly Octant* 2 Some 1 and 3	1953 to 1960	Height Period Direction	½ Metre 2 Seconds 10°	2 3	Speed Direction		Diff.	Northern Hemisphere *Octant 1 90° - 180°W 2 180° - 90°E 3 90° - 0°E
		1,250,000	Mainly Octant* 2 Some 1 and 3	Since 1961	Height Period Direction	½ Metres 2 Seconds 10°	2	Speed Direction		Yes	
NETHERLANDS		8,000,000	All	1854 to 1940	State of Sea			Speed Direction	Beaufort 16 Points	Yes	
K.N.M.I. De Bilt		2,212,000	All	Since 1949	Height Period Direction	½ Metres 2 Seconds 10°	2	Speed Direction	Beaufort 10°	Yes	1 or 2 groups before 1958
		196,000	Lightships (4 positions)	Since 1949	Height Period Direction	½ Metres 2 Seconds 10°	2	Speed Direction	Beaufort 10°	Yes	1 or 2 groups before 1958
UNITED KINGDOM	Series 1	1,453,500	All	1854 to 1920	None	None	None	Speed Direction	Beaufort 32 Points	Yes	
Meteorological Office Bracknell Berkshire	2, 3 and 4	1,479,000	All	1921 to 1948	Sea and Swell		2	Speed Direction	Beaufort 32 Points	No	

TABLE I (Cont'd.) - Index of Punched Card Decks Carrying Wave and Wind Data

Country and Holding Agent	Deck Nos. or Series No.	Approximate No. of Cards	Areas Covered	Years Covered	Waves			Wind		Temp. Air/Sea	Remarks
					Elements	Intervals or Code	No. of Groups	Elements	Intervals or Code		
UNITED KINGDOM Meteorological Office Bracknell	7, 9, 13 and 23	3,973,000	All	Since 1945	Height Period Direction	$\frac{1}{2}$ Metres 2 Seconds 10°	2	Speed Direction	Knots 10°	Yes	Wave height 0-9 scale before 1948. Wave direction 32 points before 1953. Wind Speed-Beaufort and Wind direction 32 points before 1956.
Berkshire (Cont'd.)	6, 10, 14 18 and 24	279,000	Ocean Weather Ships North Atlantic	Since 1947	Height Period Direction	$\frac{1}{2}$ Metres 2 Seconds 10°	2	Speed Direction	Knots 10°	Yes	Wave height 0-9 scale before 1948. Wave direction 32 points before 1953. Wind Speed-Beaufort and Wind direction 32 points before 1956.
	8, 12 and 22	144,500	Lightships	1949 to 1961	Height Period Direction	$\frac{1}{2}$ Metres 2 Seconds 10°	2	Speed Direction	Knots 10°	Yes	Waves from 1950 onwards. Wind speed Beaufort and Wind direction 32 points before 1956
Ship Division NPL		42,000	All	1953 to 1961	Height Period Direction	$\frac{1}{2}$ Metres 2 Seconds 30°	1	None	None	No	Statistical Summary Cards [1].
Feltham Middlesex		4,000	Barents Sea Davis Strait Greenland Sea	1962 to 1965	Height Period Direction	2 Feet 1 Second 30°	1	Speed Direction	Beaufort 30°	No	From Trawlers (Reference 6). Wave length also given.
U.S.A. National Weather Records Centre Asheville N. Carolina	Deck 116	6,686,000	All	1949 to 1963	Height Period Direction	$\frac{1}{2}$ Metres 2 Seconds 10°	1	Speed Direction	Knots 10°	Yes	
	Deck 128	167,000	All	Since 1963	Height Period Direction	$\frac{1}{2}$ Metres 2 Seconds 10°	2	Speed Direction	Knots 10°	Yes	Air/Sea temperatures not after 1st Jan. 1965.

APPENDIX B

U.S. NAVAL WEATHER SERVICE COMMAND

SUMMARY OF
SYNOPTIC METEOROLOGICAL OBSERVATIONS

CHINESE-PHILIPPINE COASTAL MARINE AREAS

VOLUME	AREA	NAME	CENTRAL LOCATION		NTIS NO.
1	1	Gulf of Chihli	38.8°N	120.3°E	AD 758 372
	2	Tsingtao	36.3°N	122.2°E	
	3	Yellow Sea S.W.	33.6°N	121.8°E	
	4	Shanghai	30.5°N	122.8°E	
2	5	Wenchow	27.3°N	122.3°E	AD 760 333
	6	Taiwan E.	23.2°N	122.7°E	
	7	Taiwan W.	23.4°N	119.4°E	
	8	Swatow	22.2°N	116.8°E	
3	9	Hong Kong	20.5°N	112.8°E	AD 762 423
	10	Luzon N.E.	18.8°N	123.3°E	
	11	Luzon N.W.	18.5°N	117.9°E	
	12	Hainan S.E.	17.1°N	112.6°E	
4	13	Luzon S.E.	13.5°N	123.8°E	AD 762 424
	14	Manila Bay	12.4°N	119.7°E	
	15	West York Island	12.5°N	114.0°E	
	16	Mindanao E.	9.0°N	127.0°E	
5	17	Mindanao W.	7.5°N	122.0°E	AD 762 425
	18	Balabac Strait	7.7°N	117.5°E	
	19	Brunei N.W.	7.5°N	112.5°E	
	20	Saigon 300 S.E.	6.8°N	108.6°E	

JAPANESE AND KOREAN COASTAL MARINE AREAS

VOLUME	AREA	NAME	CENTRAL LOCATION		NTIS NO.
1	1	Kushiro	42.6°N	145.8°E	AD 757 107
	2	Tomakomai	41.8°N	142.4°E	
	3	Sendai	39.5°N	142.7°E	
2	4	Tokyo	35.5°N	140.9°E	AD 754 773
	5	Hachijo Jima	32.0°N	140.5°E	
	6	Nagoya	33.8°N	137.4°E	
3	7	Nobeoka	32.3°N	133.2°E	AD 753 468
	8	Yaku Shima	30.0°N	130.0°E	
	9	Amami O Shima	28.0°N	129.5°E	
4	10	Okinawa	26.0°N	127.5°E	AD 753 216
	11	Sakishima Islands	25.0°N	124.5°E	
	12	Southern East China Sea	27.7°N	125.8°E	
5	13	Central East China Sea	30.0°N	126.0°E	AD 743 488
	14	Northern East China Sea	32.0°N	126.0°E	
	15	Nagasaki	32.0°N	129.4°E	
6	16	Sasebo	33.9°N	129.8°E	AD 743 944
	17	Inland Sea	34.2°N	133.2°E	
	18	Matsue	36.1°N	133.3°E	
7	19	Niigata	38.0°N	137.5°E	AD 742 797
	20	Akita	40.0°N	138.0°E	
	21	Hakodate	42.6°N	139.4°E	
8	22	Central Sea of Japan	39.9°N	133.7°E	AD 733-997
	23	Southern Sea of Japan	38.0°N	133.5°E	
	24	Wonsan	40.0°N	129.8°E	
9	25	Kangnung	38.1°N	129.8°E	AD 732 758
	26	Pusan	35.7°N	130.0°E	
	27	Cheju Island	34.1°N	127.4°E	
10	28	Southern Yellow Sea	34.0°N	124.5°E	AD 730 958
	29	Inch'on	36.5°N	125.3°E	
	30	Korea Bay	38.9°N	123.6°E	
11	31	Bonin Islands	27.5°N	142.5°E	AD 730 958
	32	Volcano Islands	24.5°N	141.5°E	
	33	Marcus Island	24.0°N	153.5°E	

SOUTHWEST ASIAN COASTAL MARINE AREAS

VOLUME	AREA	NAME	CENTRAL LOCATION		NTIS NO.
1	1	Akyab	19.8°N	91.8°E	AD 733 692
	2	Calcutta	19.8°N	88.5°E	
	3	Vishakhapatnam	18.3°N	85.3°E	
	4	Masulipatam	15.7°N	82.3°E	
2	5	Madras	11.9°N	81.4°E	AD 736 449
	6	N.E. Ceylon	8.8°N	81.9°E	
	7	S.E. Ceylon	5.8°N	81.2°E	
	8	W. Ceylon	8.0°N	79.5°E	
3	9	Cape Comorin	7.9°N	77.4°E	AD 735 441
	10	Mangalore	11.3°N	74.4°E	
	11	Panjim	14.4°N	72.7°E	
	12	Bombay	17.4°N	71.6°E	
4	13	Gulf of Cambay	20.3°N	70.9°E	AD 734 693
	14	N.E. Arabian Sea	20.5°N	67.0°E	
	15	N.W. Arabian Sea	20.5°N	63.0°E	
	16	S.E. Oman	20.3°N	59.8°E	
5	17	Karachi	22.9°N	68.3°E	AD 733 693
	18	Sonmiani	23.7°N	65.5°E	
	19	Gwadar	23.6°N	62.5°E	
	20	N. Gulf of Oman	25.0°N	58.7°E	
6	21	S. Gulf of Oman	23.5°N	59.0°E	AD 737 909
	22	S.E. Persian Gulf	25.3°N	53.7°E	
	23	N.E. Persian Gulf	27.7°N	51.4°E	
	24	N.W. Persian Gulf	27.5°N	50.0°E	

HAWAIIAN AND SELECTED NORTH PACIFIC ISLAND COASTAL MARINE AREAS

VOLUME	AREA	NAME	CENTRAL LOCATION		NTIS NO.
1	1	Hawaiian Windward	20.9°N	156.0°W	AD 723 798
	2	Hawaiian Leeward	20.3°N	158.2°W	
	3	Barking Sands	22.7°N	160.3°W	
	4	French Frigate Shoals	23.6°N	166.5°W	
2	5	Johnston Island	17.4°N	169.3°W	AD 725 137
	6	Midway Island	27.8°N	177.2°W	
	7	Wake Island	19.2°N	166.4°E	
3	8	Majuro	6.8°N	171.4°E	AD 725 138
	9	Kwajalein	8.8°N	167.7°E	
	10	Eniwetok	10.9°N	162.1°E	
4	11	Ponape	6.9°N	158.6°E	AD 726 740
	12	Truk	7.2°N	151.1°E	
	13	Pagan	17.5°N	145.2°E	
5	14	Saipan	14.8°N	145.4°E	AD 727 900
	15	Guam	13.0°N	144.7°E	
	16	Yap	9.6°N	139.1°E	
	17	Koror	6.9°N	134.4°E	

SOUTHEAST ASIAN COASTAL MARINE AREAS

VOLUME	AREA	NAME	CENTRAL LOCATION		NTIS NO.
1	1	Tonkin Gulf	19.5°N	108.0°E	AD 747 638
	2	Da Nang	15.7°N	109.5°E	
	3	Nha Trang	12.5°N	110.0°E	
	4	Saigon	9.3°N	107.3°E	
2	5	Southeast Gulf of Siam	9.3°N	103.7°E	AD 749 936
	6	North Gulf of Siam	12.0°N	101.0°E	
	7	Southwest Gulf of Siam	9.0°N	101.0°E	
3	8	Kuala Trengganu	5.5°N	104.4°E	AD 749 937
	9	Endau	2.6°N	104.9°E	
	10	South Malacca Strait	2.1°N	102.0°E	
	11	North Malacca Strait	6.0°N	99.0°E	
4	12	Victoria Point	10.0°N	96.8°E	AD 750 159
	13	Rangoon	14.3°N	96.5°E	
	14	Pagoda Point	15.7°N	93.3°E	

WESTERN EUROPEAN COASTAL MARINE AREAS

VOLUME	AREA	NAME	CENTRAL LOCATION		NTIS NO.
1	1	Lisbon	38.0°N	10.7°W	AD 773 141
	2	Aveiro	40.0°N	10.6°W	
	3	Porto	42.0°N	10.5°W	
	4	La Coruna	44.0°N	9.7°W	
	5	Gijon	44.2°N	5.8°W	
	6	Bordeaux	44.8°N	2.8°W	
2	7	Nantes	46.8°N	3.6°W	AD 773 594
	8	Plymouth	49.1°N	5.5°W	
	9	English Channel	49.7°N	2.8°W	
	10	Dover Strait	50.4°N	.6°E	
	11	Bristol Channel	51.1°N	6.0°W	
3	12	Irish Sea	53.7°N	4.8°W	AD 775 177
	13	Cork	50.8°N	8.3°W	
	14	S.W. Irish Coast	52.2°N	11.5°W	
	15	W. Irish Coast	54.1°N	11.8°W	
	16	Scottish Sea	56.1°N	7.4°W	
	17	Outer Hebrides	58.2°N	6.8°W	
4	18	Shetland Is. N.W.	61.0°N	4.5°W	AD 775 435
	19	Orkney Islands	59.0°N	3.4°W	
	20	Edinburgh	56.6°N	1.2°W	
	21	Grimsby	53.9°N	.9°E	
	22	Rhine Delta	52.4°N	3.1°E	
	23	Bremerhaven	54.2°N	7.0°E	
5	24	Esbjerg	55.9°N	6.5°E	AD 776 396
	25	Dogger Banks	55.2°N	3.2°E	
	26	North Sea	56.9°N	2.2°E	
	27	Shetland Is. S.E.	58.9°N	.2°E	
	28	Stavanger	57.8°N	5.7°E	
	29	Bergen	60.0°N	3.8°E	
	30	Alesund	62.2°N	4.3°E	
6	31	Olso	58.1°N	9.8°E	AD 777 049
	32	Copenhagen	55.4°N	11.2°E	
	33	Bornholm Is.	55.2°N	15.3°E	
	34	Gulf of Danzig	56.1°N	19.2°E	
	35	Stockholm	58.4°N	18.4°E	
	36	Gulf of Riga	58.5°N	21.2°E	

WESTERN EUROPEAN COASTAL MARINE AREAS (Continued)

VOLUME	AREA	NAME	CENTRAL LOCATION		NTIS NO.
7	37	Gulf of Finland	60.0°N	25.5°E	AD 777 133
	38	Gulf of Bothnia S.	61.0°N	19.4°E	
	39	Gulf of Bothnia N.	63.9°N	21.8°E	
	40	Murmansk	70.3°N	32.9°E	
	41	Andenes	70.2°N	17.4°E	
	42	Central Norwegian Coast	66.0°N	10.0°E	
	43	OSV Mike	66.0°N	2.0°E	
8	44	Iceland S.E.	63.8°N	14.6°W	AD 777 601
	45	Reykjavik	64.0°N	24.1°W	
	46	Iceland N.W.	66.2°N	25.1°W	
	47	Iceland N.	66.6°N	18.8°W	
	48	Iceland N.E.	66.3°N	13.4°W	
	49	Angmagssalik	64.9°N	37.5°W	
	50	Cape Farewell S.E.	58.0°N	38.5°W	

MEDITERRANEAN MARINE AREAS

VOLUME	AREA	NAME	CENTRAL LOCATION		NTIS NO.
1	1	Rota	36.4°N	7.8°W	AD 713 992
	2	Tangier	35.0°N	7.7°W	
	3	Malaga	36.0°N	3.4°W	
2	4	Oran	36.5°N	.3°W	AD 714 288
	5	Cartagena	37.7°N	.5°E	
	6	Barcelona	40.4°N	1.9°E	
	7	Marseille	42.6°N	5.0°E	
3	8	N. Menorca	40.8°N	5.2°E	AD 713 779
	9	Mallorca	38.9°N	4.6°E	
	10	Algiers	37.4°N	3.9°E	
	11	Corsica	42.7°N	8.4°E	
4	12	Sardinia	39.0°N	9.1°E	AD 713 780
	13	Annaba	37.6°N	7.9°E	
	14	Rome	41.2°N	12.0°E	
	15	S. Tyrrhenian Sea	39.1°N	13.4°E	
5	16	S.W. Sicily	36.8°N	12.2°E	AD 713 648
	17	Tripoli	34.1°N	12.3°E	
	18	N. Adriatic Sea	43.9°N	14.7°E	
	19	S. Adriatic Sea	41.5°N	18.1°E	
6	20	W. Ionian Sea	37.9°N	16.8°E	AD 713 295
	21	Malta	35.3°N	16.7°E	
	22	Gulf of Sidra	32.7°N	18.3°E	
	23	E. Ionian Sea	37.6°N	20.4°E	
7	24	N. Aegean Sea	39.9°N	24.8°E	AD 713 084
	25	S. Aegean Sea	37.9°N	25.1°E	
	26	Crete	35.8°N	24.9°E	
	27	Benghazi	33.9°N	22.9°E	
8	28	Rhodes	35.7°N	29.9°E	AD 713 085
	29	Central Levantine Basin	34.0°N	27.5°E	
	30	Alexandria	32.2°N	27.8°E	
	31	N. Cyprus	35.7°N	34.3°E	
9	32	S. Cyprus	33.9°N	31.9°E	AD 712 761
	33	Nile Delta	32.3°N	31.0°E	
	34	Beirut	34.2°N	34.9°E	
	35	Port Said	32.2°N	33.3°E	

NORTH AMERICAN COASTAL MARINE AREAS (Revised)

VOLUME	AREA	NAME	APPROXIMATE CENTRAL LOCATION	
1	1	Belle Isle Strait	50.5°N	58.3°W
	2	OSV Bravo	51.5°N	51.0°W
	3	NE Newfoundland Coast	49.2°N	52.7°W
	4	SE Newfoundland Coast	47.0°N	51.5°W
	5	Placentia Bay South	46.0°N	54.5°W
	6	Cabot Strait	46.8°N	58.3°W
	7	Anticosti Island	49.6°N	62.5°W
2	8	St. Lawrence River	49.4°N	66.9°W
	9	Gulf of St. Lawrence	47.8°N	62.4°W
	10	Cape Brenton Island SE	44.9°N	58.9°W
	11	Halifax	48.7°N	63.7°W
	12	Boston	43.4°N	68.3°W
	13	Quonset Point	40.8°N	70.4°W
	14	New York	40.4°N	72.7°W
3	15	Atlantic City	39.0°N	72.5°W
	16	Norfolk	37.0°N	74.5°W
	17	Cape Hatteras	34.7°N	74.8°W
	18	Bermuda	32.0°N	65.0°W
	19	Charleston	32.9°N	77.4°W
	20	Jacksonville	30.5°N	79.7°W
	21	Miami	27.0°N	79.2°W
4	22	Guantanamo	19.0°N	75.0°W
	23	Key West	24.0°N	81.0°W
	24	Fort Myers	25.8°N	83.2°W
	25	Apalachicola	28.6°N	84.4°W
	26	Pensacola	28.7°N	87.5°W
	27	New Orleans	28.2°N	90.5°W
	28	Galveston	28.4°N	93.5°W
	29	Corpus Christi	27.3°N	96.2°W

CARIBBEAN AND NEARBY ISLAND COASTAL MARINE AREAS

VOLUME	AREA	NAME	APPROXIMATE CENTRAL LOCATION	
1	1	British Honduras	17.5°N	87.5°W
	2	Ciudad del Carmen	19.5°N	92.5°W
	3	Veracruz	19.5°N	95.0°W
	4	Cape Rojo	21.5°N	96.5°W
	5	Yucatan	22.5°N	89.5°W
	6	Isle of Pines	21.5°N	82.5°W
2	7	Cayman	19.5°N	80.5°W
	8	Jamaica West	18.0°N	79.0°W
	9	Jamaica South	17.0°N	77.0°W
	10	Jamaica North	19.0°N	77.0°W
	11	Jamaica Southeast	17.0°N	75.0°W
3	12	Hispaniola South	17.0°N	72.5°W
	13	Windward Passage	20.0°N	74.0°W
	14	Grand Bahama	26.5°N	77.5°W
	15	Nassau	25.0°N	77.0°W
	16	San Salvador	24.0°N	:75.0°W
	17	Acklins Island	21.5°N	·73.5°W
4	18	Hispaniola North	19.5°N	69.0°W
	19	Santo Domingo	17.5°N	69.5°W
	20	Mona Passage ·	18.5°N	68.0°W
	21	Puerto Rico South	17.5°N	66.5°W
	22	Puerto Rico North	19.5°N	66.5°W
	23	Vieques	18.5°N	65.6°W
5	24	Virgin Islands	18.0°N	64.0°W
	25	Leeward Islands	16.5°N	62.0°W
	26	Windward Islands	13.5°N	60.5°W
	27	Trinidad	11.0°N	61.5°W
	28	Barcelona	11.5°N	64.5°W
	29	Caracas	11.5°N	67.0°W
6	30	Gulf of Venezuela	12.5°N	69.5°W
	31	Riohacha	12.5°N	72.5°W
	32	Cartagena	11.5°N	75.5°W
	33	Colon	10.0°N	80.0°W
	34	Gulf of Panama	8.0°N	79.5°W
	35	Galapagos Islands	.5°S	90.5°W

INDONESIAN COASTAL MARINE AREAS

VOLUME	AREA	NAME	· APPROXIMATE CENTRAL LOCATION	
1	1	Southeast Sumatra	04.3°S	101.7°E
	2	Christmas Island	10.5°S	105.5°E
	3	Sunda Strait	6.1°S	105.7°E
	4	Northwest Java Sea	4.0°S	107.5°E
	5	Bangka Island Northwest	.8°S	105.5°E
	6	Natuna Island	3.5°N	108.0°E
	7	Sarawak	3.8°N	111.8°E
2	8	West Borneo	.7°N	107.8°E
	9	Karimata Strait	2.7°S	109.2°E
	10	Southwest Java Sea	5.5°S	109.6°E
	11	South Central Java	8.4°S	110.6°E
	12	Southeast Java	9.7°S	115.2°E
	13	Southeast Java Sea	6.3°S	113.1°E
	14	Northeast Java Sea	4.4°S	113.9°E
3	15	Bali Sea	7.8°S	116.5°E
	16	Flores Sea	7.8°S	119.9°E
	17	Northwest Flores Sea	6.0°S	117.5°E
	18	South Makassar Strait	4.2°S	117.8°E
	19	Central Makassar Strait	2.0°S	117.8°E
	20	North Makassar Strait	.1°S	118.7°E
	21	Southwest Celebes Sea	2.2°N	120.3°E
4	22	Northwest Celebes Sea	3.8°N	120.2°E
	23	East Celebes Sea	3.0°N	123.5°E
	24	Northeast Molucca Sea	3.0°N	127.0°E
	25	Southeast Molucca Sea	1.0°S	126.7°E
	26	Northeast Banda Sea	5.5°S	131.0°E
	27	Timor Northwest	7.8°S	124.5°E
	28	North Timor Sea	8.4°S	129.3°E
5	29	Melville Island	11.2°S	130.8°E
	30	West Arafura Sea	9.3°S	133.3°E
	31	East Arafura Sea	9.6°S	136.8°E
	32	West Torres Strait	10.5°S	140.5°E
	33	East Torres Strait	10.8°S	143.8°E
	34	Gulf of Papua Southeast	10.3°S	146.8°E
6	35	Southeast New Guinea	10.7°S	151.5°E
	36	Northwest Solomon Sea	6.9°S	148.7°E
	37	Admiralty Islands East	1.8°S	149.0°E
	38	New Ireland Northeast	2.1°S	152.6°E
	39	North Solomon Sea	5.5°S	153.5°E
	40	Southeast Solomon Sea	8.5°S	154.5°E

EAST AFRICAN AND SELECTED ISLAND COASTAL MARINE AREAS

VOLUME	AREA	NAME	APPROXIMATE CENTRAL LOCATION	
1	1	Kuria Muria Is	18.0°N	58.0°E
	2	West Arabian Sea	16.0°N	57.0°E
	3	Qamr Bay	15.3°N	53.0°E
	4	Socotra Is	13.3°N	54.4°E
	5	Gulf of Aden NE	13.5°N	49.0°E
	6	Gulf of Aden NW	12.6°N	45.7°E
2	7	Red Sea South	14.6°N	42.3°E
	8	Red Sea South Central	17.5°N	40.5°E
	9	Red Sea Central	20.5°N	38.5°E
	10	Red Sea North Central	23.5°N	37.0°E
	11	Red Sea North	26.4°N	35.3°E
	12	Gulf of Suez	28.5°N	-33.2°E
3	13	Gulf of Aden SW	11.4°N	45.7°E
	14	Gulf of Aden SE	12.4°N	51.5°E
	15	Somali Coast NE	9.4°N	52.3°E
	16	Somali Coast East	6.5°N	51.4°E
	17	Somali Coast SE	3.4°N	48.9°E
	18	Somali Coast South	.5°N	45.8°E
4	19	Kenya Coast	2.5°S	42.8°E
	20	Zanzibar	5.5°S	41.6°E
	21	Tanzania Coast SE	8.5°S	41.8°E
	22	Porto Amelia	11.5°S	42.3°E
	23	Lumbo	14.4°S	42.2°E
	24	Mazambique Channel NW	17.5°S	40.0°E
	25	Mozambique Channel SW	20.6°S	37.2°E
5	26	Lourenco Marques	24.5°S	37.4°E
	27	Tulear	25.0°S	42.2°E
	28	Mozambique Channel SE	20.5°S	41.7°E
	29	Mozambique Channel NE	13.2°S	46.3°E
	30	Diego Garcia	8.5°S	72.5°E
	31	Gan	.5°N	73.0°E
	32	Minicoy Is	8.0°N	73.0°E

SIBERIAN COASTAL MARINE AREAS

VOLUME	AREA	NAME	APPROXIMATE CENTRAL LOCATION	
1	1	Wrangel Island	72.0°N	178.5°W
	2	North Cape	69.0°N	175.0°W
	3	Anadyrskiy Gulf	64.0°N	177.0°W
	4	Khatyrka	60.5°N	176.0°E
	5	Khatyrka 340S	57.0°N	175.0°E
2	6	Karaginskiy Island	58.0°N	166.0°E
	7	Kronoki	54.5°N	162.5°E
	8	Commander Islands	54.0°N	168.0°E
3	9	Kuril Strait W	51.5°N	156.0°E
	10	Kuril Strait E	51.5°N	159.5°E
	11	Kuril Strait 400E	51.5°N	167.0°E
4	12	Magadan	58,5°N	147.5°E
	13	Shelikhova Gulf	60.0°N	158.5°E
	14	Sakhalinskiy Gulf	55.0°N	143.0°E
	15	Sobolevo 240 NW	55.5°N	153.0°E
	16	Sobolevo	54.4°N	155.5°E
5	17	Tartar Strait N	51.0°N	141.5°E
	18	Tartar Strait S	48.0°N	140.5°E
	19	Sakhalin NE	52.0°N	146.0°E
	20	Sakhalin SE	49.0°N	146.0°E
6	21	Okhotsk Sea SE	52.5°N	152.0°E
	22	Onekotan Island 135W	49.5°N	152.0°E
	23	Onekotan Island	48.0°N	155.5°E
	24	Soya Strait W	45.5°N	139.5°E
7	25	Soya Strait E	46.0°N	145.5°E
	26	Urup Island	46.5°N	151.0°E
	27	Vladivostok	42.0°N	131.5°E
	28	Ol'ga	42.5°N	135.5°E

Publications Volumes 1 through 6 still in production.

NTIS No. for Volume 7 is AD 733 988.

NORTH AMERICAN COASTAL MARINE AREAS

VOLUME	AREA	NAME	BOUNDARY	(C=COASTLINE)	NTIS NO.
1	1	Argentina	45–47°N	53–56°W	AD 706 357
	2	Bermuda	30–34°N	63–67°W	
	3	Guantanamo	18–20°N	74–76°W	
2	4	Boston	42°N–C	66°W–C	AD 707 699
	5	Quonset Point	40–42°N	69–72°W	
	6	New York	40°N–C	72°W–C	
	7	Atlantic City	38–40°N	72°W–C	
3	8	Norfolk	36–38°N	73°W–C	AD 707 700
	9	Cape Hatteras	34–36°N	73°W–C	
	10	Charleston	32–34°N	75°W–C	
4	11	Jacksonville	29–32°N	78°W–C	AD 707 701
	12	Miami	25–29°N	78–81°W	
	13	Key West	23–25°N	79–83°W	
5	14	Fort Myers	25–27°N	81–84°W	AD 709 973
	15	Apalachicola	27°N–C	C–86°W	
	16	Pensacola	27°N–C	86–89°W	
6	17	New Orleans	27°N–C	89–92°W	AD 710 770
	18	Galveston	27°N–C	92–95°W	
	19	Corpus Christi	26°N–C	95°W–C	
7	20	Baja	28–31°N	C–120°W	AD 709 054
	21	San Diego 200SW	28–31°N	120–125°W	
	22	San Diego	31–34°N	C–120°W	
	23	Santa Rosa	31–34°N	120–125°W	
8	24	Point Mugu	34–36°N	C–125°W	AD 710 771
	25	San Francisco	36–38°N	C–126°W	
	26	Point Arena	38–40°N	C–127°W	
9	27	Eureka	40–42°N	C–127°W	AD 709 939
	28	North Bend	42–44°N	C–127°W	
	29	Newport	44–46°N	C–127°W	
10	30	Astoria	46–48°N	C–127°W	AD 710 829
	31	Seattle	48–50°N	C–129°W	
11	1	Vancouver	50–53°N	C–134°W	AD 716 721
	2	Queen Charlotte	53–56°N	C–135°W	
	3	Sitka	56–60°N	C–140°W	

NORTH AMERICAN COASTAL MARINE AREAS (Continued)

VOLUME	AREA	NAME	BOUNDARY (C=COASTLINE)		NTIS NO.
12	4	Cordova	57°N-C	140-146°W	AD 714 360
	5	Seward	57°N-C	146-151°W	
	6	Kodiak	56°N-C	151-157°W	
13	7	Unimak	53°N-C	157-165°W	AD 717 949
	8	Dutch Harbor	51-55°N	165-172°W	
	9	Adak	51-55°N	172-180°W	
	10	Attu	51-55°N	172-180°E	
14	11	Bristol Bay	55-59°N	C-165°W	AD 719 345
	12	St Paul	55-59°N	165-172°W	
	13	St Paul 180W	55-59°N	172-180°W	
15	14	Nunivak	59-62°N	C-171°W	AD 718 346
	15	St Matthew	59-62°N	171-178°W	
	16	St Lawrence	62-66°N	C-172°W	
	17	Cape Lisburne	66-70°N	C-170°W	
	18	Barrow	70-74°N	154-170°W	

Summary of Synoptic Meteorological
Observations for Great Lakes Areas

Volume	Area
1	Ontario
1	Erie East
1	Erie West
2	Huron South
2	Huron Central
2	Huron Northwest
2	Georgian Bay
3	Michigan North
3	Michigan South
4	Superior East
4	Superior East Central
4	Superior West Central
4	Superior West

APPENDIX C

SAMPLE TABLES
OF WAVE OBSERVATIONS
FROM VARIOUS SOURCES

TABLE C-1

SAMPLE TABLES FROM "SUMMARY OF SYNOPTIC METEOROLOGICAL OBSERVATIONS"

FOR (VARIOUS AREAS)," U.S. DEPT. OF COMMERCE, NOAA, ENVIRONMENTAL DATA SERVICE

PERIOD1 (PRIMARY)
(OVER-ALL) 1963-1969

DECEMBER

AREA 0007 WAKE ISLAND
19.3N 166.4E

TABLE 18 (CONT)

WIND SPEED (KTS) VS SEA HEIGHT (FT)

HGT	0-3	4-10	11-21	22-33	34-47	48+	PCT	TOT OBS
<1	1.0	2.0	.0	.0	.0	.0	2.9	
1-2	.7	9.5	9.2	1.0	.0	.0	19.3	
3-4	.7	8.8	18.0	1.6	.0	.0	28.4	
5-6	.0	3.9	17.6	2.6	.0	.0	24.2	
7	.0	.3	9.8	3.6	.0	.0	13.7	
8-9	.0	.3	2.6	3.3	.3	.0	6.5	
10-11	.0	.0	1.3	1.3	.0	.0	2.6	
12	.0	.0	.0	.7	.0	.0	.7	
13-16	.0	.0	.7	.0	.0	.0	.7	
17-19	.0	.0	.0	.7	.0	.0	.7	
20-22	.0	.0	.3	.0	.0	.0	.3	
23-25	.0	.0	.0	.0	.0	.0	.0	
26-32	.0	.0	.0	.0	.0	.0	.0	
33-40	.0	.0	.0	.0	.0	.0	.0	
41-48	.0	.0	.0	.0	.0	.0	.0	
49-60	.0	.0	.0	.0	.0	.0	.0	
61-70	.0	.0	.0	.0	.0	.0	.0	
71-86	.0	.0	.0	.0	.0	.0	.0	
87+	.0	.0	.0	.0	.0	.0	.0	
TOT OBS								306
TOT PCT	2.3	24.8	59.5	12.4	1.0	.0	100.0	

TABLE 19

PERCENT FREQUENCY OF WAVE HEIGHT (FT) VS WAVE PERIOD (SECONDS)

PERIOD (SEC)	<1	1-2	3-4	5-6	7	8-9	10-11	12	13-16	17-19	20-22	23-25	26-32	33-40	41-48	49-60	61-70	71-86	87+	TOTAL	MEAN HGT
<6	.9	8.5	8.9	6.2	3.4	1.7	.0	.0	.0	.0	.0	.0	.0	.0	.0	.0	.0	.0	.0	173	4
6-7	.0	1.2	6.0	10.4	10.6	3.4	1.0	.9	.5	.3	.0	.0	.0	.0	.0	.0	.0	.0	.0	201	6
8-9	.3	.2	1.9	4.4	7.5	3.1	1.4	.9	.5	.3	.3	.0	.0	.0	.0	.0	.0	.0	.0	127	7
10-11	.0	.0	.7	1.2	.9	.9	1.0	.9	1.2	.7	.5	.3	.3	.0	.0	.0	.0	.0	.0	33	10
12-13	.0	.0	.0	1.0	.3	.5	.7	.3	.7	.3	.3	.2	.2	.0	.0	.0	.0	.0	.0	24	10
>13	.0	.0	.0	.3	.2	.2	.2	.0	.7	.2	.2	.2	.2	.0	.0	.0	.0	.0	.0	7	10
INDET	1.4	.5	.7	.5	.2	.2	.2	.0	.8	.2	.4	.0	.0	.0	.0	.0	.0	.0	.0	20	3
TOTAL	15	61	106	135	135	57	26	15	21	8	4	2	2							585	6
PCT	2.6	10.4	18.1	23.1	23.1	9.7	4.4	2.6	3.6	1.4	.7	.3	.2							100.0	

TABLE C-2

SAMPLE TABLE FROM U.S. NAVAL OCEANOGRAPHIC OFFICE (1963)
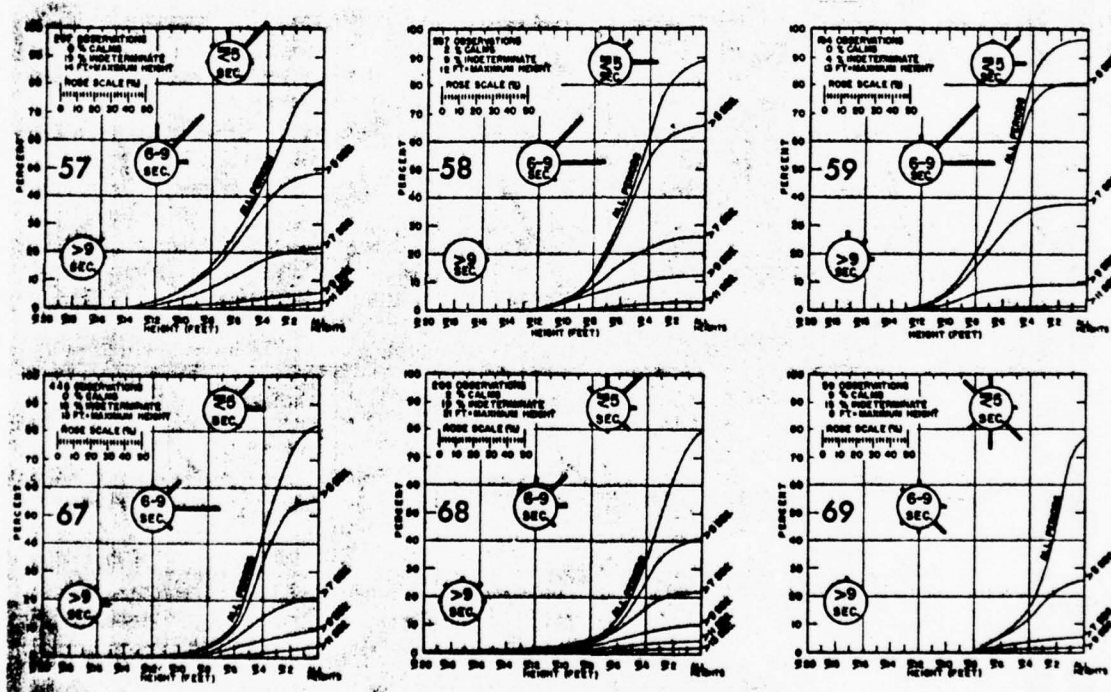
TABLE C-III

SAMPLE TABLE FROM YAMANOUCHI AND OGAWA (1970)

TABLE C-IV

SAMPLE TABLE FROM HOGBEN AND LUMB (1967)

C-3

APPENDIX D

A DESCRIPTION OF WAVE MEASURING SYSTEMS

adapted from

"The Theory and Applications of Ocean Wave Measuring Systems at and
Below the Sea Surface, on the Land, from Aircraft and from Spacecraft"

by

Willard J. Pierson, Jr.

The Tucker Shipborne Wave Recorder

A routinely operated system for recording ocean waves is the Tucker Shipborne Wave Recorder as described by Tucker (1956). This particular instrument has been in virtually continuous use on the European weather ships since the time of the publication of the above reference and many hundreds of records have been obtained in various places in the eastern North Atlantic since that time. During SKYLAB for the month of January 1974, the winds over the North Atlantic were extremely high and an area of high winds where the winds exceeded 65 knots (32.5 meters per second), equal roughly to the area of the United States east of the Mississippi, occurred and lasted for a number of days. European weather ships on station in the North Atlantic recorded the waves during this period with this instrument for use in the interpretation of SKYLAB data.

The Tucker Shipborne Wave Recorder consists of two pressure-sensitive transducers mounted with a water-tight seal on each side of the hull of a ship on the inside at a point below the water line. They are provided access to the ocean by means of small holes drilled through the hull plates. The function of these two pressure transducers is to provide the average value of the pressure caused by the height of the water on the outside of the ship above this point. The idea of these two transducers to record that part of the wave motion is that these two signals are averaged before further processing. On the line connecting these two points, which are located near midships on the particular ship being used, is an accelerometer. The design of this accelerometer is quite simple, and the signal recorded by the accelerometer is double integrated continuously as a function of time to yield a function that represents the rise and fall of that point. The signal from the pressure transducer is then added to this doubly integrated acceleration signal and the output is graphed as a function of time on a piece of chart paper. The ships on which these wave recorders are installed are typically quite small, being of the order of 150 to 200 feet long (say, 50 to 65 meters long). When extremely high waves are being recorded, the waves are typically four or five times longer than the ship and the ship rides up and down on these waves and follows the wave profile quite closely. The correction added by the pressure transducer is thus a relatively small part of the total vertical excursion sensed by the ship. If the ship did not move up and down on the waves, it would be flying part of the time and acting like a submarine during the other part of the time. A sample record from this recorder is shown in Fig. D-1. The date, time and other pertinent information is also shown on the figure.

The wave record obtained by the Tucker Shipborne Wave Recorder needs to be corrected as a function of frequency. The double integration is not perfect so that some waves are over amplified by the process for some frequencies and others are attenuated. Also, the added correction for the pressure fluctuation due to the shorter period waves is a function of the depth of the pressure transducer on the side of the hull and of other dimensions of the ship. A calibration curve needs to be derived for each ship on which this recorder is installed. The procedures for deriving this calibration curve were given by Cartwright (1961).

Wave records obtained by this instrument, as used on many different ships, have been spectrally analyzed and corrected according to the appropriate calibration curve by many different scientists. Pertinent references are Moskowitz, Pierson and
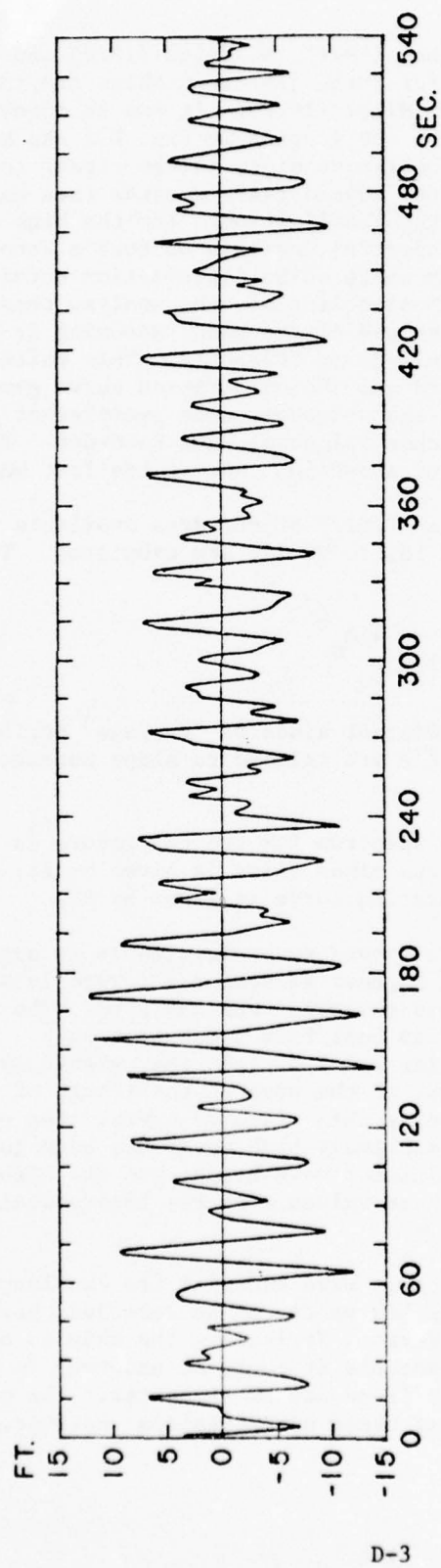
Figure D-1. Sample Wave Record from the Shipborne Wave Recorder 0250 GMT 18 March 1956, 45° 15' N, 15° 31' W.

Mehr (1962, 1963, 1965), Ewing and Hogben (1971), M. Miles (1972) and Hoffman (1974. a). Sample calibration curves for three different ships are tabulated as a function of frequency in Table D-1 from Miles (1972). It can be noted that a spectrum estimated from a record such as the one graphed in Fig. D-1 has to be multiplied by values greater than one for low frequencies, values closer to one for certain intermediate frequencies, and values considerably greater than one as the frequency increases towards the upper range of definition. For the high end of the frequency band typically covered in a spectral analysis of such a record, the amplification factors are very high, and any white noise digitization error in the records can lead to unrealistic values. Most scientists who analyze these records calculate the white noise level at the high end of the band, assuming it to be all white noise and well above some unknown Nyquist frequency. This white noise level is then subracted from the entire record and the calibration curve given by the above table is then applied. Fig. D-2 and D-3 shows some examples of spectra calculated from the data obtained by the Tucker Shipborne Wave Recorder. The peak of the first spectrum is at a spectral value of about 50; that of the last one is at 0.07.

Table D-2 shows a sample from Miles (1972) of the data available from these records. The parameters of records NW 181 to NW 210 are tabulated. The significant height is related to m_o by

$$H_{\frac{1}{3}} = 4 m_o^{\frac{1}{2}}$$

The values T(-1), T(1) and T(2) are different kinds of "average" period, based on various moments of the spectrum. The K's are related to slope parameters of the spectrum.

Table D-3 shows the values of the spectrum for the top record in Fig. D-2. The raw spectrum is given by SO, the spectrum minus noise is given by S1, and the spectrum after multiplication by the calibration curve is given by S3.

The data from this instrument have proved to be invaluable to naval architects. Over the years the records for the ten highest sequences observed in a twenty minute interval in the North Atlantic have been assembled and analyzed. The very highest waves had a significant wave height of 55 feet from crest to trough. This implies that one wave in one hundred at that time was 1.5 times that significant wave height, or somewhere near 82 feet from the crest of the wave to the trough of the wave as it passed the weather ship that was recording this train of waves. The probabalistic structure of the wave motion for such extremely high waves has been quite well verified by calculating the so-called significant wave height and the highest wave in a twenty minute interval and comparing these values with the theoretical results obtained by Longuet-Higgins.

The advantages of the Tucker Shipborne Wave Recorder are considerable. It can be mounted on any relatively small ship and waves can be recorded wherever that ship is stationed. The water can have any depth. Typically, the ship is hove to while the waves are being recorded but in principle it could be underway in head seas and record the waves as a function of their frequency of encounter. The calibration problem is somewhat more difficult under these circumstances, however, so that this

TABLE D-1

FREQUENCY RESPONSE CORRECTION FUNCTIONS
[from Miles (1972)]

		WEATHER EXPLORER	WEATHER REPORTER	WEATHER ADVISER
N	OMEGA	A(N)	B(N)	C(N)
0	0.00	1.0000	1.0000	1.0000
1	0.05	1.0000	1.0000	1.0000
2	0.10	1.0000	1.0000	1.0000
3	0.15	1.0000	1.0000	1.0000
4	0.20	1.4524	1.4245	1.6677
5	0.25	1.3253	1.2787	1.2979
6	0.30	1.2048	1.1442	1.1392
7	0.35	1.1394	1.0622	1.0673
8	0.40	1.1294	1.0303	1.0400
9	0.45	1.1519	1.0256	1.0402
10	0.50	1.1999	1.0405	1.0599
11	0.55	1.2703	1.0584	1.0956
12	0.60	1.3641	1.1107	1.1456
13	0.65	1.4829	1.1635	1.2098
14	0.70	1.6301	1.2307	1.2888
15	0.75	1.8093	1.3103	1.3839
16	0.80	2.0277	1.4046	1.4970
17	0.85	2.2948	1.5162	1.6307
18	0.90	2.6214	1.6470	1.7882
19	0.95	3.0173	1.7979	1.9737
20	1.00	3.5052	1.9751	2.1922
21	1.05	4.1087	2.1830	2.4499
22	1.10	4.8559	2.4256	2.7545
23	1.15	5.7837	2.7084	3.1157
24	1.20	6.9462	3.0409	3.5451
25	1.25	8.4121	3.4329	4.0575
26	1.30	10.2667	3.8940	4.6710
27	1.35	12.6353	4.4413	5.4087
28	1.40	15.6792	5.0934	6.2990
29	1.45	19.6103	5.8701	7.3782
30	1.50	24.7277	6.8016	8.6918
31	1.55	31.4321	7.9219	10.2980
32	1.60	40.2735	9.2728	12.2707
33	1.65	52.0057	10.9108	14.7046
34	1.70	67.7020	12.9024	17.7216
35	1.75	88.8481	15.3343	21.4788
36	1.80	117.4970	18.3199	26.1804
37	1.85	156.6320	21.9977	32.0919
38	1.90	210.5760	26.5521	39.5609
39	1.95	285.3370	32.2142	49.0439
40	2.00	389.2020	39.2524	61.1438

TABLE D-2

SAMPLE DATA SUMMARY FOR SBWR FREQUENCY SPECTRA
[Miles (1972)]

RECORD	DATE (HR-DY-MO-YR)	H(1/3) (METERS)	CONFIDENCE INTERVAL ON H(1/3) UPPER 95%	LOWER 5%	T(-1) (SEC)	T(1) (SEC)	T(2) (SEC)	K(-1)	K(1)	K(2)
NW181	12-22-12-61	3.648	4.033	3.300	11.03	9.84	9.12	1.35	1.34	1.35
NW182	12-27-12-61	4.102	4.491	3.748	9.33	8.56	8.11	1.08	1.09	1.13
NW183	12-28-12-61	5.331	5.756	4.938	8.67	7.70	7.23	0.88	0.86	0.88
NW184	12-22- 1-62	9.229	10.285	8.282	11.95	10.62	9.74	0.92	0.91	0.90
NW185	12-28- 1-62	4.551	4.976	4.162	10.58	9.41	8.75	1.16	1.14	1.15
NW186	12-29- 1-62	6.968	7.765	6.252	10.08	9.06	8.45	0.89	0.89	0.81
NW187	12-31- 1-62	10.048	11.315	8.923	11.54	10.03	9.08	0.85	0.82	0.90
NW188	12- 9- 2-62	6.357	7.024	5.753	10.31	9.17	8.48	0.95	0.94	0.95
NW189	12-10- 2-62	13.657	15.170	12.294	12.11	10.13	8.97	0.76	0.71	0.68
NW190	12-11- 2-62	10.084	11.107	9.156	11.42	9.88	8.97	0.84	0.81	0.80
NW191	12-13- 2-62	5.064	5.635	4.551	11.17	10.17	9.50	1.16	1.17	1.19
NW192	12-15- 1-64	5.036	5.553	4.568	9.05	8.00	7.42	0.94	0.92	0.93
NW193	12-20- 1-64	4.739	5.173	4.342	9.29	8.35	7.83	1.00	0.99	1.01
NW194	12-21- 1-64	6.668	7.446	5.972	12.62	11.12	10.11	1.14	1.12	1.10
NW195	12-23- 1-64	3.592	3.975	3.246	11.33	10.29	9.67	1.39	1.41	1.44
NW196	12-24- 1-64	2.427	2.679	2.198	10.62	9.58	8.92	1.59	1.59	1.61
NW197	12-29- 1-64	8.047	8.990	7.203	10.53	9.40	8.68	0.87	0.86	0.86
NW198	12-30- 1-64	11.327	12.772	10.046	12.20	10.81	9.88	0.85	0.83	0.83
NW199	12- 3- 2-64	8.197	9.047	7.426	11.04	9.81	9.09	0.90	0.89	0.89
NW200	12- 4- 2-64	6.332	7.019	5.712	11.00	9.67	8.84	1.02	1.00	0.99
NW201	12- 5- 2-64	2.189	2.400	1.997	9.15	8.30	7.83	1.44	1.45	1.49
NW202	12-26- 7-64	2.926	3.221	2.659	7.90	7.41	7.11	1.08	1.12	1.17
NW203	12-23- 7-64	3.336	3.684	3.022	9.73	8.94	8.46	1.24	1.27	1.30
NW204	12-29- 7-64	1.600	1.744	1.468	8.27	7.63	7.30	1.53	1.56	1.63
NW205	12-30- 7-64	3.804	4.222	3.427	8.79	8.23	7.91	1.05	1.09	1.14
NW206	12- 4- 8-64	3.328	3.712	2.983	8.83	8.17	7.79	1.13	1.16	1.20
NW207	12- 5- 8-64	3.602	4.016	3.230	9.67	8.96	8.50	1.19	1.22	1.25
NW208	12- 8- 8-64	1.337	1.453	1.231	8.09	7.40	7.10	1.63	1.66	1.73
NW209	12-13- 8-64	0.698	0.750	0.650	7.30	6.45	6.13	2.04	2.00	2.07
NW210	12-15- 8-64	1.208	1.305	1.118	6.35	5.83	5.66	1.35	1.38	1.45

TABLE D-3 WAVE DISPLACEMENT SPECTRUM [MILES (1972)]

1200   Feb. 10, 1962   Ship-<u>Weather Reporter</u>   Record No. NW189

Variance- 11.6438 M**2   Sig. Wave Hgt. - 13.6568 M

Noise Level- 0.2993 M**2/RPS   CUT-OFF- 0.225 RPS

DOF- 26   Total DOF- 120

T(-1)- 12.1150 sec   T(1)- 10.1342 sec   T(2)- 8.9675 sec

K(-1)- 0.7650   K(1)- 0.7108

N	ω (RPS)	S0 (M**2/RPS)	S1 (M**2/RPS)	S2 (M**2/RPS)
0	0.00	0.0000	0.0000	0.0000
1	0.05	0.0000	0.0000	0.0000
2	0.10	0.0000	0.0000	0.0000
3	0.15	0.0000	0.0000	0.0000
4	0.20	0.0000	0.0000	0.0000
5	0.25	1.4003	1.1010	1.4078
6	0.30	2.6504	2.3511	2.6902
7	0.35	15.6533	15.3540	16.3087
8	0.40	41.8450	41.5457	42.8062
9	0.45	45.7956	45.4963	46.6592
10	0.50	30.0550	29.7557	30.9617
11	0.55	16.2779	15.9786	16.9113
12	0.60	9.2435	8.9441	9.9341
13	0.65	7.0654	6.7661	7.8723
14	0.70	4.2780	3.9787	4.8960
15	0.75	4.4176	4.1182	5.3962
16	0.80	2.6207	2.3214	3.2608
17	0.85	2.1931	1.8938	2.8714
18	0.90	1.9518	1.6525	2.7216
19	0.95	2.0900	1.7907	3.2195
20	1.00	2.4724	2.1731	4.2920
21	1.05	2.0685	1.7692	3.8621
22	1.10	1.5042	1.2048	2.9224
23	1.15	0.9857	0.6864	1.8591
24	1.20	0.8697	0.5704	1.7346
25	1.25	1.1481	0.8488	2.9139
26	1.30	1.0156	0.7162	2.7890
27	1.35	0.6277	0.4234	1.8803
28	1.40	0.6198	0.3289	1.6753
29	1.45	0.6456	0.3320	1.9487
30	1.50	0.6142	0.3281	2.2319
31	1.55	0.6359	0.3062	2.4254
32	1.60	0.5359	0.2040	1.8920
33	1.65	0.3057	0.0569	0.6209
34	1.70	0.2777	0.0000	0.0000
35	1.75	0.2335	0.0000	0.0000
36	1.80	0.2703	0.0000	0.0000
37	1.85	0.3921	0.0455	1.0009
38	1.90	0.3248	0.0309	0.8214
39	1.95	0.2793	0.0018	0.0573
40	2.00	0.3209	0.0008	0.0319

Fig. D-3 – Sample Spectra from Tucker Shipborne Wave Recorder Data
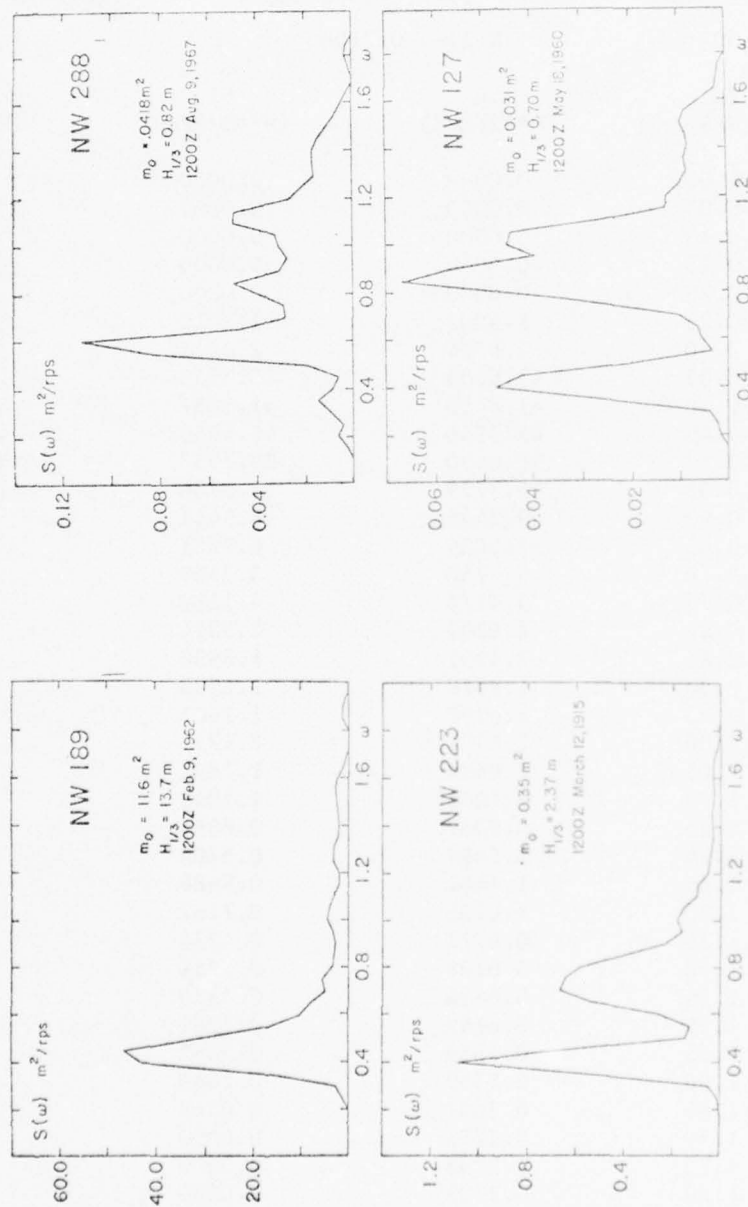
Fig. D-2 – Sample Spectra Estimated from Tucker Shipborne Wave Recorder Data.

is not done very often. This particular instrument has yielded a wealth of data on the wave conditions just to the west of the British Isles over a period of almost twenty years. Data on wave statistics can be found, for example, in a report by Draper and Squires (1967). The Tucker Shipborne Wave Recorder has also been installed on a ship off the coast of South Africa for a number of years and is currently in use on the weather ships from Canada that occupy weather station PAPA in the North Pacific.

Data Buoys

The February 1975 issue of the "Data Buoy Technical Bulletin" (Volume 1 No. 6) published by the NOAA data buoy office, NSTL, Bay St. Louis, Mississippi, contains a description of a modification of the experimental buoys developed by NOAA so that they now provide real time wave spectral data. The article in this technical bulletin describes the system quite completely, and there is little point in paraphrasing it. Therefore, the article is quoted in full below.

BUOYS NOW PROVIDE REAL TIME WAVE SPECTRAL DATA

"A new experimental wave measuring system was installed on two environmental data buoys in early December 1974. Both EB-01 (deployed in the Atlantic off Norfolk, Virginia) and EB-03 (deployed in the Gulf of Alaska) are 12-meter diameter discus buoys configured to produce, each 3 hours, raw data from which wave spectra are computed. These buoys are equipped with payloads that include an on-board programmable computer. The wave sensor hardware on board these two buoys consists of an accelerometer and a two-stage electronic double integrator sensor system that produces analogs of acceleration, velocity, and displacement for the vertical heave motion. The on-board computer has been programmed to produce data from which heave displacement spectra are computed. A total of 51 data words associated with measurement of spectra is reported to the Miami Shore Collection Station (SCS) once every 3 hours.

"The instantaneous acceleration analog voltage is sampled each second by the buoy multiplexer and analog-to-digital converter. Readings are taken for approximately 15 minutes; the on-board digital computer processes these samples into 51 autocovariances of acceleration, corresponding to lags of 0,1, 2 --- 50 seconds. These autocovariances are encoded and relayed to the SCS. They are then partially decoded and relayed to the Data Handling Center at the National Space Technology Laboratories. There, raw spectral densities are produced from the autocovariances, Hanning smoothing is applied, noise corrections are made, and the spectrum is modified to account for the ocean platform transfer function. Finally, the heave displacement spectrum is produced by assuming superposition and operating on each spectral density with ω^{-4}. These computations result in the graphic presentation of spectral density for heave displacement at frequencies of 0.01, 0.02 --- 0.49, 0.50 Hz.

"The performance of these systems has been determined by comparison of the spectra produced by the EB-03 system to spectra produced by a Waverider buoy deployed nearby. Shown below are results of this comparison test, during which EB-03 was not anchored, but tethered to a ship standing by. Other tests have been performed and evaluations are continuing, but all preliminary analysis indicate that

the spectral data are excellent.

"Both EB-01 and EB-03 have been producing these spectra each 3 hours since early December 1974. These buoys are being used to test the new measurement concept from both the engineering and operational points of view, with the objective of installing similar systems on future operational buoys.

-- NDBO Contact: K. Steele"

As can be seen from Fig. D-4, which accompanied this article, the spectra compare quite favorably. It is hoped that this experimental program will be extended to include the other operational buoys presently on station in the North Pacific, the Gulf of Mexico, and off the east coast of the United States. If this were done, there would be a total of five experimental buoys, two in the Gulf of Alaska, two off the east coast, and one in the Gulf of Mexico that will be able to obtain wave spectra every three hours routinely.

It is noted that these experimental buoys are quite a bit smaller than weather ships and that they probably track the rise and fall of the sea surface quite well at the frequencies involved in the gravity wave spectrum. Thus only minor modifications are required to relate the twice-integrated vertical accelerations recorded by the sensor installed inside the buoy to the wave spectrum.

It might also be noted that there have been a number of variations of the basic Tucker principle tested on various ships. A device with a laser on it that projects over the bow of a ship can be used to measure the distance between the instrument containing the laser and the surface of the water below. This distance plus the twice integrated acceleration of the laser then yields a wave record. The problem with this instrument is that the bow of the ship, especially when the ship is under way, may plunge below the surface of an oncoming wave and the entire instrument system may be damaged, or torn completely loose from its mounting, and lost at sea. However, for not too high waves such a system does provide better information on the high frequencies in the wave pattern.

Wave Poles and Wave Wires

Another system for recording the rise and fall of the sea surface as a function of time at a fixed point is a wave pole, or a wave wire mounted in a fixed structure. Also pipes with spark plugs sticking out of the side at fairly close intervals have been used. The rising water shorts out these spark plugs as it rises and the signal that is produced is a measure of the position of the last shorted out spark plug. These wave poles or wave wires work on a variety of principles. Some sense the change in capacitance induced by the rising and falling of water, others sense a change in resistance. However, the output is simply a graph of the rise and fall of the water at the point involved. For all such systems, the frequency response of the recorder is usually a problem, and there tends to be some roll-off at some frequency that in general is not too high. In considering the work of Stacy (1974) it appears that the very high-frequency part of the spectra of hurricane waves in the Gulf of Mexico may have undergone some attenuation due to this roll off. Such a recording
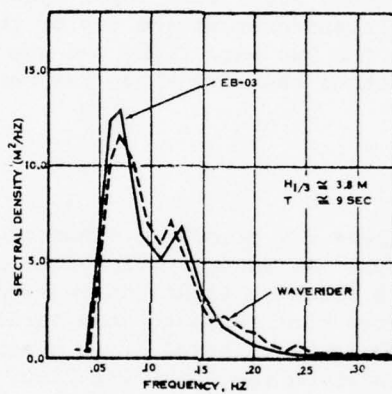
Figure D-4. Comparison of Displacement Spectra from EB-03 and
Waverider at Latitude 48° 54' N, Longitude 126° 22' W.

system has the disadvantage that it requires a fixed platform for installation. Consequently wave poles and wave wires can only be operated in shallow water. Wave recorders referred to as Baylor gages were installed on oil drilling platforms in the Gulf of Mexico by a consortium of oil companies a number of years ago in order to record the waves generated by hurricanes that passed near by. Later, the same oil companies supported a program to develop a numerical wave specification and numerical wave forecasting procedure for hurricanes in the Gulf of Mexico.

The Baylor gauge is described in a report by Draper and Fortnum (1974). Two models are available. One contains the electronics and transducer in a stainless steel housing that can operate when submerged; the other is more conventional. The wave staff consists of two tensioned steel wire ropes spaced about 9 inches apart and electrically connected to a transducer at the top of the staff. The sea water acts as a short circuit between the two wire ropes and the transducer measures the a.c. impedance so that the length of the wire above the water surface is known.

The Waverider Buoy

The Waverider buoy is a sphere 0.7 meters in diameter. It is weighted to float with a preferred upward direction. An antenna sticks out the top, and the upper portion is transparent so that a flashing light can be seen inside the buoy. The sensing system is an accelerometer that tends to stay vertical as the sphere pitches and rolls on the waves. The sphere is tethered by an elastic line to a submerged buoyant float that produces tension on the anchoring line. It behaves essentially like a small fluid particle of sea water and follows the orbital velocity of the passing waves essentially in circles of varying radius with time. The vertical component of the acceleration of the buoy is recorded and double integrated. The output is therefore a representation of wave elevation versus time in Lagrangian coordinates. To first order, a spectrum from such a record is essentially the same as the spectrum from waves passing a fixed point (see for example Chang (1968)). Of the many commercially available wave recording systems, this one appears to have been very successful. A study by Briscoe and Goudriaan (1972) describes the various ways that the data can by analyzed and shows numerous spectra obtained from the data recorded by this system.

Calibration of Wave Recorders

Draper and Humphery (1973) have compared the calibration of the shipborne wave recorder and the Waverider buoy. One of the problems in calibrating an instrument that senses the vertical acceleration of its motion is that it is difficult to build a device that will accelerate and decelerate the recorder over distances much larger than three meters. The shipborne wave recorder and the Waverider buoy have been calibrated for simulated waves of about three meters in height, but this did not demonstrate the full capabilities of these recorders which are frequently used to measure much higher waves. In order to simulate waves of much greater height arrangements were made to use the "Big Wheel" Ferris wheel, or merry-go-round, at South Sea Fun Fair. This Ferris wheel has a diameter of 14 meters and could be rotated to give simulated wave periods from about 13.6 seconds to 30 seconds. The ac-

celerometer part of the Tucker shipborne wave recorder and the Waverider buoy were fastened to a seat of the Ferris wheel and the Ferris wheel was rotated at various speeds, as rapidly as 13.6 seconds per rotation. The output of the recording system should be, after double integration, a sinusoid with height given by the diameter of the wheel after correction for known calibration effects.

The conclusions of this study were essentially that both instruments function as predicted except that the shipborne wave recorder response was better for long periods than had been theoretically calculated and that a slight correction to the previous calibration for long period waves might be made under certain circumstances in analyzing the data. The errors in the measurement of the waves as a function of the frequency spectrum are very small indeed compared to the problems of sampling variability for the data. The two systems can be considered to have been thoroughly calibrated by these techniques and by the studies that had been carried out previously.

APPENDIX E

A Tabulation of Available Measured Spectra

	Pierson & Marks (1952)	Moskowitz, Pierson & Mehr (1962, 1963, 1965)	Inoue, T. 1967
Record Length	1500 sec. (750 data)	approx. 900 sec. (approx. 600 data)	$3^{hr} - 30^{min}$
Sample Rate	$\Delta t = 2$ sec.	1-1/2 sec.	3 sec.
Analysis Method	Correlation 30 lags	Correlation (B & T) 60 lags	Correlation from 2 sensors' data, 120 lag
Smoothing	Hamming	Hamming	Hamming
Corrections		Noise average of last ten values was subtracted	Noise ratio
Freq. Range		$1/180 - 1/3$ sec^{-1}	$1/720 - 1/6$ sec^{-1}
Units Energy	$C_m^2 \cdot sec$	$(ft)^2 \cdot sec$	m^2 sec
Units Freq.	sec^{-1}	sec^{-1}	sec^{-1}
Assoc. Para.	90% confidence band variance	95%, 5% confidence band var. significant ht. Average $T(\to T_o)$	$H_{1/3}$
Instrumentation	pressure gauge 32.5 ft.	Tucker Shipborne Wave Recorder	Vibrotron press transd. at depth of 30.6, 88.1 m
Time (Year)	1951	1955 - 1960	1963
Location	Long Beach, NJ	OWS in Atlantic	FLIP North Pacific
No. of Spectra		400	460

	Pickett (1962) Lazanoff (1964)	Brown, Scringer & Kelly (1966)	Miles, N. (1972)
Record Length	20 min.	1/2 hour	10^{min}, 15^{min}
Sample Rate	1 sec.		$\Delta t = 0.613$ sec
Analysis Method	Correlation 60 lags	Auto-correlation 120 lags	FFT
Smoothing			20 point averages 10 point overlap
Corrections			low pass anti-aliasing filter average low freq. Cut off high freq. smoothing and white noise subtraction
Freq. Range	$1/120 \sim 1/2$ sec^{-1}		$0 \sim 5.12$ rps computed $0 \sim 2$ rps
Units Energy	ft^2 sec.	ft$^2 \cdot$ sec	m^2/rps
Units Freq.	sec^{-1}	sec^{-1}	radians per sec (rps)
Assoc. Para.	Total Energy	Total Energy	var., sig. wave ht. $T(-1)$, $T(1)$, $T(2)$ analogue → dig. → analog + low pass filt. →digit.
Instrumentation	Resistance Wire Staff	Spar Buoy	Tucker Shipborne Wave Recorder
Time (Year)	1961, 1962	1966	14 years, 1954-1967
Location	Argus Island	Pacific	Station India, OWS Weather Explorer, Reporter III, Adviser
No. of Spectra	100		323

	Snodgrass, et al (1966)	Moskios & Deleonibus (1965)	Schule, et al (1971)
Record Length	5400 x 8 sec = 10800 sec = 3 hr.	mostly 30 min.	9.5 nautical miles (17.6 km)
Sample Rate	$t = 2$ sec.	$\Delta t = 0.5$ sec.	0.04 sec that correspond = 15 ft. (46 m) roughly
Analysis Method	Auto-correlation	Correlation	Correlation and also FFT
Smoothing	'Parzen fader' (to avoid neg. side bands 0.0030,0.0617,0.2471, 0.3762,0.2471,0.0617, 0.0030		Blackman & Tukey
Corrections		Correction by ship speed	low-pass by Butterworth filter
Freq. Range	0 – 250 m c/s ($T = \to 4$ sec)	$.03 \sim 1$ cps	$0 \sim 0.11$ ft.$^{-1}$ (0.35 m^{-1})
Units Energy	$e(cm^2/mc/s)$ (log scale)	ft^2/sec^{-1}	$ft^3(m^3)$
Units Freq.	mc/s	cps	ft^{-1}, m^{-1}
Assoc. Para.	Wave direction (partially), events identification tides are removed by num. high-pass filtering	$H_{1/3}$	Linear and exponential growth parameters
Instrumentation	Vibrotron depth 20 m	Shipboard Wave Height Sensor	Airborne Laser
Time (Year)	1965	1963 – 1964	1969
Location	6 points in Pacific along a great-circle route between Antarctica and Australia	Near Argus Island	Cape Henlopen, Del.
No. of Spectra		12	10

	Barnett and Wilkerson (1967)	Bennett (1968)	Rudnick (1969)
Record Length	1200 - 1700	1800 sec (1800 data)	1728 sec (864 data)
Sample Rate	0.05 sec. correspond	$\Delta t = 1$ sec	$\Delta t = 2$ sec
Analysis Method	Correlation	Correlation 60 lags	Correlation 64 lags
Smoothing	Hamming	Parzen lag window	Hamming
Corrections	Airplane motion was filtered, freq. was transformed		
Freq. Range	.05 ~ .25 cps	0 ~ 0.5 Hz (used 0 ~ 0.2)	
Units Energy	m^2 sec	log-power density IN^2/Hz	
Units Freq.	cps	Hz	cps
Assoc. Para.	growth of wind wave	Directional	Directional
Instrumentation	radar wave profiler & accelerometer (resolution 1 ft. in vertical 100 ft. horizontal)	Bottom Pressure Instrument Array (6 probes)	FLIP - Press sensor at 30 m, two horizontal acc.
Time (Year)	1965	1965	1963
Location	Offshore areas of the Middle Atlantic States	Gulf of Mexico off Panama City, Florida	near 39°20'N 148°30'W
No. of Spectra			

	Caul and Brown (1967)	Ewing and Hogben (1971)	Yamanouchi (1969)
Record Length	15 mm (900 data)	10 min.	10 min.
Sample Rate	$\Delta t = 1$ sec	$\Delta t = 1$ sec	$\Delta t = 0.5$ sec.
Analysis Method	Correlation 45 lag	Correlation	Correlation 60 lags
Smoothing	Blackman & Tukey	Hamming 1/4,1/2,1/4	Q filter −0.06, 0.24,0.64,0.24, −0.06
Corrections	high and low freq. range were cut off	noise correction	
Freq. Range	$0 \sim 0.5$ Hz $(0 \sim 0.35)$	$0 - 0.25$ Hz	$0 - 2$ rps
Units Energy	FT^2/Hz	m^2 sec	m^2 sec
Units Freq.	Hz	Hz	circular freq. rps
Assoc. Para.		B.F. No Hs Tz, Wind Dir., Wave Dir.	var $H_{1/3}$
Instrumentation	press. gauge in FFWM (free-floating wave meter) & accelerometer for Monster Buoy	Tucker Shipborne Wave Recorder	Shipborne Encounter Wave Recorder
Time (Year)	1966-1967	1963	1968
Location	Bermuda and off San Diego	Marsden Square 285,286,287,217, 218,219,251,252,222	off Honshu
No. of spectra	6	97	

	Longuet-Higgins, Cartwright & Smith (1963)	Ewing (1969)
Record Length	12-17 min. (about 2000 data)	25 min.
Sample Rate	$\Delta t = 0.5$ sec	$\Delta t = 0.5$ sec.
Analysis Method	Correlation (57-66 lags)	Correlation 100 lags
Smoothing	Hamming 1/4,1/2,1/4	
Corrections	subtracted noise energy	
Freq. Range	0.4 - 4.0 rps	0.8 - 0.24 cps
Units Energy	FT^2 sec	m^2 sec
Units Freq.	circular freq. rps	0.8 - 0.24 cps
Assoc. Para.	directional spectra	directional spectra
Instrumentation	Roll-Pitch Buoy	Cloverleaf Buoy
Time (Year)	1955-1956	1967
Location	England	R.R.S. Discovery 56°45' N 18°57' W
No. of Spectra		

	Hafer (1970)	Lockheed (1974)	Larsen and Fenton (1974)	Ploeg (1971)
Record Length	1 hr.	8,10,20 min.	30 min.	20 min.
Sample Rate		$\Delta t = .61035$	$\Delta t = .8789$	
Analysis	Correlation	Correlation	FFT	B & T
Smoothing / Correction		/ limited	/ mean and trend removed	Hamming /
Freq. range	.04-.2 Hz	.053-2.0		
Units Energy	ft^2/Hz	m^2/rps	$m^2/rps + ft$	ft^2/rps
Units Freq.	Hz	rps	rps	rps
Assoc. Para.				
Instrumentation	acc. & press + read	Tucker	Vibratron	accelerometer
Time	1967-69	1971-73	1972-73	
Location	Coast of BC	Pacific - between Seattle & Japan	Cobb Seamount	
# of Spectra	425	176	614	4,000
Notes		Ship at speed		46 published

	Ferdinande, V. et al, (1975)	Lockheed (1971) Lockheed (1973) Hoffman, (1974a)	Hoffman, (1975)
Record Length	12 min.	15 min.	12 min.
Sample Rate	$\Delta t = 1$ sec.	$\Delta t = .60$	$\Delta t = .3059$
Analysis	Auto-correlation 60 lag	Auto-correlation 100 lag	FFT
Smoothing / Correction	Hamming/correction from encounter freq.	Hamming	3 point avg. .25,.5,.25
Freq. range	hi freq. cut off $\omega = 1.4$	$\omega = 0-2.0$ rps	0-2.0 rps / selected low-freq. cutoff
Units Energy	m^2 sec	ft^2 sec.	$m^2/$ rps
Units Freq.	sec^{-1}	sec^{-1}	rps
Assoc. Para.			
Instrumentation	Tucker	Tucker	Tucker
Time			
Location	N. Atlantic	Station 'Papa' N. Pacific	Station 'Kilo' N. Atlantic
# of Spectra	45	355 & 305	93
Notes	Ship at speed		

	Saetre (1974)	NDBO (see text)	FNWC (see text)
Record Length	13 min.	15 min every 12 hours	every 12 hours
Sample Rate		Δt = 1 sec	
Analysis	FFT	auto-correlation 51 lag	
Smoothing / Correction	avg. over 6 harmonics / equilib. law tail at hi freq.	Hanning / buoy transfer function known	
Freq. range	.02-.2 Hz	.01-.50 Hz	.04-.16 Hz
Units Energy	m^2/Hz	m^2/Hz	ft^2/Hz
Units Freq.	Hz	Hz	Hz
Assoc. Para.			
Instrumentation	Tucker	Accel.	Computer forecast using Pierson/NYU spectral model
Time	Winters 69-70,71-72,72-73		Continuous
Location	North Sea	EBO 03 56°N,147.9°W EBO 13 36.5°N, 73.5°W EBO 12 26°N, 94°W	Northern Hemisphere
# of Spectra	41	System still under development	2275 grid points in N. Pacific
Notes	Storm spectra	large no. of spectra available, potential for large amounts of high quality spectra	12 direction, 15 frequency components at each grid point

APPENDIX F

Catalog of Tucker Shipborne Wave Recorder Data
From ISSC 1973 Committee 1 Report

ATLANTIC AND EUROPEAN WATERS

ADDRESS OF HOLDING AGENT	REFERENCE TO PUBLISHED DATA	NUMBER OF RECORDS	MONTHS AND YEARS COVERED	LOCATION	ANALYSIS	DATA FORMAT	REMARKS
Centre Belge de Recherches Navales 26 Rue des Drapiers 1050 Brussels 5 Belgium	Series of papers by Prof G Aertssen in the transactions of the Royal Institution of Naval Architects	849 20 minute records	1960 to 1971	Voyages ranging over the North and South Atlantic between ports in Europe, North and South America and Africa including 3 voyages through the Straits of Magellan to Chile	Extraction of heights and periods. Spectral analysis mostly by methods of Tukey a few by Fourier analysis	693 estimates of height and period 71 spectra	
KNMI Utrechtseweg 297 De Bilt Netherlands		About 1300 records of 30 minutes duration	8 years intermittently 1964-1971	Scattered over Ocean Weather Stations A 62° N 33° W I 59° N 19° W J 52.5° N 20° W K 45° N 16° W M 66° N 2° E in the North Atlantic	Estimates of height and period from about 100 records. Spectra from about 30 records	Analysis not completed	Comparisons with results from other instruments included
Meteorologie Nationale 1 Quai Branly 75 Paris 7ème France	DEVILLAZ et BARBOTTIN "l'Analyse Automatique des Enregistrements de Houle" l'EXEM No 240 June 1967	20 minute records twice daily at 0000 and 1200 hours and special records in storms	8 years intermittently 1962-1971	North Atlantic Ocean Weather Stations A 62° N 33° W Marsden Square 220 J 52.5°N 20° W Marsden Square 182/183 K 45° N 16° W Marsden Square 146	Inspection of records and spectral analysis using 500 Fourier Harmonics averaged over 1 sec bands over range 3 to 26 seconds	Unchecked raw data on 5 hole punched tape and also on 7 track magnetic tape. Tabulated and Plotted Spectra and Statistical Distributions of Height also available on punched cards	
National Institute of Oceanography Wormley Near Godalming Surrey	Papers by Draper et al	2,400 records from Station India and 1,440 records from Station Juliett all of 12 minutes duration	1953 to 1964	North Atlantic Weather Stations India (59°N 19°W) and Juliett (52°30'N 20°W) Marsden Square 182	Heights and periods abstracted from records	Statistical distributions of heights and period in standard format recommended in reference 5.10	Intermittent unanalysed records also available for North Atlantic Weather stations Alpha and Kilo from 1953 to present
		Records of 15 minutes duration every 3 hours throughout 1 complete year at each of 9 stations in the Irish Sea, English Channel and North Sea	1 year at each station	Light Vessels in the Irish Sea(Morecambe Bay and Mersey Bar) English Channel (Sevenstones, Owers & Varne) and North Sea (Tongue, Smith Knoll & North Carr also, Vessel Facits at station 57°30N 3°E in North Sea). All in Marsden Squares 181 and 216	Heights and periods abstracted from records	Statistical distributions of heights and periods in standard format recommended in reference 5.10	Similar analysis is being carried out for other UK light vessels (Shambles, Helwick, Dowsing and Galloper)

ATLANTIC AND EUROPEAN WATERS

ADDRESS OF HOLDING AGENT	REFERENCE TO PUBLISHED DATA	NUMBER OF RECORDS	MONTHS AND YEARS COVERED	LOCATION	ANALYSIS	DATA FORMAT	REMARKS
Superintendent Ship Division NPL Faggs Road Feltham Middlesex (holds analogue traces) Director National Institute of Oceanography Wormley Near Godalming Surrey (holds punched cards)		526 records of 15 minutes duration	Intermittently over 5 years 1963 to 1968	From British Research Trawler cruises. Scattered over Marsden Square Nos. 145, 181, 182, 215, 216, 217, 218, 219, 251 and 252	Estimates of height and period from 526 records. Computation of Spectra from 97 (highest) records	Statistical distributions of height and period from 526 analogue records. Tabulated and plotted spectra from 97 (highest records) and associated punched cards	Comparisons made with visual observations. Further records have been taken from a trawler support vessel off Iceland since 1971
Mr C Van Cauwenberghe Head of the Coast Hydrographic Office Ministerie Van Openbare Werken Bestuur der Waterwegen Christinastraat 113 Ostend Belgium	Publication expected soon	15 minute records twice per day	(1) 7 years Intermittently from mid 1960 to mid 1967 (2) 13 years Intermittently from late 1958 to late 1971	Wandelaar Light Vessel 51° 22.4'N 2° 47.4'E West Hinder Light Vessel 51° 23'N 2° 26.4'E Marsden Square 216	Extraction of highest and significant wave height and period from each record	Tables of heights and periods	
Engineer in Chief Commissioners of Irish Lights 16 Lower Pembroke St Dublin 2 Eire	To be published by Instifition of Engineers of Ireland	10 minute records every 3 hours starting at midnight	(i) 1 year October 1964 to November 1965 (ii) 1 year April 1966 to May 1967 (iii) Nearly 3 yrs September 1957 to June 1970	(i) Kish Bank Light Vessel 53°19'N 5°55'W (ii) Barrels Light Vessel 52°06'N 6°24'W (iii) Daunt Light Vessel 51°43'N 8°16'W Marsden Square 181	Estimates of Height and Period by inspection of records	Standard format recommended by Draper	Recorder is now in Codling Light Vessel 53°03'N 5°41'W

AUSTRALIAN WATERS

RAN Research Laboratory New Beach Rd Edgecliffe N S W Australia				Marsden Square No 428	Estimates of height and period	Raw Data	

BAY OF BENGAL

The Commissioners for the Port of Calcutta Hydraulic Study Department 20 Garden Reach Road Calcutta 43	Departmental Report	2 hour records twice daily and special records in severe conditions	6 years intermittently from 1965 to 1971	Bay of Bengal (i) 21°15'22"N 85°12'02"E (ii) 20°59'40"N 83°13'40"E (iii) 21°25'57.5"N 83°09'48.5"E Marsden Square 100		Statistical Distribution of Heights and Periods. Tabulated and Plotted Spectra for year 1965	

F-2

MEDITERRANEAN

ADDRESS OF HOLDING AGENT	REFERENCE TO PUBLISHED DATA	NUMBER OF RECORDS	MONTHS AND YEARS COVERED	LOCATION	ANALYSIS	DATA FORMAT	REMARKS
Saclant ASW Research Centre NATO Viale San Bartolomeo La Spezia Italy			Intermittent periods of recording since May 1968	Ionian and West Ligurian Seas in Mediterranean Marsden Squares 143 and 180	Some hand analysis some analogue analysis to obtain height and period and some analog spectra Digital spectra from Waveriders	Mostly strip chart recordings but some analog mag tape. Digital spectra available from Waveriders	Measurements have been made with 'Waverider' and AURE buoys as well as ' shipborne wave recorders and results have been compared

PACIFIC

Mr G L Holland Canadian Wave Climate Study Oceanographic Section Department of the Environment 615 Booth St Ottawa Canada	Paper on Wave Observation from Station 'P' in preparation. Abstract submitted to Coastal Engineering Conference Vancouver 1972	20 minute records every 3 hours	3½ years October 1968 to present	Ocean Weather Station 'P' 50° N 145° W and line east to Victoria BC. Marsden Squares 157-158-159	Heights and Periods by NIC inspection method	Graphs such as histograms and exceedances to describe wave climatology	
Defence Research Board Defence Research Establishment Pacific Forces Mail Office Victoria British Columbia Canada	HAPER R A "Wave Measurements from the Drilling Rig SEDCO 135F off the Coast of British Columbia DRSP Report -- 70-3 July 1970	Continuous recording for days covered at each site	Over 2 years 5 January 1967 to 18 April 1969	48°19'N 125°44'W to 55°33'N 131°25'W Marsden Squares 157 and 194	Spectral analysis by electronic filtering for 1 hour duration samples at 0600, 1200 and 1800 hours each day	Power Spectra and Significant Wave heights. Recorded Data is on file on Magnetic tape at DRSP	Pace Engineering Co Model CP 51 Pressure Transducer Mounted 30 feet below surface on rig

SOUTH AFRICAN WATERS

Hydraulics Research Unit P O. Box 320 Stellenbosch South Africa (holds Ocean Wave Records) Department of Oceanography University of Capetown Rondebosch Capetown South Africa (holds specialised area records)	Various reports published by the CSIR Hydraulics Research Unit and some confidential contract reports	Mostly 15 or 20 minute records 4 times daily at 0000 0600 1200 and 1800 hours	7 years 1964 to present	Scattered over Marsden Squares 367, 368, 403, 404, 406, 407, 440, 441, 442, 476, 477, 478 including Ocean Weather Station at 40°S 10°E	Mostly by inspection of records but some spectral analysis	Tables of height and period distribution and some spectra in special areas. The Hydraulics Research Unit has incorporated the results into an overall record of wave characteristics in the area	The Tucker Shipborne Wave recorder was used for most of the records. Waverider buoys an inverted echo sounder and a Boersma wave height meter were also used for some cases

WORLD CRUISE (OCEANOGRAPHIC RESEARCH VESSEL ATLANTIS II)

Bedford Oceanographic Institution Nova Scotia		20 minute record at each hydrographic station	6 months 6 July to 20 December 1963 5 months 16 February to 31 July 1965	Cruises 8 and 15 of Atlantis II. Atlantic Mediterranean Red Sea Indian and Pacific Oceans	Power Spectrum program has been developed for use at sea	Analogue records and punched tape	

APPENDIX G

SOURCES OF UNPUBLISHED MEASURED DATA

FROM

REPORT OF THE INTERNATIONAL COMMISSION

FOR THE

STUDY OF WAVES

Excerpt from Bulletin No. 15 (Vol. II/1973)

of the

Permanent International Association of Navigation Congresses

AFRIQUE DU SUD — SOUTH AFRICA

1. Hydraulics Research Unit
   S.A. Council for Scientific and Industrial Research
   P.O. Box 320
   Stellenbosch (Cape)

2. Oceanography Department
   University of Cape Town
   Private Bag
   Rondebosch (Cape)

3. Oceanographic Research Unit
   Anglo American Corporation
   Oranjemund (South West Africa)

4. Fisheries Development Corporation
   P.O. Box 539
   Cape Town (Cape)

5. Oceanography Division
   National Physical Research Laboratory
   P.O. Box 1
   Congella (Natal)

ALLEMAGNE RÉPUBLIQUE FÉDÉRALE — GERMANY FED. REP

1. Seewetteramt Hamburg
   des Deutschen Wetterdienstes

2. Deutsches Hydrographisches Institut
   2 Hamburg 4 Bernhard-Nocht-Strasse 78

3. Bundesanstalt für Wasserbau
   Karlsruhe

4. Institut für Geophysik der Universität Kiel
   23 Kiel Neue Universität, Haus B 2

5. Technische Universität Hamburg
   2 Hamburg 36 Jungiusstrasse 9

6. Biologische Anstalt Helgoland
   2192 Helgoland

7. Bundesforschungsanstalt für Fischerei
   2 Hamburg 50 Palmaille 9

8. — Strom — und Hafenbau Hamburg
    Forschungsgruppe Neuwerk

9. Forschungsstellen auf den Inseln
    Norderney
    Helgoland
    Sylt

10. Hydraulik — bzw. Wasserbauinstituten der Universitäten
    e.a.
    Franziusinstitut der T.U. Hannover
    Leichtweissinstitut der T.U. Braunschweig
    Institut für theoretische Geophysik der Universität Hamburg
    Ozeanographische Forschungsanstalt Kiel
    Institut für Meereskunde Kiel
    Biologische Anstalt Helgoland
    Bundesforschungsanstalt für Fischerei

BELGIQUE — BELGIUM

1. Monsieur l'Hydrographe en Chef
    Service Spécial de la Côte
    Rue Christine 113
    8400 Ostende

CANADA — CANADA

1. Chief Engineer
    Design Branch, Department of Public Works
    Sir Charles Tupper Building, Riverside Drive, Ottawa 8 (Ontario)

2. The Director
    Marine Sciences Branch
    Environment Canada
    615 Booth Street, Ottawa (Ontario)
    KIA OE6 Canada

3. The Head
    Hydraulics Laboratory
    Division of Mechanical Engineering
    National Research Council
    Montreal Road, Ottawa (Ontario)
    KIA OR6 Canada

DANEMARK — DENMARK

1. Vandbygningsinstituttet
    (Danish institute of Applied Hydraulics)
    Oster Voldgade 10
    Dk 1350 Copenhagen, K

2. Vandbygningsdirektorated
   (Danish Board of Maritime Works)
   Kampmannsgade 1
   DK 1604 Copenhagen, V

ETATS-UNIS D'AMÉRIQUE — U.S.A.

1. U. S. Army,
   Coastal Engineering Research Center
   Kingman Building
   Fort Belvoir, Virginia 22060
   U. S. A.

ESPAGNE — SPAIN

1. Laboratorio de Puertos Ramon IRIBARREN
   Alfonso XII, 3 — Madrid — 7

FINLANDE — FINLAND

1. Finnish Meteorological Institute
   Vuorikatu 24
   00100 Helsinki 10

2. Finnish Oceanographical Institute
   Vuorimiehenkatu 1
   00140 Helsinki 14

FRANCE — FRANCE

1. Service Technique des Phares et Balises (1)
   12, route de Stains
   94 — Bonneuil-sur-Marne

2. Météorologie Nationale Française (2)
   1, Quai Branly
   75 — Paris 7e

3. Centre National d'Exploitation des Océans (CNEXO)
   39, Avenue d'Iéna
   75 — Paris 16e

4. Institut Français du Pétrole (I.F.P.)
   1, Avenue de Bois-Préau
   92 — Rueil-Malmaison

---

(1) Stations d'enregistrement au large du Havre (2 stations), à Roscoff et à Port Haliguen + 3 bouées d'enregistrement en Méditerranée + observations visuelles.
Off-shore recording stations in front of Le Havre (2 stations), at Roscoff and at Port Haliguen + 3 recording buoys in the Mediterranean + visual observations.

(2) Deux frégates avec enregistreurs Tucker aux points météorologiques K et A (ou J) + observations visuelles.
Two frigates with Tucker recording instruments at meteorological points K and A (or J) + visual observations.

5. SOGREAH
    84/86 Avenue Léon Blum
    Cedex n° 172
    38 — Grenoble-Gare

6. Laboratoire Central d'Hydraulique de France
    10, Rue Eugène Renault
    94 — Maisons-Alfort

7. Laboratoire National d'Hydraulique
    6, Quai Watier
    78 — Chatou

8. Centre de Recherches et d'Etudes Océanographiques
    2, Avenue Rapp
    75 — Paris 7^e

GRANDE-BRETAGNE — UNITED KINGDOM

1. British Oceanographic Data Service
    Institute of Oceanographic Sciences
    Wormley Godalming (Surrey)
    GU 8 5 UB

2. Meteorological Office (Marine Division)
    Eastern Road
    Bracknell (Berkshire)

IRLANDE — IRELAND

1. Meteorological Service
    44 Upper O'Connell Street
    Dublin I

2. National Committee for Geodesy and Geophysics
    Study Group of Oceanographic Observers
    (Chairman : Mck Bary of University College, Galway)

ISRAËL — ISRAËL

1. The Israël Ports Authority
    Coast study Division
    P.O.B. 15
    Ashdod

2. The Israëli Meteorological Service
    Climatological Division
    P.O.B. 25
    Beit Dagon

ITALIE — ITALY

1. Istituto Centrale di Statistica
    Direzione Generale Servizi Tecnici
    Reparto SF
    00100 Roma

2. Station stéréophotogrammétrique et dynamométrique en service depuis 15 ans :
    (Stereophotogrammetrical and dynamometrical station operating since 15 years) :
    Ufficio del Genio Civile per le Opere Marittime
    Napoli

3. Istituto Talassografico « F. Vercelli »
    via Romolo Gessi 2
    Trieste (dépendant du Ministère de l'Agriculture — controlled by the Ministry of Agriculture)

4. Istituto Idrografico della Marina
    Genova (dépendant de la Marine Militaire — controlled by the Navy)

JAPON — JAPAN

1. Chief of the Construction Section
    Harbour Bureau Ministry of Transport
    3-1-2, Kasumigaseki, Chiyoda-Ku
    Tokyo

2. The Fisheries Agency (Ministry of Agriculture and Forestry)

3. The Ministry of Construction

4. The Universities

MAROC — MOROCCO

1. Service de la Météorologie Nationale
    7, rue du Docteur Veyre
    Casablanca

2. Bibliothèque Générale du Ministère des Travaux Publics
    Rabat

NORVÈGE — NORWAY

1. The Norwegian Meteorological Institute
    Niels Henrik Abelsvei 40
    Oslo

2. Det Norske Veritas
    Research Department
    Oslo

3. Dept. of Port and Ocean Engineering
    The Technical University of Norway
    7034 Trondheim

PAYS-BAS — NETHERLANDS

1. Rijkswaterstaat
   Directie Waterhuishouding en Waterbeweging
   Koningskade 25
   's-Gravenhage

2. Rijkswaterstaat
   Deltadienst
   Van Alkemadelaan 400
   's-Gravenhage

3. K.N.M.I. (Institut Royal Météorologique)
   De Bilt

4. Waterloopkundig Laboratorium
   B.P. 177
   Delft

5. Rijkswaterstaat
   Studiedienst Vlissingen
   Prins Hendrikweg 3
   Vlissingen

6. Rijkswaterstaat
   Deltadienst
   Meetdienst voor afsluitingswerkzaamheden en metingen in de Zeeuwse Wateren
   Van Veenlaan 1
   Zierikzee

7. Rijkswaterstaat
   Deltadienst
   Meetdienst voor het Benedenrivierengebied
   Kanaalweg 2 (OZ)
   Hellevoetsluis

8. Rijkswaterstaat
   Directie Waterhuishouding en Waterbeweging
   Afdeling Hydrometrie
   Koningskade 25
   's-Gravenhage

9. Rijkswaterstaat
   Studiedienst IJmuiden
   De Wetstraat 3
   IJmuiden

10. Rijkswaterstaat
    Studiedienst Hoorn
    Grote Oost 26
    Hoorn

11. Rijkswaterstaat
    Directie Groningen
    Afdeling Studiedienst
    Farsumerzijl 10
    Delfzijl

12. Rijkswaterstaat
    Zuiderzeewerken
    Afdeling Waterloopkunde
    Kanaalweg 3
    's-Gravenhage

POLOGNE — POLAND

1. Institut Polonais d'Hydrologie et de Météorologie
   Section Maritime
   Gdynia
   ul. Wazyntona 42

2. Institut des Constructions Hydrotechniques de l'Académie Polonaise des Sciences
   Gdansk-Oliwa
   ul. Cystersow 11

3. Institut Maritime
   Gdansk Dlugi Targ 41/43

PORTUGAL — PORTUGAL

1. Laboratorio Nacional de Engenharia Civil
   Avenida do Brasil
   Lisboa 5

2. Instituto Hidrografico
   (Ministerio de Marinha)
   Rua das Trinas 49
   Lisboa 2

3. Direcçào des Serviços Maritimos
   Rua das Portas de Santo Antào 167
   Lisboa 2

4. Serviço Meteorologico Nacional
   Rua Saraiva de Carvalho 2
   Lisboa 3

U.R.S.S. — U.S.S.R.

1. State Oceanographic Institute
   6 Kropotkinski pereulok
   Moscow

2. Oceanology Institute of the U.S.S.R. Academy of Sciences
   1. Letnjaja ulitza, Lublino
   Moscow

DOCUMENTATION CONCERNANT LES ENREGISTREMENTS DE LAMES
INFORMATION RELATED TO WAVES RECORDS

PAYS COUNTRIES	Organismes + adresses Organizations + Addresses	Endroit de l'enregistrement Recording Site	Longitude	Latitude	effective > 6 mois effective > 6 months	écoulée dès début elapsed since beginning	C.O. (1)	C.C. (2)	N. (3)	M. (4)
Afrique du Sud South Africa	Hydraulics Research Unit S.A. Council for Scientific and Industrial Research P.O. Box 320 Stellenbosch (Cape)	Richard Bay	32° 06' 58'' E	28° 48' 30'' S	10	48	x			x
		Mossel Bay	22° 12' 98'' E	34° 13' 48'' S	16	33		x		
		Saldanha Bay	17° 57' 03'' E	33° 06' 36'' S	8	8		x		
		Möwe Point	12° 42' 10'' E	18° 22' 90'' S	9	26		x		
	Fisheries Development Corporation P.O. Box 539 Cape Town (Cape)	Gansbaai	19° 20' 00'' E	34° 35' 00'' S	38,4	48		x		
		Lambertsbaai	18° 19' 00'' E	32° 10' 00'' S	33,6	32		x		
		Möwe Point	12° 40' 00'' E	19° 22' 00'' S	36,9	41		x		
		Kalkbaai	18° 28' 00'' E	34° 08' 00'' S	0,4	6		x		
		Gansbaai	19° 20' 00'' E	34° 35' 00'' S	8,15	19		x		
		Kalkbaai	18° 28' 00'' E	34° 08' 00'' S	5,30	12		x		
Allemagne (Rép. Féd.) Germany (Fed. Rep.)	Deutsches Hydrographisches Institut 2 Hamburg 4 Bernhard-Nocht-strasse 78	Büsum-Scholloch	8° 51' 24'' E	54° 07' 36'' N	28	28			x	
		Büsum-Tertius	8° 40' 16'' E	54° 06' 35'' N	30	30			x	
		Büsum-Tonne 16	8° 50' 19'' E	54° 07' 35'' N	30	30			x	
		Eider	8° 29' 42'' E	54° 13' 00'' N	12	12			x	
		Flensburg	9° 27' 02'' E	54° 48' 39'' N	23	23			x	
		Kalkgrund	9° 53' 23'' E	54° 49' 35'' N	14	14			x	
		Wesierland	8° 17' 38'' E	54° 54' 56'' N	24	24			x	
		Wittsand	8° 05' 37'' E	53° 46' 23'' N	14	14			x	
		Olpenitz	0° 02' 33'' E	54° 39' 33'' N	52	52			x	
		Mittelgrund	8° 31' 08'' E	53° 58' 06'' N	12	12			x	
		Wangerooge	7° 55' 43'' E	53° 48' 22'' N	27	27			x	
		Mellum-Plate	8° 05' 37'' E	53° 46' 23'' N	13	13			x	
		Scharhörn-N.	8° 25' 25'' E	53° 58' 37'' N	29	29			x	
		Scharhörn-Riff	8° 20' 36'' E	53° 59' 05'' N	39	39			x	
	Marschenbauamt Husum Wasserwirtschaftsamt Herzog Adolf strasse 1 Postfach 1440 225 Husum	Ile de Sylt	8° 17' 00'' E	54° 54' 00'' N	6	6		x		

Coordonnées géographiques / Geographical Coordinates — Durée d'enregistrement (en mois) / Recording Period (month) — But / Objective

Organization / Country	Location	Longitude	Latitude	No.	C.O.	C.C.	N.	M.
Leichtweiss Institut für Wasserbau der T.U. Pockelstrasse 4, 33 Braunschweig	Ile de Sylt	08° 15' 00'' E	54° 55' 00'' N	6	X			
Canada — The Director, Marine Sciences Branch, Environnement Canada, 615 Booth street, Ottawa (ont.), K1A OE6 Canada	Glace Bay, Nova Scotia	59° 27' 00'' W	46° 10' 24'' N					
	Halifax Harb. Nova Scotia	63° 36' 00'' W	44° 39' 00'' N					
	Georgia Strait Brit. Columbia	123° 27' 00'' W	49° 16' 00'' N					
	Port Borden, Prince Edw. Island	63° 42' 00'' W	46° 15' 00'' N		X			
	Come-by-Chance Newfoundland	54° 01' 18'' W	47° 47' 45'' N				X	X
	Western Head, Nova Scotia	64° 36' 10'' W	44° 00' 49'' N				X	X
	Cape Roseway, Nova Scotia	65° 19' 28'' W	43° 37' 20'' N				X	X
	Osborn Head, Nova Scotia	63° 27' 50'' W	44° 32' 40'' N				X	
	Sept Iles, Quebec	66° 23' 00'' W	50° 12' 00'' N				X	
	Main Duck Island, Lake Ontario	76° 49' 39'' W	43° 47' 45'' N				X	
	Tofino, Brit. Columbia	125° 54' 00'' W	49° 09' 00'' N				X	X
Hydraulics Laboratory, Division of Mechanical Engineering, National Research Council, Montreal Road, Ottawa (On.), K1A OR6 Canada	Battle Island, Ontario	87° 33' 00'' W	48° 41' 06'' N	8				X
	North Superior Minnesota	90° 17' 09'' W	47° 40' 09'' N	8				X
	Eagle Harbour Michigan	88° 09' 05'' W	47° 33' 01'' N	8				X
	Grand Marais Michigan	86° 02' 04'' W	46° 45' 09'' N	8				X
	Cap Chat, Quebec	66° 46' 05'' W	49° 10' 03'' N	12				X
	Sept Iles, Quebec	66° 18' 05'' W	49° 58' 00'' N	8				X
	Cap d'Espoir, Quebec	64° 14' 00'' W	48° 20' 07'' N	10				X
	West Point Anticosti Island, Quebec	64° 39' 03'' W	49° 48' 07'' N	9				X
	Heath Point Anticosti Island, Quebec	61° 42' 01'' W	49° 00' 00'' N	6				X
	Cape Whittle, Quebec	60° 03' 03'' W	50° 04' 09'' N	6				X
	Bird Rock, Magdalen Island, Quebec	61° 09' 00'' W	47° 55' 05'' N	6				X
	North Point, Prince Edw. Isl., Can.	64° 06' 00'' W	47° 07' 07'' N	6				X

(1) C.O. = Off-shore structure.
(2) C.C. = Coastal structure.
(3) N. = Nautical.
(4) M. = Meteorological.

(1) C.O. = Construction en pleine mer.
(2) C.C. = Construction à lit côte.
(3) N. = Nautique.
(4) M. = Météorologique.

PAYS / COUNTRIES	Organismes + adresses / Organizations + Addresses	Endroit de l'enregistrement / Recording Site	Coordonnées géographiques / Geographical Coordinates		Durée d'enregistrement (en mois) / Recording Period (month)		But / Objective			
			Longitude	Latitude	effective > 6 mois / effective > 6 months	écoulée dès début / elapsed since beginning	C.O. (1)	C.C. (2)	N. (3)	M. (4)
		East Point, Prince Edw. Isl., Can.	61° 52' 02" W	46° 31' 04" N		8			x	
		Cape Breton, Nova Scotia, Can.	60° 16' 04" W	47° 06' 09" N						
		Presqu'île Point, Brighton, On.	77° 44' 03" W	43° 53' 04" N		12			x	
Danemark / Denmark	Vandbygningsinstituttet Danish Hydraulics Instit. Øoster Voldgade 10 DK 1350 Copenhagen K	Hanstholm Harb. (North Sea)	08° 35' 31" E	57° 07' 39" N	45	104		x		
		Hirtshals Harb. (North Sea)	09° 57' 06" E	57° 35' 54" N	9	24		x		
		Karachi Harb. (Arabian Sea)	66° 58' 12" E	24° 47' 06" N	23	36		x		
		Saint-Louis, Senegal	17° 47' 36" E	15° 59' 35" N	7	24		x		
France	Service Technique des Phares et Balises Route de Stains 12 91 — Bonneuil-s-Marne		05° 03' 12" E	43° 19' 00" N	12		x	x		
	Laboratoire National d'Hydraulique Quai Watier 6 78 — Chatou	Dunkerque (points 1-2-3)	02° 19' 10" E	51° 03' 47" N	22			x		
		Dunkerque (point 4)	01° 57' 10" E	51° 01' 14" N	10			x		
		Dunkerque (point 5)	01° 49' 07" E	51° 00' 52" N	13			x		
		Dunkerque (point 6)	02° 12' 27" E	51° 03' 15" N	22			x		
		Dunkerque (point 7)	02° 08' 12" E	51° 04' 42" N	11			x		
		Dunkerque (point 8)	02° 09' 14" E	51° 02' 53" N	16			x		
		Dunkerque (point 9)	02° 09' 00" E	51° 01' 55" N	10					
		Boulogne-s-Mer	01° 34' 28" E	50° 45' 04" N	27					
		Le Havre	00° 08' 30" W	40° 31' 55" N	25			x		
		Barfleur	01° 15' 23" W	49° 42' 09" N	13			x		
		Granville	01° 36' 28" W	48° 49' 35" N	8			x		
		Baie du Mont-Saint-Michel	01° 49' 30" W	48° 49' 15" N	55			x		
		Pointe du Grouin	01° 49' 55" W	48° 45' 05" N	23			x		
		Brest	04° 40' 56" W	48° 19' 45" N	7			x		
		La Turballe	02° 36' 07" W	47° 20' 15" N	13			x		
		Phare du Four	02° 40' 25" W	47° 17' 33" N	14			x		

Organisme / Pays	Lieu	Longitude	Latitude			X
	Le Chatelier (chenal extér, Loire)	02° 17' 43'' W	47° 10' 10'' N	9		
	Pointe de Grave	01° 23' 00'' W	45° 39' 36'' N	16		
	Biscarosse	01° 19' 00'' W	44° 28' 00'' N	37		× ×
	Cap-Breton	01° 28' 03'' W	43° 39' 28'' N	9		× × × × ×
	Saint-Cyprien	03° 04' 00'' E	42° 37' 10'' N	13		
	Sète	03° 41' 08'' E	43° 22' 00'' N	15		
	Cap Couronne (Ouest)	05° 03' 13'' E	43° 19' 20'' N	11		× × × × × ×
	Cap Couronne (Est)	05° 03' 32'' E	43° 19' 24'' N	11		
	La Bálancelle (Golfe de Fos)	04° 54' 50'' E	43° 20' 22'' N	28		
	Lavera	04° 59' 30'' E	43° 22' 54'' N	9		× × ×
	Antibes	07° 08' 30'' E	43° 35' 10'' N	16		
	Nice	07° 13' 30'' E	43° 39' 12'' N	31		
	Bejaïa (Algérie)	05° 06' 36'' E	36° 44' 30'' N	7		
	Arzew (Algérie)	00° 17' 05'' W	35° 50' 07'' N	22		
	Kuwait (Golfe arabique)	47° 58' 00'' E	29° 27' 00'' N	10		
	Estuaire du Gabon	00° 16' 29'' E	00° 24' 33'' N	12		
	Naples (Italie)	14° 15' 00'' E (environ)	40° 50' 00'' N (environ)	9		
Grande-Bretagne United Kingdom						
British Oceanographic Data Service	Milford Haven	5° 05' 00'' W	51° 40' 00'' N	9	9	
Institute of Oceanographic Sciences Wormley Godalming Surrey GU8 5UB	Perranporth, Newquay	5° 05' 00'' W	50° 20' 00'' N	12	> 12	
	Morecambe Bay LV (Irish Sea)	3° 30' 00'' W	53° 52' 00'' N	12	24	
	Mersey Bar LV (Irish Sea)	3° 19' 00'' W	53° 33' 00'' N	12	36	
	Sevenstones LV (Engl. Channel)	6° 10' 00'' W	50° 00' 00'' N	12	80	
	Shambles LV (Engl. Channel)	2° 20' 00'' W	50° 31' 00'' N	12	24	
	Owers LV (Engl. Channel)	0° 47' 00'' W	51° 01' 00'' N	12	24	
	Varne LV (Engl. Channel)	1° 24' 00'' E	51° 01' 00'' N	12	24	
	Tongue LV (North Sea)	1° 58' 00'' E	51° 30' 00'' N	12	24	
	Galloper LV (North Sea)	1° 50' 00'' E	51° 40' 00'' N	12	35	
	Smith's Knoll (North Sea)	2° 18' 00'' E	52° 44' 00'' N	12	12	
	Dowsing LV (North Sea)	0° 50' 00'' E	53° 34' 00'' N	12	24	
	North Carr LV (North Sea)	2° 34' 00'' W	56° 18' 00'' N	12	12	
	Famita (North Sea)	3° 00' 00'' E	57° 30' 00'' N	6	36	
	OWS Station India (Atl.)	19° 00' 00'' W	59° 00' 00'' N	12	15	
	OWS Station, Julicit (Atl.)	20° 00' 00'' W	52° 30' 00'' N	12	100	
	Wylfa, Anglesey	4° 25' 00'' W	53° 25' 00'' N	8	100	
	Camp Pendleton, California	118° 00' 00'' W	33° 00' 00'' N	24	8	
	Benghazi, Libya	20° 00' 00'' E	32° 00' 00'' N	24	72	×
Sir Alexander Gibb & Partners Telford House 14 Tothill Street London SW1H 9NG	Clovelly, N. Devon	2° 25' 00'' W	50° 34' 00'' N	6	12	×
	Heysham,				6	
	Morecambe Bay	2° 56' 00'' W	54° 03' 00'' N	12	12	

PAYS / COUNTRIES	Organismes + adresses / Organizations + Addresses	Endroit de l'enregistrement / Recording Site	Coordonnées géographiques / Geographical Coordinates		Durée d'enregistrement (en mois) / Recording Period (month)		But / Objective			
			Longitude	Latitude	effective > 6 mois / effective > 6 months	écoulée des début / elapsed since beginning	C.O. (1)	C.C. (2)	N. (3)	M. (4)
	Hydraulics Research Station Wallingford Berkshire	Portland, S. Ship Channel	2° 25' 00" W	50° 34' 00" N		24		x		
		Portland, Oiling Jetty (Long waves)	2° 26' 00" W	50° 34' 00" N		18				
		Port Talbot, S. Wales	3° 48' 00" W	51° 35' 00" N		36				
		Christchurch Harb., New Zealand	112° 43' 00" E	43° 36' 00" S		18				
		Christchurch Harb., New Zealand (Long waves)	112° 43' 00" E	43° 36' 00" S		18				
	Rendel, Palmer & Tritton Southwark Bridge House 61 Southwark street London SE1 1SA	Liverpool	3° 19' 00" W	53° 32' 00" N		12		x		
		Port Talbot, S. Wales	3° 03' 00" W	53° 28' 00" N		12		x		
		Port Authority, Paradeep, Orissa, India	3° 48' 00" W	51° 35' 00" N		18		x		
			86° 44' 00" E	20° 20' 00" N		?		x		
	Allot and Lomax 23 Ashton Lane Sale M33 1WP	Belfast Lough	5° 41' 03" W	54° 46' 06" N	12	12				
	Binnie and Partners Artillery House Artillery Row London SW1P 1RX	Kwun Mun (H. Kong)	114° 22' 33" E	22° 21' 45" N		8				
		Waglan (H. Kong)	216 metres from Waglan, Light on bearing 213° True			11				
	Babtie, Shaw and Morton 95 Bothwell street Glasgow G2 7HX	Scrabster Caithness	3° 33' 00" W	50° 36' 30" N	12	12				
	Institute of Oceanographic Sciences (Taunton) Crossway, Taunton TA1 2DW	Orfordness	1° 28' 00" E	52° 04' 30" N	12	19				
		Wyke Regis, Chesil Beach	2° 30' 00" W	50° 35' 30" N	12	15				
		West Bexington, Chesil Beach	2° 40' 00" W	50° 40' 20" N	12	16				
	West Indies: Regional Bench Erosion Control Programme Facility of Engineering, University of West Indies Trinidad. West Indies	Belleplaine, Barbados (East Coast)	59° 33' W	13° 14' N	12	12		x		
		Sandy Bay, St. Kitts	62° 15' W	17° 15' N	12	12		x		

							x x x x	x x x		x x				x x x x x x x x x x x x x x x x
															x x x x x x x x x x x x x x x
								x				x		x		
							x x x x								

Pays / Country	Meteorological Service	Station	Longitude	Latitude		
Irlande / Ireland	Meteorological Service 44 Upper O'Connell str. Dublin I	Kish Lightship	03° 55' 00" W	53° 19' 00" N		
		Barrels Lights	06° 24' 00" W	52° 06' 00" N		
		Daunt Lightship	05° 03' 00" W	53° 03' 00" N		
		Codling Lights	05° 44' 00" W	53° 03' 00" N		
Israël	The Israeli Meteorological Service Climatological Division P.O.B. 25 Bet Dagon	Ashdol-Port			12	152
		Nahariya			13	100
		Haifa-Harbour			11	28
		Eilat			11	81
Italie / Italy	Consiglio Superiore dei LL.PP. Via Nomentana 2 00161 Roma	Port de Venise (plate-forme CNR et canal Grande)	12° 30' 08" E	45° 18' 08" N	temps mesure continu V 1/18 du temps global	
Norvège / Norway	The Norwegian Meteorological Institute Niels Eendrik Abelsvei 40 Oslo	Weather ships M.	02° 00' 00" E	66° 00' 00" W		252
		Weather ships, Familia	03° 00' 00" E	57° 05' 00" N		156
Pays-Bas / The Netherlands	Rijkswaterstaat Directie Waterhuishouding en Waterbeweging Koningskade 25 's-Gravenhage	Katwijk	04° 21' 42" E	52° 12' 20" N		125
	Rijkswaterstaat Studiedienst Vlissingen Prins Hendrikweg 3 Vlissingen	Cadzand	03° 22' 39" E	51° 22' 48" N	36	
	Rijkswaterstaat Deltadienst Van Alkemadelaan 100 's-Gravenhage	Ha - I				6
		Ha - VI				6
		Ma - III				6
		E - 70				6
		BG - I				6
		Bg - II				6
		OS - IV				
	Koninklijk Nederlands Meteorologisch Inst. Utrechtseweg 297 De Bilt	KA 01 NH	2° 34' 00" E	51° 39' 00" N	84	84
		KB 02 GR	3° 40' 00" E	51° 56' 00" N	81	81
		KB 03 TX	3° 22' 00" E	53° 01' 00" N	71	71
		KW 01 NW	4° 22' 00" E	52° 15' 00" N	15	15
		KW 02 NW	4° 17' 00" E	52° 17' 00" N	11	11
		KW 04 NW	3° 57' 00" E	52° 24' 00" N	31	31
		KW 06 YM	4° 04' 00" E	52° 33' 00" N	9	9
		KW 2 B			13	13
		KT 0			96	96
		KW 04 NM	3° 57' 00" E	52° 24' 00" N	1	1
		KW 20 BL	4° 32' 00" E	53° 59' 00" N	3	3
		KB 01 NH	2° 34' 00" E	51° 39' 00" N	9	9
		KB 02 GR	3° 40' 00" E	51° 56' 00" N		
		KB 03 TX	4° 22' 00" E	53° 01' 00" N		
		KW 20 BL	4° 32' 00" E	53° 54' 00" N	10	10

PAYS / COUNTRIES	Organismes + adresses / Organizations + Addresses	Endroit de l'enregistrement / Recording Site	Coordonnées géographiques / Geographical Coordinates		Durée d'enregistrement (en mois) / Recording Period (month)		But / Objective			
			Longitude	Latitude	effective > 6 mois / effective > 6 months	écoulée dès début / elapsed since beginning	C.O. (1)	C.C. (2)	N. (3)	M. (4)
		KW 21 BK	3° 20' 00'' E	53° 28' 00'' N	1	1			x	x
		KW 22 BF	4° 54' 00'' E	55° 00' 00'' N	2	2			x	x
		KW 23 BL	4° 34' 00'' E	53° 51' 00'' N	1	1			x	x
		KW 24 BL	4° 41' 00'' E	53° 57' 00'' N	1	1			x	x
		KW 25 DK	3° 54' 00'' E	53° 13' 00'' N					x	x
		KW 26 BK	3° 31' 00'' E	53° 05' 00'' N	7	7			x	x
		KW 06 YM	4° 04' 00'' E	52° 33' 00'' N	9	9			x	x
		KB 03 TX	4° 22' 00'' E	53° 01' 00'' N	12	12			x	x
		KB 01 NH	2° 34' 00'' E	51° 39' 00'' N	9	9			x	x
		KB 02 GR	3° 40' 00'' E	51° 56' 00'' N	1	1			x	x
		OWS Cumulus A			1	1			x	x
		K			1	1			x	x
		L			4	4			x	x
		Y			7	7			x	x
		M			↑	↑			x	x
		L								x
	Rijkswaterstaat Studiedienst Hoorn Grote Oost 26 Hoorn	Wadden Sean	5° 40' 05'' E	53° 24' 27'' N	25	28	x	x		
		Wadden Sea	5° 38' 29'' E	53° 20' 14'' N	23	26	x	x		
Pologne Poland	Institut Polonais d'Hydrologie Section maritime Gdynia ul. Wazyntona 42	Rozewie			120	120		x	x	
		Ustka			120	120		x	x	
		Kolobrzeg			60	60		x	x	
		Dziwnów			60	60		x	x	
		Swinoujscie						x	x	
Portugal	Laboratorio Nacional de Engenharia Civil Avenida do Brasil Lisboa 5	Figueira da Foz	8° 54' 00'' W	40° 10' 00'' N	72	72		x	x	
		Leixões	8° 44' 00'' W	41° 11' 00'' N	36	36		x	x	
		Portimão	8° 32' 00'' W	37° 05' 00'' N	48	48		x	x	
		Sines	8° 52' 00'' W	37° 56' 00'' N	6	6		x	x	
		Cabinda (Ang.)	14° 10' 00'' E	5° 20' 00'' S	12	12		x	x	
		Lobito (Ang.)	13° 32' 00'' E	12° 20' 00'' S	12	12				
		Ponta Dobelo (Mozambique)	32° 34' 00'' E	25° 06' 00'' S	11	11		x		
		Ka-Ho (Macau)	113° 37' 00'' E	22° 08' 00'' N	8	8		x		
		Morro Carregado (S. Tomé)	6° 37' 00'' E	00° 24' 00'' N	8	8		x		
		Luanda (Angol.)	12° 30' 00'' E	9° 30' 00'' S	12	12		x		

Organization	Station	Longitude	Latitude		
Servico Meteorologico Nacional Rua Saraiva de Carvalho 2 Lisboa 3	Ancora	8° 52' 00'' W	41° 49' 00'' N		
	Viana do Castelo	8° 50' 00'' W	41° 41' 00'' N		
	Leixões	8° 42' 00'' W	41° 11' 00'' N		
	Aveiro	8° 45' 00'' W	40° 38' 00'' N		
	Cabo Mondego	8° 54' 00'' W	40° 11' 00'' N		
	Barra do Mondego	8° 52' 00'' W	40° 09' 00'' N		
	Nazaré	9° 05' 00'' W	39° 36' 00'' N		
	Cabo Carvoeiro	9° 24' 00'' W	39° 22' 00'' N		
	Ericeira	9° 25' 00'' W	38° 58' 00'' N		
	Cabo da Roca	9° 30' 00'' W	38° 47' 00'' N		
	Cabo Raso	9° 29' 00'' W	38° 42' 00'' N		
	Monte Estoril	9° 24' 00'' W	38° 42' 00'' N		
	S. Julião	9° 19' 00'' W	38° 40' 00'' N		
	Calcilhas	9° 09' 00'' W	38° 41' 00'' N		
	Cabo Espichel	9° 13' 00'' W	38° 25' 00'' N		
	Oufão	8° 56' 00'' W	38° 29' 00'' N		
	Sines	8° 53' 00'' W	37° 57' 00'' N		
	Sagres	8° 57' 00'' W	37° 00' 00'' N		
	Ponta da Piedade	8° 40' 00'' W	37° 05' 00'' N		
	Praia da Rocha	8° 32' 00'' W	37° 08' 00'' N		
	Alfanzina	8° 26' 00'' W	37° 05' 00'' N		
	Cabo de Santa Maria	7° 52' 00'' W	36° 58' 00'' N		
	Lourenço Marques (Mozamb.)	32° 57' 05'' E	25° 55' 00'' S		
	Beira (Mozamb.)	34° 51' 00'' E	19° 50' 00'' S		
	Ilha de Goa (Mozambique)	40° 47' 03'' E	15° 03' 02'' S		
Costal Engineering Research Center 5201 Little Falls Road NW Washington D.C. 20016	Assateague, Md.	75° 09' 20'' W	38° 11' 30'' N	21	
	Assateague, Va.	75° 20' 18'' W	37° 53' 24'' N	21	
	Atlantic City, N.J.	74° 25' 53'' W	39° 21' 21'' N	120,53	147
	Atlantic, N.C.	76° 18' 35'' W	38° 51' 30'' N	42	
	Belmar, N.J.	74° 00' 48'' W	40° 10' 36'' N	21	
	Black Pt Oahu, Ha.	157° 48' 00'' W	21° 15' 00'' N	10	
	Boca Raton, Fla.	80° 04' 01'' W	26° 22' 20'' N	10 8	45
	Bolinas Ca.	122° 41' 04'' W	37° 54' 17'' N	33	
	Bolsa Chica, Ca.	118° 02' 10'' W	33° 41' 01'' N	13	
	Brigantine, N.J.	74° 23' 54'' W	39° 23' 04'' N		31
	Buzzards Bay, Mass.	71° 02' 00'' W	41° 24' 00'' N	18	
	Cape Cod., Mass.	69° 57' 01'' W	41° 51' 37'' N	22	
	Cape Decision, Ak.	134° 08' 00'' W	56° 00' 00'' N	191	
	Cape Hattery, Wash.	124° 44' 05'' W	48° 23' 30'' N		65
	Cape Henry, Va.	76° 00' 00'' W	36° 55' 00'' N		
	Cape Hinchinbrook, Ak.	146° 39' 00'' W	60° 15' 00'' N		
	Cape St. Elias, Ak.	144° 36' 00'' W	59° 13' 00'' N	23	
	Cape San Blas, Fla.	85° 21' 23'' W	29° 40' 00'' N	211	
	Cape Sarichef, Ak.	164° 55' 00'' W	54° 36' 00'' N	23	
	Carlsbad, Ca.	117° 20' 43'' W	33° 08' 49'' N	33	
	Carpinteria, Ca.	119° 31' 14'' W	34° 23' 35'' N	9 17	
	Centerville, Ca.	124° 21' 00'' W	40° 34' 24'' N	15	
	Chesapeake Bay Bridge Norfolk, Va.	76° 07' 00'' W	36° 58' 00'' N		49
	Chesapeake Beach, Md.	76° 30' 00'' W	38° 37' 00'' N		56½
	Clearwater, Fla.	82° 50' 00'' W	27° 58' 00'' N		38¾
	Crystal Beach, Fla.	86° 26' 36'' W	30° 23' 00'' N	12	128½
	Daytona Beach, Fla.	80° 58' 00'' W	29° 09' 00'' N		

U.S.A.

PAYS COUNTRIES	Organismes + adresses / Organizations + Addresses	Endroit de l'enregistrement / Recording Site	Coordonnées géographiques / Geographical Coordinates		Durée d'enregistrement (en mois) / Recording Period (month)		But / Objective			
			Longitude	Latitude	effective > 6 mois / effective > 6 months	écoulé dès début / elapsed since beginning	C.O. (1)	C.C. (2)	N. (3)	M. (4)
		Deal, N.J.	74° 00' 30''	40° 14' 41''	20					
		Destin, Fla.	80° 26' 36''	30° 23' 00''	17					
		Doheny, Ca.	117° 41' 03''	33° 27' 43''	36					
		El Capitan, Ca.	120° 01' 09''	34° 27' 33''						
		El Segundo, Ca.	118° 25' 00''	33° 55' 00''	12	57				
		Enderts, Ca.	124° 08' 36''	41° 42' 30''				×		
		Fort Walton Beach, Fla.	86° 35' 06''	30° 23' 24''	29			×		
		Francis, Ca.	122° 26' 49''	37° 28' 30''	30			×		
		Frying Pan Shoals, N.C.	77° 34' 00''	33° 28' 00''				×		
		Galveston, Texas	94° 47' 00''	29° 17' 00''		16		×		
		Gilgo Beach, LI, N.Y.	73° 25' 00''	40° 37' 00''		85		×		
		Goat Rock, Ca.	123° 07' 38''	38° 26' 46''		47		×		
		Grand Isle, La.	90° 00' 00''	29° 13' 45''	47					
		Grand Isle, La.	85° 59' 00''	29° 13' 00''	16	117‡		×		
		Grayton Beach State Park, Fla.	86° 08' 18''	30° 19' 06''	15,17			×		
		Hampton Bch, H.H.	70° 47' 30''	43° 56' 30''	147			×		
		Hanalei, Hawaii	159° 30' 11''	22° 12' 29''	10			×		
		Hillsboro Inlet, Fla.	80° 05' 00''	26° 15' 30''	210‡	15		×		
		Holden Beach, N.C.	78° 17' 20''	33° 54' 36''	21			×		
		Hollywood Bch, Fla.	80° 06' 48''	26° 02' 30''	40			×		
		Huntington Bch, Ca.	117° 59' 14''	33° 38' 49''	46			×		
		Huntington Bch, Ca.	118° 00' 00''	33° 38' 00''		287		×		
		Jones Bch, Li, N.Y.	73° 31' 00''	40° 33' 00''	52			×		
		Jupiter Beach, Fla.	80° 04' 30''	26° 58' 15''	40			×		
		Kahului Harbor, Ha.	156° 28' 00''	20° 54' 00''		18‡		×		
		Laguna Beach, Fla.	85° 55' 12''	30° 14' 18''	17			×		
		Lake Worth, Fla.	80° 02' 00''	26° 43' 00''		64		×		
		Leo Carrillo, Ca.	118° 56' 17''	34° 02' 39''	41			×		
		Long Beach is., N.J.	74° 10' 56''	39° 38' 14''	52			×		
		Long Branch, N.J.	73° 59' 00''	40° 18' 00''		66‡		×		
		Los Angeles (Venice Pier) Ca.	118° 28' 00''	33° 58' 00''	52	42		×		
		Ludlam Is., N.J.	74° 41' 30''	39° 09' 09''	15			×		
		Mad River, Ca.	124° 08' 00''	40° 56' 00''	21			×		
		Mackerricher, Ca.	123° 47' 40''	39° 29' 30''	16			×		
		Manchester, Ca.	123° 42' 23''	38° 59' 02''	41			×		
		Mc Grath, Ca.	119° 15' 53''	34° 14' 11''				×		
		Melbourne, Fla.	80° 35' 00''	28° 13' 00''	52	14‡		×		
		Misquamicut, R.I.	71° 56' 30''	41° 18' 12''				×		

G-16

Location					
Monmouth Bch, N.J.	73° 58' 30"	40° 20' 30"	211	108½	x
Moose Peak, Me.	67° 32' 00"	44° 28' 30"	214	102½	x
Nags Head, N.C.	75° 36' 30"	35° 56' 00"		179	x
Natural Bridges, Ca.	122° 03' 25"	26° 08' 00"	32		x
Nauset, Mass.	69° 57' 00"	41° 51' 30"	44		x
Navarre Beach State Park, Fla.	86° 59' 24"	30° 21' 30"	12		x
Navarro, Ca.	121° 45' 24"	39° 11' 18"	10		x
New Brighton, Ca.	121° 56' 06"	36° 58' 43"	13		x
Newport, Ca.	117° 56' 16"	33° 37' 06"	37		x
Oak Isl., N.C.	78° 02' 00"	33° 53' 30"	171½		x
Ocean Cape, Alaska	139° 51' 00"	59° 32' 00"	28		x
Ocean City, Md.	75° 05' 15"	38° 19' 30"	211	96	x
Palm Beach, Fla.	80° 02' 00"	26° 42' 00"			x
Panama City Beach (Hilton) Fla.	85° 53' 36"	30° 12' 24"	17		x
Panama City Beach, Fla.	85° 44' 36"	30° 07' 48"	17		x
Panama City (St. Andrew State Park) Fla.	85° 40' 00"	30° 05' 00"	17,12		x
Pea Island, N.C.	75° 28' 49"	35° 41' 01"	22		x
Piedras Blancas, Ca.	121° 17' 00"	35° 40' 00"	69		x
Pismo, Ca.	120° 38' 34"	35° 08' 29"	39		x
Point Arena, Ca.	123° 44' 15"	38° 57' 20"	211		x
Point Arguello, Ca.	120° 39' 00"	34° 34' 30"	190	30	x
Point Conception Ca.	120° 28' 00"	34° 27' 00"	94		x
Point Judith, R.I.	71° 29' 00"	41° 21' 31"	211		x
Point Loma, Ca.	117° 07' 00"	32° 39' 52"	25	25	x
Point Mugu, Ca.	119° 01' 42"	34° 04' 42"	34	172	x
Point Mugu(Peg)Ca.	119° 09' 30"	34° 07' 06"	57		x
Ponce de Leon, Fla.	80° 54' 48"	29° 04' 00"			x
Port Hueneme, Ca.	119° 09' 00"	34° 07' 00"			x
Port St. Joe (St.Joseph St. Park) Fla.	85° 23' 12"	29° 45' 36"	17		x
Prairie Creek Redwoods, Ca.	124° 04' 30"	41° 21' 18"	33		x
Race Point, Mass.	70° 13' 12"	42° 04' 45"	8		x
Redwook Creek, Ca.	124° 05' 34"	41° 17' 00"	17		x
Russian Gulch, Ca.	123° 46' 59"	39° 19' 46"	29		x
Saint Simon Is., Ga.	87° 22' 45"	31° 08' 20"	67		x
San Buenaventura Ca.	119° 16' 46"	34° 16' 08"	25		x
San Clemente, Ca	117° 36' 14"	33° 24' 07"	42		x
San Elijo, Ca.	117° 17' 30"	33° 01' 15"	46		x
San Simeon, Ca.	121° 06' 32"	35° 33' 58"	48		x
Santa Rosa Isl, Fla.	87° 16' 06"	30° 19' 06"	141		x
Sapelo Isl., Ga.	81° 15' 35"	31° 24' 08"	11		x
Savannah Coast Guard Tower, Ga.	80° 41' 00"	31° 57' 00"	13		x
Seacliff, Ca.	121° 54' 44"	36° 58' 10"	48		x
Shelter Cove, Ca.	124° 03' 54"	40° 01' 24"	30		x
Short Beach, N.Y.	73° 33' 25"	40° 35' 30"	57		x
Silver Strand, Ca.	117° 10' 00"	32° 40' 00"	47		x
Shouthampton Bch, N.Y.	72° 24' 38"	40° 51' 38"	22		x

PAYS COUNTRIES	Organismes + adresses Organizations + Addresses	Endroit de l'enregistrement Recording Site	Coordonnées géographiques Geographical Coordinates		Durée d'enregistrement (en mois) Recording Period (month)		But Objective			
			Longitude	Latitude	effective > 6 mois effective > 6 months	écoulée dès début elapsed since beginning	C.O. (1)	C.C. (2)	N. (3)	M. (4)
		South Assateagua, Md.	75° 20' 30"	37° 53' 00"	13			x		
		South Carlsbad, Ca.	117° 22' 30"	33° 07' 56"	26			x		
		Spruce Cape, Alaska	152° 20' 00"	57° 46' 00"	23			x		
		Stinson, Ca.	122° 38' 10"	37° 53' 36"	42			x		
		Stratford Pt. Conn.	73° 06' 15"	41° 09' 00"	70			x		
		Sunset, Ca.	121° 50' 19"	36° 53' 48"	20			x		
		Sunset, Hawaii	158° 03' 06"	21° 40' 15"	12			x		
		Thornton, Ca.	122° 29' 50"	37° 41' 55"	28			x		
		Toms River, N.J.	74° 04' 20"	39° 56' 00"	61½			x		
		Torrey Pines, Ca.	117° 15' 11"	32° 54' 02"	33			x		
		Twin Lakes, Ca.	121° 59' 46"	36° 57' 42"	20			x		
		Umpqua River, Ore.	124° 11' 55"	43° 39' 54"	211			x		
		Van Damme, Ca.	123° 47' 23"	39° 16' 23"	9	101½		x		
		Virginia Beach, Va.	75° 58' 25"	36° 51' 10"	177			x		
		Westhampton Bch., N.Y.	72° 40' 26"	40° 41' 12"	52			x		
		Willapa Bay, Wash.	123° 58' 00"	46° 42' 20"	49			x		
		Wright, Ca.	123° 05' 53"	38° 24' 09"	47			x		
		Wrightsville, Bch., N.C.	77° 47' 20"	34° 12' 48"	22			x		
		Yaquina Bay, Ore.	124° 03' 40"	44° 37' 26"	209½	25½		x		

APPENDIX H

A COMPARISON OF THE DRAPER AND SPECTRAL METHODS OF ANALYSIS

This is a part of Hoffman (1974), "Analysis of
Wave Records and Application to Design," Inter-
national Symposium on Ocean Wave Measurement and
Analysis, New Orleans, 1974, Vol. II, pages 235-
253.

The methods of data collection and analysis are closely linked to the specific application for which the wave data are intended. While for response calculation of most types the spectrum is ideally suited, the maximum expected wave height is the criterion for determining the height of a jack-up platform above the mean water level. For long-term statistics the distributions of wave heights and periods in various ocean zones are required which are often presented in histogram format giving the probability of exceedance and the frequency of occurrence of such conditions. It is therefore desirable to establish the appropriate analysis technique for each application and, furthermore, to illustrate the relationship between the results obtained by different analysis methods.

A large amount of wave measurement data is available to date only in an analog form on paper strip charts. These represent data collected over the past twenty years, such as thousands of records at Weather Stations A, I, J, K in the eastern Atlantic, and other locations around the British Isles, recorded by pen recorders. During the last few years the development of portable mini recording devices, along with the advent of the digital computer industry, have led to more economical data storage such as tape cassettes as well as on-line digitizing and processing of data using analog to digital converters in conjunction with a digital computer. While wave records stored on magnetic tape are usually easy to reduce and analyze, the analysis or transfer of paper strip charts to magnetic tape are usually time consuming and require variable amounts of manual work.

A substantial amount of the available wave records in deep water was collected using a Tucker wave meter mounted on small ships or trawlers and a standard analysis technique of the data was formulated through the years and recently presented by Draper (1966). Each record, approximately 12 minutes long is characterized by six parameters including the highest and second highest crests and troughs about the mean line, and the number of zero upcrossings as well as the total number of crests. From the above parameters significant wave height ($H_{1/3}$) is calculated, as well as the predicted maximum for a specific steady state duration such as three hours. The zero crossing period $\bar{T}_z$ and the crest period $\bar{T}_c$ are also calculated as well as the spectral width parameter ε_T defined as

$$\varepsilon_T = \left[1 - \left(\frac{N_z}{N_c} \right)^2 \right]^{1/2}$$

Most of the data analyzed as described above, which include but are not limited to Draper (1965, '67, '71), are presented on an annual as well as a seasonal basis including the following:

1) Bar charts of the probability of exceedance of $H_{1/3}$ and H_{max}.

2) Histogram of zero-crossing periods ($\bar{T}_z$).

3) Histogram of spectral width parameter (ε_T).

4) Scatter diagrams illustrating the probability of occurrence of wave conditions within limited height and period bands such as usually customary to describe visual wave statistics.

Two additional presentations suggested by Draper (1966) are diagrams which illustrate the persistance of a range of wave heights of a given wave condition, once a threshold height is achieved and the lifetime wave which is an estimate of the most probable value of the height of the highest wave in the lifetime of a structure.

A recent analysis of 323 wave records from Station "India" was performed using a routine similar to that advocated by Draper as well as spectral analysis, Miles (1971). All records were originally on strip charts approximately 12-15 minutes long and cover primarily noon records collected over a period of twelve years (1954-1966) at that location by three different weather ships, i.e., the Weather Explorer, Weather Recorder and Weather Reporter. The records were selected from a list supplied by the National Institution of Oceanography (NIO) in Wormley, England, and were selected to include all records of Beaufort 6 and above which were available as well as a fair sample of records representing Beaufort 5 and below. The spectral analysis was performed using a computer controlled x-y Bendix digitizer taking 333 samples per inch of time axis by simply following the curve with a light weight cursor, and then carrying out a digital spectrum analysis.

The manual analysis of the records was performed at Webb Institute of Naval Architecture. For each record, a 720 second period was selected and the number of crests and zero crossing periods was first determined. In several cases where the records length was shorter than 12 minutes, the actual available record length was used. All crests were defined as such only if a definite positive and negative slope could be detected. For the purpose of defining the zero crossing period the mean line of the record was usually taken as the geometrical center of the record and adjustments for off center records was only called for in a few cases. The number of crests (N_C) vary between 140 and 60 and the number of zero crossings (N_z) vary from 119 to 53. The maximum height (H_{max}) was the combined sum of the highest wave crest and the lower wave trough in a given record, which varied from 63.41 ft. to 1.00 ft.

Based on the above 3 parameters the following quantities were calculated:

$$H_{1/3} = \frac{f_2}{f_1} H_{max}$$

where f_1 and f_2 are a function of $\overline{T}_z$ and $\overline{T}_c$ respectively, and

$$\overline{T}_z = \frac{L}{N_z} \qquad\qquad \overline{T}_c = \frac{L}{N_C}$$

where L is the length of record in seconds usually L = 720.

The spectral width parameter ε_T was also evaluated.

$$\varepsilon_T = \sqrt{1 - \left(\frac{N_z}{N_C}\right)^2}$$

based on the derivation of Longuet-Higgins (1952).

The function f_1 was also given above as follows:

$$f_1 = \frac{\sqrt{2}}{2}\left[(\ln N_C)^{\frac{1}{2}} + \tfrac{1}{2}\gamma\,(\ln N_C)^{-\frac{1}{2}}\right]$$

where $\gamma = .5772$ is the Euler number. Values of f_1 were found to vary between 1.664 to 1.532 corresponding to N_C values of 140 and 60 respectively. The function f_2 is a function of the number of zero crossings and represent a frequency dependent correction to account for the dynamic correction applied to the pressure record as measured by the Tucker wave meter.

The frequency response correction f_2 is given as a function of frequency and can assume high values for the higher frequency range. Hence, each spectral estimate is multiplied by a different constant. In the above analysis a mean value representing the square root of the frequency response correction must be applied to the measured height and it is usual to select the constant corresponding to the zero crossing frequency. For each of the three ships, a different frequency response correction table was obtained and f_2 values varied from 1.020 for zero crossing frequency of .48 rad/sec to 1.872 at a zero crossing frequency of 1.00 rad/sec.

The $H_{1/3}$ value obtained from spectral analysis were calculated from the square root of the area under the spectrum (rms) times four, i.e.,

$$H_{1/3} = 4 \sqrt{\int_0^\infty S(\omega) \, d\omega} = 4\sqrt{m_o}$$

All spectra were represented at discrete frequencies between $0 - 2.0$ rad/sec at increments of .05 rad/sec.

The comparison between the $H_{1/3}$ values obtained by the two methods is illustrated graphically in Figures H-1 - 4. The overall agreement is rather good, though a slight tendency toward a lower estimate of $H_{1/3}$ from H_{max} is somewhat evident. For the 0-10 ft. wave height group, the approximation technique seems to slightly overestimate the $H_{1/3}$ by roughly 10%. Over the next range of 10-20 ft. as well as 20-30 ft. there seems to be an increase in the scatter about the mean line. However, the distribution about the mean line is approximately equal, indicating an excellent agreement between the two techniques with a standard deviation of approximately ± 2.5 ft.

The data for $H_{1/3}$ larger than 30 ft. are rather scarce; only 14 of the 323 records fall within this range. Most of the data falls below the idealized mean line, with only one point above it and two points lying on it. Hence, in general it can be stated that the predicted $H_{1/3}$ is a reasonably good estimate. This, however, should be further investigated due to the fact that the relationship between $H_{1/3}$ and H_{max} shown previously was made under the assumption of a narrow band process. In reality, the value of ε_T as calculated from the ratio of N_z and N_c varies between 0.20-0.70, rather than the assumed case of $\varepsilon_T = 0$.

The general relationship between H_{max} and $H_{1/3}$ was developed by Cartwright and Longuet-Higgins (1956) using the distribution of maxima.

$$\frac{\eta_{max}}{\mu_2'^{1/2}} = \frac{\left[\ln \, (1-\varepsilon^2)^{1/2} \, N \right]^{1/2} + \frac{1}{2}\gamma \left[\ln \, (1-\varepsilon^2)^{1/2} \, N \right]^{1/2}}{(1 - \frac{1}{2}\varepsilon^2)^{1/2}}$$

where $\eta = \xi/m_o^{1/2}$

$\mu_2' = 2 - \varepsilon^2$, i.e., the second moment about the origin

$N =$ the number of crests

$\varepsilon_T =$ the process width parameter

$\gamma =$ Euler number

$m_o =$ the zeroth moment of the process,   rms $= m_o^{1/2}$

$\xi =$ peak to mean, or mean to trough variation

H-3
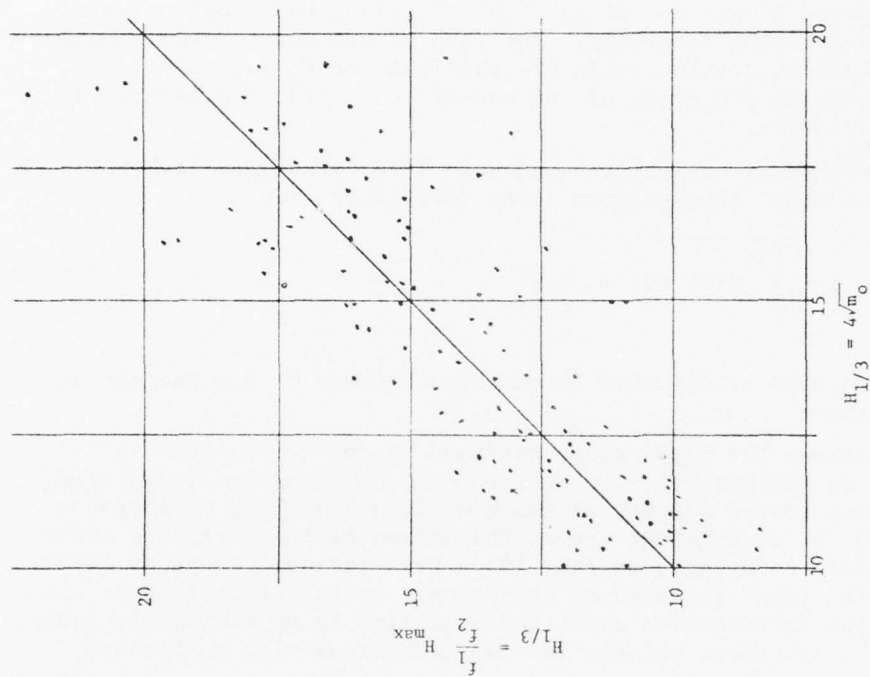
Fig. H-2 – Relationship between values of $H_{1/3}$ calculated from spectral analysis and H_{max} (10-20 ft)
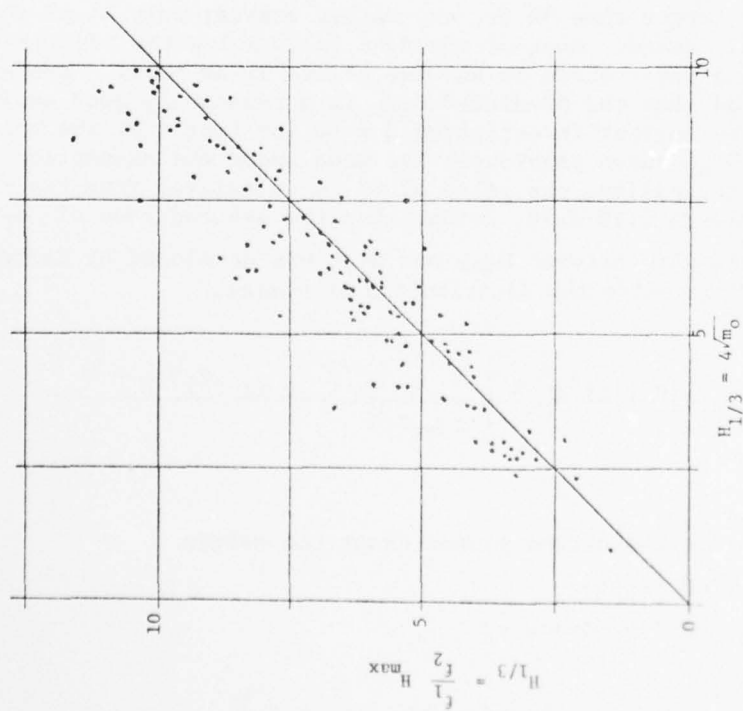
Fig. H-1 – Relationship between values of $H_{1/3}$ calculated from spectral analysis and H_{max} (0-10 ft)

1.0

4.5
5.0

2.8

2.5

1.1

3.2

2.2

3.6

4.0

2.0

1.8

1.25

1.4

1.6

MICROCOPY RESOLUTION TEST CHART

NATIONAL BUREAU OF STANDARDS-1963-A

$H_{1/3} = \dfrac{f_1}{f_2} H_{max}$

$H_{1/3} = 4\sqrt{m_0}$

Fig. H-4 – Relationship between values of $H_{1/3}$ calculated from spectral analysis and H_{max} (30-40 ft).

$H_{1/3} = \dfrac{f_1}{f_2} H_{max}$

$H_{1/3} = 4\sqrt{m_0}$
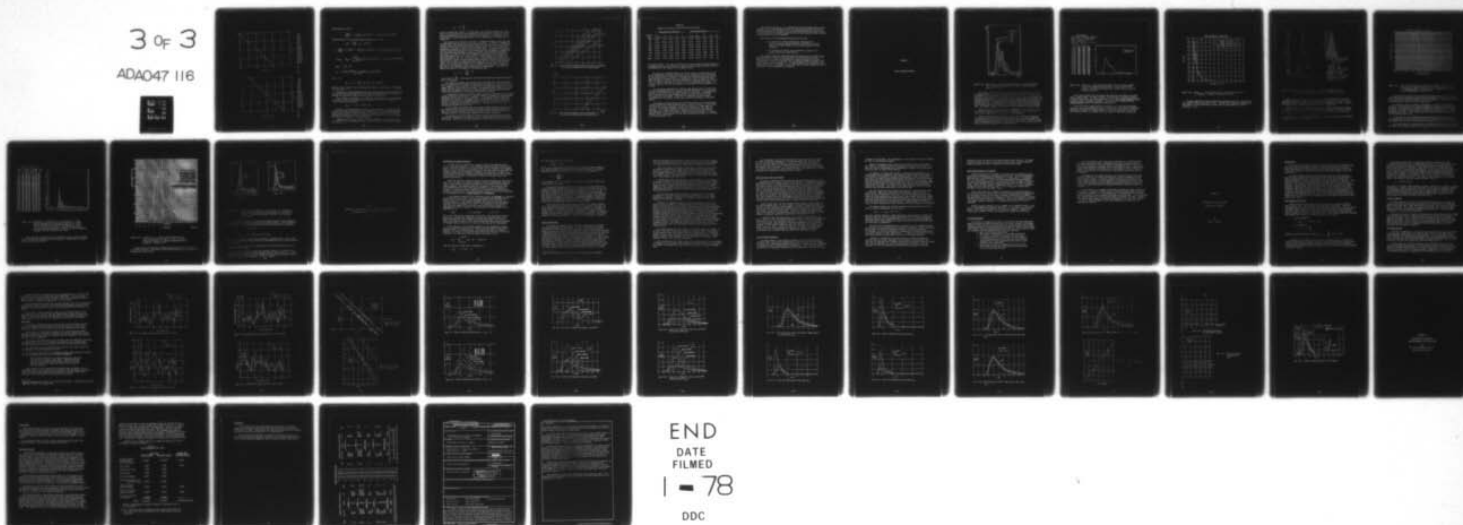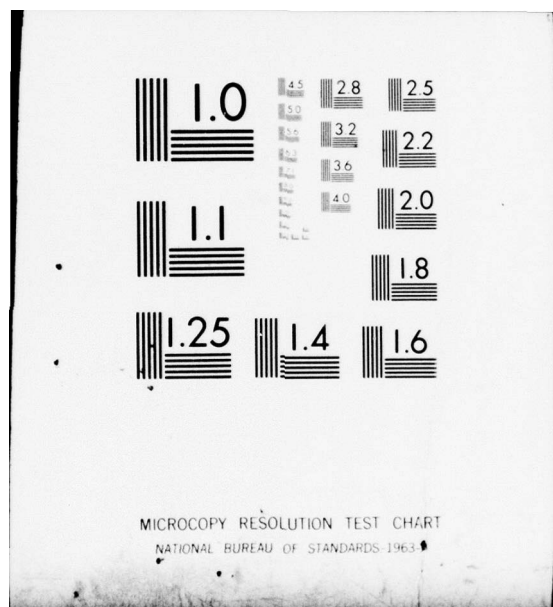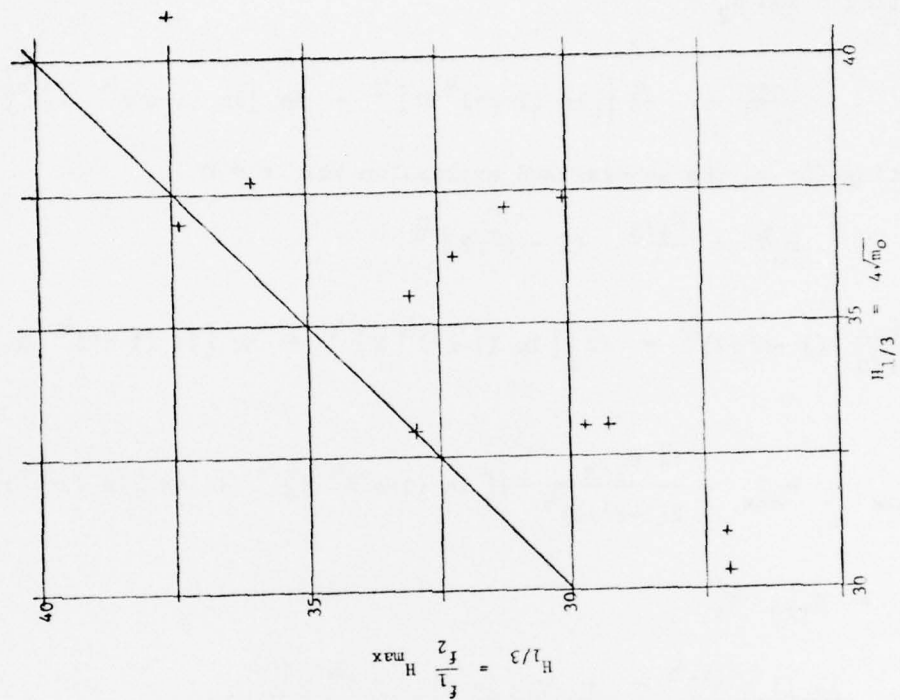
Fig. H-3 – Relationship between values of $H_{1/3}$ calculated from spectral analysis and H_{max} (20-30 ft).

Substituting η and μ_2'

$$\frac{\xi_{max}}{m_o^{\frac{1}{2}}} = \sqrt{2} \left\{ \left[\ln (1-\epsilon^2)^{\frac{1}{2}} N \right]^{\frac{1}{2}} + \frac{1}{2}\gamma \left[\ln (1-\epsilon^2)^{\frac{1}{2}} N \right]^{\frac{1}{2}} \right\}$$

Substituting for m_o the generalized expression for $\epsilon \neq 0$

$$m_o^{\frac{1}{2}} = \frac{H_{1/3}}{4} (1 - \epsilon^2/2)^{-\frac{1}{2}}$$

$$4 \frac{\xi_{max}}{H_{1/3}} (1 - \epsilon^2/2)^{\frac{1}{2}} = \sqrt{2} \left\{ \left[\ln (1-\epsilon^2)^{\frac{1}{2}} N \right]^{\frac{1}{2}} + \frac{1}{2}\gamma \left[\ln (1-\epsilon^2)^{\frac{1}{2}} N \right]^{-\frac{1}{2}} \right\}$$

$$2 \xi_{max} = H_{max} = \frac{\sqrt{2} H_{1/3}}{2(1-\epsilon^2/2)^{\frac{1}{2}}} \left\{ \left[\ln (1-\epsilon^2)^{\frac{1}{2}} N \right]^{\frac{1}{2}} + \frac{1}{2}\gamma \left[\ln (1-\epsilon^2)^{\frac{1}{2}} N \right]^{-\frac{1}{2}} \right\}$$

$$H_{max} = H_{1/3} f_1'$$

$$f_1' = \frac{\ln (1 - \epsilon^2)^{\frac{1}{2}} N + \frac{1}{2}\gamma \left[\ln (1 - \epsilon^2)^{\frac{1}{2}} N \right]^{-\frac{1}{2}}}{(2 - \epsilon^2)^{\frac{1}{2}}}$$

for $\epsilon = 0$

$$f_1' = f_1 = \frac{\sqrt{2}}{2} \left[(\ln N)^{\frac{1}{2}} + \frac{1}{2}\gamma (\ln N)^{-\frac{1}{2}} \right]$$

where N is the number of zero crossings (N_z) which is equivalent to the number of crests (N_c).

Values for ϵ_T were calculated using the relationship between N_z and N_c and it was found that the range of f_1' shift upward by approximately 8-10% hence, causing an equivalent decrease in the predicted $H_{1/3}$ value.

This, however, was offset by a correction of approximately the same order to the $H_{1/3}$ values calculated for the spectrum as a result of inclusion of ϵ in the following relationship:

$$H_{1/3} = 4 (1 - \epsilon^2/2)^{\frac{1}{2}} \sqrt{m_o}$$

Values of ϵ_T calculated from N_z and N_c were compared with those obtained by the second and fourth moment of the process $-\epsilon_s$. It can be generally concluded that in spite of the fact that the difference in the order of 40-50% existed between the $H_{1/3}$ values obtained by the two methods the general agreement shown in Figures H-1 - 4 was maintained.

Comparison of the zero crossing period T_z estimated for the record with the calculated zero crossing period as obtained from the second moment of the spectrum, i.e.,

H-6

$$T_2 = 2\pi \frac{m_o}{m_2}$$

are of a rather poor quality. In most cases, the predicted period was in the order of 10-25 higher than the calculated T_2 and only 10-15 records out of 323 were approximately equal or lower than the $\overline{T}_z$ calculated. In general, the $\overline{T}_z$ values were in closer agreement with T_{-1} or T_1 respectively as illustrated in Figure H-5.

The relatively large error in T and ε is expected because of the crude way of measuring N_z and N_c directly from the strip chart. It should be remembered, however, that even though the absolute value of T and ε may be in error the distribution of the data is valid and is extremely useful for a quick relatively inexpensive analysis of waves in various ocean zones. It should also be noted that the large differences in T and ε between the two techniques as compared to the relatively good agreement of the $H_{1/3}$ ratios can be logically explained. While $H_{1/3}$ is related to the zero[th] moment of the process T is a function of the second moment and ε is a function of the fourth moment both of which are more dependent on the tail of the spectrum. At this region, the Tucker wave meter results require an increasingly larger frequency response correction function which is often of a magnitude larger than the rest of the lower frequency range. The tendency may therefore be to exaggerate the spectral ordinate in the tail of the spectrum in some cases, which in turn will cause a larger moment with a corresponding greater increase with fourth moment. It will also affect the value of ε_s as shown by the expression below

$$\varepsilon_s = (1 - \frac{m_2^2}{m_o m_4})^{\frac{1}{2}}$$

As a result of $\frac{m_2^2}{m_4}$ decreasing the term under the radical sign gets larger and hence ε increases.

The comparison between the predicted and calculated zero crossing periods and the spectral width parameter is illustrated in Figs. H-5, H-6, respectively. It is apparent that in the case of the period, the prediction method is generally higher than the calculated $\overline{T}_z$ by 10-20%. The spectral width parameter ε_T as obtained from the number of crests, is generally much lower than the calculated value from the moments of the record in the order of 20-30%.

A comparison of seven records all having a period T_1 between 8.5-9.0 seconds and $H_{1/3}$ between 11.50-15.00 ft. is given in Table H-1 showing the characteristic parameters as obtained by the two methods. It is evident from the table that the mean value of $H_{1/3}$ is extremely close by both methods and $\overline{T}_z$ corresponds better to a period lying somewhere between T_{-1} and T_1, the energy average period and the average wave period respectively. The mean deviation of ε_T is substantial and amounts to about 25%.

It is further illustrated that the values obtained from the analog records are consistent and the deviation about the mean, though somewhat larger than that of the values obtained from spectral analysis are all the same, which is extremely useful in defining wave conditions at various locations.

It should be also noted that for several of the records the $H_{1/3}$ was calculated by averaging the 1/3 highest peak to trough heights over the length of the record. The results obtained were within 3-5% of the calculated $H_{1/3}$ from
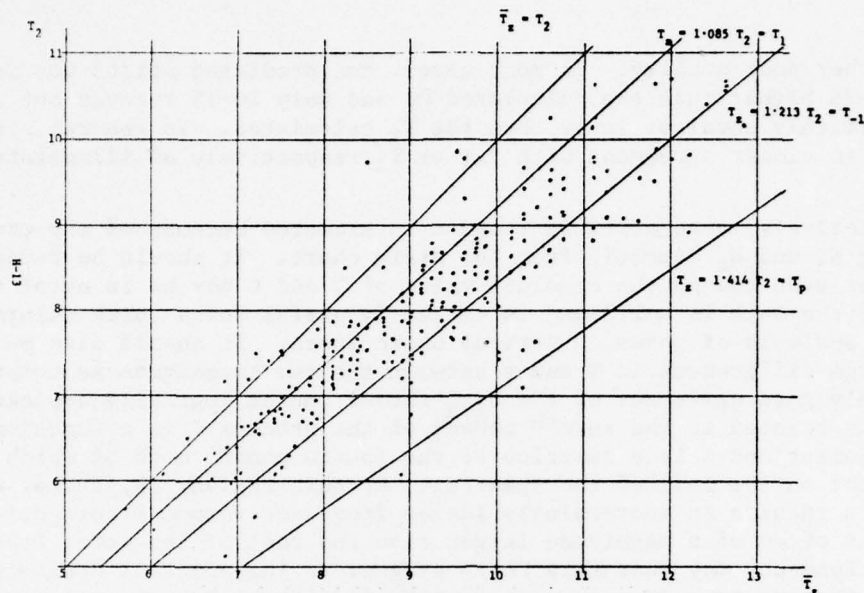
Fig. H-5 - Relationship between values of T_2 and $\bar{T}_z$ calculated from spectral analysis and the analog record.
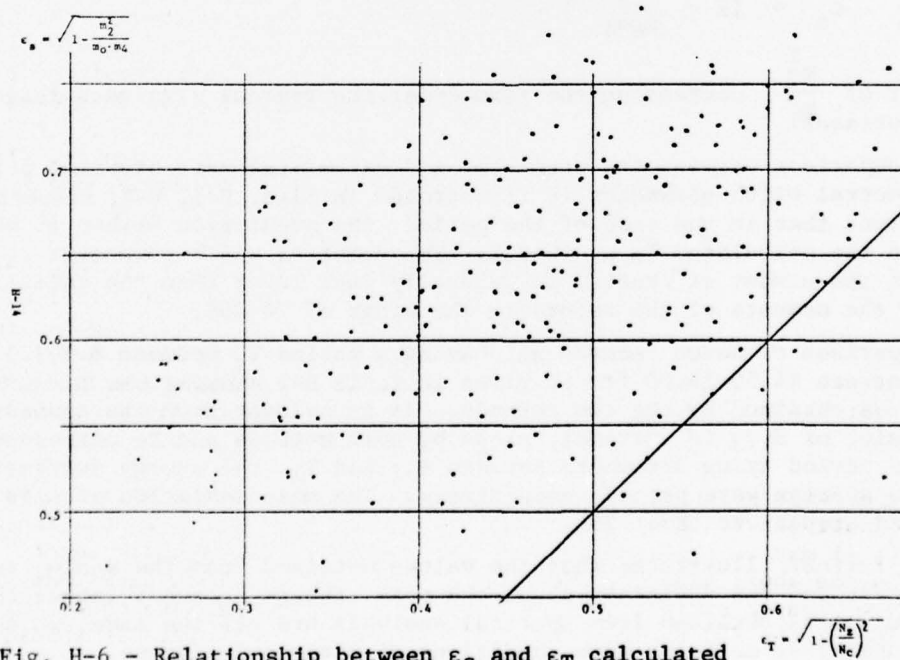
Fig. H-6 - Relationship between ε_S and ε_T calculated from spectral analysis and the analog record.

TABLE H-1

Comparative Results of Two Wave Analysis Methods

Record No.	From Spectral Analysis					From Analog Record				
	$H_{1/3}$	T_{-1}	T_1	T_2	ε_s	$H_{1/3}$	H_{max}	$\overline{T}_z$	ε_T	N_c
182	13.45	9.33	8.56	8.11	.624	15.34	22.07	8.89	.391	90
224	14.01	10.60	8.84	8.02	.700	14.44	21.48	9.35	.586	95
228	11.47	9.61	8.72	8.24	.628	10.10	14.83	9.35	.465	85
265	13.58	9.80	8.98	8.44	.658	13.87	19.80	9.35	.586	95
268	14.57	9.81	8.86	8.31	.662	13.50	18.75	9.11	.513	80
273	14.90	9.76	8.73	8.20	.638	16.20	22.50	9.00	.553	80
277	14.78	9.94	9.00	8.29	.687	14.60	20.79	9.86	.585	75
Mean	13.87	9.83	8.82	8.24	.660	14.00	20.03	9.27	.526	86

the spectral area. The only correction to the actual peak-to-trough heights was a constant correction for frequency response, which was applied using the value corresponding to the frequency of the spectral peak.

The excellent agreement between the values of $H_{1/3}$ calculated by the different techniques is of great importance and is indicative of the flexibility of the Draper method of analysis. Although when comparing individual records some substantial deviation may occur occasionally, for statistical purposes where the mean is required, excellent agreement is shown in Table H-1 for $H_{1/3}$. If T_z is taken as the mean of T_{-1} and T_1, a close approximation results. It is felt, however, that the discrepancy in the periods by the two methods is of concern.

The preceding comparison is of further significance since it covers both the most comprehensive and the simplest possible approaches to data analysis. Several other methods fall in between these two techniques. For example, the rms of the record can be determined directly from the record, and hence, the significant wave height. Similarly, by analyzing the peak-to-mean distribution of the record, the $H_{1/3}$ can be directly obtained, as mentioned above.

The degree of sophistication that should be applied to the data analysis should be compatible with the method used to collect the data. If the latter is deficient, it may be useless to carry the analysis to a high degree of accuracy. In the above example, the source of the data in both cases was identical, i.e., paper strip charts recorded by a NIO Tucker wave meter. The limitation of the NIO recorder at high frequencies is known. It should, however, have a limited effect on the zero-crossing period which is a function of the second moment only.

The broadness factor, ϵ, is a function of the fourth moment which is more dependent on the high-frequency tail of the spectrum, which may be affected in both techniques by the nature of the record obtained from the Tucker meter. The discrepancies are therefore large and very little similarity exists between results obtained by the two methods.

The purpose of the preceding evaluation was two-fold:

1. To evaluate the Draper technique by comparing with spectral analysis and hence provide a criterion of acceptance for the large amount of data already analyzed by this technique.

2. To determine the extent one is justified in using it for general analysis of strip charts.

The complete answer to these questions can only be given in terms of the ship responses as predicted using one source of wave data or the other. If, however, one has to judge the reliability of such data based on the wave characteristics only it is apparent that the method proposed in Draper (1966) only provides a partial answer, i.e., a good estimate of the significant wave height, but fails to supplement it with additional required information such as the period or other parameters of interest.

APPENDIX I

SAMPLE MEASURED SPECTRA
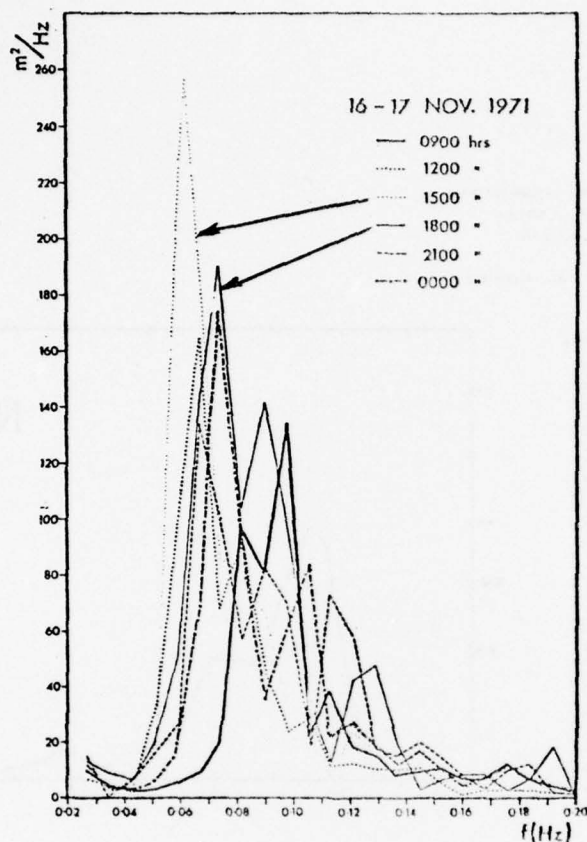
Sample from: Saetre, H.J., "On High Wave Conditions in the Northern North Sea," Institute of Oceanographic Sciences, Surrey England, Report No. 3, 1974.

This report contains an analysis of waves measured during three winters by M/V <u>Famita</u> in the northern part of the North Sea (57° 30' N, 3° 00' E). The 41 spectra were selected from the six most severe storms in order to study growth and decay of the spectra. It is concluded that storm spectra from the North Sea (and North Atlantic) have the same form and that their shapes are similar to the JONSWAP spectrum, i.e., the spectrum has a much sharper peak than the Pierson-Moskowitz spectrum. In general the wave spectrum 3 hours before the spectrum with maximum total energy is sharper and has more energy in the peak frequency band. For example, compare the spectra for 1500 and 1800 in the above sample.

Saetre finds good correlation between parameters derived using the moments of the spectra and those derived by Tucker's method of visually inspecting the wave record except in the case of spectral width parameter.

Based on all the records collected over the three winters, he draws the following conclusions from the long term statistics: The Gumbel probability distribution gives the best fit to the complete time series. The Gumbel probability distribution gives higher extrapolated, predicted wave heights than the Weibull distribution applied to the same data set.

1-1

WAVE DISPLACEMENT SPECTRUM

1760 NOV. 29, 1960   SHIP=WEATHER REPORTER   RECORD NO. NW147

VARIANCE= 1.4996 M==2   SIG. WAVE HGT.= 4.9011 M

NOISE LEVEL= 0.0235 M==2/RPS   CUT-OFF= 8.225 RPS

DOF= 28   TOTAL DOF= 184

T(-1)= 10.5136 SEC   T(1)= 9.2633 SEC   T(2)= 8.5860 SEC

K(-1)= 1.1682   K(1)= 1.0845

NW147

Sample from: Miles, M., "Wave Spectra Estimated from a Stratified Sample of 323 North Atlantic Wave Records," Report LTR-SH-118A, Division of Mechanical Engineering, National Research Council, Canada, May 1972.

This report presents the 323 spectra and describes the analysis procedure used to compute them. As shown in Table 1 in this report (frequency response correction functions), the correction factor for the OWS Weather Explorer becomes extremely large as frequency increases. For this reason, records from the Weather Explorer should be regarded as questionable.

These records were not selected to represent fully developed conditions. Except for 16 records selected in order to facilitate a short study of spectral variation with time over limited periods, all records were taken at noon and were chosen randomly to represent the total range of conditions encountered.

DISPLACEMENT SPECTRUM

RMSA = 1.95 FT
$H_S = 4 \times 1.95 \times (C_1 \times C_2) = 11.70$ FT
$\left. \begin{array}{l} C_1 = 1.20 \\ C_2 = 1.25 \end{array} \right\}$ SEE PAGES 22, 23

(y-axis: FT^2 / RPS, values 0 to 10)
(x-axis: FREQUENCY IN RPS, values 0 to 6.5)
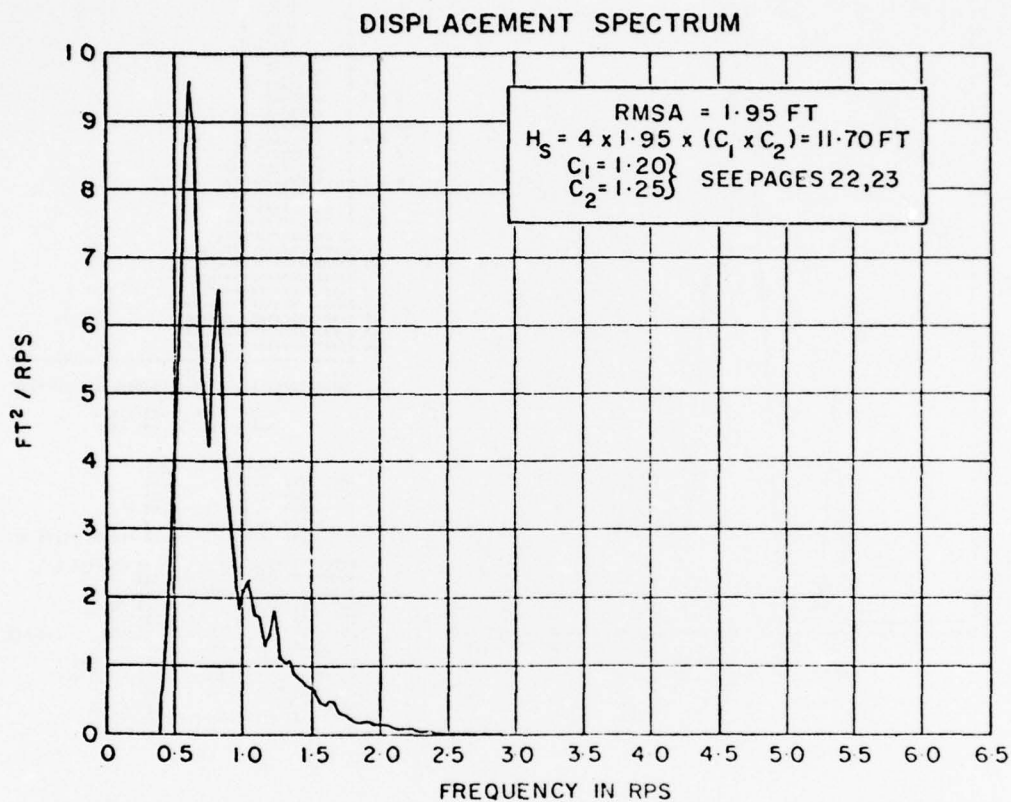
Sample from: Ploeg, J., "Wave Climate Study -- Great Lakes and Gulf of
St. Lawrence," SNAME T & R Bulletin No. 2-17.

The data tabulated by Ploeg includes $H_{1/3}$ and peak period ω_o. The spectra
are available only in the form of plots. Tabulations of spectral ordinates were
never made. Of the 4,000 spectra, there are only approximately 10 spectra
with $H_{1/3} > 16$ ft.

Sample from: Larsen, L.H. and Fenton, D., "Open Ocean Wave Studies,"
University of Washington, Department of Oceanography, DATA
Report 1-73, February 1974.

This report includes 615 spectra measured using a **vibrating wire pressure
transducer (vibratron)** placed on the top of Cobb Seamount in the North Pacific.
The first volume of this report (Discussion of Data Analysis) provides a **complete**
description of the instrument used and the method of analysis.

The vibratron is an extremely accurate and low noise instrument throughout
its recording range; thus these spectra are quite reliable. The authors include
a comparison with a measurement made using a Tucker wave meter on a ship above
the Seamount and find the agreement excellent.

It should be noted that Cobb Seamount is located near major Pacific **shipping**
routes (46° 46.4' N – 130° 48.8' W).

WAVE DISPLACEMENT SPECTRUM
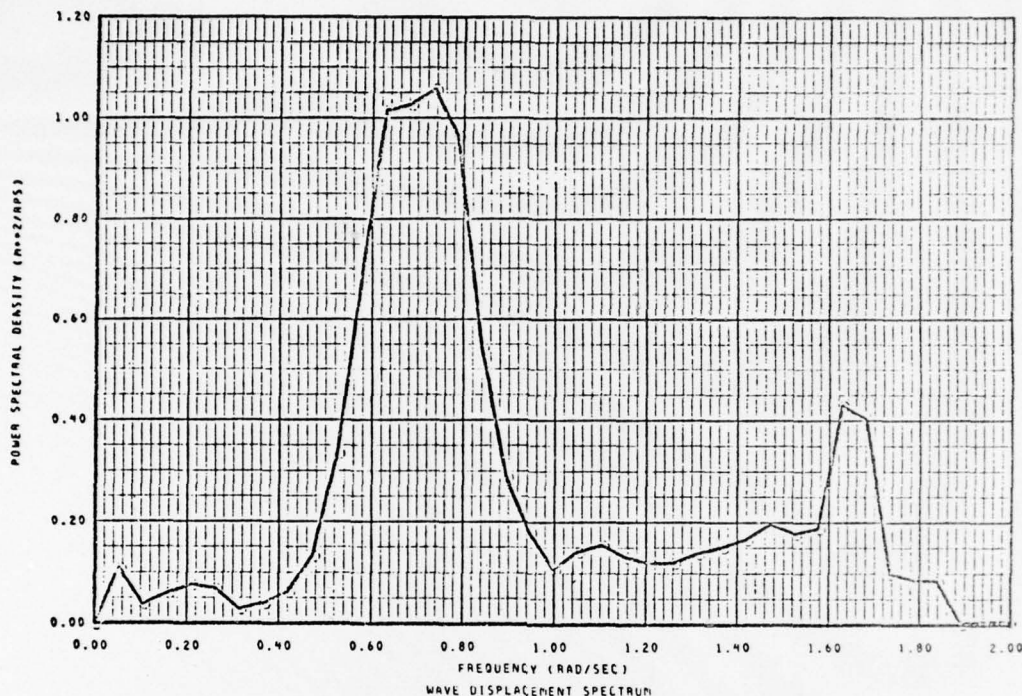
Sample from: Lockheed Shipbuilding and Construction Company, "Instrumentation
and Analysis of Data Collected on the S.S. Japan Mail and the
S.S. Philippine Mail from December 1971 to July 1973," Report
to Sea Use Foundation, Seattle, 1974.

This report describes the data reduction techniques used on data gathered
with Tucker meters installed on ships crossing the Pacific. The method described
is not unusual and the description of it is straightforward. They fail, however,
to mention several factors of crucial importance.

In almost all cases, the ship is traveling at a speed of approximately
20 knots. This means that the frequency measured is actually the frequency of
encounter. If the direction in which the waves are traveling and the heading
and speed of the ship are all known, the frequency of encounter can be related
to absolute frequency. This information can be extracted from the ships logs
which accompany this report.

If the waves are not predominantly from one direction but consist rather
of a combination of local wind waves and swell, as is often the case, then
measurements from the ship at speed cannot be analyzed to give the true spectrum.

The dynamic effects of ship motion on the Tucker wave meters have not been
discussed. The possible influence of such effects warrants careful consideration.

HINDCASTING SPECTRA   COMPUTED APRIL 1963

DATE = 5/ 3/58   AV. T=   7.5   RECORD =   JHC201
HOUR = 21   SIG.HGT. =   22.7   UPPER HGT. =   24.9
TOTAL OF =149   CORR. VAR. =   32.1   LOWER HGT. =   20.6
                        NOISE LEVEL =   .0094   WIND SPEED =   40

Sample from: Moskowitz, L., Pierson, W.J., Jr. and Mehr, E.,   "Wave
               Spectra Estimated from Wave Records Obtained by the OWS
               Weather Explorer and the OWS Weather Reporter,"   Parts
               1, 2 and 3, New York University, College of Engineering,
               Research Division, Department of Meteorology and Oceanography,
               November 1962, March 1963 and June 1965.

    These data were collected to study the shape of fully developed spectra.
Hence, the spectra included cannot be considered a random sample of typical
spectra encountered by ships.
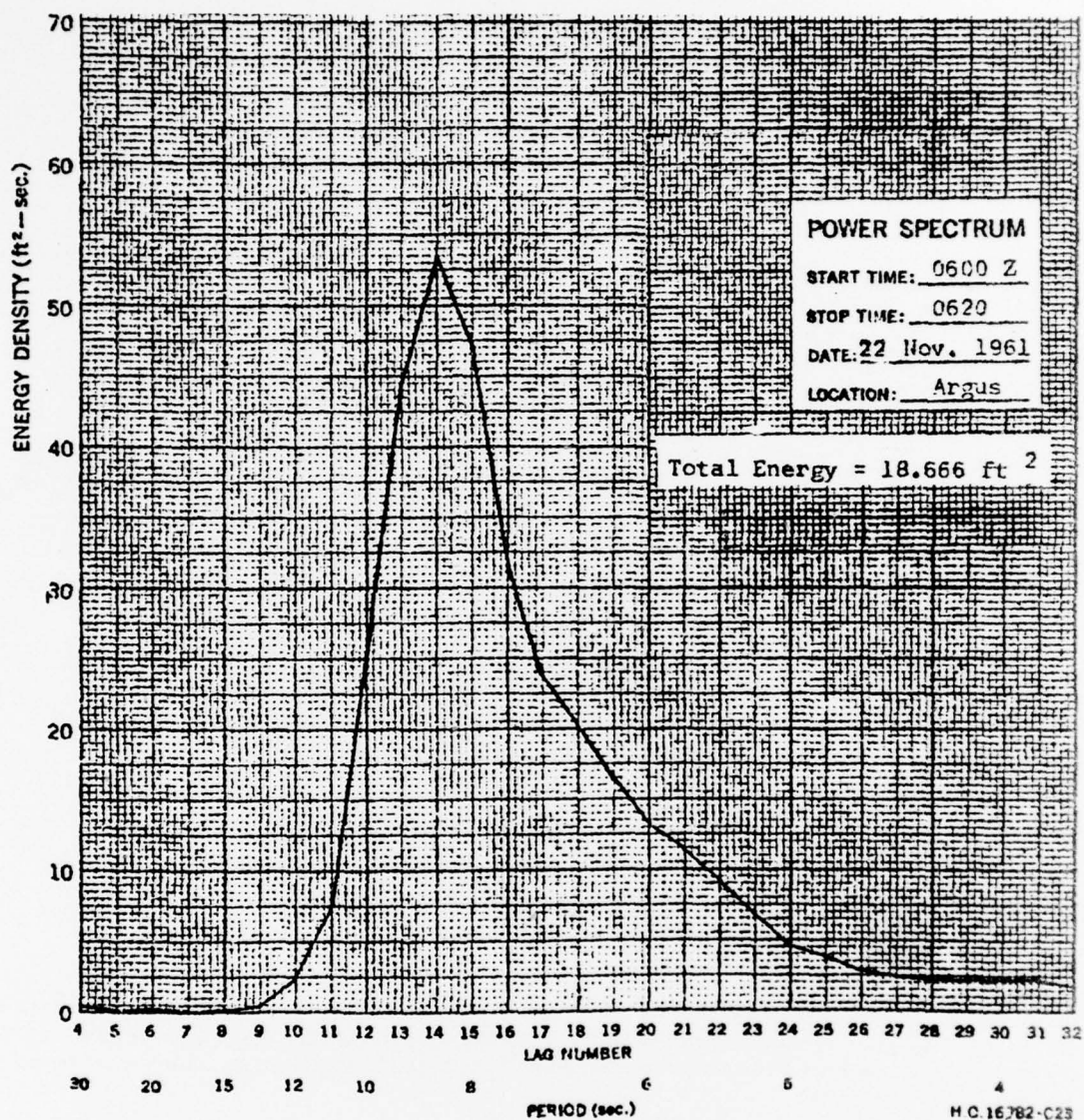
Sample from: Pickett, R.L., "A Series of Wave Power Spectra,"
               Unpublished manuscript, IMR No. 0-65-62, Marine
               Science Department, U.S. Naval Oceanographic Office,
               Washington, November 1962.

     These spectra were measured at Argus Island Tower (31° 56' N, 65° 10' W)
in 192 feet of water. The effects of this limited depth must be considered in
dealing with these spectra.
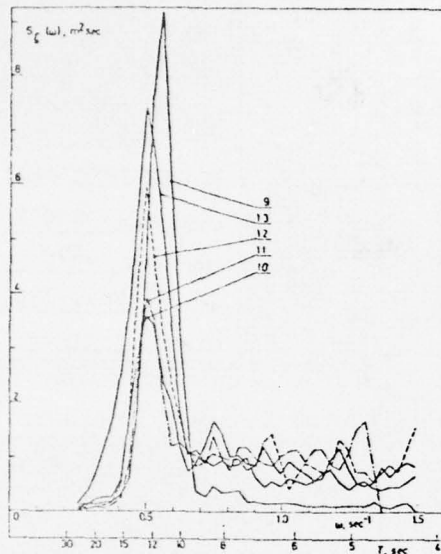
Fig. 1c)
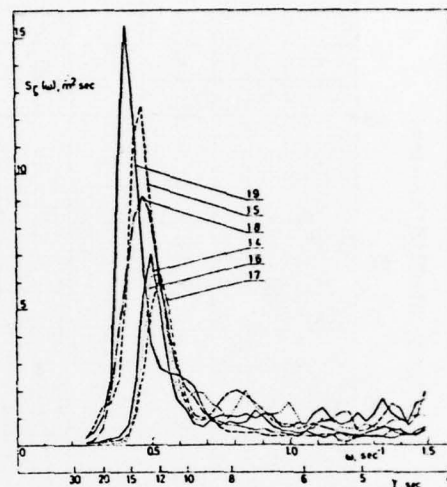
Fig. 1d)

Samples from: Ferdinande, V., DeLambre, R. and Aertssen, G., "Spectres de Vagues de l'Atlantique Nord (Sea Spectra from the North Atlantic)," Association Technique Maritime et Aeronautique, 1975 Session.

The spectra included in this report were made using the Tucker Shipborne Wave Recorder on French naval vessels in the North Atlantic. The measurements were made while the vessels were at speed and corrected using the equations:

$$\omega_e = \omega - \omega^2 \frac{V}{g} \cos \mu$$

$$S_\zeta(\omega) = \left(1 - 4 \frac{V}{g} \omega_e \cos \mu\right)^{\frac{1}{2}} S(\omega_e)$$

where V is the ship speed, ω_e is the encounter frequency, and μ is the angle between the direction in which the ship is traveling and that in which the waves are traveling.

The dynamic effects of the ship motion on the Tucker wave meter are not considered in the report.

Based on the spectra included the authors conclude $p = 4.9$ and $q = 3.5$ provide a better mathematical approximation than the usual choice of $p = 5$ and $q = 4$. Based on similar work done at Webb with a much larger group of spectra, we cannot support this conclusion. See text, chapter V.

I-8

APPENDIX J

REMARKS ON OCEAN WAVE SPECTRAL PARAMETERIZATION TECHNIQUES
AND THEIR APPLICATIONS IN NAVAL ARCHITECTURE

by

Willard J. Pierson, Jr.

Statistics and Random Variables

In 1949, when J.W. Tukey wrote a paper entitled "The Sampling Theory of Power Spectrum Estimates", a new technique became available to study ocean waves. The total variance of the wave record could be resolved into frequency bands in such a way that the contributions to the total variance from different frequency bands could be graphed or tabulated as a spectrum. A highly correlated time history and a highly correlated covariance function were replaced by a sequence of essentially independent numbers in frequency space that formed the spectrum.

There are important parallels between spectral estimation and the estimation of the variance of a normal population. Given an independent sample of size n from a normal population, the mean and the variance can be estimated from the sample. The estimated mean has a "student t" distribution, and the estimated variance has a Chi-Square distribution with n-1 degrees of freedom. A fiducial confidence interval on both the mean and the variance can also be constructed. The essential point, however, is that these estimates of the parameters are both <u>random variables</u> and <u>statistics</u>.

In the spectral analysis of an ocean wave record, an <u>estimate</u> of a function called a spectrum is found. Just as in the example from the normal distribution where μ and σ^2 must be distinguished from $\bar{x}$ and $\hat{\sigma}^2$ (the mean, μ, and the variance, σ^2, are unknown constants, and the second two are random variables that are estimates of μ and σ^2), the spectrum of the population from which the sample wave record was taken as defined by $S(\omega)$ must be distinguished from the estimate of the spectrum at a finite number of frequencies, as in

$$\hat{S}(\omega_j) \qquad\qquad \omega_j = 2\pi j / 2p\Delta t \qquad\qquad j = 0 \text{ to } p$$

The point of the paper by Tukey was to show that, with the method he used, every other estimate was independent and that these estimates had a Chi-Square distribution, whose degrees of freedom were known. The values of $\hat{S}(\omega_j)$ are random variables. Fast Fourier Transforms (FFTs) make it possible to estimate spectra such that all values of the spectrum are independent.

Since each point on a spectrum estimated by the techniques of Tukey, either as originally proposed or in terms of the more modern square filter smoothed FFTs, is a random variable, the complete spectrum is a random function. Or stated in statistical terms, if $S(\omega)$ is the true, but unknown, spectrum of the infinitely long stationary time series, and if

$$M_{oj} = \int_{\omega_j - \Delta\omega/2}^{\omega_j + \Delta\omega/2} S(\omega) \; d\omega \approx S(j\Delta\omega) \; \Delta\omega$$

then the variance in that band is estimated by

$$\hat{M}_{oj} = \hat{S}(j\Delta\omega) \; \Delta\omega$$

The expected value of $\hat{M}_{oj}$ is given by

$$E(\hat{M}_{oj}) = M_{oj}$$

and $\hat{M}_{oj}$ has a Chi-Square distribution with an unknown scaling parameter, M_{oj}, with the degrees of freedom given by Tukey in which M_{oj} is unknown and in which $\hat{M}_{oj}$ is an estimate of it in exactly the same sense as

$$\hat{\sigma}^2 = \frac{1}{n} \sum_{j}^{n} x_i^2$$

is an estimate of σ^2 in a sample of size n from a univariate normal population with a zero mean.

The spectral estimates, $\hat{S}(j\Delta\omega)$, j=0, 1...p, in the older method are weakly correlated in that $\hat{S}(j\Delta\omega)$ is not independent of $\hat{S}((j+1)\Delta\omega)$, but independent in that $\hat{S}(j\Delta\omega)$ is independent of $\hat{S}(q\Delta\omega)$ if $q \neq j-1, j, j+1$. In both cases, however, since each spectral estimate is a random variable, each and every one of the spectra that have been estimated from ocean wave records over the course of the years is a random function. Plotting the 90% fiducial confidence intervals on a number of spectral estimates with typically 50 to 100 degrees of freedom, is a convincing way to learn how poorly the true population parameters have been located.

In the same sense that each spectral estimate is a random variable, it is also true that each spectral estimate is a "statistic" and that the entire sequence of frequency ordered spectral estimates is a sequence of "statistics". It is true that these "statistics" are computed using a blend of Fourier series concepts plus probabilistic concepts. The spectral estimate is some linear combination of the observed data where the linear combination involves trigonometric terms; it is nevertheless a statistic.

Target Populations

In statistical sampling theory, the first requirement is to define the target population to be sampled. If one is interested in selling clothes for 10 year old girls in New York City, it does little good to study the sizes of 5 year old boys in Manila. Only in the study by Moskowitz (1964),* which led to the so-called Pierson-Moskowitz spectrum, was the target population defined and only in that study was it shown that the spectra could indeed have been samples from the target population. In each of five different wind speeds, the target population was the spectra of those records that might be obtained for "infinite" fetch and duration, generated by a wind blowing for a long time with a constant speed and direction over an infinite ocean. It was postulated that, for the wind speeds actually used, "infinite" duration and fetch were actually fairly finite as to the time the wind needed to blow and the distance over which it blew. All other

---

* Note that the first word in the title of this paper is "Estimates".

spectral parameterization procedures that have been proposed have ignored
the two most essential aspects of statistical procedures, namely defining
the target population and proper consideration of sampling variability.

Since this study by Moskowitz is more than a decade old, much could
be learned by repeating it, using better calibrated wave data and FFT
spectral estimates, a much larger sample, and the correct application of
the Kolmogorov-Smirnov test (Crutcher, 1975). Of great importance would
be a careful study of the high-frequency tail of the spectrum. The equili-
brium range probably does not exist.

A second important situation where a target population can probably
be defined is that of the fetch-limited case. To simplify things, it would
be useful to use wave records where the upwind end of the fetch is land,
where the wind is always from the same direction, and where the range of
admissable wind speeds is severely restricted to one or two knots. The true
population spectra would then be functions only of wind speed, since the
fetch would be fixed.

For the open ocean, far from land, in a region where a continuous
procession of transient cyclones and anticyclones moves by, the target
population is difficult to define. An attempt to define a third target
population is, however, necessary.

Consider, for example, a point on the ocean surface, and a circle
around it with a radius of 10 nautical miles. Now imagine a wave record
taken for 20 minutes for every two-mile intersection on a square grid inside
this circle, all starting at the same time. There would be about 78 such
records. No two would be exactly alike, and the correlation between nearby
records and spectra would be vanishingly small. If each spectrum were
estimated over exactly the same frequency bands for exactly the same algorithm,
these 78 different spectra could be averaged. The average would still be
a random function, but the confidence intervals would be about one-ninth
as wide as those for one spectral estimate. The target population spectrum
is then some spectrum, probably within the 90% confidence intervals of this
averaged estimate. The individual spectra from the 20-minute records
should fluctuate about this "averaged" spectrum in ways predictable from
sampling theory.

The target population is the limit in an infinite number of degrees of
freedom of this kind of spectral estimate at each grid point of the model.
If wave spectra could be estimated with 5000 or 4000 degrees of freedom, as
opposed to about 30 to 100, many of these problems could go away. A recent
study by Pierson (1975) suggests that this may indeed be possible if wave
imaging techniques can be further developed.

Wave records taken for longer times at a point are usually not the answer.
Increasing the record length from 20 minutes to 2,000 minutes (33 hours) leads
to problems of changing wind speed and direction over the longer recording
time.

As an exception, in the trade wind areas of the world oceans, it might
be a most interesting experiment to record wind speed, wind direction and
waves for several days continuously. Except for swell from some distant
source, that will usually be in different frequency bands, this long record
may respond only to the minor (?) fluctuations in the strength of the trades.
Its analysis could provide a very precise estimate of the spectrum of a target
population with sampling variability greatly reduced.

Numerical Wave Prediction Models

    Insofar as a numerical wave forecasting and wave specification (or hind-
casting) method that attempts to describe the spectra of wind-generating gravity
waves and of swell is a valid method, it can only hope to predict, or specify,
the expected value of the wave spectrum that will be observed at a particular
point on the ocean surface (or in a particular area) for a particular time
(+20 to 30 minutes) of observation. The actual spectrum computed from a
wave record at that point in space and time will not, and cannot be expected
to, agree with the predicted spectrum in exact detail because of the fundamen-
tal nature of the waves. The random part of the problem cannot be predicted.
The target population is the third example given above in the most general
case and at various points in the model at various times, the target population
becomes either a fully developed sea or a fetch or duration-limited sea.

    Stated another way, wave forecasting methods attempt to specify $S(\omega)$ to
be varified against $\hat{S}(\omega)$. In this context, it should be emphasized that all
theories of wave generation and propagation are really working with $S(\omega)$, and
$S(\omega,\psi)$, and are only indirectly concerned with the problem of verifying what
they predict in terms of actual data. It may be, though, that some of the
more recent aspects of wave generation theory have falsely attributed certain
effects of sampling variability incorrectly to some physical cause.

    A numerical wave forcasting theory can be wrong in several different
ways. One way is that the idealized spectrum, $S(\omega)$, is really not an adequate
description of the true population spectrum. A second is that the physics
of wave generation, wave propagation and wave dissipation is not correctly
modeled. A third would be that the winds that "generate" the waves are not
given correctly. Even if perfectly correct in all three of the above ways,
there would still be the problem of comparing the numerically predicted
spectrum with the estimated spectrum, using valid sampling concepts.

Curve Fitting Procedures

    The great danger in the present procedures for curve fitting spectral
estimates lies in the lack of appreciation of the fact that they are indeed
estimates with a substantial sampling variability. Insofar as these "estimates"
are equated, without considering the consequences, to the true, but unknown,
spectrum of the conceptual population for the seaway under consideration, then

a mistake is being made. The consequences of this mistake are hard to define, but they are nevertheless present.

Numerous fundamental points arise as to the best way to use estimated wave spectra, as random functions, in problems of naval architecture. It is here that various deterministic and probabilistic concepts are in sharp contrast and even, at times, sharp conflict.

For example, in towing tank studies a long-crested approximation to a random seaway can be generated. The response of this model to that seaway is in principle a deterministic problem in hydrodynamics. The fact that the spectrum of the seaway produced might depart substantially from the prototype wave conditions that attempts were being made to model is not critical. For example, a modeled spectrum that was twice too high in a given frequency band would produce an output in a linear theory that was twice too high in the spectrum of the motion. The motion of the model predicted from the forcing function that was used would still be the correct one.

The real problems of Naval Architecture should be concerned with short-crested seas. Under these conditions, the coherency between the ship motion and the forcing waves is not one. Most of the research in the time domain in towing tanks does not carry over to real oceanic conditions. Model tests are quite different from observing the waves at one point on the ocean, observing a ship's motion in an area a few miles away and then trying to relate the motion spectra to the wave spectra. (Someone might try this as a thesis in naval architecture; nearly everyone will be interested in the result).

The lengthy debate over the ISSC spectrum and the validity of the free choice of the two parameters A and B, as in,

$$S(\omega) \quad = \quad A \exp \ (-B \ \omega^{-4}) \ /\omega^5$$

has never properly defined a target population, never checked on whether the spectral form lies within the appropriate limits of the variable estimates, and never looked at the sampling variability of A and B as multiple spectral estimates from a target population. Were this done it would now become clear that the model is inadequate.

The new spectral parameterization technique used in the JONSWAP program is even worse. The procedures fail to account for sampling variability effects and stratify the spectra by using the "estimate" that was accidentally the maximum. Its routine application is guaranteed to provide biased spectra for design purposes in naval architecture. A paper has been written on this particular subject, Pierson (1975), but has not yet been published.

Attempts to parameterize ocean wave spectra in terms of analytical functions and two or more constants, to be defined, are motivated by the idea that the new function is somehow better than the spectrum that was fitted. Even this is debatable. To use the resulting spectral form, it must be evaluated at a set of frequencies and multiplied by appropriate transfer

functions so that the result will predict various ships' motions. Are these predicted motions any better in any way from those that would be predicted using the original spectral estimates for each frequency band?

Other Parameterization Techniques

Various attempts have been made to stratify spectra according to wind speed only and according to non-dimensional concepts. The Pierson-Moskowitz spectrum used a non-dimensional frequency, $\bar{f} = f\ U/g$, where f is frequency, and U is wind velocity. $\bar{S}\ (\bar{f})$ had a non-dimensionalized form independent of F and t (fetch and duration). This may have been an accident, since more recent results suggest that the equilibrium range does not exist for high winds. There are also reasons to doubt that S(f, U, F, t) can be non-dimensionalized to the form $S(f\ U/g;\ g\ F/U^2)$ for t large and F finite, and $S(f\ U/g,\ f\ t/U)$ for F large and t finite.

For U alone fixed as a parameter, the family of all possible spectra for a given U does not seem to have a properly defined target population even for one single location on the ocean, as shown by Moskowitz, for example. The sample space will have to be defined in terms of a distribution of distributions, and this is difficult to formalize. This is the concept of a stratified sample, somewhat analogous to the sampling techniques of political pollsters.

Another popular technique (as for example in the JONSWAP project) is the use of a non-dimensional frequency given by $\bar{f} = f/f_m$ where f_m is the frequency of the spectral maximum for the estimated spectrum. As shown in a recent paper (Pierson, 1975), this procedure is fraught with difficulty.

Concluding Remarks

All in all, it seems that the need to think about the basic meaning of spectral estimation, sampling variability, the terms "statistic" and random sample, and the concept of a target population should precede curve fitting techniques applied to individual estimates of spectra. Before further debate about present spectral parameterization techniques and before other new ones are attempted, the following questions need to be answered:

1. What are the target populations?
2. What causes the parameters of the target populations to vary as a function of the physics of the waves?
3. Can sampled spectra be picked such that the parameters of the target population are fixed, and then can these parameters be in turn estimated from the spectra estimated for these conditions?
4. In what ways, if any, do parameterized spectra yield more useful results than using spectral estimates from a set of actual wave records?

So at the present state of wave data collection it is recognized that the target population cannot be defined as precisely as might be desired. This does not mean that this goal connot be accomplished in the future as a better understanding is developed of the climatology of waves. Essentially, samples from different populations have to be combined, and the overall probability distribution for a new kind of climatological population needs to be derived.

One segment of the target population is the fully-developed seas generated by a wind that is constant in direction, without contamination from other storms or swell. It would be grossly inaccurate to use this as the entire target population of seas expected to be encountered by ships, since account must be taken of waves caused by both growing and decaying seas, of effects of sudden wind shifts, of combined effects of different storms and of swell.

In this report it is assumed that without defining the target population precisely it is possible to make a useful stratified random sample of spectra at specific locations. It is recognized that the sample must be stratified over all seasons, so that seasonal variations can be included. It is recognized that results apply only to the location where the samples are taken. However, when results from several locations are compared (as, in this case, Stations I, K and P) limited judgments can be made regarding the variability with geographical location.

APPENDIX K

A COMPARISON OF WAVE BUOY AND

HINDCAST WAVE SPECTRA

By

David A. Walden

Introduction

Wave data for the month of March 1975 were obtained from the NOAA Data Buoy Office for buoy EB-03 located at 56.0° N - 148.0° W in the Gulf of Alaska. These data consist of spectral ordinates for frequencies from 0.01 to 0.50 Hz. in 0.01 Hz increments. The spectra are based on 16-minute samples taken every three hours.

The predicted directional wave spectra produced by the Fleet Numerical Weather Central (FNWC) Spectral Ocean Wave Model (SOWM) were obtained from the Naval Oceanographic Office. These analyzed spectra are based on the best available wind data, including measurements and the previous wind hindcast. They differ from the spectral forecasts produced by FNWC, which are based on wind forecasts. Both hindcasts and forecasts include the wave state of the previous hindcast. These spectra, again for March 1975, are the hindcasts for a computational grid point located at 56.236° N - 147.537° W, 15 nautical miles ENE of EB-03. These spectra consist of 180 numbers, representing the spectral variance in 15 frequency bands for 12 directions, which are computed every three hours with winds updated every six hours. If at each frequency the variance is summed over the 12 directions, the one-dimensional frequency spectrum for a grid point can be derived.

Wave Heights and Periods

The first step in this study was to plot $H_{1/3}$ and T_1 from both FNWC and EB-03, versus date. These plots are shown in Figs. K-1 and K-2. It can be seen from Fig. 2 that the T_1 results from EB-03 are usually lower than the results from FNWC. This is due to the fact that the plots are based on the assumption that the highest frequency for the FNWC spectrum is 1.03 rps, while the buoy spectra extend to 3.14 rps. It has since been learned that the FNWC high frequency band extends from .164 Hz to .400 Hz (1.03 rps to 2.51 rps).

$H_{1/3}$ is defined by

$$H_{1/3} = 4\sqrt{m_o} \quad , \text{ and}$$

T_1 is defined by,

$$T_1 = 2\pi \frac{m_o}{m_1}$$

where m_o, m_1 are the moments defined by $\displaystyle m_n = \int_0^\infty S_\zeta(\omega)\ \omega^n\ d\omega$

The effect of the high frequency tail of the EB-03 spectra is to make m_1 larger and therefore T_1 smaller. Figs. K-3 and K-4 show $H_{1/3}$ and T_1 versus date with $H_{1/3}$ and T_1 computed from EB-03 spectra which are cut off at 1.068 rps. It can be seen that the agreement is greatly improved for wave period and slightly improved for height.

Since most response RAO's of medium-size ships have significant values at frequencies above 1.03 rps, the FNWC spectra which, in its present form, lack definition in this high frequency are not ideally suited for predicting the motions and stresses of such ships. Thus the inclusion of only one band from 1.03 to 2.51 rps is a significant shortcoming. As can be seen from the effect on T_1, the lack of accuracy in describing high frequency components significantly affects higher moments of the spectra. Figs. K-5 and K-6 show the skewness γ defined by $\gamma = m_3/m_2^{3/2}$ for the FNWC cut off at 1.03 rps spectra and the EB-03 spectra with and without the tail. The lines are least squares fit to the data points. Also shown is the ISSC relation between γ and $H_{1/3}$

$$\gamma = 6.1458 \; H_{1/3}^{-1}$$

The results for another shape parameter, flatness, defined by $\beta = m_4/m_2^2$, are shown in Figure K-6. Similar results from Stations "I," "P" and "K" indicated a fairly close agreement with the ISSC line. Thus, the large scatter of the EB-03 data with the tail included about the ISSC lines, compared with the scatter of the Station "P" data, raises some doubts about the buoy results, particularly the high frequency tail which strongly affects m_2 and m_3.

Groups of Spectra

The next step was to create a group of spectra based on $H_{1/3}$. The spectra selected were those for which $H_{1/3}$ was between 2 and 3 meters for both FNWC and EB-03 at the same times. Eight such spectra were found. The results are shown in Figs. K-7 and K-8. In spite of the selection of spectra where the wave height agreed fairly well, the agreements between the means is poor. This difference is important in predicting ship responses.

The next group was of 8 spectra from consecutive observation where $H_{1/3}$ ranged from 1½ meters to 3 meters. Again the means, as seen in Figs. K-9 and K-10, show poor agreement. The last group was of 8 consecutive spectra including the largest $H_{1/3}$ value (7.0 m). Figs. K-11 and K-12 show that the magnitudes of the means do not agree. Fig. K-13 shows the non-dimensional means. It can be seen that the means are in only fair agreement with each other and with the ISSC spectrum, but the shapes are similar.

Individual Spectra

A one-to-one comparison of the spectra near the peak of the $H_{1/3}$ versus date curve was made. These results are shown in Figs. K-14, K-15 and K-16, and in non-dimensional form in Figs. K-17, K-18 and K-19. The poor agreement in Figs. K-14 - K-16 and the somewhat improved agreement in the non-dimensional Figs. K-17 - K-19 shows that there are large differences in significant height, $H_{1/3}$, and mean period, T_1, but that some similarity in spectrum shape exists.

At the suggestion of Professor Pierson, the confidence intervals for the EB-03 spectra were investigated. The 90% confidence intervals based on the 36 degrees of freedom at each ordinate are shown in Figs. K-14, K-15, K-16 and K-23. It can be seen that even if the actual spectra corresponded to the extremes of the confidence intervals, the agreement with the FNWC spectra is still poor.

Professor Pierson also suggested that the disagreement near 27 March might be due to an error in the arrival time in the FNWC model. For this reason, Fig. K-23 shows the FNWC spectrum for 1200Z 27 March and the EB-03 spectrum for 1200Z 26 March. Significant disagreement is still apparent.

The non-dimensional results also show good agreement with the non-dimensional ISSC spectrum. This is expected since these cases approximate the pure fully-developed, wind-generated sea on which the ISSC spectrum and the FNWC model are based.

Fig. K-20 is a scatter diagram of FNWC $H_{1/3}$ versus EB-03 (based on the full spectra out to 3.14 rps). The leat squares lines through the origin has slope 1.2, which indicates that the FNWC model is predicting an average total energy excess of about 20% over that measured by the buoy for this period.

Wind Speed

In seeking an explanation for the differences between the FNWC and EB-03 results, we examined the wind speed, which was given for both sets of data. The results shown in Fig. K-21 indicate quite poor agreement in wind speed.

On the basis of a preliminary version of this report supplied to NDBO, and other information, they have re-examined the wind data from EB-03 for March and have discovered that there were problems with the anemometers and therefore all wind data are unreliable.

It has also been learned that only after March 1975 has FNWC been correcting all wind speeds to 19.5 m. This includes observations used in determining the wind field and the values printed in the output with the spectral values.

Fig. K-22 shows that the wind directions agree for most cases within 30°. This agreement can be considered fairly good.

The following quotation from the Mariner's Weather Log* indicates that March 1975 was an exceptionally mild one in the Gulf of Alaska.

> "More storms tracked into the eastern Bering Sea, and fewer
> into the Gulf of Alaska, than normal. Higher-than-normal
> pressure over extreme northern Canada diverted the storms
> away from the Gulf of Alaska and further south along the
> U.S. west coast."

This explains the low significant wave heights for this period. It is unfortunate that it was not possible to compare the FNWC and EB-03 results for a period when higher wave heights prevailed because it is these higher waves that are of more significance in predicting ship responses.

_____

*Mariner's Weather Log, "Smooth Log, North Pacific Weather -- March and April 1975," MWL, Vol. 19, No. 5, September 1975.
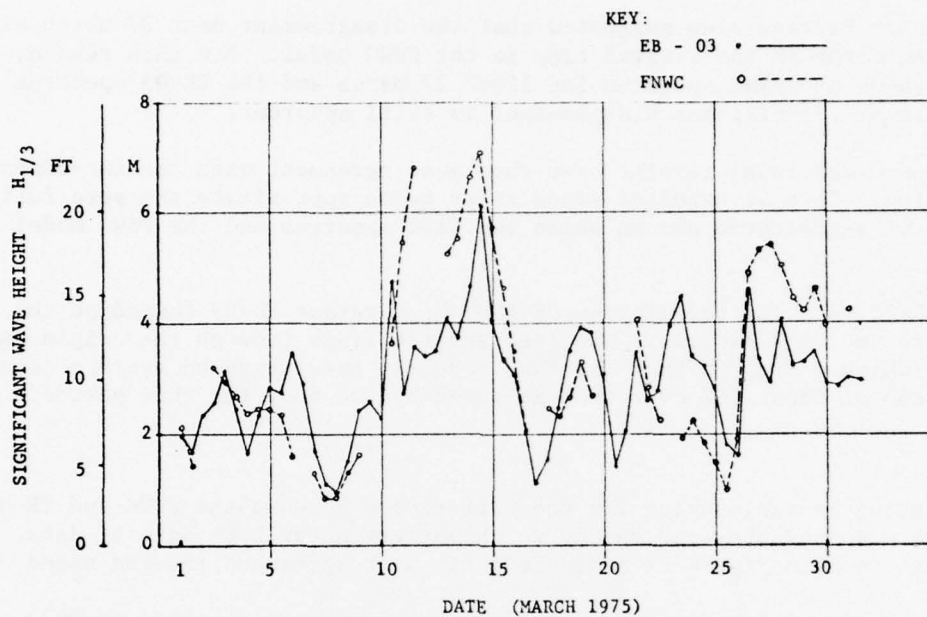
Fig. K-1 – $H_{1/3}$ FNWC and $H_{1/3}$ EB-03 (with tail) vs Date
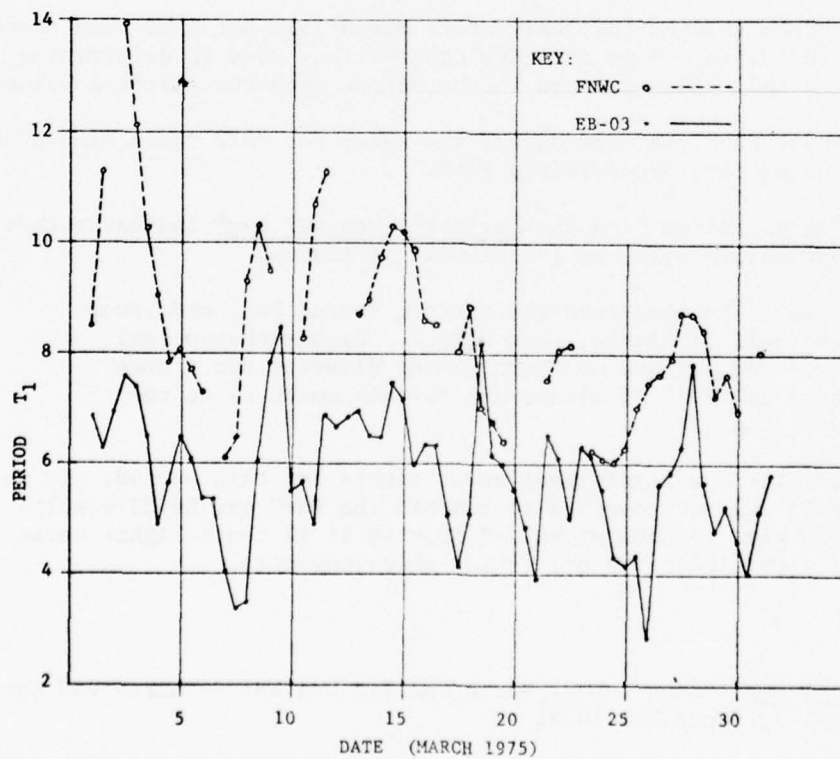
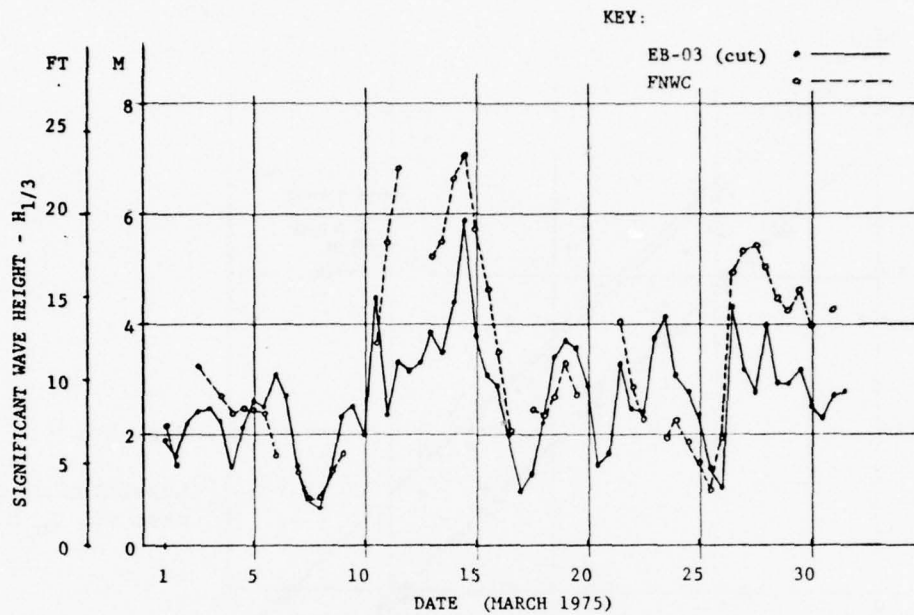**Fig.** K-2 – T_1 FNWC and T_1 EB-03 (with tail) vs. Date

K-4

Fig. K-3 - $H_{1/3}$ FNWC and $H_{1/3}$ EB-03 (without tail) vs Date
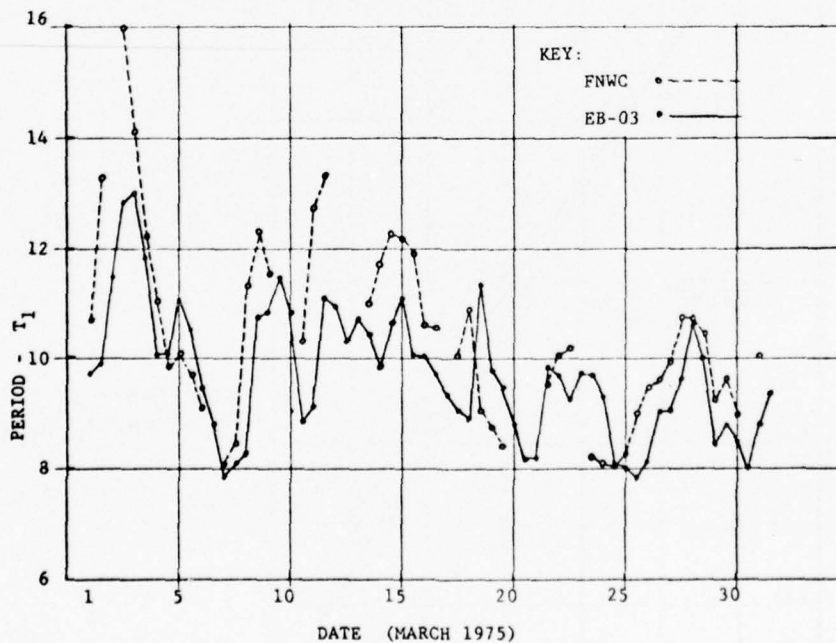

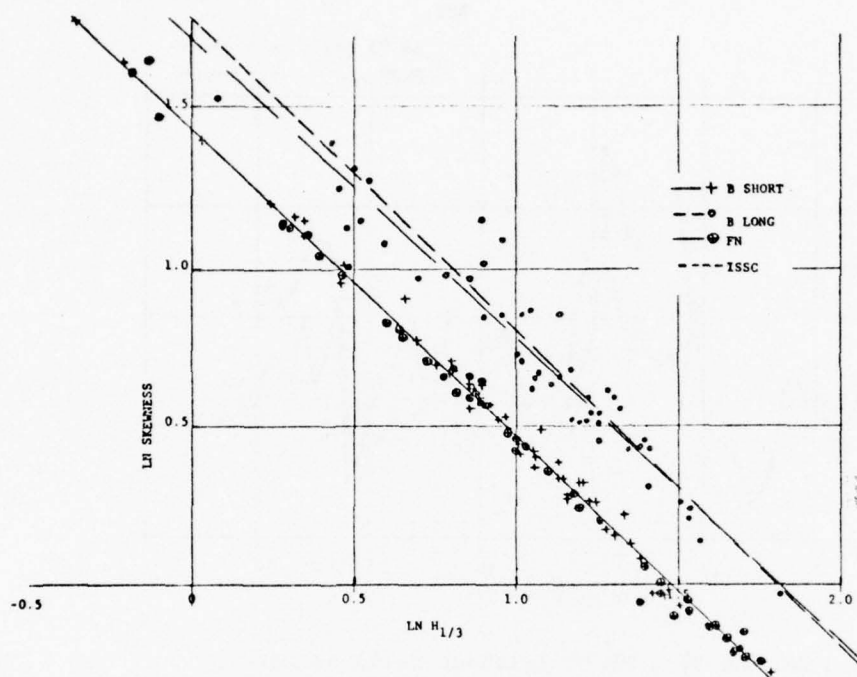Fig. K-4 - T_1 FNWC and T_1 EB-03 (without tail) vs Date
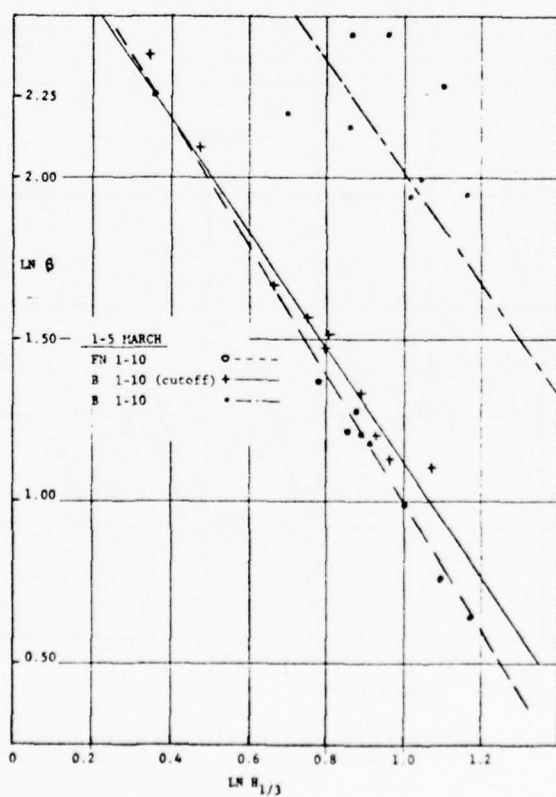
Fig. K-5 –

Logarithm of Skew-
ness vs. $l_n H_{1/3}$

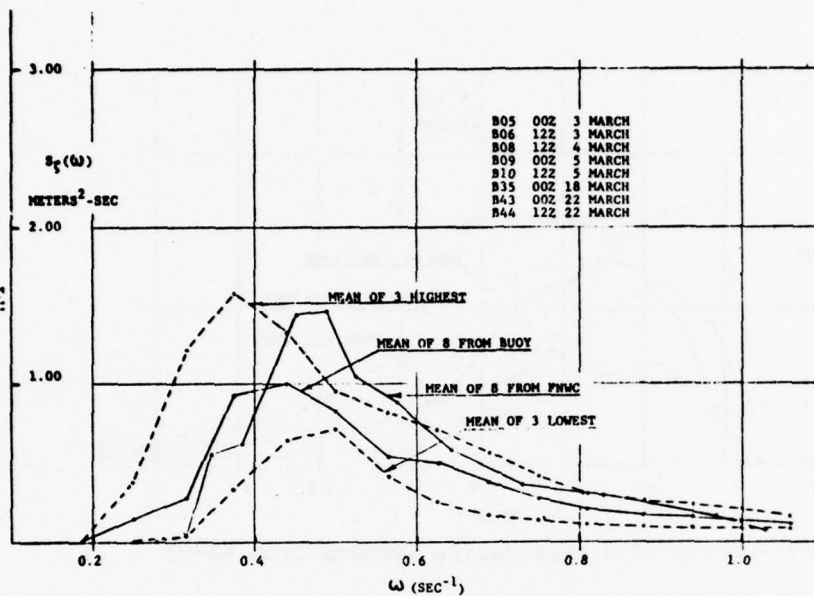Fig. K-6 – $l_n \beta$ (flat-
ness) vs. $l_n H_{1/3}$

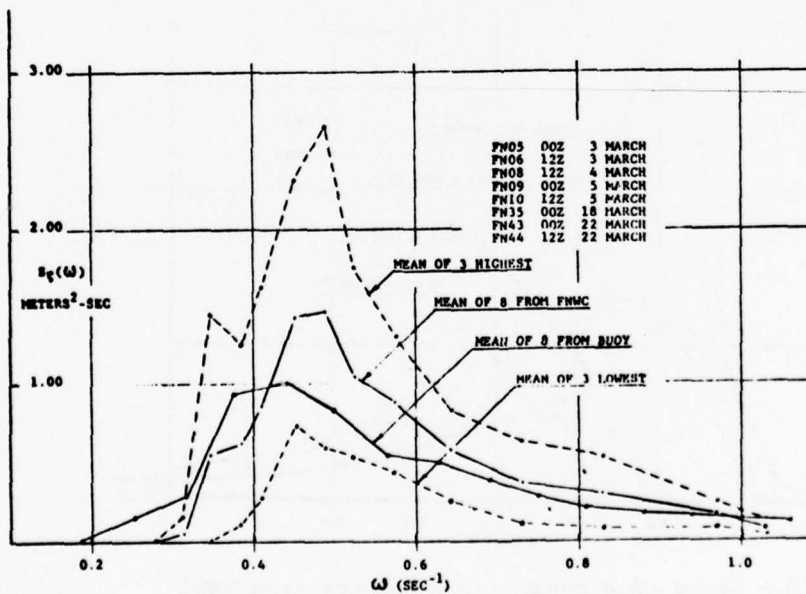Fig. K-7 - Group of EB-03 spectra with $2_m < H_{1/3} < 3_m$

Fig. K-8 - Group of FNWC spectra with $2_m < H_{1/3} < 3_m$
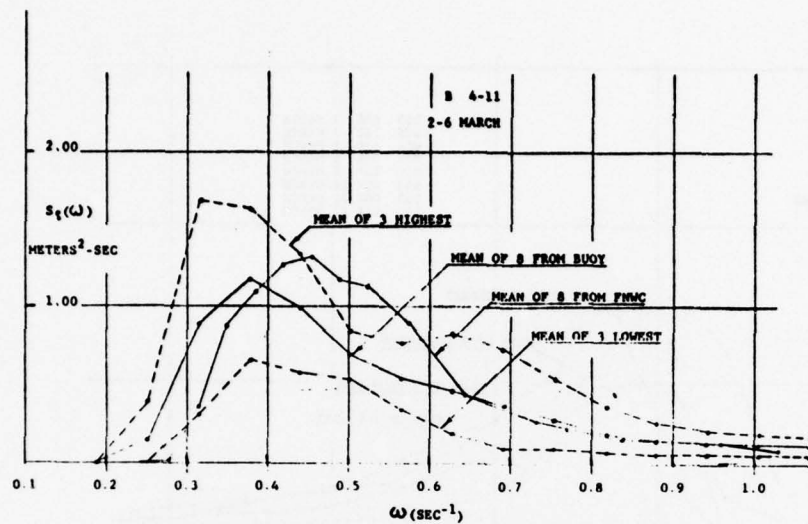
Fig. K-9 – Group of 8 consecutive spectra from EB-03
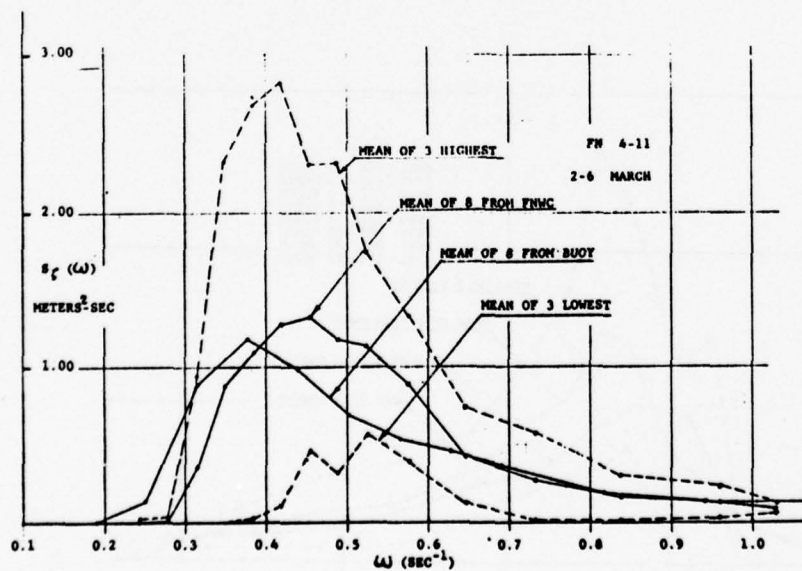
Fig. K-10 – Group of 8 consecutive spectra from FNWC

K-8
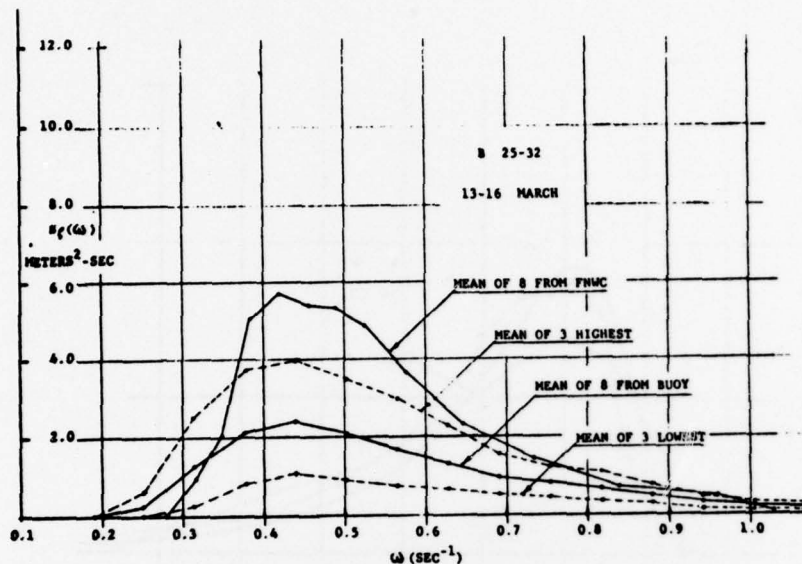
Fig. K-11 — Group of 8 consecutive spectra from EB-03
(bracketing peak $H_{1/3}$)
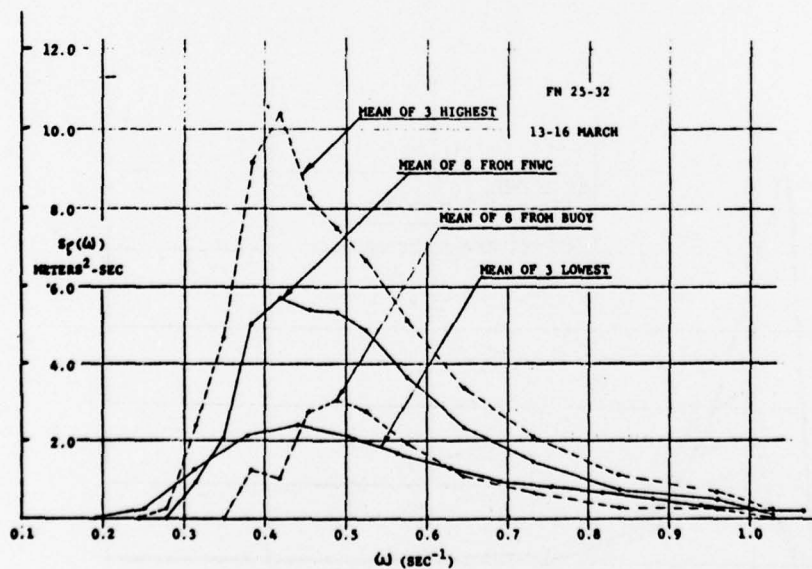
Fig. K-12 — Group of 8 consecutive spectra from FNWC
(bracketing peak $H_{1/3}$)
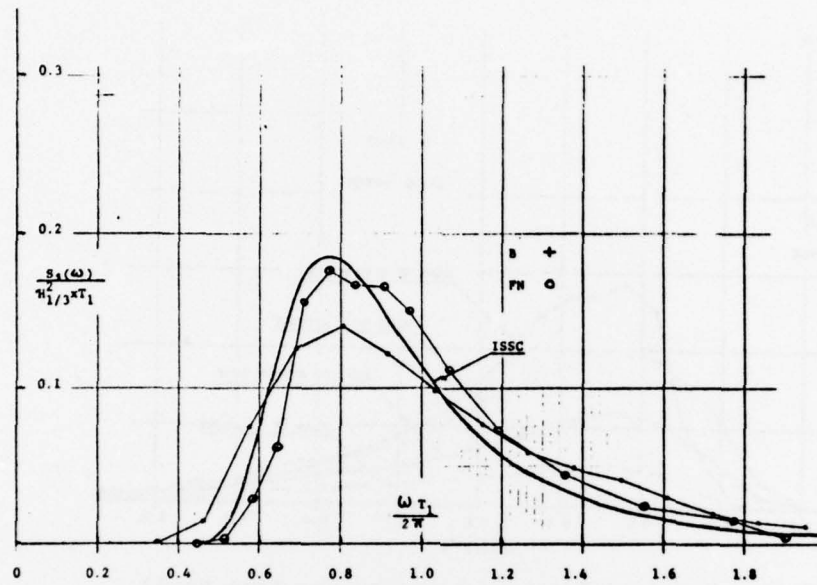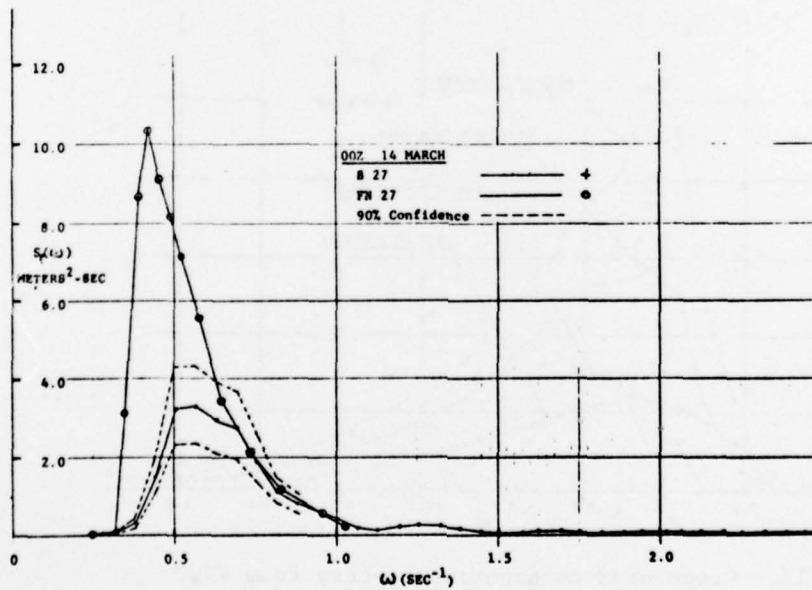
Fig. K-13 - Non-dimensional means from EB-03 & FNWC spectra bracketing peak $H_{1/3}$
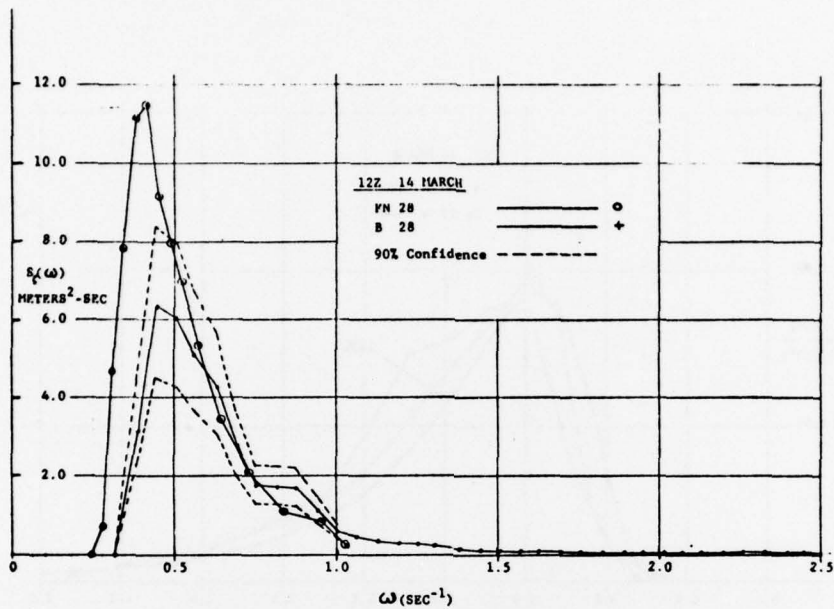

Fig. K-14 - EB-03 and FNWC spectra near peak $H_{1/3}$
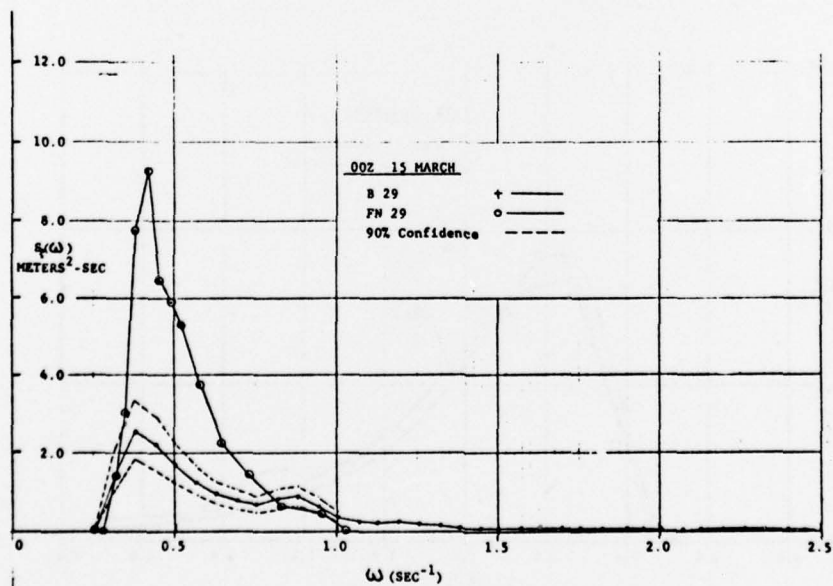
Fig. K-15 - EB-03 & FNWC spectra near peak $H_{1/3}$
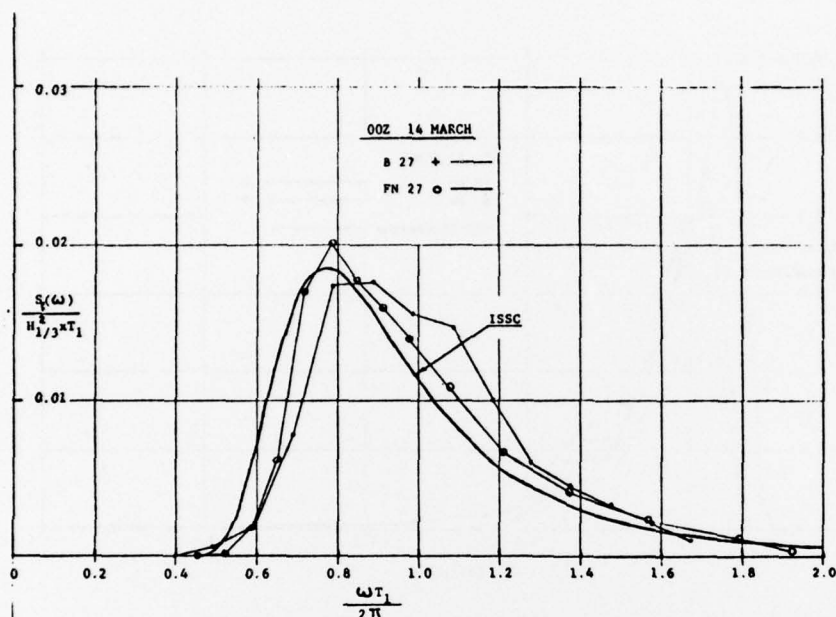

Fig. K-16 - FB-03 and FNWC spectra near peak $H_{1/3}$

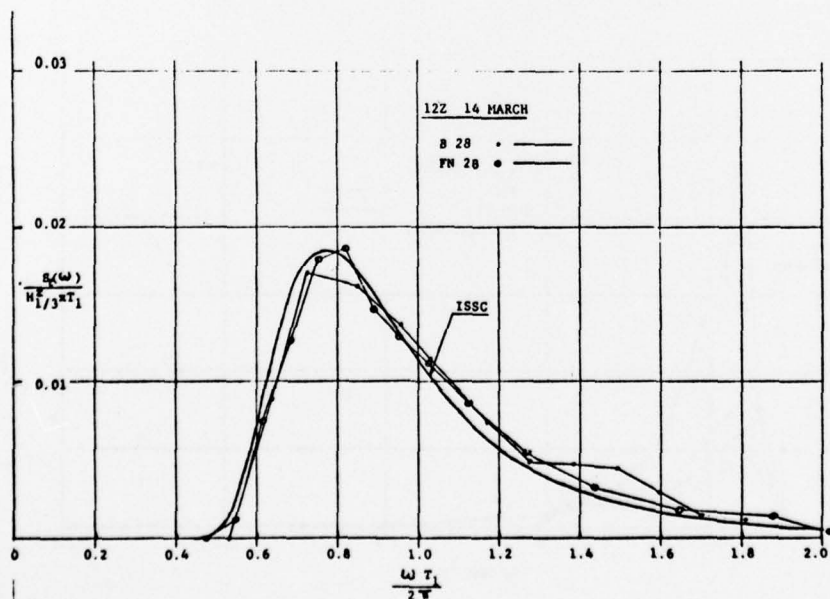Fig. K-17 – Non-dimensional EB-03 & FNWC spectra near peak
$H_{1/3}$

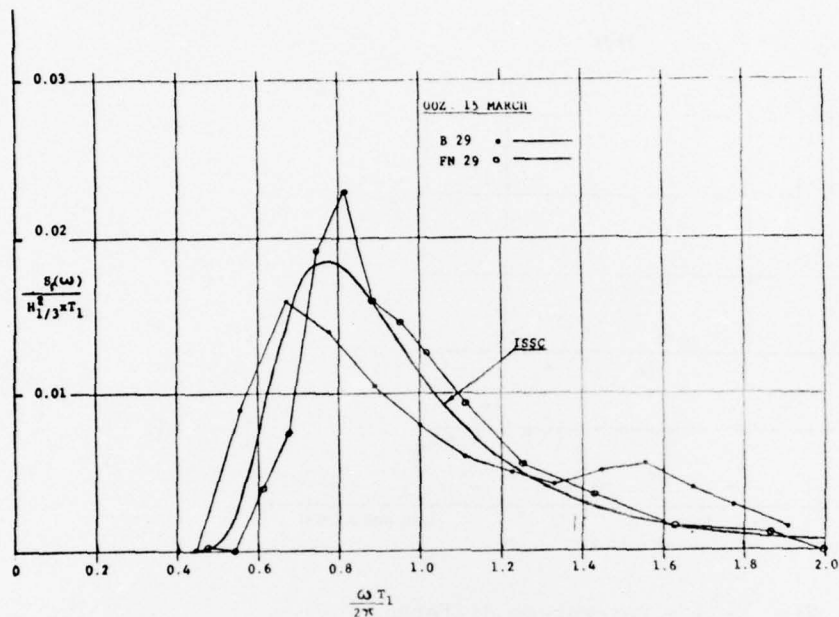Fig. K-18 – Non-dimensional EB-03 & FNWC spectra near peak
$H_{1/3}$

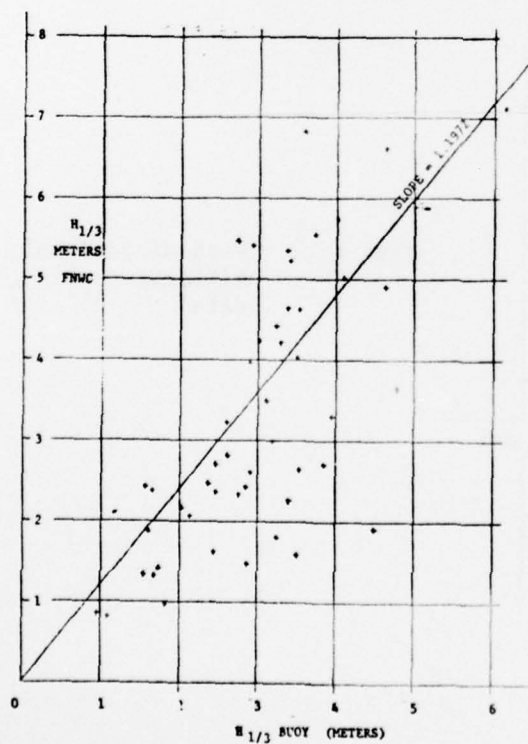**Fig. K-19-** Non-dimensional **EB-03** & FNWC spectra near Peak $H_{1/3}$

Fig. K-20 – Scatter diagram
$H_{1/3}$ FNWC and $H_{1/3}$
EB-03

Fig. K-21 – Percentage difference
in wind speed vs. date

Fig. K-22 – Wind directional
difference vs.
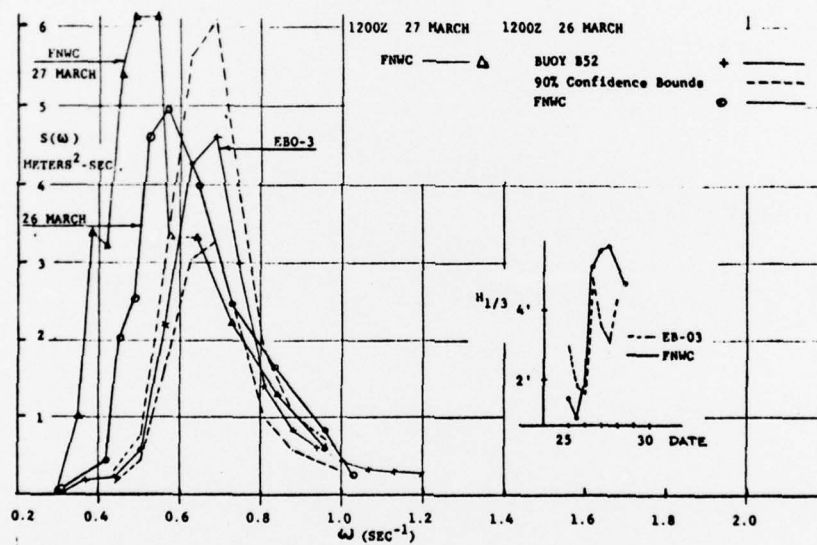date
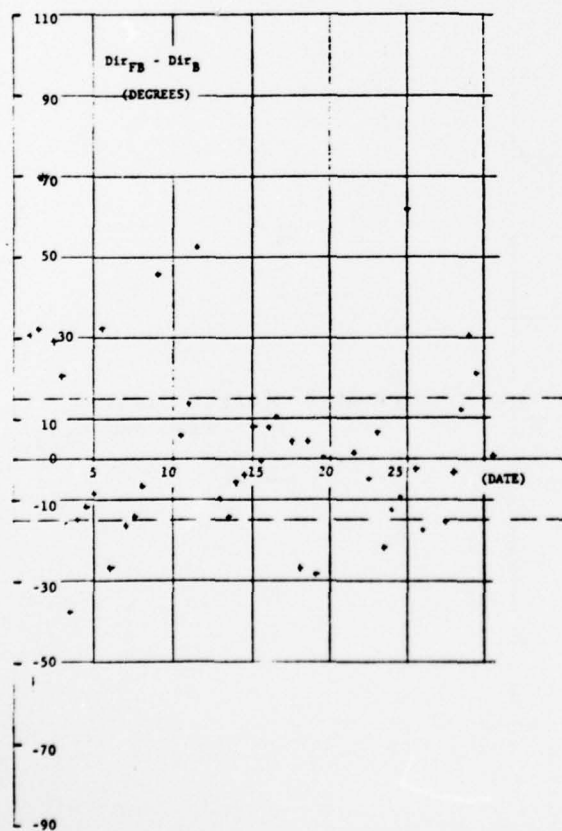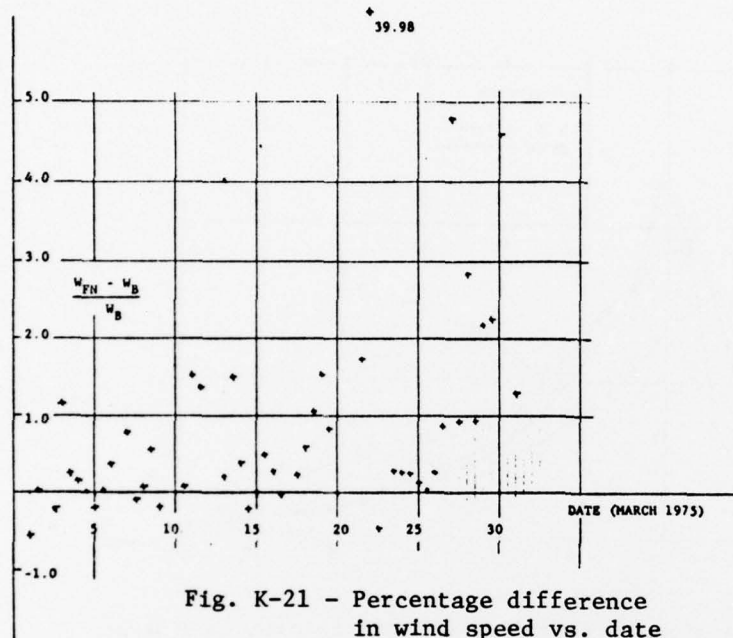
Fig. K-23 - FNWC and EB-03 Spectra for 26-27 March

APPENDIX L

PROPOSED BUOY SYSTEM FOR
WAVE MEASUREMENT OFF SOUTH AFRICA

by

Cdr. C.S. Niederman, U.S.C.G.

NOAA Data Buoy Office

Introduction

This appendix reviews, in brief, a proposal submitted by the NOAA Data Buoy Office to the American Bureau of Shipping (ABS) during December 1975. It represents the state-of-the-art in proven wave measurement capability from a buoy reporting on a long-term basis in a severe ocean environment. A description of the buoy system, its data output, costs, and schedule, are presented.

At the present time, June 1976, ABS is seeking additional monies from shipping interests to assist them in funding such a buoy.

System Description

The system was designed to survive severe storms and strong currents and to report wave conditions on a three-hour synoptic basis for a period of at least a year. Thus it would be expected to report the severe seas off the South African coast which have resulted in serious ship damage or loss. The system was to consist of a 40-foot (12-meter) diameter discus hull and a battery powered payload which transmitted in the HF range by relay to a U.S. shore communication station. Unfortunately, the location is beyond presently available UHF satellite coverage, which is more reliable and less expensive than the HF system. In addition to the wave measurement capability, wind vector, air temperature and pressure measurements were proposed, since their inclusion made little difference in cost and they would be parameters of interest in relation to the recorded waves.

The proposed wave measurement system consists of a hull-mounted accelerometer and a wave spectrum analyzer which filters the acceleration data into twelve discrete frequency bands, which can be selected during assembly to best describe the anticipated spectra. At the NOAA shore communication station (SCS) these inputs are converted to twelve-point displacement spectra.

The data at the SCS are then available on a real-time basis for use by forecasters and ship routers and on an archival basis for use by naval architects. The wave data available in the one-dimensional spectral form can be converted easily, if desired, to wave heights and periods.

The system proposed was selected from existing hardware wherever possible to reduce production costs. The mooring costs were conservative since the mooring line length and diameter were chosen to withstand a maximum Agulhas Current profile, which occurs in deep water off the continental shelf. Costs would be less for mooring over the continental shelf, where water is shallower and currents are less strong. The payload, including the sensors, the data processing and control unit, and the communications set were mostly on-hand items. The communications were to be set up from Miami to the buoy on a direct

command link and from the buoy via Ascension Island and Patrick Air Force
Base on the data link. A tape recorder was included on the buoy to provide
a record of data that might be lost in transmission. Logistic costs were
based on one repair trip during the year. Transportation costs to South
Africa were not included since it was felt that transportation might be
available from a shipping beneficiary of the program. Redundancy of the pay-
load was proposed as an option for added reliability, but the single-repair
trip cost was also retained. The costs were based on one year of operation
with a second year of operation proposed as an option for a redundant system.

Estimated costs, assuming the buoy to remain the property of the U.S.
Government, are given in table K-1.

Table K-1
WAVE MEASUREMENT BUOY COSTS

| | FIRST YEAR | | SECOND YEAR |
	Single System	Redundant System	Redundant System
Payload & Spares, Including Wave Spectral Analyzer	$ 33,000	$ 95,000**	$ 4,000
Power Supply	2,000	4,000	4,000
Integration & Test	7,000	13,000	
Tape Recorder	5,000	5,000	
Hull Refurbishment	20,000	20,000	
Mooring* (11,000 ft. in Agulhas Current)	60,000	60,000	
Communications & Data Processing	23,000	23,000	5,000
Logistics (Deploy, Repair, Recover)	25,000	25,000	11,000
On-Load & Off-Load on Transport	20,000	20,000	
TOTAL	$195,000	$265,000	$20,000 Additional

* Reduced to approximately $10,000 if moored on continental shelf at
600-foot depth.

** This is more than twice as expensive as the single system since the
first consists of parts on hand, while the second requires some new
procurement.

Conclusion

It is believed that the system described here would be a feasible method for obtaining reliable, long-term wave data for an ocean area for which data are scarce. Furthermore, the spectra obtained would be consistent with other data being collected in U. S. coastal waters.

The cost does not seem high in relation to the value and quality of data to be obtained and financial assistance may be obtained from the operators of ships regularly engaged in service around the Cape of Good Hope.

METRIC CONVERSION FACTORS

Approximate Conversions to Metric Measures

When You Know	Multiply by	To Find	Symbol
LENGTH			
inches	*2.5	centimeters	cm
feet	30	centimeters	cm
yards	0.9	meters	m
miles	1.6	kilometers	km
AREA			
square inches	6.5	square centimeters	cm²
square feet	0.09	square meters	m²
square yards	0.8	square meters	m²
square miles	2.6	square kilometers	km²
acres	0.4	hectares	ha
MASS (weight)			
ounces	28	grams	g
pounds	0.45	kilograms	kg
short tons (2000 lb)	0.9	tonnes	t
VOLUME			
teaspoons	5	milliliters	ml
tablespoons	15	milliliters	ml
fluid ounces	30	milliliters	ml
cups	0.24	liters	l
pints	0.47	liters	l
quarts	0.95	liters	l
gallons	3.8	liters	l
cubic feet	0.03	cubic meters	m³
cubic yards	0.76	cubic meters	m³
TEMPERATURE (exact)			
Fahrenheit temperature	5/9 (after subtracting 32)	Celsius temperature	°C

*1 in = 2.54 (exactly). For other exact conversions and more detailed tables, see NBS Misc. Publ. 286, Units of Weights and Measures. Price $2.25, SD Catalog No. C13.10:286.

Approximate Conversions from Metric Measures

When You Know	Multiply by	To Find	Symbol
LENGTH			
millimeters	0.04	inches	in
centimeters	0.4	inches	in
meters	3.3	feet	ft
meters	1.1	yards	yd
kilometers	0.6	miles	mi
AREA			
square centimeters	0.16	square inches	in²
square meters	1.2	square yards	yd²
square kilometers	0.4	square miles	mi²
hectares (10,000 m²)	2.5	acres	
MASS (weight)			
grams	0.035	ounces	oz
kilograms	2.2	pounds	lb
tonnes (1000 kg)	1.1	short tons	
VOLUME			
milliliters	0.03	fluid ounces	fl oz
liters	2.1	pints	pt
liters	1.06	quarts	qt
liters	0.26	gallons	gal
cubic meters	35	cubic feet	ft³
cubic meters	1.3	cubic yards	yd³
TEMPERATURE (exact)			
Celsius temperature	9/5 (then add 32)	Fahrenheit temperature	°F

SECURITY CLASSIFICATION OF THIS PAGE (When Data Entered)

REPORT DOCUMENTATION PAGE		READ INSTRUCTIONS BEFORE COMPLETING FORM
1. REPORT NUMBER SSC-268	2. GOVT ACCESSION NO.	3. RECIPIENT'S CATALOG NUMBER
4. TITLE (and Subtitle) Environmental Wave Data for Determining Hull Structural Loadings		5. TYPE OF REPORT & PERIOD COVERED Final Report
		6. PERFORMING ORG. REPORT NUMBER
7. AUTHOR(s) Dan Hoffman and David A. Walden		8. CONTRACT OR GRANT NUMBER(s) N00024-75-C-4209
9. PERFORMING ORGANIZATION NAME AND ADDRESS Webb Institute of Naval Architecture Glen Cove, NY 11542		10. PROGRAM ELEMENT, PROJECT, TASK AREA & WORK UNIT NUMBERS SF43-422-703-06 Task 2022
11. CONTROLLING OFFICE NAME AND ADDRESS Naval Ship Systems Command		12. REPORT DATE
		13. NUMBER OF PAGES 222
14. MONITORING AGENCY NAME & ADDRESS(if different from Controlling Office) Ship Structure Committee		15. SECURITY CLASS. (of this report) Unclassified
		15a. DECLASSIFICATION/DOWNGRADING SCHEDULE

16. DISTRIBUTION STATEMENT (of this Report)

Distribution is unlimited.

17. DISTRIBUTION STATEMENT (of the abstract entered in Block 20, if different from Report)

18. SUPPLEMENTARY NOTES

19. KEY WORDS (Continue on reverse side if necessary and identify by block number)

Ocean waves	Wave hindcasting	Wave measuring buoys
Ship hull loads	Wave statistics	
Wave spectra	Wave data collection	

20. ABSTRACT (Continue on reverse side if necessary and identify by block number)

A summary is given of the trade routes of U.S. ships, followed by suggestions for new projects and extension and improvement of current projects to meet the need for additional data on sea conditions encountered by U.S. ships. It is concluded that the greatest benefit can be obtained by making a direct effort to obtain wave spectra for the ocean areas on important sea routes that are known to experience severe sea conditions, probably by the use of moored buoys, and by further verification and improvement of wave hindcast techniques

DD FORM 1473 EDITION OF 1 NOV 65 IS OBSOLETE
1 JAN 73
S/N 0102-014-6601 |

SECURITY CLASSIFICATION OF THIS PAGE (When Data Entered)

20. Abstract

for eventual application to obtaining wave spectra for design. At the same
time, steps should be initiated that may lead to the availability of wave data
in the future, as seeking oil company data.

It is felt that attention should also ge given to the further analysis of
available data, and of new data produced by buoy deployment and hindcast
procedures, including the measurement of directional spectra and their
application to design. Hindcast techniques should be extended to the southern
hemisphere, and new techniques for wave data collection -- disposable buoys
and satellite systems -- should continue to be developed.

A survey evaluation is given of observed and measured wave data covering
major U.S. routes, with appendices, tabulations and maps. The introduction
of theoretical formulations leads to the discussion and evaluation of wave
spectral hindcasting techniques. The methods used to predict ship motions
and loads are explained followed by a section discussing the wave data format
required for predicting short and long-term loads and motions as well as
numerical examples showing the effect on and sensitivity of predictions to
variation in wave data format.

Based on the preceding discussion, presently available data suggested for
use in determining ship loads are given. The use of a combination of
statistics based on observations on the frequency of occurrence of various
wave heights and a spectral family of measured spectra grouped by wave height
is recommended. Finally, a survey of current and planned data collection
projects is given.

The opinions and conclusions presented in this paper are those of the
authors and not necessarily those of the Ship Structure Committee nor of the
Department of the Navy.